Preparation, Characterization, and *In Vitro* Evaluation of Polymer-based Wound Dressings for the Management of Chronic Wounds

University of Fort Hare

Together in Excellence

Alven Sibusiso

University of Fort Hare
Together in Excellence

Supervisor: Prof B. A. Aderibigbe

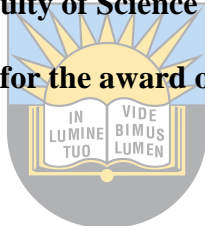Co-Supervisor: Prof. K. Varaprasad

2022

Preparation, Characterization, and *In Vitro* Evaluation of Polymer-based Wound Dressings for the Management of Chronic Wounds

By

Alven Sibusiso (201214199)

Being a thesis submitted to the Faculty of Science and Agriculture in fulfilment of the requirements for the award of the degree of

Doctor of Philosophy in Chemistry at the

University of Fort Hare

Supervisor: Prof. B.A. Aderibigbe

Co-Supervisor: Dr K. Varaprasad

Declaration by candidate

"I hereby declare that this thesis submitted for Doctor of Philosophy degree in Chemistry, at the University of Fort Hare, chemistry department, is my original work without plagiarism and has not been previously submitted to any other institution of higher learning. I further declare that all the cited sources are indicated and acknowledged through a comprehensive list of references".

<u>20/06/2022</u>

Date   Alven. S

University of Fort Hare
Together in Excellence

Dedication

I hereby dedicate this thesis to my lovely wife, Alven Esona Zozibini, and my sons, Alven Imolathile Blessing, Alven Ungcwele Favoured, and Alven Ingcwele Favour.

Acknowledgements

Research Outputs

Published Papers

1. S. Alven, S. Peter, Z. Mbese, and B.A. Aderibigbe. Polymer-Based Wound Dressing Materials Loaded with Bioactive Agents: Potential Materials for the Treatment of DiabeticWounds. *Polymers* **2022**, 14, 724. https://doi.org/10.3390/polym14040724.

2. S. Alven and B.A. Aderibigbe. Hyaluronic Acid-based Scaffolds as Potential Bioactive Wound Dressings. *Polymers* **2021**, 13, 2102. https://doi.org/10.3390/polym13132102.

3. S. Alven, V. Khwaza, O.O. Oyedeji, and B.A. Aderibigbe. Polymer-based Scaffolds loaded with Aloe Vera extract for Wound Treatment. *Pharmaceutics* **2021**, 13, 961. https://doi.org/10.3390/pharmaceutics13070961.

4. S. Alven, B. Buyana, Z. Feketshane, and B.A. Aderibigbe. Electrospun Nanofibers/Nanofibrous Scaffolds Loaded with Silver Nanoparticles as Effective Antibacterial Wound Dressing Materials. *Pharmaceutics* **2021**, 13, 964. https://doi.org/10.3390/pharmaceutics13070964.

5. S. Alven and B.A. Aderibigbe. Fabrication of Hybrid Nanofibers from Biopolymers and Poly (vinyl alcohol)/ Poly (ε-caprolactone) for Wound Dressing Applications. Polymers, **2021**, 13, 2104. https://doi.org/10.3390/polym13132104.

6. Z. Mbese, S. Alven and B.A. Aderibigbe. Collagen-Based Nanofibers for Skin Regeneration and Wound Dressing Applications. *Polymers* **2021**, 13, 4368. https://doi.org/10.3390/polym13244368.

7. S.P. Ndlovu, K. Ngece, S. Alven, and B.A. Aderibigbe. Gelatin-Based Hybrid Scaffolds: Promising Wound Dressings. *Polymers* **2021**, 13, 2959. https://doi.org/10.3390/polym13172959.

8. S. Peter, S. Jama, S. Alven, and B.A. Aderibigbe. Artemisinin and Derivatives-Based Hybrid Compounds: Promising Therapeutics for the Treatment of Cancer and Malaria. Molecules **2021**, 26, 7521. https://doi.org/10.3390/molecules26247521.

9. S. Alven, X. Nqoro, and B.A. Aderibigbe. Polymer-Based Materials Loaded with Curcumin for Wound Healing Applications. *Polymers* **2020**, 12, 2286; doi:10.3390/polym12102286.

10. S. Alven and B.A. Aderibigbe. Chitosan and Cellulose-Based Hydrogels for Wound Management. *International Journal of Molecular Science* **2020**, 21, 9656; doi:10.3390/ijms21249656.

11. S. Alven and B.A. Aderibigbe. Nanoparticles Formulations of Artemisinin and Derivatives as Potential Therapeutics for the Treatment of Cancer, Leishmaniasis and Malaria. *Pharmaceutics* **2020**, 12, 748; doi:10.3390/pharmaceutics1208074.

12. S. Alven and B.A. Aderibigbe. Efficacy of Polymer-Based Nanocarriers for Co-Delivery of Curcumin and Selected Anticancer Drugs. Nanomaterials **2020**, 10, 1556, doi:10.3390/nano10081556.

13. S. Alven and B.A. Aderibigbe. The Therapeutic Efficacy of Dendrimer and Micelle Formulations for Breast Cancer Treatment. *Pharmaceutics* **2020**, 12, 1212; doi:10.3390/pharmaceutics12121212.

14. S. Alven, X. Nqoro, B. Buyana, and B.A. Aderibigbe. Polymer-Drug Conjugate, a Potential Therapeutic to Combat Breast and Lung Cancer. *Pharmaceutics* **2020**, 12, 406; doi:10.3390/pharmaceutics12050406.

15. S. Alven and B.A. Aderibigbe. Combination Therapy Strategies for the Treatment of Malarial. *Molecules* **2019**, *24*, 3601; doi:10.3390/molecules24193601.

Published Book Chapters
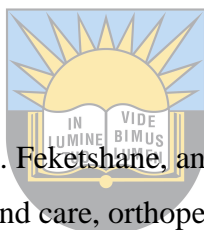
1. S. Alven, Z. Mbese, S. Peter, Z. Feketshane, and B.A. Aderibigbe. The efficacy of injectable biomaterials for wound care, orthopedic application, and tissue engineering Polymeric Biomaterials for Healthcare Application **2022**, 285-320.

2. S. Alven and B.A. Aderibigbe. Nanoformulations of old and new antimalarial drugs. Applications of Nanobiotechnology for Neglected Tropical Diseases **2021**, 191-216.

3. B. Buyana, S. Alven, X. Nqoro, B.A. Aderibigbe. Antibiotics Encapsulated Scaffolds as Potential Wound Dressings. Antibiotic Materials in Health Care **2020**, 111-128.

Accepted Manuscripts

1. X. Nqoro, S. Alven, and B.A. Aderibigbe. Chitosan-Based Hybrid Wound Dressings Encapsulated with Bioactive Agents. Int. J. Mol. Sci., **2021** 22, x. https://doi.org/10.3390/xxxxx.

2. S. Peter, S. Alven, R.B. Maseko, and B.A. Aderibigbe. Doxorubicin-Based Hybrid Compounds as Potential Anticancer Agents: A Review *Molecules* **2022**, *27*, x. https://doi.org/10.3390/xxxxx.

Manuscripts *submitted*

1. S. Alven and B.A. Aderibigbe. Carboxymethyl Cellulose/Poloxamer Topical Gels Enriched with Essential Oil and Ag Nanoparticles for Wound Treatment. **2022**.

2. S. Alven and B.A. Aderibigbe. Gelatin/PEG Sponges Co-Loaded with Metronidazole and Ag Nanoparticles for Management of Chronic Wounds. **2022**.

3. S. Alven, S. Peter, and B.A. Aderibigbe. Polymer-based Hydrogels Enriched with Essential Oils: Potential Strategy for the Treatment of Wounds. **2022**.

4. Z. Feketshane, S. Alven, and B.A. Aderibigbe. Gellan Gum in Wound Dressing Scaffolds. **2022**.

University of Fort Hare
Together in Excellence

Abstract

Microbial infections are responsible for the retarded recovery process of chronic wounds. Polymer-based scaffolds possess features suitable for the treatment of chronic injuries. However, these scaffolds are commonly encapsulated with therapeutic agents to enhance their biological activities, including antibacterial efficacy. In this research, two types of polymer-based scaffolds were formulated and evaluated as effective formulations for the treatment of chronic wounds: sponges and topical gels. Sponges were formulated from cross-linking of gelatin and PEG. Ag nanoparticles and metronidazole were incorporated into the sponges to improve their antibacterial activity. Topical gels were loaded with essential oils and Ag nanoparticles and prepared from CMC and poloxamer. The prepared sponges and topical gels were evaluated using various analysis and characterization techniques.

SEM/EDX, FTIR, and TGA were employed to characterize gelatin/PEG hybrid sponges followed by porosity, *in vitro* biodegradability, cytotoxicity, and antibacterial studies. FTIR, SEM/EDX, and TGA confirmed their physicochemical properties and successful fabrication of sponges loaded with metronidazole and Ag nanoparticles. The sponges were biodegradable, indicating their capability to induce skin regeneration. The drug release studies showed a rapid release of metronidazole (28.32-71.97%) from the sponges over the first hour, followed by a sustained drug release. The Ag nanoparticles were released in a sustained manner, suggesting that these sponges can rapidly destroy bacteria and inhibit persisting bacterial infections as well as protect the lesion bed from further bacteria infections. The *in vitro* antibacterial studies of sponges displayed superior antibacterial activity against most of the Gram-negative and Gram-positive bacteria strains commonly found in chronic wound infections with a MIC value of 15.625 μg/mL. *In vitro* cytotoxicity experiments revealed excellent biocompatibility with a % cell viability of more than 70%. The *in vitro* wound scratch healing assay exhibited that the sponges encapsulated with only metronidazole promoted high cell migration than the dual drug-loaded sponges and untreated cells, suggesting its potential to quicken the wound healing process.

CMC/Poloxamer topical gels were also characterized by FTIR, followed by pH, viscosity, spreadability, cytotoxicity, and antibacterial studies. FTIR showed successful preparation of CMC/Poloxamer topical gels loaded with essential oils and Ag nanoparticles. The topical gels exhibited pH in the range of 5.20-6.68, spreadability between 5.4 and 5.9 cm, and viscosity ranged from 216 to 1200 cP at 50 rpm and 210–858 cP at 100 rpm. The *in vitro* drug release studies demonstrated that Ag nanoparticles were released from the topical gels in a sustained

manner. Most formulated topical gels demonstrated superior antimicrobial efficacy against Gram-positive and Gram-negative bacteria strains than the blank gel and controls. The cytotoxicity analysis displayed more than 90.83% cell viability for the topical gels, revealing excellent biocompatibility. The outcomes revealed that the topical gels enriched with essential oils (lavender and tea tree) and Ag nanoparticles and sponges incorporated with metronidazole and Ag nanoparticles are potential wound dressing scaffolds that can be employed for the treatment of chronic infected injuries. The *in vitro* wound healing experiments showed that the HaCaT cells cultured with gels co-enriched with lavender oil and Ag nanoparticles possessed a higher rate of closure in comparison to the untreated cells for 96 hours.

University of Fort Hare
Together in Excellence

List of abbreviations and symbols

- ❖ PVP: Poly (Vinyl Pyrrolidone)
- ❖ PEG: Poly (ethylene glycol)
- ❖ PHEMA: poly(hydroxyethyl methacrylate)
- ❖ PCL: poly(ε-caprolactone)

- ❖ PU: Polyurethane
- ❖ PVA: Poly (vinyl Alcohol)
- ❖ PGLA: Poly (lactic-co-glycolic acid)
- ❖ CMC: Carboxymethyl cellulose
- ❖ HA: hyaluronic acid
- ❖ Ag: Silver
- ❖ Cu: Copper
- ❖ Ti: Titanium
- ❖ Zn: Zinc
- ❖ TTO: Tea Tree Oil
- ❖ AMP: Ampicillin
- ❖ STM: Streptomycin
- ❖ NLD: nalidixic acid
- ❖ ROS: Reactive Oxygen Species
- ❖ UV-Vis: Ultraviolet-visible Spectroscopy
- ❖ EDX: Energy-dispersive X-ray
- ❖ SEM: Scanning Electron Microscopy
- ❖ TEM: Transmission Electron Microscopy
- ❖ FTIR: Fourier Transform Infrared Spectroscopy
- ❖ TGA: Thermogravimetric Analysis
- ❖ %: Percentage
- ❖ ºC: Degrees Celsius
- ❖ h: hour
- ❖ min: minutes
- ❖ g: grams
- ❖ μg: microgram
- ❖ mg: milligram

- ❖ mL: millilitre
- ❖ cm: centimetre
- ❖ nm: nanometre
- ❖ cP: centipoise
- ❖ MPa: mega Pascal
- ❖ rpm: revolutions per minute
- ❖ WHO: World Health Organisation
- ❖ NHS: National Health Service
- ❖ US: United States
- ❖ UK: United Kingdoms
- ❖ MIC: Minimum inhibition concentration
- ❖ MRSA: Multi-Resistant *Staphylocucccos Aureus*
- ❖ HDFs: Human Dermal Fibroblasts
- ❖ ECM: Extracellular matrix
- ❖ GFs: Growth Factors
- ❖ DFUs: diabetic foot ulcers
- ❖ CaCl$_2$: Calcium chloride
- ❖ AgNO$_3$: Silver nitrate
- ❖ SLNs: solid lipid nanoparticles
- ❖ NLCs: nanostructured lipid nanocarriers

Table of Contents

List of Tables

List of Figures

List of Schemes

University of Fort Hare

Together in Excellence

CHAPTER 1: INTRODUCTION

1.1. Background

Skin is the most extensive and exposed human organ that functions as a barrier and defensive mechanism against shocks, microbes, and foreign bodies [1][2]. The disruption of a skin's epithelial lining or mucosa induced by thermal or physical damage is called a wound [3]. The factors resulting in wounds include corrosive chemicals, accidents, mechanical injuries (tears, abrasions, or surgical procedures), radiation, diseases, etc. [2]. Wounds are usually categorized into two groups depending on their healing timeline as acute and chronic wounds [4]. Acute wounds are lesions that generally heal in a period that ranges between 2 and 3 months, depending on their extent, size, and depth in the epidermis or dermis layer of skin. Chronic wounds are life-threatening injuries that do not follow a timely and orderly way of wound recovery [5]–[7]. These injuries are characterized by a delayed wound-healing process that needs special clinical attention. The common chronic wounds in patients include decubitus ulcers, infectious wounds, diabetic foot ulcers, leg ulcers, and ischemic wounds [8]. Factors such as malnutrition, smoking, obesity, prolonged bed rest, microbial invasion, and diseases (e.g., cardiovascular diseases, diabetes mellitus, and cancer) can make acute wounds become chronic. Whether acute or chronic, a wound requires appropriate clinical care to accelerate its process of wound healing [9].

Among the clinical strategies that are presently utilized in the arena of wound healing, the wound dressing approach is the most employed one. Numerous kinds of wound dressing scaffolds are commercially available. Despite the wide variety of dressing products, there is no universally effective wound dressing that makes healthcare workers select wound dressing products that are most appropriate for each specific wound type [6]. An ideal wound dressing should possess these properties: excellent antibacterial and antioxidant efficacy, good hemostatic activity, easy sterilization, high porosity and swelling capacity, high water uptake, moderate water vapour transmission rate, ability to promote wound debridement, ability to provide suitable moisture for the wound, offer O_2 and CO_2 gaseous diffusion, ability to be incorporated with drugs, and good biocompatibility [4][10][11]. Furthermore, the wound dressing material must be able to preserve moisture, be soft, and no pyrogen and bad reaction. It must stimulate skin regeneration, accelerate wound healing and decrease scar development [12]. The wound dressing material with these aforementioned properties can significantly result in fast wound recovery. Polymers are materials that are frequently employed for the preparation of wound dressing scaffolds, and they are classified into two categories such as synthetic and

biopolymers (natural polymers) [13]. Natural polymers that are frequently employed in the fabrication of dressing scaffolds include chitosan, alginate, elastin, collagen, dextran, fibrin, elastin, hyaluronic acid, gelatin, and cellulose [13]–[15]. These polymers demonstrate interesting features that make them appropriate in wound care: non-toxicity, good biocompatibility and biodegradability, non-immunogenicity, readily available and cost-effective [13]. Biopolymers commonly suffer from poor mechanical performance, and cross-linking them with synthetic can enhance their mechanical properties.

Some synthetic polymers that are frequently combined with biopolymers for the formulation of the polymer-based hybrid wound dressing scaffolds are poly(ethylene glycol)(PEG)/poly(ethylene oxide)(PEO), poly (lactic-co-glycolic acid) (PLGA), polyvinyl pyrrolidone (PVA), poly(hydroxyethyl methacrylate) (PHEMA), poly(vinyl pyrrolidone), (polyglycolic acid (PGA), poly(ε-caprolactone), polylactide (PLA), and polyurethanes (PUs) [16]–[19]. The polymer-based wound dressings are usually designed for different wound types and healing stages, such as bandages, foams, films, gel, membranes, wafers, patches, and sponges [6]. Most presently developed polymer-based wound dressings suffer from poor biological activities (i.e., antimicrobial and anti-inflammatory or antioxidant efficacy). Incorporating therapeutic agents into the wound dressing materials can significantly improve the biological efficacy of wound dressing scaffolds, especially antibacterial activity.

The loaded bioactive agents are released from the wound dressing scaffolds through the hydrolysate influence of injury enzymes that are found in wound exudates or other biological fluids [20]. Furthermore, various approaches such as diffusion, swelling, and hydrates are utilized to release the therapeutic agents from the wound dressing material into the injury site [21]. Bioactive agents that are usually loaded into the wound dressings include antibiotics (e.g. ciprofloxacin, norfloxacin, metronidazole, ampicillin, and others) [22]–[25], metal-based nanoparticles (e.g. silver and zinc nanoparticles) [26], essential oils (e.g. tea tree oil, lavender oil, lemongrass, cinnamon, and peppermint) [27], and plant extracts (e.g. curcumin, quercetin, and thymol)[21][28]–[33], stem cells, and vitamins.

1.2. Problem Statement

Chronic wounds such as diabetic wounds are life-threatening and usually result in limb or leg amputation. Bacterial invasion of wounds is another significant factor that causes retarded wound healing. The management of these wounds causes negative socio-economic impacts, especially in developed countries. For example, the United States of America (USA) spends approximately USD 20 billion every year on treating chronic injuries, while the United

Kingdom (UK) in 2012 spent around GBP 184 million on chronic wound care [34]. Some of the wound dressing products that are currently used in clinical applications suffer from various shortcomings such as poor mechanical properties, poor antimicrobial efficacy, and do not offer the required moist environment for the quickening of the wound recovery process. There is an urgent need to develop advanced wound dressing scaffolds by biomedical researchers that are affordable and effective for chronic wound management.

1.3. Motivation and Rationale

The combination of biopolymers with synthetic polymers to form polymer-based hybrid wound dressing materials present interesting physicochemical and biological properties. The porous nature of polymer-based sponges can promote high cell migration and proliferation, good gaseous permeation, and high wound exudate absorption resulting in the acceleration of the wound healing mechanism. In the last few decades, the encapsulation of bioactive agents to wound dressing scaffolds has been shown as a potential strategy for managing chronic wounds. The application of therapeutic agents in wound management is effective in the clinical care of non-healing chronic injuries. Furthermore, the loading of antibacterial agents into polymer wound dressings prevents the invasion of bacterial strains to the wound site and is appropriate for managing bacteria-infected wounds.

1.4. Aims and Objectives
1.4.1. Aims

This research project aims to prepare, characterize, and evaluate *in vitro* polymer-based wound dressing scaffolds to manage chronic wounds.

1.4.2. Objectives

1. Polymer-based sponges loaded with Ag nanoparticles and metronidazole were prepared using gelatin and PEG as biopolymer and synthetic polymer, respectively.
2. Characterization of polymer-based sponges using FTIR, SEM/EDX, and TGA, porosity, and biodegradation studies of sponges.
3. Perform *in vitro* antibacterial, cytotoxicity, drug release, and scratch wound healing assays on the polymer-based sponges.
4. Preparation of topical gels loaded with Ag nanoparticles and essential oils (lavender and tea tree) using CMC as biopolymer and poloxamer as a synthetic polymer.

3

5. Characterization of the topical gels using FTIR, pH, viscosity, and spreadability studies.
6. Perform *in vitro* antibacterial studies, drug release, cytotoxicity, and scratch wound healing assays on the topical gels.

References

[1]   Abou-okeil, A.; Fahmy, H.M.; El-Bisi, M. K.; Ahmed-Farid, O. Hyaluronic acid/Na-alginate films as topical bioactive wound dressings. *Eur. Polym. J.* **2018**, 109, 101–109. doi: 10.1016/j.eurpolymj.2018.09.003.

[2]   Borda, L.J.; Macquhae, F.E.; Kirsner, R.S. Wound Dressings: A Comprehensive Review. *Curr. Dermatol. Rep.* **2016**, 5, 287–297. doi: 10.1007/s13671-016-0162-5.

[3]   S. Dhivya, V. V. Padma, and E. Santhini, "Review article Wound dressings – a review," *BioMedicine*, vol. 5, pp. 24–28, 2015, doi: 10.7603/s40.

[4]   Aderibigbe, B. A.; Buyana, B. Alginate in Wound Dressings. *Pharmaceutics* **2018**, 10, 42. doi: 10.3390/pharmaceutics10020042.

[5]   Schreml, S.; Szeimies, R.; Prantl, L.; Karrer, S.; Landthaler, M.; Babilas, P. Oxygen in acute and chronic wound healing. *Br. J. Dermatol.* **2010**, 2, 257-268. doi: 10.1111/j.1365-2133.2010.09804

[6]   Debele T.A.; Su, W. Polysaccharide and protein-based functional wound dressing materials and applications. *Int. J. Polym. Mater. Polym. Biomater.***2020**, 10.1080/00914037.2020.1809403. doi: 10.1080/00914037.2020.1809403.

[7]   Nunan, R.; Harding, K.G.; Martin, P. Clinical challenges of chronic wounds : searching for an optimal animal model to recapitulate their complexity. *Dis. Model. Mech.* **2014**, 7, 1205–1213. doi: 10.1242/dmm.016782.

[8]   Fredric, S.; Gowda, D.V.; Yashashwini, M. Wafers for wound healing. *J. Chem. Pharm. Res.* **2015**, 7, 450–468. ISSN : 0975-7384.

[9]   Alven, S.; Nqoro, X.; Aderibigbe, B.A. Polymer-Based Materials Loaded with Curcumin for Wound Healing Application. *Polymers (Basel).***2020**, 12, 2286. doi:10.3390/polym12102286.

[10]   Alven, S.; Aderibigbe, B.A. Chitosan and Cellulose-Based Hydrogels for Wound Management. *Int. J. Mol. Sci.* **2020**, 21, 9656. doi:10.3390/ijms21249656.

[11]   Li, S.; Li, L.; Guo, C.; Qin, H.; Yu, X. A promising wound dressing material with excellent cytocompatibility and proangiogenesis action for wound healing: Strontium loaded Silk fibroin/Sodium alginate (SF/SA) blend films. *Int. J. Biol. Macromol.* **2017**, 104, 969–978. doi: 10.1016/j.ijbiomac.2017.07.020

[12]   Deng, C.; He, L.; Zhao, M.; Yang, D.; Liu, Y. Biological properties of the chitosan-gelatin sponge wound dressing. *Carbohydr. Polym.* **2007**, 69, 583–589. doi: 10.1016/j.carbpol.2007.01.014.

[13]   Hussain, Z.; Thu, H.E.; Shuid, A.N.; Katas, H.; Hussain, F. Recent Advances in Polymer-based Wound Dressings for the Treatment of Diabetic Foot Ulcer: An Overview of State-of-the-art. *Curr. Drug Targets* **2017**, 19, 527–550. doi: 10.2174/1389450118666170704132523.

[14]   Ye, S.; Jiang, L.; Su, C.; Zhu, Z.; Wen, Y.; Shao, W. Development of gelatin/bacterial cellulose composite sponges as potential natural wound dressings. *Int. J. Biol. Macromol.* **2019**, 133, 148–155. doi: 10.1016/j.ijbiomac.2019.04.095.

[15]   Pei, Y.; Ye, D.; Zhao, Q.; Wang, X.; Zhang, C.; Huang, W.; Zhang, N.; Liu, S.; Zhang, L. Effectively promoting wound healing with cellulose/gelatin sponges constructed

directly from a cellulose solution†.*J. Mater. Chem. B* **2015**, 3,7518. doi: 10.1039/c5tb00477b.

[16] Fang, Y.; Zhu, X.; Wang, N.; Zhang, X.; Yang, D.; Nie, J.; Ma, G. Biodegradable core-shell electrospun nanofibers based on PLA and -PGA for wound healing. *Eur. Polym. J.* **2019**, 116, 30–37. doi:10.1016/j.eurpolymj.2019.03.050

[17] Shi, R.; Geng, H.; Gong, M.; Ye, J.; Wu, C.; Hu, X.; Zhang, L. Long-acting broad-spectrum antimicrobial electrospun poly (e-caprolactone)/gelatin micro/nanofibers for wound dressing. *J. Colloid Interface Sci.* **2018**, 509, 275–284. doi: 10.1016/j.jcis.2017.08.092

[18] Poonguzhali, R.; Basha, S.K.; Kumari, V. S. Synthesis and characterization of chitosan-PVP-nanocellulose composites for in-vitro wound dressing application. *Int. J. Biol. Macromol.* **2017**, 105, 111–120. doi: 10.1016/j.ijbiomac.2017.07.006.

[19] Choi, Y.S.; Lee, S.B.; Hong, S.R.; Lee, Y.M.; Song, K.W.; Park, M.H. Studies on gelatin-based sponges . Part III : A comparative study of cross-linked gelatin/alginate, gelatin / hyaluronate and chitosan / hyaluronate sponges and their application as a wound dressing in full-thickness skin defect of rat. *J. Mater. Sci. Mater. Med.* **2001**, 2, 67–73.

[20] Boateng, J.; Catanzano, O. Advanced Therapeutic Dressings for Effective Wound Healing - A Review. *J. Pharm. Sci.* **2015**, 104, 3653–3680. doi: 10.1002/jps.24610.

[21] Dias, A.M.A.; Braga, M.E.M.; Seabra, I.J.; Ferreira, P.; Gil, M.H.; De Sousa, H.C. Development of natural-based wound dressings impregnated with bioactive compounds and using supercritical carbon dioxide. *Int. J. Pharm.* **2011**, 408, 9–19. doi: 10.1016/j.ijpharm.2011.01.063.

[22] Negut, I.; Grumezescu, V.; Grumezescu, A. M. Treatment Strategies for Infected Wounds. *Molecules* **2018**, 23, 392. doi: 10.3390/molecules23092392.

[23] Simões, D.; Miguel, S.P.; Ribeiro, M.P.; Coutinho, P.; Mendonça, A.G.; Correia, I.J. Recent advances on antimicrobial wound dressing: A review. *Eur. J. Pharm. Biopharm.* **2018**, 127, 130–141.

[24] Shi, R.; Niu, Y.; Gong, M.; Ye, J.; Tian, W.; Zhang, L. Antimicrobial gelatin-based elastomer nanocomposite membrane loaded with ciprofloxacin and polymyxin B sulfate in halloysite nanotubes for wound dressing. *Mater. Sci. Eng. C* **2018**, 87, 128–138. doi: 10.1016/j.msec.2018.02.025.

[25] Ahmed, A.; Getti, G.; Boateng, J. Ciprofloxacin-loaded calcium alginate wafers prepared by freeze-drying technique for potential healing of chronic diabetic foot ulcers. *Drug Deliv. Transl. Res.* **2018**, 8, 1751–1768. doi: 10.1007/s13346-017-0445-9.

[26] Rajendran, N.K.; Kumar, S.S.D.; Houreld, N.N.; Abrahamse, H. A review on nanoparticle based treatment for wound healing. *J. Drug Deliv. Sci. Technol.* **2018**, 44, 421–430. doi: 10.1016/j.jddst.2018.01.009.

[27] Liakos, I.; Rizzello, L.; Hajiali, H.; Brunetti, V.; Carzino, R.; Pompa, P.P.; Athanassiou, A.; Mele, E. Fibrous wound dressings encapsulating essential oils as natural antimicrobial agents. *J. Mater. Chem. B* 2015, 3, 1583, 2015, doi: 10.1039/c4tb01974a.

[28] Bajpai, S. K.; Ahuja, S.; Chand, N.; Bajpai, M. Nano cellulose dispersed chitosan film with Ag NPs / Curcumin : An in vivo study on Albino Rats for wound dressing. *Int. J. Biol. Macromol.* **2017**, 104, 1012–1019. doi: 10.1016/j.ijbiomac.2017.06.096.

[29] Rramaswamy, R.; Mani, G.; Venkatachalam, S.; Venkata, R.Y.; Lavanya, J.S.; Choi, E. Tetrahydro curcumin loaded PCL-PEG electrospun transdermal nano fi ber patch : Preparation, characterization, and in vitro diffusion evaluations. *J. Drug Deliv. Sci. Technol.* **2018**, 44, 342–348. doi: 10.1016/j.jddst.2018.01.016.

[30] Nguyen, M.; Lee, S.E.; Tran, T.; Bui, C.; Nguyen, T.; Vu, N.; Tran, T.T.; Nguyen, T.-P.-T.; Nguyen, T.-T.; Hadinito, K. A simple strategy to enhance the in vivo wound-healing activity of curcumin in the form of self-assembled nanoparticle complex of curcumin and oligochitosan. *Mater. Sci. Eng. C* 2018, 98, 54–64. doi: 10.1016/j.msec.2018.12.091.

[31] Zahiri, M.; Khanmohammadi, M.; Goodarzi, A.; Ababzadeh, S.; Farahani, M.S.; Mohandesnezhad, S.; Bahrami, N.; Nabipour, I.; Ai, J. Encapsulation of curcumin loaded chitosan nanoparticle within poly (e -caprolactone) and gelatin fiber mat for wound healing and layered dermal reconstitution. *Int. J. Biol. Macromol.* **2019**, 153, 1241–1250. doi: 10.1016/j.ijbiomac.2019.10.255.

[32] Saeed, S.M.; Mojgan, M.; Jalal, Z.; Jalal, B. Designing and fabrication of curcumin loaded PCL / PVA multi- layer nanofibrous electrospun structures as active wound dressing. *Prog. Biomater.* **2017**, 6, 39–48. doi: 10.1007/s40204-017-0062-1.

[33] Shefa, A.A.; Sultana, T.; Park, M.K.; Lee, Y.S.; Gwon, J.; Lee, B. Curcumin incorporation into an oxidized cellulose nanofiber-polyvinyl alcohol hydrogel system promotes wound healing. *Mater. Des.* **2020**, 186, 108313.doi: 10.1016/j.matdes.2019.108313.

[34] Aderibigbe, B.A.; Buyana, B. Alginate in Wound Dressings. *Pharmaceutics* **2018**, 10, 42. doi:10.3390/pharmaceutics10020042.

CHAPTER 2: LITERATURE REVIEW

2.1. Structure and Functions of the Human Skin

Understanding the structure and functions of human skin is very important in the treatment of wounds. The human skin contributes to approximately 15% of the entire body weight and has a higher surface area of around 1.5-2 m^2, making it the most significant human body organ [1]–[3]. The skin is a biological barrier that protects the body from destructive environmental effects and controls the hydration conditions of the body [3]–[5]. Furthermore, the skin also plays a crucial role in excretion, perception, absorption, immunity, and metabolism [6]. The structural integrity of the human skin is also very important for maintaining physiological roles. The human skin is comprised of two major layers, the epidermis and dermis, that are positioned over the subcutaneous tissue as the third layer contains abundant fats (**Figure 1**). The epidermis is the outermost layer of the human skin. The main cell of the epidermis is the keratinocyte which comprises over 95% of this skin layer. Merkel cells, Langerhans, and melanocytes only contribute to the remaining 5% [7].
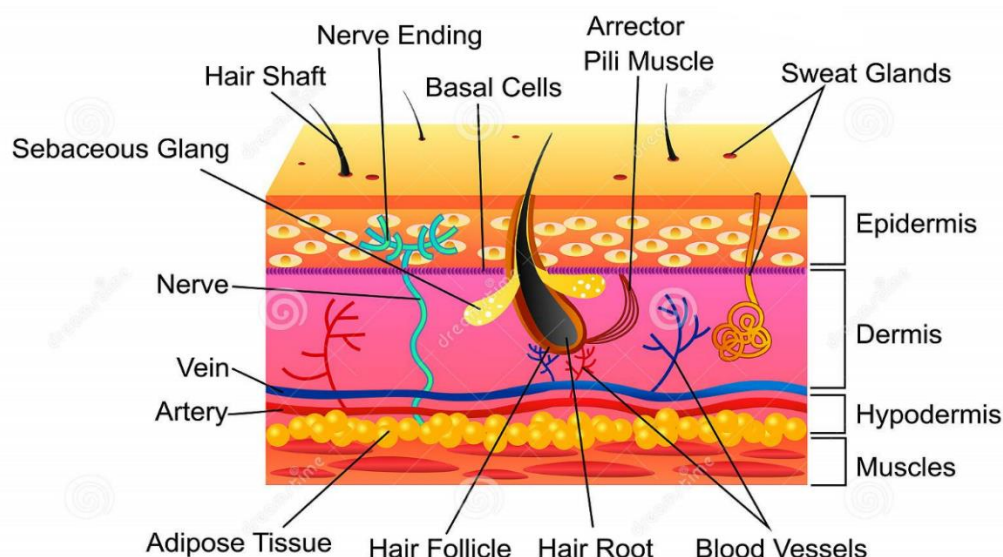
Figure 1: The structure of human skin

The epidermis is made up of four essential layers depending on the state of differentiation of keratinocytes. The first layer of the epidermis is named the basal layer or stratum basale, which is the inner layer and is made up of a single layer of keratinocytes. Keratinocytes grow and cause daughter cells to terminate differentiation, leading to the development of the stratum corneum [8]. The second layer of the epidermis, known as the stratum spinosum, comprises melanocytes, which are dendritic cells obtained from the neural crest. Melanocytes produce melanin, which is found in subcellular organelles (melanosomes) and then carried to the adjacent basal keratinocytes. Each melanocyte provides melanin to about 30-40 neighbouring keratinocytes.

The surface pH of human skin ranges between 4.3 and 5.3, which is lower in individuals with darker skin due to the acidic conditions of melanin by-products [9]. The third layer known as stratum granulosum comprises brick-like shape keratinocytes supplied by a cytoskeleton and composed of intermediate filaments of keratin. The keratinocytes turn compacted as the epidermis differentiates, due to the action of filaggrin, a protein constituent of keratohyalin granules, on the keratin filaments. Filaggrin and keratin make up 80 to 90% of the epidermis mass. The last layer of the epidermis is called the stratum corneum and is the outermost layer. The cells in this layer are called corneocytes and do not have cytoplasmic and nuclei organelles. The corneocyte plasma membranes carry very insoluble cornified envelopes produced by the cross-linking of precursors of soluble protein, including loricrin and involucrin [10]. If present, the fifth layer just before the stratum corneum is called stratum lucidum and is a thin clear layer comprising eleidin (transformation product of keratohyalin); it normally appears in thick skin only [10].

The dermis is the second layer of the human skin, and it is divided from the epidermis by the cutaneous basement membrane zone [11]. The dermis thickness is about 0.5-5 mm depending on the human body's location. For example, a thin dermis is obtained around the eyelid while a thick dermis is found on the back. This layer is divided into two major parts: papillary dermis (it is in interaction with the cutaneous basement membrane zone and is richly provided with sensory nerve terminations and blood vessels) and reticular dermis (it is the main portion of the dermis that is attached to the subcutis) [12]. The dermis is made up of interstitial (ground substance, collagen fibres, elastic tissue) and cellular components (fibroblast, mast cell, histiocyte, lymphocytes, plasma cell, dermal dendritic cell). It is also composed of lymphatic channels, sensory nerves (free nerve endings, end-corpuscles), and blood vessels (superficial and deep Plexi) [13]. Approximately 70% of the dermis dry weight is composed of collagens,

mainly types I and III. Elastic fibres are less tough when compared to collagen fibres but impart extendable features to the skin, contribute about 5% of the dermis dry weight and are composed of elastic and elastin microfibrils [14]. Elastic and collagen fibres are deposited by fibroblast cells [15]. Several subpopulations of fibroblasts differentially contribute to skin wound healing, skin homeostasis, scarring, and hair follicle formation. Lastly, the dermis also contains histiocytes, antigen-presenting cells that play a vital role in degrading foreign matters and providing antigens to T cells [16].

The third layer of the human skin is the subcutis, also called hypodermis, the innermost layer and mainly made up of lipocytes. These cells are organized into fat lobules that are divided from each other by fibrous septae. Packs of fibres mainly produced by the skin dermis and extending into the subcutis layer support the connection between these two sections. Almost 80% of all body fat is situated in the subcutis in non-obese people. Fat also possesses an endocrine role, producing hormones (e.g., leptin) that regulate appetite and control metabolic energy [17]. The human skin is normally subjected to different degrees of wounds due to its main function as a physical barrier against environmental surroundings. In healthy people, skin injuries less than 1 mm deep are usually able to restore spontaneously via a wound healing process that involves four consecutive phases: hemostasis phase, inflammation phase, proliferation phase, and maturation phase [18]. Nevertheless, an injury that extends into the deeper dermis is prolonged to heal with slow wound closure and scarring, normally causing lasting damage to skin appearance, structure, and role. Injuries in the skin with underlying physiological conditions (such as diabetes or vasculopathy) often fail to recover, leading to chronic wounds. Chronic injuries can result in serious systemic infections, and injuries that are not instantly life-threatening can cause significant undesirable effects on one's quality of life [18].

2.2. Chronic Wounds and Their Negative Socio-Economic Impacts

It has been reported that over 1-2% world population in developed countries suffers from chronic wounds [19]. Although there are many current advances in wound care, about 50% of chronic wounds still fail to recover [20]. In the US, chronic injuries affect about 5.7 million people, and about 20 billion dollars are spent yearly on wound treatment [21]. These wounds are characterized by slow rate of healing and fail to accomplish full re-epithelization in a suitable sequential manner of skin tissue recovery. In clinical practice, the chronic injury mode of healing is different from acute injury healing. Chronic wounds could take many years to fully heal in contrast some of them do not heal, causing pain, releasing excess exudates,

decreased mobility, social isolation, sleep disorders, mephitis, emotional stress, anxiety, and even depression [22]. Chronic wounds are characterized by high inflammatory cells, proteases, low mitogenic response, and senescent. Several factors can lead to the delayed wound healing process for chronic wounds, including underlying infection, necrotic tissue, poor blood supply, high levels of matrix metalloproteinases, neoplasia, and persistent trauma. Other factors include cold temperature, malnutrition, hormonal deficiency, and Zn shortage. The inflammation phase of the wound healing process is retarded by these factors through consistently recruiting neutrophils and macrophages in the injury area. The extended inflammatory phase is accompanied with the constant disruption of eosinophil cationic protein (ECP), impeding the mechanism of wound recovery [23].

2.2.1. Diabetic wounds

Diabetes is a metabolic condition resulting from elevated blood sugar levels (hyperglycemia) over a prolonged period caused by a relative lack of insulin or resistance to this vital hormone [24]–[26]. This disorder affects more than 422 million people around the world, including approximately 9.3% (29.1 million people) of the US population [27]. A major obstacle in people with diabetes is delayed or poor recovery of wounds; subsequently non-healing chronic wounds are one of the major difficulties related to diabetes. They are predicted to happen in 15% of patients with diabetes and result in more than 27% of the annual $176 billion in diabetic health care expenses in the US [27][28]. Among the classes of diabetic wounds, a predominantly significant and challenging category are diabetic foot ulcers (DFUs) [29]. Annual incidence rates of DFUs are predicted to be 6.3% in diabetic people worldwide. DFUs result in 20% of all diabetic hospital admissions in the US and contribute to at least 60% of lower-limb amputations yearly, with only a 40% 5-year survival rate post-amputation [24][27][30]. The costs and negative impacts of chronic diabetic wounds are anticipated to increase sharply, encouraging the urgent need for novel advanced wound dressing materials [27].

Investigational and clinical facts have demonstrated that the recovery of diabetic injuries and other correlated chronic wounds does not follow the ordinary phases of wound healing as acute injuries. Retarded wound-healing process in diabetes is caused by the combination of factors that stimulate inflammation and interrupt epithelialization and wound closure [31]. Three main factors disturb the wound-healing process in diabetic injuries: vasculopathy, neuropathy, and infections [32]. In vasculopathy, the distal arteries are incapable of delivering nutrients and oxygen efficiently to the injury environment, and this causes the wound healing process to be

delayed. In neuropathy: sensory, motor and autonomic fibres are all damaged in diabetic patients, so these sensory shortages in diabetes fail to sense external stimuli such as injuries, pressure, and heat [32][33]. Therefore, the process of wound healing can be slower than the normal wound healing process. The absence of pain with the irregular vasodilator autoregulation also results in pathogenesis that further decreases the rate of wound closure and reduces the ability to notice pressure. Therefore, neuropathy plays a significant role in the formation of bacterial load and infection in injured tissues [32]. The third factor (infection) is discussed below in the infected wounds subsection.

2.2.2. Chronic Ulcers

Except for DFUs, some ulcers are also considered chronic wounds because of their non-healing behaviours. The most recognized chronic ulcers are venous and pressure ulcers [34]. There were 2.2 million adult patients (about 4.5% of the adult people) treated by the National Health Service (NHS) of the UK between 2012 and 2013 with injuries at the cost of about £4.5 to £5.0 billion per annum [35]. Over 1 million of these patients were confirmed to be suffering from diabetic, venous, and pressure ulcers, with the wound care of 731 thousand chronic ulcers costing approximately £1.94 billion [35]. Venous ulcers are a predominant and reoccurring type of complex injury, leading to a significant public healthcare problem with serious economic and social issues [36]. The risk factors that contribute to chronic venous ulcers include underlying diseases related to poor venous return (including obesity and congestive heart failure) and primary disruption of the venous system (including recreational injected drug use, prior deep venous thrombosis, venous valvular dysfunction, and phlebitis) [37]–[39]. Both surgical and medical therapies are used to treat venous ulcers although no effective cure is yet available [40]. Venous ulcers affect 1% of the world's population, with the incidence increasing to more than 4% in older people. This class of chronic wounds are characterized by severe discomfort, pain, and social isolation or embarrassment and is the cause of poor quality of life in people with congestive cardiac failure [41]. As the ageing population is intensely increasing in size, chronic venous ulcers will result in a heavy burden on patient morbidity and health care expenses. Treatment of patients that suffer from venous ulcers costs the US more than $2.5 billion yearly, and the annual estimated cost in the UK ranges between £300 and £600 million [42]. The overall expenses are alike in most western countries, expending about 1% of their total health care finances, further affecting the emotional costs to patients and highlighting the necessity for improved wound therapeutics [43][44].

On the other hand, pressure ulcers, also called pressure wounds, are localized injuries to the human skin and underlying tissue resulting from pressure or pressure combined with shear [45]. Pressure ulcers involve disrupting the skin's soft tissues, including dermal, epithelial, and subcutaneous tissues (such as muscle or fat). These chronic ulcers are caused by extended mechanical deformation of soft tissues between internal stiff anatomical structures (tendon, cartilages, bones) and external stiff support surfaces (e.g., seats or mattresses), or contact with medical devices [46]. The first pressure ulcer cases were documented thousands of years ago, yet they still often happen in all age groups and settings. Due to pressure ulcers being predominantly related to chronic illness, care dependency, and advanced age, the incidence and burden of these chronic ulcers are particularly high in long-term care and intensive settings [47]. Recent epidemiologic information concerning pressure ulcers in the US is limited, but their incidences have been estimated to be 1 to 3 million annually [48]. The reported prevalence rates in hospitalized patients vary significantly, affecting approximately 5% to 15% of patients overall but affecting constantly higher percentages of patients in intensive care units [49][50]. The cost of Hospital-acquired pressure ulcers only is more than $11 billion per annum [49][51]. The typical cost of a hospital stay for patients with pressure ulcers is around $72,000, while for those without pressure ulcers are about $32,000 [52]. A study conducted in the UK has demonstrated that the average individual cost of pressure ulcer management is around $1500 for stage 1 while it is about $18,000 for stage 4 ulcers [49].
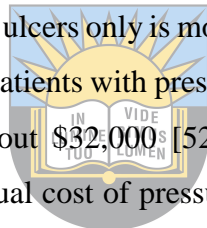
2.2.3. Burn Wounds

Severe burn wounds are the most physically devastating traumatic wounds that affect almost every organ system and result in a high mortality rate worldwide [53]. These wounds are considered the most life-threatening type of wounds that has troubled humankind since the days of yore with fatal well-being outcomes. There were approximately 11 million people around the world that received medical assistance for burn wounds in 2004, with a reported incidence of about 265,000 deaths from burns yearly described more lately (normally determined in in-patient hospital sectors) [54][55]. In 2014, about 400,000 burn/fire wounds were reported in the USA in a population of approximately 300 million, including 0.78% mortality (3196 deaths) [56]. According to WHO statistics, about 1 million people in India get moderately or severely affected yearly by burn injuries. It happens in various age groups, and severity may probably differ from extremely minor (no specific treatment needed) to extremely severe (intensive treatment needed) [57]. Burn injuries require important attention as a large number of cases of these injuries happen daily, particularly in war regions. Burn injuries have

been demonstrated to be capable of having difficult consequences both cosmetically and functionally, fascinating the need for enhanced and more effective therapeutics [58].

Etiologically, burn injuries are categorized as burnt by fire (overheated corroded air), low voltage current (less than 200 mV) (power transmission of electrical movement through fabrics) and high voltage current (greater than 1000 mV), chemical (antacids or acids), burning by hot liquids or by touching hot solids. These injuries can also be classified into three classes based on their depth: first-degree (those that only occur in the skin epidermis); second-degree (occur both on the epidermis and papillary/ reticular dermis), and third-degree (occur in all layers of the skin and muscles) [59]. Patients with severe burn injuries do not only suffer from psychological and physical distress from the wound itself, but they also have to cope with everyday painful experiences from therapeutic procedures such as wound care or physical therapy, i.e., debridement, washing, removal of wound dressing materials, and application of fresh wound dressings [60][61]. The pain from burn wounds has been established as being highest during therapeutic methods, and wound debridement might be more painful than the burn wound itself [60][62].

2.2.4. Infected Wounds

Infections are the leading cause of the delayed process of wound healing of chronic wounds (diabetic wounds, burn injuries, etc.). For example, for patients with burn wounds, it is estimated that 75% of mortality is associated with infections [63]. Bacterial infections represent a serious cause of chronic wounds, using various modes to hinder innate inflammatory pathways, and they can result in drug resistance against traditional therapeutics [64][65]. Infections are an important cause of morbidity in chronic wound patients with several consequences such as delayed healing, hospitalization, and amputation. Conditions such as osteomyelitis, cellulitis, and abscesses need instant medical attention [66]. Wound infections cause trauma in patients and lead to financial burdens in the healthcare system. For instance, patients with postoperative surgery are usually infected in a surgical position. The severity of the burden has become serious because of the increased incidence of infections related to multidrug-resistant (MDR) bacteria. The WHO reported that more than 2 million infections are caused by MDR bacteria, with indirect and direct costs surpassing USD 55 billion yearly [67]. These microbial infections can quickly occur in diabetic injuries and ulcers. A higher load of bacteria without the characteristics associated with infection is also unfavourable in recovering ulcers and injuries. Consistent hypoxia at the injury bed is treated as a very harmful condition as it exaggerates physiological related actions and may lead to reperfusion of the wound by

generating oxygen radicals. Furthermore, Clinicians that are responsible for the treatment of infected chronic injuries must have the ability to distinguish between injury contamination, colonization, and infection [67].

Injury contamination: All chronic injuries are considered contaminated. The contaminants resulted from the surrounding environment and/or the indigenous microbiota [68]. Wound colonization is explained by multiplying bacteria in the injury site without a response from the host, and this process is prevalent. The microorganisms that commonly cause wound colonization are ordinary skin microbiota such as *Staphylococcus epidermis*, other coagulase-negative Staphylococcus *Corynebacterium sp.*, *Proprionibacterium acnes*, *Pityrosporum sp.*, *Brevibacterium sp*. [68]. At the wound infection point, bacteria's proliferation occurs not only on the injury surface but also into the deeper tissue on the periphery of the injury, provoking a host reaction. Microbial pathogens that are commonly found in the infected wound include *Staphylococcus aureus* (*S. aureus*), *Escherichia coli* (*E. coli*), *Klebsiella pneumoniae (K. pneumoniae)*, *Proteus*, Beta-hemolytic *Streptococcus* (*Streptococcus agalactiae*, *Streptococcus pyogenes*), *Pseudomonas, Stenotrophomonas* (*Xanthomonas*), *Acinetobacter* [68][69]. It has been demonstrated that ordinary skin microbiota is predominant in primary acute injury. Beta-hemolytic *Streptococcus* and *S. aureus* quickly follow. These are common microorganisms occurred in DFUs [68]. Long-term chronic wounds usually comprise more anaerobes bacteria in comparison with aerobes bacteria. For instance, *Stenotrophomonas* (*Xanthomonas*), *Pseudomonas*, and *Acinetobacter* are frequently found in chronic wounds [68]. The increase in morbidity and mortality rate in infected wound cases is that the currently used antimicrobial therapeutic suffer from multi-drug resistance, especially for *P. aeruginosa* [70].

2.3. Phases of Wound healing Process

The study and understanding of the process of wound healing are very important, especially in the management of chronic wounds. The mechanism of wound recovery is explained as a significant complex mechanism that results in restoring the anatomical and physiological structure of the injured skin tissue [71]. This process involves the association of several cells, extracellular matrix (ECM) components, growth factors (GFs), and proteinases [72]. The wound healing process comprises four consecutive phases that normally overlap: the hemostasis phase, inflammation phase, proliferation phase, and maturation (remodelling) phase

(**figure 2**) [73]. These wound-healing phases are normally used to identify what kind of wound dressing is needed for wound treatment.
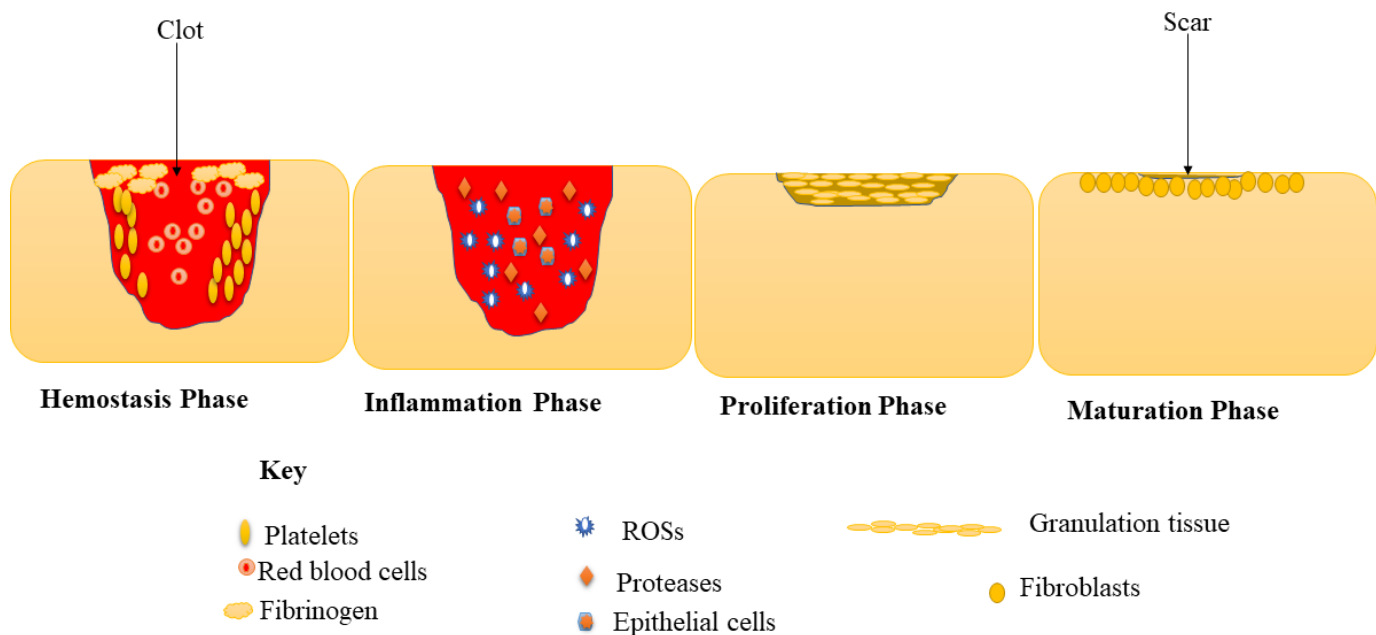
Figure 2: Consecutive phases of the wound healing process

2.3.1. Haemostasis Phase

The hemostasis phase is the initial step of the wound recovery mechanism. It happens instantly and rapidly after the wound; it results in coagulation of the blood and wound exudate to stop bleeding [74]. This phase happens in three phases: vasoconstriction, primary, and secondary hemostasis. The significant cells involved in this phase are platelets, whereby the important matrix component is fibrinogen [75]. When the skin tissue is disrupted, the instant reaction to terminate bleeding is called vasoconstriction. During vasoconstriction, vessels quickly constrict to decrease bleeding from burst microvasculature. This is accomplished by automatic vascular smooth muscle contracture and is activated by vasoconstrictors such as endothelin, released from the disrupted endothelium [76]. Vasoconstriction is followed by primary and secondary hemostasis that happens in two simultaneous and mechanistically entangled ways. Primary hemostasis involves platelet accumulation and the development of platelet plugs provoked by collagen exposure [77]. Secondary hemostasis is based on the stimulation of the blood-clotting cascade whereby soluble fibrinogen is transformed into insoluble components that produce the fibrin network. The fibrin mesh and the platelet plug combine to make up the thrombus, which terminates blood bleeding, releases growth factors and complements and

offers a temporary material for penetrating cells which is crucial for wound healing within the subendothelial matrix [77].

2.3.2. Inflammation Phase

The inflammatory phase typically occurs at the same time or nearly after the hemostasis phase and involves the release of ROS, proteases, and neutrophils that are responsible for the protection of the wound from bacterial infections and the removal of debris to offer an appropriate condition for the fast wound healing process [78]. The signal for the recruitment of proteases, neutrophils, and other inflammatory cells is caused by lipid mediators, damage-associated molecular patterns (DAMPs), and chemokines that are released by injured skin cells. Several research experiments have demonstrated that the fast production of hydrogen peroxide (H_2O_2), one of the ROS, can significantly result in reduced wound infections, recruits neutrophils from the promyelocytes in the bone marrow, stimulate keratinocyte regeneration, and promotes new vessel development [79]. The neutrophils make up about 50% of all cells in the damaged skin after the day of the injury. Stimulated neutrophils possess the ability to release factors to amplify and prolong extra infiltration of neutrophils. Neutrophils disrupt infectious threats by constructing an oxidative burst, releasing toxic granules, creating neutrophil extracellular traps (NETs), and starting phagocytosis [77].

Proteases contain the central part of all the poisonous granules. They are also very vital for both antimicrobial efficacy and disruption of the ECM and basement membrane, permitting neutrophils to come out from the blood vessels and enter the damaged tissue. The key serine proteases are protease 3, elastase, and cathepsin G, and they are found in the azurophilic granules and break down laminin, fibronectin, elastin, collagen IV, and vitronectin. These proteases are also responsible for the activation matrix metalloproteinases (MMPs) and hinder protease inhibitors aggravating the proteolytic feedback [80]. Furthermore, other cells called exudate leucocytes that are involved in this wound healing phase are responsible for the soreness and redness of the wound and sometimes erythema, swelling, and warmth of the wound. The epithelial cells migrate to the wound bed to substitute disrupted cells. The time of the hemostasis, together with the inflammatory phase, depends on the severity of the wound [81]. Although the above inflammatory cells are vital in wound healing, their prolonged activity that can result from continuous microbial invasion may be life-threatening in many patients by disrupting normal skin cells (e.g., fibroblasts, keratocytes) and end up slowing the wound healing mechanism [82].

2.3.3. Proliferation Phase

The proliferation stage of the wound recovery process involves the simultaneous formation of granulation tissue or connective tissue with other progressions of wound healing, including immunomodulation, re-epithelialization, and neovascularization. Granulation tissue is largely produced by stimulated fibroblasts, which make new ECM and assist wound contraction [83]. It also aids as a scaffold for other components and cells such as new blood vessels, newly formed ECM, and inflammatory cells. Granulation tissue is substituted by ordinary connective tissue in the last phase (maturation/remodelling) of the wound healing process. Neovascularization, the formation of new blood vessels, is vital for effective injury recovery. It also plays an essential role in the nutrient distribution and maintaining oxygen homeostasis, promoting tissue regeneration and cellular proliferation [83]. Endothelial cells line the inner blood vessel surface and are the key cell type responsible for the formation of new vessels. Endothelial cell activation needs GFs from adjoining cells, proteolytic enzyme production that permits the invasion of endothelial cells within the fibronectin/fibrin-rich clot, endothelial cell interactions with adjoining perivascular cells, and intracellular endothelial cell response to hypoxia. Endothelial cells are also responsible for angiogenesis, where in response to pro-angiogenic signals such as fibroblast growth factor (FGF), vascular endothelial growth factor (VEGF), transforming growth factor β (TGF-β), platelet-derived growth factor B (PDGF-B), and angiopoietins, they migrate and proliferate [84].

2.3.4. Maturation or Remodelling Phase

The maturation phase is the last stage of wound healing, also named the remodelling phase. The ECM component named collagen is remodelled by crosslinking to decrease the scar thickness with full injury contraction. Apoptosis takes place at the maturation phase, whereby the cells that take part in the wound recovery but are no longer beneficial are eliminated. This is a very fragile phase, and an injury failure to reach this phase makes the wound chronic. This wound-healing phase can continue for some months or even years. Skin cells named fibroblasts play a very important role in the maturation phase by affecting epidermal-dermal interactions during wound healing, stimulating Wnt/β-catenin for the development of hair follicles, resulting in anatomical heterogeneity displaying different forms of gene expression when separated from various positions, and synthesizing a huge quantity of ECM that can contribute to scarring [77].

2.4. Trends in Wound Treatment

It is vital to take proper care of the wound, whether an acute or chronic injury to avoid a retarded process of wound healing that may result from microbial infections and other harmful factors; this procedure typically includes the application of wound dressings. Wound dressing materials are formulated to be in interaction with the injury, making them different from the bandages that just hold the wound dressing in position. Previously, wet-to-dry wound dressings were employed widely to provide debridement in injuries. The linen strips saturated in grease or oil enclosed with plasters were utilized to treat injuries in 1600 BC. Mesopotamians utilized clay tablets to cure injuries during 2500 BC. They used to clean injuries with water or milk before treating them with honey and resin. The ancient Greece Hippocrates employed vinegar or wine to rinse lesions during 460-370 BC. In the 19th century, there was a great discovery in the antiseptic procedure whereby antibiotics were presented to control microbial infections and reduce morbidity. Then the innovation of modern wound dressing materials occurred during the 20th century [85].

Subsequently, in the late 20th century, the formulation of occlusive wound dressing materials was useful in providing protection and moisture to the injury. These wound dressing materials assist in collagen synthesis, quicker re-epithelialization, stimulate angiogenesis by generating hypoxia to the lesion site and reduce the pH of the injury bed, resulting in decreased wound infection. In the 1890s, the greatly employed dressing was woven absorbent cotton gauze [86]. Until the mid-1900s, injuries were believed to recover faster in dry and exposed conditions, but it was discovered in 1615 BC that closed wounds healed more rapidly than open wounds. Oscar Gilje defined the moist chamber effect for recovering ulcers in 1948. During the 1980s, the foremost modern wound dressing was developed, which was characterized by significant features, absorbing fluids and moisture (e.g., iodine-containing gels, polyurethane foams, hydrocolloids). In the middle of the 1990s, synthetic wound dressing materials extended into different formulations such as hydrocolloids, vapour-permeable adhesive films, hydrogels, synthetic foam dressing, alginates, tissue adhesives, silicone meshes, and collagen/silver-containing wound dressing [87].

Currently, wound dressing materials are anticipated to cover the injury and quicken the wound healing mechanism. A wound dressing material is chosen based on the depth, extent, type, and position of the injury, infection, wound adhesion, and the quantity of discharge. Although over 300 kinds of wound dressing products are commercially accessible, not even one dressing is suitable for managing all kinds of wounds [88]. Wound dressing scaffolds are crucial in wound

19

treatment, especially in clinical practice. Several properties that ideal wound dressings must be displayed include high water-absorbing capacity, high porosity, non-toxicity, possess mechanical protection, excellent gaseous permeation, good water vapour transmission rate, decreased surface necrosis of wound, protection of injury from microorganisms and infections, relieve the wound pain, cost-effective, eliminate excess exudates, easily removed and changed, and ability to sustain moisture at the wound site to accelerate the process of wound recovery [89].

2.5. Classification of Wound Dressing Materials

Although several ways are used to classify wound dressings, they are often categorized as traditional (passive) dressings, modern wound dressings that include bioactive dressings, and tissue-engineered skin substitutes.

2.5.1. Traditional Dressings

Traditional wound dressings (inert or passive dressings) are wound dressing materials used to protect wounds from foreign substances or contaminations. These wound dressing materials terminate excessive bleeding, absorb exudates, cushion the injury, and cover the wound. Traditional wound dressing products include bandages (synthetic or natural), gauze, cotton wool, plasters, and lint [90]. Gauze wound dressings formulated from rayon, woven or non-woven fibres of polyesters, and cotton present some defence for injury against infections caused by bacteria. Certain antiseptic gauze pads are utilized for absorbing wound fluids and exudates in open injuries with the aid of fibres in these wound dressings. The common limitation of gauze and other traditional dressings is that they require frequent changing during their application which can cause more skin damage. Also, excessive wound drainage can result in dressings being moistened and adherent to the injury, causing pain during removal [91].

 Xeroform™ (non-occlusive wound dressing product) is petrolatum gauze with 3% Bismuth tribromophenate employed to manage minor and non-exudating injuries. The bandages formulated from natural wool and synthetic bandages prepared from polyamide materials demonstrate diverse benefits. For example, cotton bandages are regularly utilized for high compression bandages, short-stretch compression bandages and retention of light dressings offer continuous compression in venous ulcers. Other examples of traditional wound dressings are tulle dressings (e.g., Jelonet, Paratulle, and Bactigras) that are available at the market; and are preferred for superficial clean wounds. Usually, traditional wound dressings are designated for dry and clean injuries with slight wound exudate levels or employed as secondary wound

dressings. Since traditional wound dressings cannot offer moisture to the lesion bed, they have been substituted by modern wound dressings that demonstrate more interesting properties [92].

2.5.2. Mordern Wound Dressings

Modern wound dressing materials have been formulated to improve the wound-healing process of the injury instead of just covering it. These wound dressings are developed to offer a moist environment and suitable water vapour transmission rate (WVTR) that stimulate the process of wound healing by inducing granulation and reepithelialization. Morden dressings are regularly produced from synthetic polymers and are categorized as bioactive and interactive dressing products. Interactive wound dressings are occlusive or semi-occlusive and are found in several forms such as nanofibers, hydrogels, hydrocolloids, films, and foams. The key function of interactive dressings is the defensive mechanism against invasion of bacteria into the wound site. These wound dressing materials are often fabricated using either synthetic polymers or biopolymers such as PGA, PLA, PLGA, hyaluronic acid (HA), chitosan, gelatin, cellulose, alginate, etc. [93].

2.5.2.1. Hydrogel Dressings

Hydrogels are explained as 3-dimensional polymeric cross-linked wound dressing materials that possess hydrophilic properties. The ability of hydrogel dressings to absorb a huge amount of water and other physiological liquids is their main advantage. The features of hydrogels that result in them being attractive in wound treatment include high porosity, high water uptake, the ability to be enriched with therapeutic agents, excellent biocompatibility, and biodegradability [94]. The high-water content of hydrogels ranges between 70 and 90% which benefits epithelium and granulation tissues in moist conditions. Hydrogel dressings usually possess soft elastic nature that helps in simple application and removal from the injury without causing further skin tears. These materials are frequently used for dry chronic wounds, burns, necrotic, and pressure ulcers. They are also not reactive with the biological tissue, non-irritant, and penetrable to metabolites. Although hydrogels demonstrate these fascinating properties, they possess some shortcomings such as exudate accumulation that can cause maceration and microbial proliferation leading to a bad smell in the wound bed. Furthermore, they can result in wound dehydration if not covered and display weak mechanical performance in swollen conditions. Examples of hydrogels that are currently used in wound treatment include Intrasite™, Nu-gel™, Aquaform™ polymers, etc. [87].
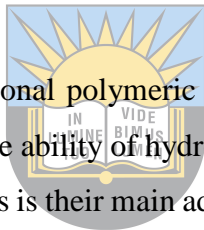
2.5.2.2. Film/Membrane Wound Dressing Materials

Films are wound dressing materials that are mainly made up of adherent and transparent polyurethanes that permit the permeation of gases (O_2 and CO_2 gas) and water vapour between the injury and the surrounding. Originally, film dressings were prepared from nylon derivatives with an adhesive polyethylene frame as the supporting materials, which caused them to be occlusive. Films demonstrate the capability to improve the process of wound recovery and protect the lesion from infections caused by bacteria. The transparency of films provides the observation of injury healing without their removal. Hence, they are very suitable wound dressings for epithelizing wounds, shallow wounds, and superficial wounds. The currently employed film wound dressings possess high flexibility and elasticity properties that make them be changed to any shape or form without requiring additional tapping [95]. Examples of film wound dressing products that are commercially available include Biooclusive™, Opsite™, and Tegaderm™, which differ in terms of their vapour permeability, conformability, extensibility, and adhesive features. Nevertheless, film wound dressings are inappropriate for excess exudate injuries because they fail to absorb a high quantity of exudates and other biological fluids [96]. On the other hand, membranes are wound-dressings that demonstrate similar features as the films. Membranes display some advantages as wound dressings such as their ability to retain biological fluids under pressure, absorb a high amount of exudate, preserve a suitable moist environment for the fast process of wound healing, require infrequent dressing changes, present potential cleaning activity, and reduce the interruption at the wound bed. Furthermore, membranes exhibit excellent mechanical features such as comfortability, flexibility, stretchability, and softness [97].

2.5.2.3. Foam Dressings

Foam wound dressing materials are produced from hydrophobic and hydrophilic foam with adhesive boundaries from time to time. The hydrophobic nature of the external layer keeps the wound from the fluid but allows gaseous transmission and water vapour permeation. Silicone rubber foam contours and moulds to injury shape. Foam dressings present the ability to absorb varying amounts of wound drainage depending upon the injury depth [98]. These wound dressings are appropriate for moderate to highly exudating wounds and lower leg ulcers and are also preferred for granulating wounds. Foams are normally utilized as principal wound dressing materials for the absorption of exudates, and secondary wound dressings are not essential due to their high moisture vapour permeability and absorbency. The limitations of foam wound dressings include their requirement for repeated dressing and their

inappropriateness for dry lesions, dry scars, or low exudating lesions. The foam wound dressing products that are commercially available include Allevyn™, Tielle™, and Lyofoam™ [98].

2.5.2.4. Alginate Dressings

Alginate wound dressings are mainly formulated from sodium and calcium salts containing guluronic and mannuronic acid units in the form of flexible foams and fibres. The biodegradable and absorbent alginates are obtained from seaweed. The calcium constituent in alginate dressings can be advantageous in blood coagulation and act as a haemostat. The absorption capability of alginate dressings is accomplished by strong hydrophilic gel production, which restricts exudates and reduces microbial invasion [99]. Once alginate-based wound dressings are placed on the injury, ions in the alginate are replaced with blood to produce a defensive film. The key feature of alginate dressings is the absorption of excess high wound exudates up to approximately twenty times their mass because of high porosity and non-stick [100]. These wound dressings are appropriate for mild to high exudate wounds and for third-degree burn injuries, dry lesions, and severe injuries with visible bone. Furthermore, they need secondary dressings due to their ability to dehydrate the injury, which retard wound healing. The commercially available alginate dressing includes Kaltostat™, Algisite™, and Sorbsan™ [100].
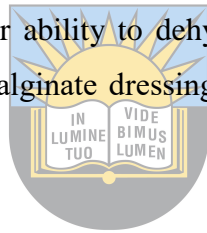
2.5.2.5. Hydrocolloid Dressings

Hydrocolloid wound dressings are made from colloidal materials with alginates and elastomers. These wound dressings can be formulated by dissolving biopolymers such as collagen, carboxymethyl cellulose (CMC), and gelatin with water. They are generally biocompatible, biodegradable and appropriate for surface sores, such as bruises, shock injuries, and minor burns. Hydrocolloid wound dressings are not suitable for deeper injuries, particularly injuries with bacterial contamination that require oxygen to improve the wound healing process. Hydrocolloids possess the ability to absorb a minimal to moderate quantity of injury exudates. Hydrocolloid wound dressings are occlusive, preventing bacteria, oxygen, and water from entering the injury. Moreover, hydrocolloids reduce the wound pH and can enable hindering bacteria proliferation [101][102]. These dressings adhere to the skin and may produce an odour sometimes due to dressing breakdown. When hydrocolloids are in interaction with the wound exudate, gels are formed. They offer a moist environment that protects the granulation tissue by absorbing wound exudates. The hydrocolloid wound dressings that are commercially available are Comfeel™, Tegasorb™, and Granuflex™, and they exist as thin

sheets or films. Hydrocolloid dressings are not appropriate for high exudating injuries or neuropathic ulcers. They are also typically employed as secondary wound dressings [103].

2.5.3. Bioactive Wound Dressings

Bioactive dressings are also considered modern dressing scaffolds fabricated from biomaterials which play a vital role in wound healing. These wound dressings are recognized for their excellent biodegradability, biocompatibility, and non-toxic nature and are generally fabricated from natural sources such as elastin, alginate, HA, collagen, cellulose, and chitosan. These polymers can be utilized alone but are regularly used together with other polymeric materials because they suffer from poor mechanical performance [104]. Bioactive wound dressings are commonly incorporated with antibiotics and GFs to improve the process of wound healing. HA is a glycosaminoglycan constituent of ECM with distinctive physicochemical and biological features. This biopolymer is biodegradable, biocompatible, and lacks immunogenicity naturally. Collagen is a main structural protein and has been considered by several biomedical researchers because of its active role in the wound-healing process. Collagen triggered the development of fibroblasts and accelerates the migration of endothelial cells upon contact with injured tissue. Chitosan stimulates the development of granulation tissue during the proliferation phase of wound healing. Bioactive wound dressings are described as the most superior to other types of wound dressing materials because they possess no obvious limitation [105].
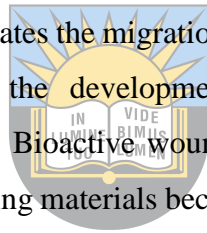
2.5.4. Tissue-Engineered Skin Substitutes

Tissue-engineered skin substitutes are wound dressing materials that are formulated to replace the disrupted skin and are made up of dermal and epidermal layers created from fibroblasts and keratinocytes on a collagen matrix. These substitutes can adapt to their environment to release cytokines and GFs loaded in wound dressings. These dressings are preferred for treating venous leg ulcers and DFUs [87]. Apligraf is one of the tissue-engineered skin substitutes approved by the FDA, and it is composed of fibroblasts and keratinocyte-loaded collagen for the management of venous ulcers. The commercially available examples of skin substitutes include Alloderm™ (made of human fibroblasts) and Integra™ artificial skin (comprises chondroitin 6 sulphate/collagen matrix covered with a thin silicone sheet). Other tissue-engineered skin substitutes are Biobrane™, Laserskin™, Hyalograft3-DTM, and Bioseed™. The shortcomings of skin substitutes that hampered them in the field of wound management include the chances of transmission of infections, host rejection, and limited survival time in the wound environment [87].

2.6. Polymers in Wound Management

Wound dressing materials, especially modern dressings (e.g., films, hydrogels, alginate dressing, hydrocolloids), composite wound dressings, and bioactive dressings, are commonly fabricated from polymers. The properties of most polymers that cause them to be beneficial in wound management include non-cytotoxicity, antibacterial effects, non-antigenicity, good biocompatibility, bioadhesive nature, good biodegradability, etc. Furthermore, polymers are usually utilized in wound treatment because they offer flexibility for chemical modification, leading to a chemical composition appropriate for producing distinct 3-dimensional structures and modified surface functionality [106]. Polymers are also used as drug delivery systems due to their unlimited diversity in chemistry, topology, and dimensions [107]. Polymers are classified into two groups based on their sources: natural polymers (biopolymers) and synthetic polymers.

2.6.1. Natural Polymers (Biopolymers) in Wound Healing Application: Gelatin and Carboxymethyl Cellulose

Natural polymers (biopolymers) are found in natural sources such as plants, animals, and microorganisms. These polymers possess many benefits in health-related applications compared to synthetic polymers, including excellent biological activity, biodegradability, and biocompatibility. The origin of natural polymers results in them being appropriate for the replacement of natural ECM constituents and skin cellular background [108]. In addition, biopolymers' molecular structures possess various functionalities that can be transformed with some derivatives, which can lead to the fabrication of versatile materials appropriate for several tissue regeneration requirements. These polymers are also produced by-products when exposed to enzymatic degradation that is normally well endured by living organisms without exacerbating poisonous responses [109]. The natural polymers obtained from animal sources include gelatin, collagen, silk fibroin, and keratin. The natural polymers that are derived from plant sources include cellulose, chitosan, chitin, alginate, hyaluronic acid, dextran, elastin, and pectin [110]. The molecular structures of biopolymers are shown in **Figure 3**.
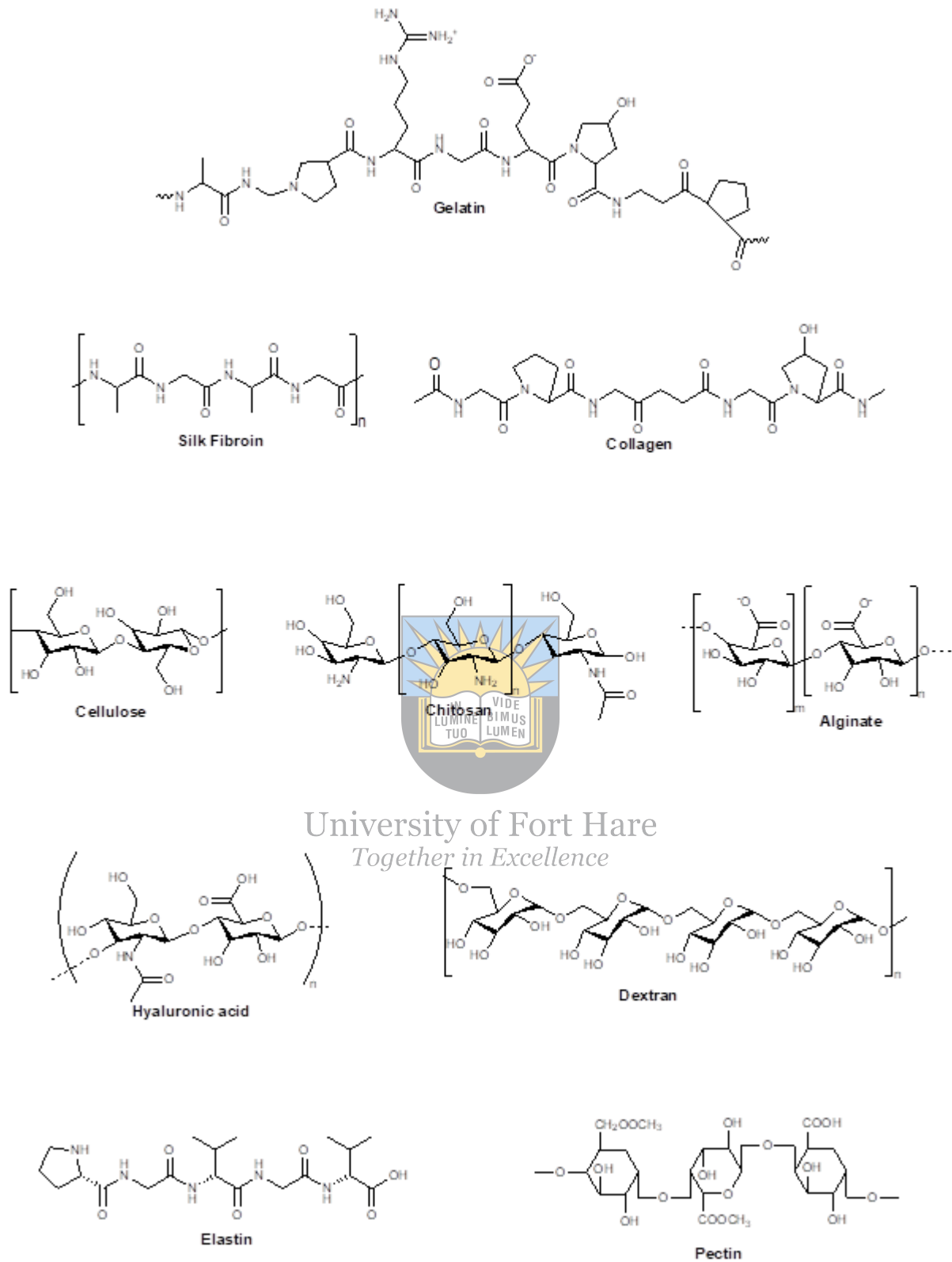
Figure 3: Molecular structures of biopolymers

The natural polymers that will be used in this research project are gelatin (fish gelatin) and carboxymethyl cellulose (CMC) (which can also be classified as a semi-synthetic polymer). Gelatin is classified as a natural polymer that is broadly utilized in manufacturing industries, particularly in cosmetic, food, processing photographic, and pharmaceutical products because of its unique functional features. This biopolymer is a solid, tasteless, colourless material produced from collagen hydrolysis. Gelatin can be categorized based on its source as fish gelatin, bovine gelatin, or porcine gelatin. Porcine gelatin and bovine gelatin are widely employed all over the world because of their substantial availability and lower price [111]. Nevertheless, as Bovine Spongiform Encephalopathy (BSE), swine influenzas, and tooth-and-mouth diseases cause public health issues, porcine products have been restricted in Jewish and Muslim countries. Fish gelatin is not only useful due to its consistent alternative to the other gelatin types but also because of its special applications and functional properties. Although fish gelatin has attracted much attention from researchers since the 1960s, its extraction efficiency and applications are still scalable and a lot can be improved [111][112].

Fish gelatin is made up of 85–92% protein, water, and mineral salt. This gelatin type is formed via collagen hydroxylation under certain conditions (e.g., alkali, acid, high temperature, and enzyme). The structure of fish gelatin is mostly made of numerous repetitions of "Glycine-proline-hydroxyproline" sequences [111]. Fish gelatin has several biomedical or pharmaceutical functions, including antihypertensive, antioxidant, anticancer, bone formation improvement, wound healing, and tissue engineering application. Gelatin meets the three primary requirements that are vital in wound healing and tissue engineering application: (i) the interaction between the host cell and the biomedical material must result in metabolic and tissue-specific structural demands; (ii) the performance of the matrix should be experimented both *in vivo* and *in vitro* utilizing quantitative histological and molecular studies; (iii) the biomedical material which supports the matrix should possess good biocompatibility and ability to be processed into the anticipated shape [113][114].

The properties of fish gelatin that demonstrate these requirements include high biodegradability, excellent biocompatibility, good processability, low antigenicity, and the ability to promote cell growth or proliferation. Furthermore, fish gelatin has been designed for the loading and delivery of growth factors, genes, nutrients, proteins, and antibiotics to the target tissues [96][115][116]. The shortcomings of fish gelatin that hamper its application in wound healing and tissue engineering are poor antibacterial activity, rapid biodegradation, and stiffness. These drawbacks are normally resolved by the encapsulation of bioactive

antimicrobial agents in gelatin-based scaffolds, a blend of gelatin materials with synthetic polymers, and the use of cross-linkers. Various gelatin/collagen-based dressing products are commercially available and are suitable for the treatment of full- and partial-thickness pressure, diabetic, vascular, and venous ulcers. Commercial wound dressing products include Surgifoam, Gelfoam, Catrix®, CollaSorb®, BIOSTEP®, BCG®, and PROMOGRAN PRISMA® Matrix [88][117]. Besides, these commercial dressings can possess some limitations that must be considered, such as the likely manifestation of impurities (due to the process of extraction to obtain gelatin), low mechanical stability, and high production costs.

The second natural polymer that will be used in this research project is a cellulose derivative called carboxymethyl cellulose (CMC). Cellulose is the main structural component of the cell walls of plants and is the greatest plentiful biopolymer on Earth. This biopolymer is a renewable biomaterial readily obtainable at an affordable price. Cellulose is a linear biopolymer composed of b-1,4 linked D-glucose parts that are combined to produce cellobiose reiterating parts [118]. Some research biomedical experiments have demonstrated that cellulose and its derivatives possess outstanding biocompatibility because of their lesser inflammatory response as external materials. Also, the resorption of cellulose in cells does not occur due to the inability of cells to produce an enzyme called cellulases [119]. The experiments on the efficacies of cellulose in wound healing have shown it can accelerate the mechanism of wound healing via the release and maintenance of many GFs at the wound bed such as epidermal growth factor (EGF), basic fibroblast growth factor (bFGF), and phosphodiesterase growth factor. These growth factors induce the movement and proliferation of skin fibroblast cells and prevent bacterial growth at wound beds [120]. The derivatives of cellulose that are often used in wound healing applications include carboxymethyl cellulose (CMC), methylcellulose (MC), hydroxylpropylmethyl cellulose (HPMC), hydroxyethyl cellulose, ethyl cellulose (EC), hydoxypropyl cellulose (HPC), and anionic ether derivatives such as sodium carboxymethyl cellulose (NaCMC).

CMC is one of the most significant cellulose derivatives obtained from cellulose's molecular modification. The carboxymethyl functional groups ($-CH_2-COOH$), in their chemical structure, are attached to the hydroxyl functional groups of the cellulose glucopyranose chain. CMC is synthesized by 2 steps: i) alkali treatment using sodium hydroxide (NaOH) to activate cellulose; ii) esterification reaction of alkali cellulose with monochloroacetic acid whereby hydroxyl groups in cellulose are replaced with carboxymethyl group [121]. Due to the degree of substitution that ranges between 0.4 and 1.5, the CMC is presented with diverse molecular

weights that range between 90,000-2,000,000 g/mol [122]. Among the various applications of CMC (food, cosmetics, paper industry, textile industry, ceramics, adhesives, etc.), it is also broadly employed in biomedical applications (such as wound dressing) and pharmaceutical applications (antimicrobial, drug delivery). CMC-based wound dressing scaffolds are recognized for being flexible, promoting angiogenesis, the ability to absorb wound exudate and autolytic debridement. The properties of CMC that make it to be very suitable in wound healing include non-toxic to humans, hydrophilic nature, high water absorbent, swelling capacities, low immunogenicity, good biocompatibility, and biodegradability, excellent mucous and skin membrane compatibility and abundant [123].

CMC mainly sustains an optimal moist environment in the injury site for ECM development and re-epithelialization. It has been fabricated as a wound dressing material for the management of burns. Extra CMC™ and AquaRite are highly absorbent, non-woven, soft CMC-based dressing materials available commercially. Hcel® NaT is another commercially available CMC-wound dressing product that presents excellent cell proliferation and adhesion features on human dermal fibroblasts by utilizing fibrin [124]. The other example of cellulose-based wound dressing that is available on the market is Aquacel® Hydrofiber, which is recognized for its superior antimicrobial effects. After application on the injury bed, it absorbs wound exudate and makes a gel-like network to provide moisture and result in the acceleration of the process of wound recovery [125]. The other natural polymers that are often utilized in wound healing applications are summarized in **Table 1**. The common limitations of natural polymers that can hamper their applications in wound dressings are weak mechanical performance and high degradation rates or poor stability. These shortcomings can be overcome by crosslinking natural polymers with synthetic polymers.

Table 1. Other natural polymers that are commonly used in wound healing application

Polymer	Advantages	Limitations	Role in Wound Healing Application	Reference
Collagen	An essential constituent of ECM, Good cell recognition, Excellent biocompatibility.	Difficult to process, easy contamination, and expensive when formulated using recombinant technologies.	Cell attachment features by binding with extracellular integrin receptors through glycine/ arginine/ aspartate binding sites.	[126]

29

			Stimulate platelet activation and Aggregation.	
Silk Fibroin	Good biocompatibility, Slight side effects on the immune system, and High mechanical strength	Inflammation Degradation	Substrate for macrophages, endothelial cells, platelets, and fibroblasts. Clot formation and have ability Contributes to bleeding termination.	[127]
Chitosan/Chitin	Oxygen permeability, nonantigenic, non-toxic, and good biocompatibility and biodegradability	Poor stability	Possess antimicrobial efficacy, promote the granulation of injury, improves inflammatory cells, macrophages, and fibroblast functions	[128]
Alginate	Good biocompatibility and biodegradability, low toxicity, resistance in acidic media, gelling properties, and relatively low cost.	Overstimulation of Fibroblasts	Stimulate granulation tissue development, induces monocytes to cause high levels of cytokines, capacity to absorb exudates, and maintain wound moisture.	[129]
Hyaluronic acid	Good biocompatibility, forms a smaller	Fast enzymatic degradation in physiological media	Enhances proliferation of keratinocytes and fibroblasts, and	[130]

	ECM portion, Nonallergenic, and water soluble.		stimulates collagen deposition	
Elastin	A major component of skin elastic fibres		Enhanced re-epithelialization and granulation tissue formation.	[131]

2.6.2. Synthetic Polymers: poly (ethylene glycol) (PEG) and Poloxamer

In recent decades, a wide variety of synthetic biocompatible, biodegradable/non-biodegradable polymers or copolymers have been used. Synthetic polymers are well-recognized for their ability to overcome the shortcomings of natural polymers (inferior mechanical properties) by accomplishing reproducible and consistent physical and chemical properties. A huge majority of these polymers are not sensitive to enzymatic and biological activities, and therefore their biochemical and physicochemical behaviour will not differ very much from various patients. Various synthetic polymers are often used in wound dressing applications, such as PLGA, PEG/PEO, PVP, PCL, PGA, PHEMA, PLA, and poloxamers (**Figure 4**).
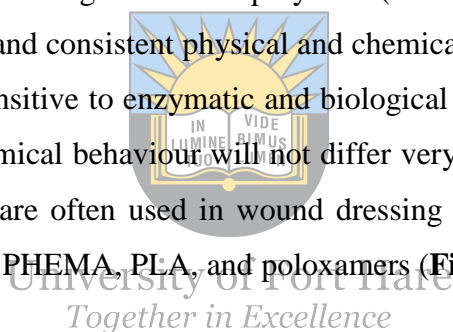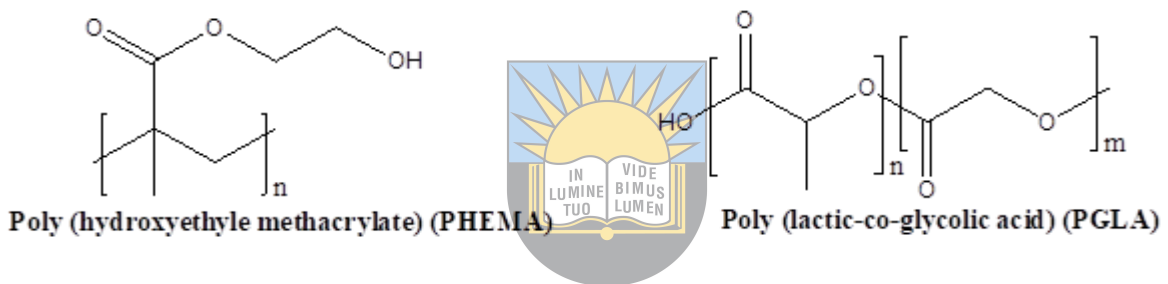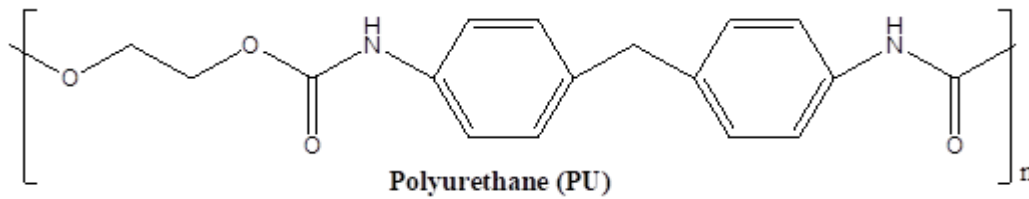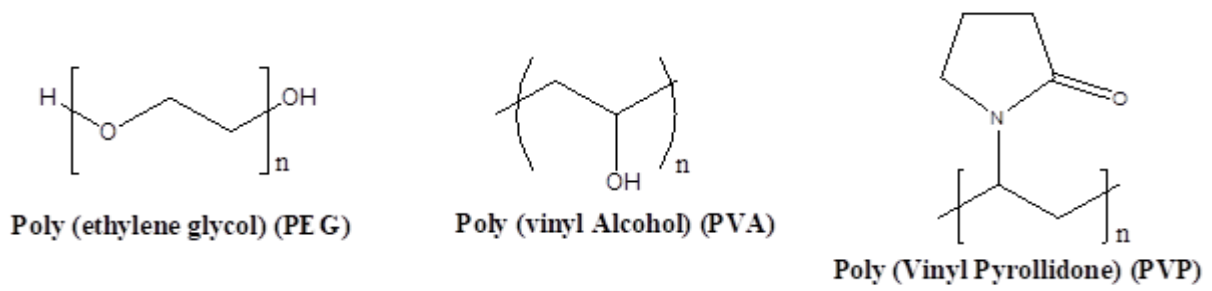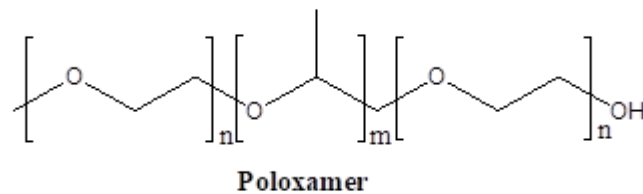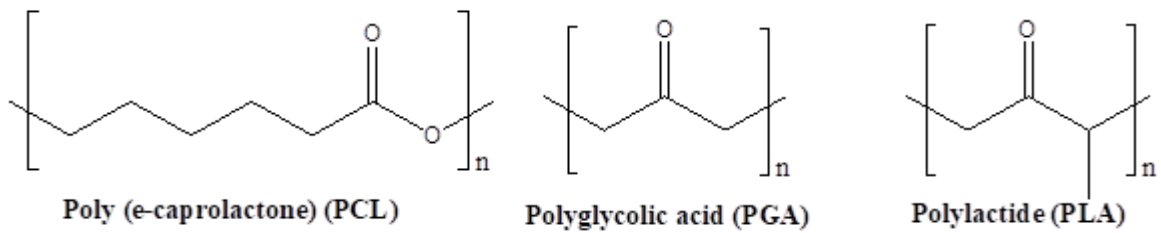
Figure 4: Molecular structures of synthetic polymers

The synthetic polymers used in this research project are PEG and poloxamer 407. PEG also known as PEO is a synthetic polymer that is inert, hydrophilic, non-immunogenic, compatible, and non-toxic making it appropriate for wound dressing, regenerative medicine and other biomedical applications [132]. Furthermore, this polymer is a water-swellable cross-linked polymer with a high degree of elasticity causing it to be a perfect candidate for tissue engineering. More significantly, the rate of degradation of the implant can be controlled by altering the chemistry of the cross-links in the polymer network. PEG is usually prepared by cationic or anionic ethylene oxide polymerization [133]. PEG is often combined with other polymers (e.g., chitosan, PGLA) to enhance its inherent solubility, thermal and mechanical features as well as crystallinity and viscosity. Some research studies have demonstrated that PEG-based hybrid wound dressing materials lead to a fast wound healing process, granulation tissue formation, complete reepithelialization, and highly improved neovascularization [134].

On the other hand, poloxamers are the main non-ionic surfactant and triblock copolymers composed of a central hydrophobic chain of poly (propylene oxide) (PPO) flanked by two hydrophilic chains of PEO). Various poloxamers have been formulated in the industry with minor different properties by adjusting the ratio of PPO: PEO [135]. Poloxamers are marketed with the trade name Pluronic, followed by a letter and number. For example, Poloxamer that will be used in this research study (Poloxamer 407) is Pluronic F-127 and is composed of a PPO molecular weight of about 3600 g/mol and 70% PEO [136]. Poloxamer 407 is a synthetic polymer and is frequently employed as a vehicle for several routes of drug administration, including topical, intranasal, parenteral, oral, recta, ocular, and vaginal. Poloxamer 407 has healing and thermo-reversibility properties. This poloxamer stimulates cell proliferation, collagen synthesis, fat metabolism, and tissue microcirculation. A poloxamer that is topically utilized sustains the stability of various water-soluble medicinal materials. The poloxamer gel offers not only a non-toxic detergent dress to the injury, but precise experiments indicate that the gel itself may also have an advantageous action, accelerating the wound healing process of injuries [137]. Other synthetic polymers that are frequently utilized in wound dressing applications are summarized in **Table 2** below.

Table 2. Other synthetic polymers that are commonly used in wound-healing applications

Polymers	Properties	References
PVP	Good biocompatibility and biodegradability, low cytotoxicity, affinity to complex hydrophobic and hydrophilic substances, high thermal and chemical resistance, and good solubility in organic solvents and water.	[138]
PVA	Hydrophilic, pH-sensitive, non-toxicity, and excellent biocompatibility.	[139]
PUs	Tough and durable, excellent biocompatibility, and degradation rate can be adapted.	[140]
PCL	Good biocompatibility and biodegradability, excellent elastic properties, hydrophobic nature, and semicrystalline.	[141]
PLA	The degradation products can be absorbed by the body, nontoxic, hydrophobic, and structurally stable.	[142]
PGA	High tensile strength, more hydrophilic than PLA, and lowers the local pH resulting in tissue and cell necrosis.	[143]
PLGA	Excellent biocompatibility and biodegradability, the rate of degradation can be controlled by altering monomer ratios.	[144]
PHEMA	Good biocompatibility, and the ability for hydrogel formulation.	[145]

2.7. Bioactive Agents used in Wound Treatment

Most of the polymer wound dressing products that are presently employed are hampered by poor biological activities, especially poor antimicrobial effects. The loading of various bioactive agents in wound dressings is the most promising approach that can be utilized to enhance therapeutic results or biological activities of polymer-based dressings. The bioactive agents that are regularly utilized in the treatment of wounds include antibiotics (e.g., ciprofloxacin), metallic nanoparticles (e.g., silver nanoparticles), plant extracts (*Aloe vera*), and essential oils (e.g., lavender oil), GFs (e.g., PDGFs), and vitamins. The bioactive agents used in this research study are antibiotics, metallic nanoparticles, and essential oils.

2.7.1. Antibiotics: Metronidazole

Once infection on the wound is established, appropriate anti-infection treatment is very important, even if debridement is done, which encompasses the local and systematic application of antimicrobial agents. Several studies have demonstrated that antibiotics can significantly help wound recovery, although their positive effect is frequently unnoticed. The mode of action of antibiotics is commonly based on their ability to disrupt some metabolic pathways of the bacteria via one of these four pathways: obstruction of major metabolic pathways, hindering the synthesis of a bacterial cell wall, inhibition of nucleic acids biosynthesis, and interference on protein biosynthesis [146]. Although antibiotics are very important in the management of infected injuries, their inappropriate application can lead to bacterial resistance. It was observed that approximately 70% of bacteria that lead to wound infections are resistant to most utilized antibiotics [147]. Various classes of antibiotics are used in biomedical applications including quinolones (e.g., ciprofloxacin, norfloxacin, amoxicillin), tetracyclines (doxycycline, minocycline, tetracycline), Aminoglycosides (e.g., gentamicin, neomycin, tobramycin), cephalosporins (e.g., cefuroxime, cefepime), and nitroimidazoles (ronidazole, metronidazole, tinidazole, nimorazole, and fluconazole) (**Figure 5**).
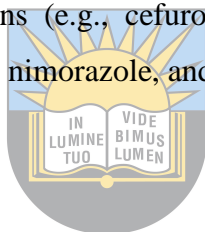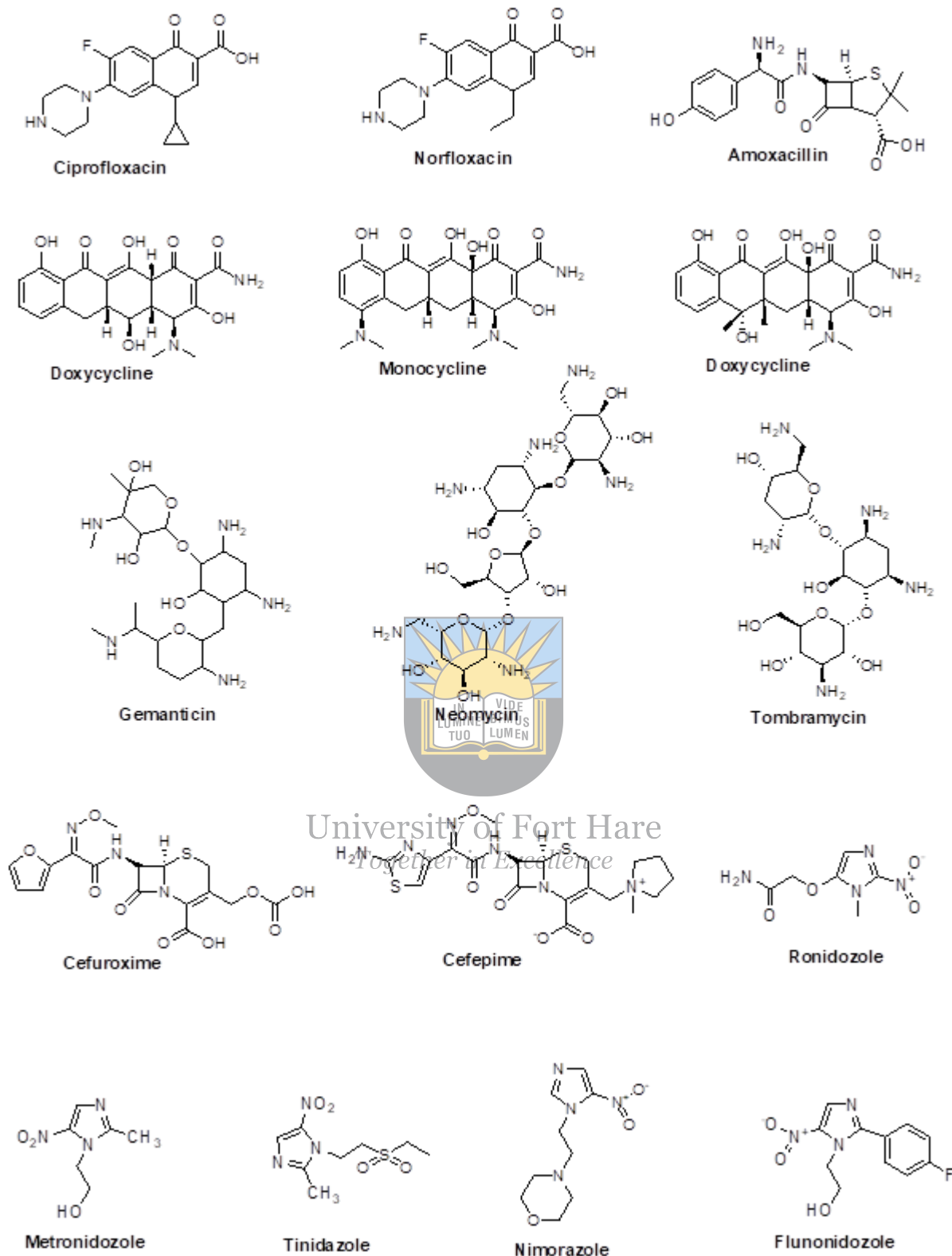
Figure 5: Chemical structures of antibiotics

Metronidazole is a nitroimidazole derivative antibiotic that is normally utilized for the treatment of several infections produced by bacteria, parasites, and anaerobes. It was first developed during the late 1950s and was initially employed for the treatment of *Trichomonas*

vaginalis infection [148]. This antibiotic exhibits antibacterial efficacy against gram-positive *bacilli*, all sporulated anaerobic *cocci*, and gram-negative anaerobic *bacilli*. The mechanism of action of metronidazole is as follows: it enters the bacterial cell first by passive diffusion in the form of a prodrug and gets triggered in the bacterial cell cytoplasm. The metronidazole is changed into temporal nitroso free radical by the intracellular reduction process. This antibiotic, in this state, is cytotoxic and can lead to interaction with the DNA molecule. The mode of action of metronidazole is not yet completely understood, but it inhibits DNA biosynthesis and DNA disruption by oxidation, leading to the breaking of double-strand and single-strands that results in DNA degradation and cell death. The reduced drug uptake of metronidazole or the altered reduction ability can result in antibiotic resistance [149], [150][151]. In wound treatment, metronidazole has been known as an effective agent in controlling wound odour [152].

2.7.2. Metal-based Nanoparticles: Silver Nanoparticles

Nanoparticles and nanocarriers have been utilized to develop medical materials and result in improved therapeutic outcomes concerning infection control and wound healing. Compared to conventional wound dressing products, nanotechnology-driven therapeutics provide unique opportunities where a specific biochemical process within the impaired wound healing process might be influenced. An excellent benefit of nanomaterial-based interventions is their tunability and versatility. For example, nanotherapeutics can be used in sustained and controlled release of bioactive agents over several long times. The nanoparticles that are frequently used in biomedical applications are classified into 3 groups: polymer nanoparticles, lipid nanoparticles, and metallic nanoparticles [93]. Polymeric nanoparticles are biocompatible colloidal materials that have been attracting great attention in the arena of biomedicine and tissue regeneration. The advantages of polymeric nanoparticles include their ability to protect incorporated drugs from premature biodegradation by wound proteases. Also, the incorporated drugs are released in a sustained and controlled way. The polymers that are frequently used to formulate these nanoparticles include chitosan, cellulose, alginate, gelatin, PLGA, etc.[153].

Lipid nanoparticles are broadly fabricated from physiological lipids or lipid molecules, and their preparation does not need the use of poisonous organic solvents. These nanoparticles are categorized into two classes solid lipid nanoparticles (SLNs) and nanostructured lipid nanocarriers (NLCs). SLNs are hydrophobic, and the bioactive agent is encapsulated in its core leading to a slowly sustained drug release. They are also known for their large surface area and low toxicity. NLCs are formulated utilizing oil, while SNLs are formulated utilizing organic

solvents. The effectiveness of lipid nanoparticles for application in topical therapeutic or cosmetic uses still requires further studies to fully understand their mode of action [154].

The metallic nanoparticles belong to the inorganic nanoparticles together with ceramic nanoparticles and carbon-based nanoparticles. Inorganic nanoparticles generally display interesting benefits in wound treatment that include excellent antimicrobial effects. The toxicity and efficacy of inorganic nanoparticles depend on crucial properties, such as architecture (smaller particle sizes are more therapeutic active), dimension, surface charge, poly-dispersity index, and surface functionalization [155]. Various metallic elements have been confirmed as potential materials to treat bacterial infections.

Silver (Ag), titanium (Ti), copper (Cu), and zinc (Zn) are widely used metallic nanoparticles in biomedical fields, including wound dressing applications, because of their potential antimicrobial properties. Ag nanoparticles are an effective bioactive agent with good antimicrobial effects against a broad variety of microorganisms such as bacteria, viruses, yeasts, and fungi [156]. Also, these nanoparticles possess excellent stability and well incorporation features into polymeric materials with good cytocompatibility and biocompatibility. The antimicrobial activity of Ag nanoparticles is due to their ability to destroy proteins of the bacterial cell membranes and interact with DNA. Ag ions possess the ability to hinder the replication of bacteria, by binding and denaturing bacterial DNA, which combines the reaction of Ag ions with a thiol functional group of proteins followed by condensation of DNA leading to apoptosis. Nano form of Ag is more reactive, and they diffuse through bacterial cell membranes, causing an accumulation of intracellular nanoparticles that lead to the dysfunction of the cells [157][158]. Nevertheless, Ag compounds, $AgNO_3$, and Ag sulfadiazine can exacerbate argyria when employed in topical formulations over a prolonged period [159].

2.7.3. Essential Oils: Tea Tree Oil and Lavender Oil

Essential oils are secondary plant metabolites that display numerous therapeutic efficacies such as antioxidant, antimicrobial, antiviral, anti-inflammatory, anti-allergic, and regenerative effects. These metabolites are usually derived from various parts of plants, including barks, leaves, roots, and seeds. Some research experiments have shown that the antimicrobial activity of essential oils enriched in wound dressing materials can be due to their various components (like carvacrol, thymol, geraniol, menthol, and cinnamaldehyde) [160]. The presence and the quantity of these constituents in essential oils depend on the sample source and extraction methods (e.g., ultrasound-assisted extraction, microwave-assisted extraction, microwave steam

diffusion, microwave-generated hydrodistillation, steam distillation, and hydrodistillation) [160].

Some research studies discussed the mode of action of essential oils on bacteria. For example, Kavvosi and co-workers demonstrated that essential oils (specifically those that contain phenolic compounds e.g., carvacrol and thymol) attack phospholipids and lipids that are found in the bacteria cell wall and plasma membranes, leading to cytoplasmic outflow, disruption of the cellular process (such as protein synthesis and DNA transcription, and ATP biosynthesis), and pH decrease. The most important benefit is that essential oils possess a very slight effect on antimicrobial resistance development than antibiotics. Nevertheless, essential oils may need high concentrations or repetitive application that may cause side effects on the patients [161]. Examples of essential oils that are mostly utilized in wound management with antimicrobial effects include tea tree oil, lavender, peppermint, lemongrass, cinnamon, thyme, eucalyptus, rosemary, etc. This research study is focused on tea tree and lavender oil-enriched polymer-based wound dressing scaffolds for the treatment of chronic injuries.

Tea tree oil (TTO) is an essential oil that is found in a well-known plant (*Melaleuca alternifolia*) in traditional remedies and current medicine because of its unique healing property. TTO is used in various products, including dermatological ointments and creams due to its interesting properties and constituents. TTO is extracted from the terminal branches and leaves of the *Melaleuca alternifolia*, and is made up of a blend of about 100 different constituents, mostly sesquiterpenes and monoterpenes, whereby 1,8-cineole and terpinen-4-ol are the most active components (with antibacterial, anti-inflammatory, antiprotozoal, analgesic activity) [162]. There are interesting data that discuss the treatment of chronic wound infections using tea tree oil loaded in various polymer-based dressings. For example, Ge and co-workers prepared chitosan-based film wound dressings enriched with TTO droplets to treat infected injuries [163]. The WVTR values of both pristine films and TTO-loaded films samples were in the range of 1400 $g \cdot m^{-2} \cdot d^{-1}$ and 2400 $g \cdot m^{-2} \cdot d^{-1}$, indicating that these films dressings could provide a suitable level of moisture without resulting in wound dehydration. The increasing concentration of TTO significantly improved the clotting effect of the film dressings, which is a significant factor in wound treatment. Also, the antimicrobial efficacy of film wound dressings was improved with an increase in TTO amount against *S. aureus*, *C. albicans*, and *E. coli*, revealing that these TTO-enriched films are effective wound dressings for the management of infected injuries. Furthermore, these films displayed high cell viability of L929 fibroblasts confirming their excellent cytocompatibility and non-toxicity [163].

In another study, Mahmood *et al*. fabricated gellan gum hydrogel films co-enriched with TTO and ofloxacin for wound treatment. The *in vitro* antimicrobial experiments demonstrated that films loaded with 25% w/w concentration of TTO displayed a high zone of inhibition against *S. aureus* and *E. coli* than the pristine films and significantly resulted in a higher antibacterial synergetic effect when co-loaded with ofloxacin. The antioxidant experiments exhibited a slight difference in the percent scavenging activity of free and loaded TTO, indicating that TTO retains its antioxidant efficacy after encapsulation into the polymeric matrix. The *in vivo* evaluations employing rat models of full-thickness injury revealed healing on the 10th day (98%) in groups dressed in films co-loaded with TTO and ofloxacin than the blank films and free bioactive agents [164]. The TTO nanoemulsions loaded with Ag nanoparticles formulated by Najafi-Taher *et al*. demonstrated good antibacterial synergistic effects, resulting in a high zone of inhibition against *S. aureus* and *E. coli*, showing their ability to be effective antibacterial wound dressing scaffolds [165].

Lee and co-workers conducted clinical studies using a 10% of topical TTO formulation for the management of chronic injuries in nursing home residents infected with methicillin-resistant *staphylococcus aureus* (MRSA) [166]. The infections in patients were eliminated after 1 month of TTO treatment. 16 colonized injuries in the TTO group healed in 28 days than the control group. Another clinical experiment performed by Edmondson and co-workers was based on the evaluation of TTO in a randomized controlled trial on chronic injuries colonized by MRSA strains. 11 patients out of 19 were treated with a water-miscible TTO (3.3%) solution which was applied at each dressing change. The infection was not fully removed even though 8 out of 11 injuries were reduced in size after treatment [166].

On the other hand, lavender oil is an essential oil obtained from the plant called *Lavandula angustifolia* and has been utilized in traditional medicine worldwide. It has been demonstrated that essential oil effectively hinders the growth of infectious microorganisms [167]. The major components of lavender oil that contribute to its antimicrobial activity are linalyl and linalool, but its antibacterial action and chemical composition are mostly due to the lavender sample source [168]. In this respect, some research studies revealed the application of lavender oil in wound treatment. Sofia *et al*. formulated and studied the electrospun polyurethane-based nanofiber co-loaded with lavender oil and Ag nanoparticles for wound dressing applications [169]. The scanning electron microscope (SEM) analysis revealed that the loading of lavender oil and Ag nanoparticles in nanofibers did not alter the morphology and the porosity of nanofiber wound dressings. The biocompatibility studies exhibited that the proliferation and

cell viability of fibroblast cells increased as the number of days increased when were incubated with dual drug-loaded nanofibers, demonstrating that these nanofibrous dressings are non-toxicity. The *in vitro* antibacterial experiments exhibited that plain polyurethane nanofiber did not hinder the growth of *S. aureus* and *E. coli*. In contrast, the nanofibers encapsulated with lavender oil and Ag nanoparticles were significantly effective in suppressing bacterial growth as they caused a high zone of inhibition against bacterial strains, indicating that the nanofibers are potential antibacterial wound dressing materials [169].

The PEG-based nanofibrous membranes enriched with lavender oil were evaluated by Eğri for bacteria-infected wounds [170]. The loading of lavender oil in membranes did not change the porosity and mechanical performance of the nanofibrous membranes. The *in vitro* drug release kinetics at physiological conditions (pH 7.4 and 37ºC) exhibited that lavender oil was initially rapidly released within the first two days and then release slowed down after the second day due to the reduction of the lavender oil present in the polymeric matrix. The *in vitro* antimicrobial experiments exhibited that plain membrane dressings did not possess any antimicrobial effects while lavender-enriched membranes resulted in superior antibacterial efficacy against *S. aureus* and *E. coli*, confirming that lavender oil-loaded scaffolds are effective antibacterial wound dressing materials [170]. Tajik and co-workers formulated keratin-PVP hybrid hydrogels encapsulated with lavender oil. The *in vitro* antibacterial analysis demonstrated superior antibacterial efficacy against *S. aureus* and *E. coli* bacteria, revealing their effective applications in wound healing [171].

2.8. Sponges

Sponges are flexible and soft wound dressing scaffolds that are characterized by their interconnected microporous structures [172]. Several advantages are due to their porous structures, which include high water absorption ability, high swelling capacity, hemostatic activity, and capacity to provide moisture for the accelerated process of wound healing and protection of the wound from bacterial invasion [173][174]. In addition, it was reported that the sponges that exhibit porosity ranging between 10 and 100 µm could lead to a high rate of cell adhesion and proliferation during the wound-healing process [175]. Polymer-based sponges fabricated from the following materials: chitosan, cellulose, graphene oxide, sodium alginate, and PVA, show good antimicrobial effects. Sponges prepared from natural polymers demonstrate excellent biocompatibility and biodegradability, intrinsic hemostatic activity, good antibacterial properties, and suitable WTVR. Generally, sponges need secondary wound dressing or tapes to fix them at the injury bed, and they are non-adhesive [176]. This research

study will focus on gelatin-based hybrid sponges for managing chronic wounds using PEG as a synthetic polymer. Due to the poor antibacterial activity of gelatin, the sponges will be loaded with antibiotics (metronidazole) and metallic nanoparticles (Ag nanoparticles). Recent experimental data discusses the activity of gelatin-based sponges loaded with therapeutic agents as potential wound dressing materials.

Naghshineh *et al*. fabricated gelatin/chitosan sponges encapsulated with curcumin using a freeze-drying method for wound treatment. The SEM results exhibited a high porosity of composite sponges that can provide high gaseous permeability and water uptake. The *in vitro* drug release studies exhibited initial rapid curcumin release from composite sponges followed by sustained drug release. The *in vivo* experiments utilizing the rat model showed that the wounds dressed in gelatin sponges encapsulated with curcumin were completely healed on the 10th day of treatment without any scars when compared to those treated with the control (gauze) [177]. These results demonstrated that the curcumin-incorporated gelatin-based hybrid sponges are effective candidates for the management of chronic wounds. Wen *et al*. fabricated gelatin-based hybrid sponges with 1% gelatin solution, 2% sodium alginate solution, and 2% CaCl$_2$ solution (as a cross-linking agent) and then incorporated them with antibiotic tetracycline hydrochloride for bacteria-infected wound treatment. The *in vitro* antimicrobial studies of antibiotic-encapsulated sponges utilizing the disc diffusion procedure exhibited excellent antibacterial activity against *E. coli*, *S. aureus*, and *B. subtilis* while the pure sponges did not demonstrate any antibacterial effects [178]. These outcomes indicated that tetracycline-loaded gelatin-based hybrid sponges have great potential for antibacterial wound dressing applications.

Tamahkar *et al*. prepared and evaluated aloe vera-enriched gelatin-sodium alginate-sodium hyaluronate sponges for wound healing applications. These sponges exhibited high swelling capacity, suggesting that they can result in high absorption of wound exudates and keep the injury site moist to provide a fast healing process. The *in vitro* drug release at pH 7.4 displayed an initial rapid release of *aloe vera* from the gelatin hybrid sponges followed by slow, sustained drug release. The antibacterial experiments employing the agar diffusion procedure showed that the pristine gelatin-based hybrid sponges didn't possess any inhibition zones for *S. aureus*, *Streptococcus pneumoniae* (SP), and *Enterococcus faecalis* (EF) while *Aloe vera*-loaded sponges displayed 15, 20, and 30 mm inhibition zones for those bacterial strains, respectively. These results demonstrate that loading aloe vera into gelatin sponges can lead to effective antibacterial sponge wound dressings [179]. The gelatin-based sponges functionalized by

Ag/Cu nanoclusters were synthesized by Wang and co-workers and they exhibited a higher inhibition zone with a diameter of about 31.9 mm for the gelatin-based sponges co-loaded with nanoclusters larger when compared to that of 25.1 mm for gelatin sponges loaded with only Au nanoclusters on *P. aeruginosa*, suggesting the excellent antibacterial efficacy dual drug-loaded sponges [180]. The improved antibacterial activity is attributed to the increased generation of ROS from the Au or Ag nanoclusters.

Zou et al. designed gelatin/konjac composite sponges co-encapsulated with gentamicin sulfate and Au nanoparticles for wound healing [181]. The X-ray diffraction (XRD) and Fourier Transform Infrared (FTIR) spectroscope confirmed the successful preparation of the dual drug-loaded gelatin-based hybrid sponges. The *in vitro* cytotoxicity analysis of gelatin-based hybrid sponges co-encapsulated with gentamicin and Au nanoparticles on L929 cells exhibited more than 89% cell viability, demonstrating non-toxicity, and excellent cytocompatibility which are characteristics of ideal wound dressing materials. The antibacterial studies of dual drug-encapsulated sponges displayed excellent antibacterial effects on MRSA, *E. coli*, and *S. aureus* while plain sponges did not show any antibacterial activity, revealing that co-loading the drugs in gelatin-based hybrid sponges can result in good biological activities with an improved wound healing mechanism. The *in vivo* experiments employing created lesions on the rabbits showed that full-thickness wounds covered with gelatin hybrid sponges encapsulated with Au nanoparticles and gentamicin recovered faster when compared to the untreated wounds. Those treated with plain sponges did not exhibit any significant healing rate. The rate of the wound recovery process was in the following order: dual drug-loaded sponges> sponges loaded with gentamicin sulphated >control [181].

Ye *et al*. prepared gelatin-bacterial cellulose composite sponges with ampicillin utilizing glutaraldehyde as the cross-linker for bacterial-infected wound management [182]. The porosity of ampicillin-loaded composite sponges was more than 92%, indicating high porosity that is very suitable for excess exuding wounds. The drug release profile displayed an initial burst release of ampicillin from the composite sponges for 12 hours, followed by continuous slow drug release for 48 hours. The *in vitro* antibacterial studies showed that the gelatin-based hybrid sponges without ampicillin did not show any antibacterial effects against *C. albicans*, *E. coli*, and *S. aureus*. In contrast, ampicillin-loaded sponges demonstrated excellent antimicrobial activity against these strains, demonstrating that these scaffolds are potential antibacterial dressing scaffolds [182]. Das *et al*. fabricated gelatin-gum odina hybrid spongy scaffolds for application in wound healing. The cytotoxicity analysis exhibited high cell

43

viability (about 90%) of NIH3T3 fibroblast cells when seeded with gelatin-based hybrid sponges for 72 hours, indicating excellent biocompatibility of gelatin sponges. The *in vivo* wound healing experiments using the wounds dressed with gelatin hybrid sponges revealed complete healing on the 18th day of treatment while those treated with the control were healed on the 21st day, confirming gelatin sponges capability to significantly accelerate the wound healing process [183]. The plain gelatin-based sponges formulated by Letha using formaldehyde as cross-linking agent exhibited non-toxicity in Balb/c 3T3 cells, while the *in vivo* experiments demonstrated that these sponges did not cause any sensitization and irritation on the guinea pig and albino rabbits [184].

The gelatin-based sponges present the properties of ideal wound dressing materials. These scaffolds display high porosity that could provide appropriate permeation of gases and cell migration that are required during the mechanism of wound healing. The gelatin-based sponges displayed high water uptake and swelling capacity, demonstrating that these sponges are appropriate materials for high-exuding wounds. Although pristine gelatin-based sponges do not promote significant antibacterial efficacy, their capability to accelerate the wound healing process *in vivo* has been reported. The antibacterial effects of gelatin-based sponges can be improved by loading antimicrobial agents (such as antibiotics, metallic nanoparticles, plant extracts, etc.) in the sponges. The gelatin sponges co-loaded with two drugs resulted in superior biological efficacy than those loaded with a single drug, suggesting that loading two drugs resulted in a synergistic effect. The *in vitro* drug release experiments revealed an initial burst release effect of the therapeutic agents from gelatin-based sponges followed by a sustained drug release. This mechanism can be caused by polymer degradation or diffusion of bioactive agents or both. This drug release mechanism can result in the killing of bacterial strains and further protect the wound from microbial invasion. Furthermore, the *in vitro* cytotoxicity of both plain and drug-loaded gelatin sponges showed non-toxicity and excellent biocompatibility when cultured with human skin cells. The gelatin-based sponges demonstrate interesting properties that make them ideal for wound dressing.

2.9. Topical Gels

Topical gels are explained as semi-solid systems whereby a liquid medium is bonded within a 3-dimensional polymeric matrix of synthetic or natural gum. These gels are usually used in topical drug delivery systems for the treatment of skin conditions or disorders like fungal or bacterial infections [185]. The ability of topical gels to penetrate the skin makes them potential wound dressing materials [186]. Several factors influence the efficiency of topical gels such as

water solubility, drug concentration, application time, mode of application, percutaneous absorption, active pharmaceutical ingredients, clearance, and protein bind capacity [187]. The drug uptake by the skin from topical gels is through passive diffusion using sweat ducts or hair follicles. Topical gel formulations offer many advantages in wound healing applications such as their ability to absorb wound exudates, control excessive bleeding, release a high amount of loaded bioactive agents at the wound bed, maintain a moist environment at the wound site, enhance gaseous penetration, cost-effectiveness, easily applied by the patients, and treat various infections [188]. The topical gels that will be focused on in this research study are based on CMC incorporated with Ag nanoparticles and essential oils (TTO and lavender oil).

Several research reports demonstrate the effectiveness of topical gels loaded with Ag nanoparticles for the treatment of various wounds. Patil *et al*. designed silk fibroin-based topical gels loaded with Ag nanoparticles for application in wound healing [189]. XRD and FTIR spectroscopy confirmed the physiochemical properties and successful fabrication of silk fibroin gels. The particle size analysis of Ag nanoparticles loaded in gels exhibited an average particles size of 56 ± 3.24 nm that are appropriate for biological applications. The antibacterial experiments showed that plain silk fibroin gels did not possess any zone of inhibition on *S. aureus* while Ag nanoparticle-loaded demonstrated a significant zone of inhibition of about 11 ± 2.12 mm, suggesting the ability of Ag nanoparticles to enhance the antibacterial efficacy of topical gels. The *in vivo* studies employing an excision wound model in albino Wistar rats showed that the wounds dressed with Ag nanoparticle-incorporated silk fibroin gels possessed the highest percent wound closure of about $97.13 \pm 1.8\%$ when compared to plain silk fibroin gel ($75.05 \pm 0.7\%$), positive control (commercial topical gels: soframycin) ($79.45 \pm 1.32\%$) and negative control (untreated wounds) ($47.77 \pm 1.21\%$) on 15th day of treatment. These *in vivo* results demonstrated that silk fibroin topical gels containing Ag nanoparticles accelerated the process of wound recovery when than other formulations [189].

Pérez-Díaz and co-workers prepared topical chitosan gels incorporated with Ag nanoparticles for the management of bacteria-infected chronic wounds. The antibacterial experiments exhibited superior antibiofilm activity of Ag nanoparticle-loaded chitosan gels against MRSA and *P. aeruginosa* when compared to free chitosan gels and Ag sulfadiazine that was used as control. The cytotoxicity analysis using fibroblast cells displayed a concentration-dependent response of Ag nanoparticles loaded in chitosan topical gels. The increase in Ag nanoparticle concentration in chitosan gels affects the morphology of fibroblasts and could disturb their proliferation, and may have an effect on the process of wound healing. Nevertheless, cell

viability was more than 75% at concentrations of 500 ppm sustaining a good relationship with the anti-biofilm treatment [190]. The Ag nanoparticle-incorporated topical Carbopol gels designed by Kaler and co-workers significantly healed the skin burn wound in the rat model effectively at a faster rate with superior cosmetic effects (no agyria and scars) than the plain Carbopol gels and marketed formulation [191].

Ontong *et al*. formulated Carbopol/ silk fibroin hybrid gels enriched with Ag nanoparticles for topical applications. The TEM results of nanoparticles-loaded topical gels exhibited a spherical shape with an average particle size ranging from 25 to 50 nm. The *in vitro* antimicrobial experiments of Ag nanoparticle-loaded topical gels revealed good bactericidal activity against *S. aureus* and *E. coli* with a minimum inhibitory concentration (MIC) of 1.05 and minimum bactericidal concentration (MBC) of more than 16.83, indicating that the topical gels are potential systems for the treatment of bacteria-infected wounds [192]. The Carbopol-based topical gels encapsulated with Ag nanoparticles were synthesized by Sharma and co-workers, and the *in vivo* wound closure studies utilizing a full-thickness excision wound model in female SD rats showed that an increased concentration of Ag nanoparticles in gels significantly improved wound contraction over 100% with dense aligned collagen fibres and increased tensile strength in dressed wound tissues than placebo and standard (Ag sulfadiazine) group. The skin toxicity analysis displayed the absence of signs of oedema, inflammation, and irritation on the dorsum of rats [193].
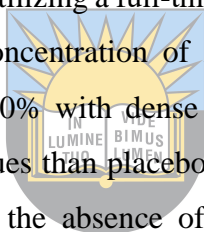
Jain and co-workers reported Carbopol-based topical gels enriched with Ag nanoparticles for the management of microbial-infected injuries. The high-resolution transmission electron microscopy (HRTEM) showed that the Ag nanoparticles were spherical with a size range of 7-20 nm. The antibacterial studies of Ag nanoparticle-loaded gels exhibited MICs values in the range of 1.56-6.25 μg/mL for all the bacterial strains (*P. aeruginosa*, *S. aureus*, *B. subtilis*, etc.) while the MBC values were 12.5 μg/mL, indicating excellent antibacterial activity that [194]. Fatima *et al*. fabricated chitosan-based topical gels incorporated with Ag nanoparticles for wound healing application. The pH test of the topical gels exhibited a pH of 6.2, suggesting that these topical formulations can be skin compatible and may not result in any dermal irritation. The biocompatibility analysis displayed that Ag nanoparticle-loaded chitosan topical gels possessed good protective effects on the red blood cells by preventing cell damage. Furthermore, *in vivo* wound closure analysis showed a progressive healing process in the wounds dressed with gels encapsulated with Ag nanoparticles than those dressed with standard (Ag sulfadiazine) and negative control (placebo) [195].

The research reports that are based on topical gels containing essential oils (TTO and lavender oil) are very few. Reichling *et al*. reported polyacrylate-based gels enriched with TTO for topical applications. The permeation studies exhibited that the key compound of TTO (terpinen-4-ol) was released from the topical gels compared to the cream, indicating that these gels are promising systems that can be used as wound-healing agents for skin injuries [196]. Wróblewska and co-workers formulated Pluronic® F-127 Gels loaded with TTO and ketoconazole. The pH test of gels exhibited pH values that range between 6.5 and 6.8, showing that these topical gels are suitable systems compatible with human skin. The *in vitro* permeation analysis demonstrated that the penetration rate of ketoconazole from the gel formulations enriched with TTO was greater when compared to formulations with ketoconazole alone, demonstrating the ability of TTO as a potential skin penetration enhancer [197].

Sharma and Nautiyal developed carbopol-based topical gels loaded with lavender oil and rosemary oil for the management of bacteria-infected wounds. These gels displayed high spreadability, although those enriched with a high amount of lavender oil possessed reduced spreadability. The pH of all the gel formulations ranged between 4 and 5.5. The *in vitro* antimicrobial experiments showed that gels enriched with lavender oil had a higher zone of inhibition against *E. coli* (3.4 cm) and *S. aureus* (3.0) compared to the marketed formulation which displayed a zone of inhibition of 2.5 and 2.7 cm, respectively. These results demonstrated that lavender oil-loaded topical gels effectively manage infected injuries [198].
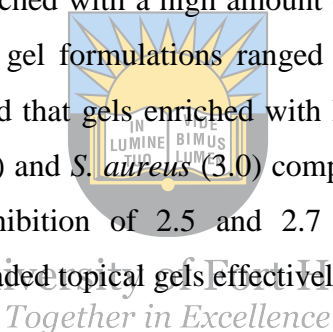
References

[1] Gomes, S.R.; Rodrigues, G.; Martins, G.G.; Roberto, M.A.; Mafra, M.; Henriques, C.M.R.; Silva, J.C. In vitro and in vivo evaluation of electrospun nanofibers of PCL, chitosan and gelatin: A comparative study. *Mater. Sci. Eng. C* **2015**, 46, 348–358. doi: 10.1016/j.msec.2014.10.051.

[2] Tottoli, E.M.; Dorati, R.; Genta, I.; Chiesa, E.; Pisani, S.; Conti, B. Skin Wound Healing Process and New Emerging Technologies for Skin Wound Care and Regeneration. *Pharmaceutics* **2020**, 17, 735, 2020. doi:10.3390/pharmaceutics12080735.

[3] Zerres, S.; Stahl, W. Carotenoids in human skin ☆. *BBA - Mol. Cell Biol. Lipids* **2019**, 1865, 158588. doi: 10.1016/j.bbalip.2019.158588.

[4] Cañedo-dorantes, L.; Cañedo-ayala, M. Skin Acute Wound Healing : A Comprehensive

Review. *Int. J. Inflammation* **2019**, 2019, 15 pages. doi: 10.1155/2019/3706315

[5]   Chouhan, D.; Mandal, B.B. Silk biomaterials in wound healing and skin regeneration therapeutics: From bench to bedside. *Acta Biomater.* **2020**, 103, 24–51. doi: 10.1016/j.actbio.2019.11.050.

[6]   Wang, Y.; Feng, Z.; Yang, M.; Zeng, L.; Qi, B.; Yin, S.; Li, B.; Li, Y.; Fu, Z.; Shu, L.; Fu, C.; Qin, P.; Meng, Y.; Li, X.; Yang, Y.; Tang, J.; Yang, X. Discovery of a novel short peptide with efficacy in accelerating the healing of skin wounds," *Pharm. Res.*, vol. 163, p. 105296, 2021, doi: 10.1016/j.phrs.2020.105296.

[7]   Niska, K.; Zielinska, E.; Witold, M.; Inkielewicz-stepniak, I. Metal nanoparticles in dermatology and cosmetology : Interactions with human skin cells. *Chem. Biol. Interact.* **2018**, 295, 38–51. doi: 10.1016/j.cbi.2017.06.018.

[8]   Wang, J.; Windbergs, M. Functional electrospun fibers for the treatment of human skin wounds. *Eur. J. Pharm. Biopharm.* **2017**, 119, 283–299. doi: 10.1016/j.ejpb.2017.07.001.

[9]   Abdo, J.M.; Sopko, N.A.; Milner, S.M. The applied anatomy of human skin : A model for regeneration. *Wound Med.* **2020**, 28, 100179. doi: 10.1016/j.wndm.2020.100179.

[10]   Sahle, F.F.; Gebre-Mariam, T.; Dobner, B.; Wohlrab, J.; Neubert, R.H.H. Skin diseases associated with the depletion of stratum corneum lipids and stratum corneum lipid substitution therapy. *Skin Pharmacol. Physiol.* **2015**, 28, 42–55. doi: 10.1159/000360009.

[11]   Blair, M.J.; Jones, J.D.; Woessner, A.E.; Quinn, K.P. Skin Structure – Function Relationships and the Wound Healing Response to Intrinsic Aging. *Adv. Wound Care* 2019, 9, 127–143. doi: 10.1089/wound.2019.1021.

[12]   Rippa, A.L.; Kalabusheva, E. P.; Vorotelyak, E.A. Regeneration of Dermis: Scarring and Cells Involved. *cells* 2019, 8, 607. ; doi:10.3390/cells8060607.

[13]   Zomer, H. D.; Trentin, A.G. Skin wound healing in humans and mice : Challenges in translational research. *J. Dermatol. Sci.* **2018**, 90, 3–12. doi: 10.1016/j.jdermsci.2017.12.009.

[14]   Dias, J.R.; Granja, P.L.; Bártolo, P.J. Advances in electrospun skin substitutes. *Prog. Mater. Sci.* **2016**, 84, 314–334. doi: 10.1016/j.pmatsci.2016.09.006.

[15] Watt, F. Mammalian skin cell biology: at the interface between laboratory and clinic. *Science* **2014**, 346, 937–940.

[16] DeMers, N.M.; Bowers, J.W.; Appin, C.; Morgan, M.B. Malignant histiocytosis of the skin: a case report and review of the literature. *J. Dermatol. Case Rep.* **2009**, 1, 4–7. doi: 10.3315/jdcr.2009.1024.

[17] Yamate, J. Chapter 19 - The Skin and Subcutis. *Boorman's Pathol. Rat (Second Ed.*, **2018**, 323–345.

[18] Fuchs, C.; Pham, L.; Henderson, J.; Stalnaker, J.R.; Anderson, K.R.; Tam, J. Multi-faceted enhancement of full-thickness skin wound healing by treatment with autologous micro skin tissue columns. *Sci. Rep.* **2021**, 11, 1668. doi: 10.1038/s41598-021-81179-7.

[19] Sen, C.K.; Gordillo, G.M.; Roy, S.; Kirsner, R.; Lambert, L.; Hunt, T.K.; Gottrup, F.; Gurtner, G.C.; Longaker, M.T. Human skin wounds: a major and snowballing threat to public health and the economy. *Wound Repair Regen*. **2009**,17, 763–771.

[20] Cha, J.; Falanga, V. Stem cells in cutaneous wound healing. *Clin. Dermatol.* **2007**, 25, 73–8.

[21] Han, G.; Ceilley, R. Chronic Wound Healing: A Review of Current Management and Treatments. *Adv. Ther.* **2017**, 34, 599–610. doi: 10.1007/s12325-017-0478-y

[22] Kumar, A.; Behl, T.; Chadha, S. A rationalized and innovative perspective of nanotechnology and nanobiotechnology in chronic wound management. *J. Drug Deliv. Sci. Technol.* **2020**, 60, 101930. doi: 10.1016/j.jddst.2020.101930.

[23] Arif, M.M.; Khan, S.; Gull, N.; Tabish, T.A.; Zia, S.; Khan, R.J.; Awas, S.M. Butt, M.A. Polymer-based biomaterials for chronic wound management: Promises and challenges. *Int. J. Pharm.* **2021**, 598, 120270. doi: 10.1016/j.ijpharm.2021.120270.

[24] Heublein, H.; Bader, A.; Giri, S. Preclinical and clinical evidence for stem cell therapies as treatment for diabetic wounds. *Drug Discov. Today* **2015**, 20, 703–717. doi: 10.1016/j.drudis.2015.01.005.

[25] Vijayakumar, V.; Samal, S.K.; Mohanty, S.; Nayak, S. K. Recent advancements in biopolymer and metal nanoparticle-based materials in diabetic wound healing management. *Int. J. Biol. Macromol.* **2019**, 122, 137–148.doi:

10.1016/j.ijbiomac.2018.10.120.

[26] Choudhury, H.; Pandey, M.; Lim, Y.Q.; Low, C.Y.; Lee, C.T.; Cheng, T.; Marilyn, L.; Seang, H.; Ping, Y.; Feng, C.; Kesharwanid, P.; Gorain, B. Silver nanoparticles: Advanced and promising technology in diabetic wound therapy," *Mater. Sci. Eng. C*, vol. 112, p. 110925, 2020, doi: 10.1016/j.msec.2020.110925.

[27] Cho, H.; Blatchley, M.R.; Duh, E.J.; Gerecht, S. Acellular and cellular approaches to improve diabetic wound healing. *Adv. Drug Deliv. Rev.* **2019**, 146, 267–288. doi: 10.1016/j.addr.2018.07.019.

[28] Sarkar, S; Mukhopadhyay, A.; Chaudhary, A.; Rajput, M.; Singh, H.; Mukherjee, R.; Das, A.K.; Banerjee, P.; Chatterjee, J. Therapeutic interfaces of honey in diabetic wound pathology. *Biochem. Pharmacol.* **2017**, 18, 21–32. doi: 10.1016/j.wndm.2017.07.001.

[29] Li, J.; Wei, M.; Liu, X.; Xiao, S.; Cai, Y.; Li, F.; Tian, J.; Qi, F.; Xu, G.; Deng, C. The progress, prospects, and challenges of the use of non-coding RNA for diabetic wounds. *Mol. Ther. Nucleic Acid* **2021**, 24, 554–578. doi: 10.1016/j.omtn.2021.03.015.

[30] Prabhakar, P. K.; Singh, K.; Kabra, D.; Gupta. J. Natural SIRT1 modifiers as promising therapeutic agents for improving diabetic wound healing. *Phytomedicine* **2020**, 76, 153252. doi: 10.1016/j.phymed.2020.153252.

[31] Den Dekker, A.; Davis, F.M.; Kunkel, S.L.; Gallagher, K.A. Targeting epigenetic mechanisms in diabetic. *Transl. Res.* **2018**, 204, 39–50, 2018, doi: 10.1016/j.trsl.2018.10.001.

[32] Shad, S.A.; Sohail, M.; Kha, S.; Minhas, M.U.; de Matas, M.; Sikstone, V.; Hussain, Z.; Abbasi, M.; Kousar, M. Biopolymer-based biomaterials for accelerated diabetic wound healing: A critical review. *Int. J. Biol. Macromol.* **2019**, 139, 975–993. doi: 10.1016/j.ijbiomac.2019.08.007.

[33] Gadelkarim, M.; Abushouk, A.I.; Ghanem, E.; Hamaad, A.M.; Saad, A.M.; M.M. Abdel-daim, "Adipose-derived stem cells : Effectiveness and advances in delivery in diabetic wound healing. *Biomed. Pharmacother.* **2018**, 07, 625–633. doi: 10.1016/j.biopha.2018.08.013.

[34] Witkowski, J.A.; Parish, L.C. Wound Healing and Leg Ulcers: Unapproved Treatments

or Indications. *Clin. Dermatol.* **1999**, 18, 211–217. PII S0738-081X(99)00113-3.

[35]   Guest, J.F.; Ayoub, N.; McIlwraith, T.; Uchegbu, I.; Gerrish, A.; Weidlich, D.; Vowden, K.; Vowden, P. Health economic burden that different wound types impose on the UK's national health service. *Int. Wound J.* **2017**, 14, 322–330.

[36]   Pascarella, L.; Shortell, C.K. Medical management of venous ulcers. *Semin. Vasc. Surg.* **2015**, 28, 21–28. doi: 10.1053/j.semvascsurg.2015.06.001.

[37]   Kokkosis, A.A.; Labropoulos, N.; Gasparis, A.P. Investigation of venous ulcers. *Semin. Vasc. Surg.* **2015**, 28, 15–20. doi: 10.1053/j.semvascsurg.2015.06.002.

[38]   Meulendijks, A.M.; Franssen, W.M.A.; Schoonhoven, L.; Neumann, H.A.M. A scoping review on Chronic Venous Disease and the development of a Venous Leg Ulcer: The role of obesity and mobility. *J. Tissue Viability* **2020**, 29, 190–196. doi: 10.1016/j.jtv.2019.10.002.

[39]   Cooper, M.A.; Qazi, U.; Bass, E.; Zenilman, J.; Lazarus, G.; Valle, M.F.; Malas, M.B. Medical and surgical treatment of chronic venous ulcers. *Semin. Vasc. Surg.* **2015**. 28, 160–164. doi: 10.1053/j.semvascsurg.2015.12.003.

[40]   Athanerey, A.; Kumar, P.; Kumar, A. Mesenchymal stem cell in venous leg ulcer: An intoxicating therapy. *J. Tissue Viability* **2017**, 26, 216–223. doi: 10.1016/j.jtv.2017.06.001.

[41]   Tan, M.K.H.; Luo, R.; Onida, S.; Maccatrozzo, S.; Davies, A. H. Venous Leg Ulcer Clinical Practice Guidelines : What is AGREEd ?. *Eur. J. Vasc. Endovasc. Surg.* **2019**, 57, 121–129. doi: 10.1016/j.ejvs.2018.08.043.

[42]   Lal, B.K. Venous ulcers of the lower extremity: Definition, epidemiology, and economic and social burdens. *Semin. Vasc. Surg.* 2015,28, 3–5. doi: 10.1053/j.semvascsurg.2015.05.002.

[43]   Lamel, S.A.; Kirsner, R.S. New approaches to enhanced wound healing: future modalities for chronic venous ulcers. *Drug Discov. Today Dis. Mech.* **2013**, 10, e71–e77. doi: 10.1016/j.ddmec.2012.12.002.

[44]   Rabe, E.; Pannier, F. Societal costs of chronic venous disease in CEAP C4, C5, C6 disease. *Phlebology* 2010, 25, 64–7.

[45] Triantafyllou, C.; Chorianopoulou, E.; Kourkouni, E.; Zaoutis, T.E.; Kourlaba, G. Prevalence, incidence, length of stay and cost of healthcare-acquired pressure ulcers in pediatric populations: A systematic review. *Int. J. Nurs. Stud.* **2021**, 115, 103843. doi: 10.1016/j.ijnurstu.2020.103843.

[46] Kottner, J.; Black, J.; Call, E.; Gefen, A.; Santamaria, N. Microclimate: A critical review in the context of pressure ulcer prevention. *Clin. Biomech.* **2018**, 59, 62–70. doi: 10.1016/j.clinbiomech.2018.09.010.

[47] Gorecki, C.; Closs, S.J.; Nixon, J.; Briggs, M. Patient-Reported Pressure Ulcer Pain : A Mixed-Methods Systematic Review. *J. Pain Symptom Manage.* **2011**, 42, 443–459. doi: 10.1016/j.jpainsymman.2010.11.016.

[48] Chou, R.; Dana, T.; Bougatsos, C.; Al., E. Pressure ulcer risk assessment and prevention: a systematic comparative effectiveness review. *Ann Intern Med.* **2013**, 159, 28–38.

[49] Mervis, J.S.; Phillips, T.J. Pressure ulcers: Pathophysiology, epidemiology, risk factors, and presentation. *J. Am. Dermatology* **2022**, 81, 881–890. doi: 10.1016/j.jaad.2018.12.069.

[50] Mcevoy, N.; Avsar, P.; Patton, D.; Curley, G.; Kearney, C.J.; Moore, Z. The economic impact of pressure ulcers among patients in intensive care units: A systematic review. *J. Tissue Viability* 2021, 30, 168–177. doi: 10.1016/j.jtv.2020.12.004.

[51] Padula, W.; Mishra, M.; Makic, M.; Sullivan, P. Improving the quality of pressure ulcer care with prevention: a cost-effectiveness analysis. *Med. Care* **2011**, 49, 385–392.

[52] Bauer, K.; Rock, K.; Nazzal, M.; Jones, O.; Qu, W. Pressure ulcers in the United States' inpatient population from 2008 to 2012: results of a retrospective nationwide study. *Ostomy Wound Manag.* **2016**, 62, 30–38.

[53] Wang, Y.; Beekman, J.; Hew, J.; Jackson, S.; Issler-fisher, A.C.; Parungao, R.; Lajevardi, S.S.; Li, Z.; Maitz, P.K.M. Burn injury: Challenges and advances in burn wound healing , infection , pain and scarring. *Adv. Drug Deliv. Rev.* **2018**, 123, 3–17. doi: 10.1016/j.addr.2017.09.018.

[54] Watt, S.M.; Pleat, J.M. Stem cells , niches and scaffolds : Applications to burns and

wound care ☆. *Adv. Drug Deliv. Rev.* **2018**, 123, 82–106. doi:
10.1016/j.addr.2017.10.012.

[55]   Markeson D.; Pleat, J.M.; Sharpe, J.R.; Harris, A.L.; Seifalian, A.M.; S. Watt, M.
Scarring, stem cells, scaffolds and skin repair. *J. Tissue Eng. Regen. Med.* **2015**, 9,
649–668.

[56]   ter Horst, B.; Chouhan, G.; Moiemen, N.S.; Grover, L.M. Advances in keratinocyte
delivery in burn wound care. *Adv. Drug Deliv. Rev.* 2018, 123, 18–32, 2018, doi:
10.1016/j.addr.2017.06.012.

[57]   Jyoti, K.; Malik, G.; Chaudhary, M.; Sharma, M.; Goswami, M.; Prakash, O.; Bala, S.;
Madan, J. Chitosan and phospholipid assisted topical fusidic acid drug delivery in burn
wound: Strategies to conquer pharmaceutical and clinical challenges , opportunities
and future panorama. *Int. J. Biol. Macromol.* **2020**, 161, 325–335. doi:
10.1016/j.ijbiomac.2020.05.230.

[58]   Ullah, S.; Mansoor, S.; Ayub, A.; Zafar, H.; Feroz, F.; Khan, A.; Ali, M. Tissue and
Cell An update on stem cells applications in burn wound healing. *Tissue Cell* **2021**, 72,
p. 101527. doi: 10.1016/j.tice.2021.101527.

[59]   Nian, Y.J.; Chen, Z.Q.; Xue, D.D.; Yin, M.F. Advances in the research of diagnosis
techniques of burn depth. *Zhonghua Shao Shang Za Zhi* **2016**, 32, 698–701.

[60]   Scheffler, M.; Koranyi, S.; Meissner, W.; Strau, B.; Rosendahl, J. Efficacy of non-
pharmacological interventions for procedural pain relief in adults undergoing burn
wound care : A systematic review and meta-analysis of randomized controlled trials.
Burns **2018**, 4,1709–1720. doi: 10.1016/j.burns.2017.11.019.

[61]   Provençal, S.; Bond, S.; Rizkallah, E.; El-baalbaki, G. Hypnosis for burn wound care
pain and anxiety : A systematic review and meta-analysis. *Burns* **2018**, 44, 1870–1881.
doi: 10.1016/j.burns.2018.04.017.

[62]   Jaspers, M.E.H.; Van Haasterecht, L.; van Zuijlen, P.P.; Mokkink, L.B. A systematic
review on the quality of measurement techniques for the assessment of burn wound
depth or healing potential. *Burns* **2018**, 45, 261–281. doi:
10.1016/j.burns.2018.05.015.

[63]   Davies, A.; Spickett-jones, F.; Jenkins, A.T.A.; Young, A.E. A systematic review of

intervention studies demonstrates the need to develop a minimum set of indicators to report the presence of burn wound infection. *Burns* **2020**, 46, 1487–1497. doi: 10.1016/j.burns.2020.03.009.

[64] Seth, A.K.; Geringer, M.R.; Hong, S.J.; Leung, K.P.; Mustoe, T.A.; Galiano, R.D. In vivo modeling of biofilm-infected wounds: A review. *J. Surg. Res.* **2012**, 178, 330–338. doi: 10.1016/j.jss.2012.06.048.

[65] Scalise, A.; Bianchi, A.; Tartaglione, C.; Bolletta, E.; Pierangeli, M.; Torresetti, M.; Marazzi, M.; Benedetto, G.D. Microenvironment and microbiology of skin wounds : the role of bacterial bio fi lms and related factors. *Semin. in Va* **2016**, 28, 151–159. doi: 10.1053/j.semvascsurg.2016.01.003.

[66] Robson, M.C.; Steed, D.L.; Franz, M.G. Wound healing: biologic features and approaches tomaximize healing trajectories. *Curr. Probl. Surg.* **2001**, *2*, 72–140. doi: 10.1067/msg.2001.111167.

[67] Yoon, R.; Chang, K.; Morales, S.; Okamoto, Y.; Chan, H. Topical application of bacteriophages for treatment of wound infections. *Transl. Res.* **2020**, 220, 153–166. doi: 10.1016/j.trsl.2020.03.010.

[68] Okur, M.E.; Karantas, I.D.; Siafaka, P. I. Recent trends on wound management : New therapeutic choices based on polymer carriers. *Asian J. Pharm. Sci.* **2020**, 15, 661–684. doi: 10.1016/j.ajps.2019.11.008.

[69] Shankar, G.; Mahendiran, B.; Gopalakrishnan, S.; Muthusamy, S.; Elangovan, S. Honey based treatment strategies for infected wounds and burns : A systematic review of recent pre-clinical research. *Wound Med.* **2020**, 30, 100188. doi: 10.1016/j.wndm.2020.100188.

[70] Hasannejad-bibalan, M.; Jafari, A.; Sabati, H.; Goswami, R.; Jafaryparvar, Z.; Sedaghat, F.; Ebrahim-Saraie, H.S. Risk of type III secretion systems in burn patients with Pseudomonas aeruginosa wound infection: A systematic review and meta-analysis. *Burns* **2020**, 47, 538-544. doi: 10.1016/j.burns.2020.04.024.

[71] Sorg, H.; Tilkorn, D.J.; Hager, S.; Hauser, J.; Mirastschijski, U. Skin Wound Healing : An Update on the Current Knowledge and Concepts. *Eur. Surg. Res.* **2017**, 58, 81–94, doi: 10.1159/000454919.

[72]   Han, R.; Ceilley, G. Chronic wound healing: a review of current management and treatments. *Adv. Ther.* 2017, 34, 599–610. doi: 10.1007/s12325-017-0478-y.

[73]   Rivera E.A.; Spencer, J.M. Clinical aspects of full-thickness wound healing. *Clin. Dermatol.* **2007**, 25, 39–48. doi: 10.1016/j.clindermatol.2006.10.001.

[74]   Zuliani-Alvarez, L.; Midwood, K.S. Fibrinogen-related proteins in tissue repair: How a unique domain with a common structure controls diverse aspects of wound healing. *Adv. Wound Care* **2015**, 4, 273–285. doi: 10.1089/wound.2014.0599.

[75]   Rumbaut, R.E.; Thiagarajan, P. Platelet-Vessel Wall Interactions in Hemostasis and Thrombosis. *San Rafael, CA Morgan Claypool Life Sci.* **2010**. PMID: 21452436.

[76]   Godo, S.; Shimokawa, H. Endothelial Functions. *Arter. Thromb Vasc Biol.* **2017**, 37, 108–114. doi: 10.1161/ATVBAHA.117.309813.

[77]   Rodrigues, M.; Kosaric, N.; Bonham, C.A.; Gurtner, G.C. WOUND HEALING : A CELLULAR PERSPECTIVE. *Physiol Rev.* **2018**, 99, 665–706. doi: 10.1152/physrev.00067.2017.

[78]   Abousamra, M.M. Nanoparticles as Safe and Effective Drug Delivery Systems for Wound Healing. *Austin J. Nanomed. Nanotechnol.* **2019**, 7, 1056.

[79]   Van der Vliet, A.; Janssen-Heininger, Y.M. Hydrogen peroxide as a damage signal in tissue injury and inflammation: murderer, mediator, or messenger?. *J Cell Biochem.* **2014**, 115, 427–435. doi: 10.1002/jcb.24683.

[80]   Wilgus, T.A.; Roy, S.; McDaniel, J.C. Neutrophils and Wound Repair: Positive Actions and Negative Reactions. *Adv Wound Care (New Rochelle)* **2013**, 2, 379–388. doi: 10.1089/wound.2012.0383

[81]   Frykberg R.G.; Banks, J. Challenges in the treatment of chronic wounds. *Adv Wound Care (New Rochelle)* **2015**, 4, 560–82. PMID: 26339534.

[82]   Las Heras, K.; Igartua, M.; Santos-vizcaino, E.; Harnandez, M. Chronic wounds: Current status , available strategies and emerging therapeutic solutions. *J. Control. Release* **2020**, 328, 532–550. doi: 10.1016/j.jconrel.2020.09.039.

[83]   Gurtner, G.C.; Werner, S.; Barrandon, Y.; Longaker, M.T. Wound repair and regeneration. *Nature* **2008**, 453, 314–321.

[84] Tonnesen, M.G.; Feng, X.; Clark, R.A. Angiogenesis in wound healing. *J Investig Dermatol Symp Proc* **2000**, 5, 40–46. doi: 10.1046/j.1087-0024.2000.00014.x.

[85] Jayesh, B.S. The history of wound care. *J. Am. Col. Certif. Wound Spec.* 2011, 3, 65–66.

[86] Ghomi, E.R.; Khalili, S.; Khorasani, S.N.; Neisiany, R.E. Wound dressings : Current advances and future directions. *J. Appl. Polym. Sci.* **2019**, 47738, 1–12. doi: 10.1002/app.47738.

[87] Dhivya, S.; Padma, V.V.; Santhini, E. Wound dressings – a review. *BioMedicine* **2015**, 5, 24–28. doi: 10.7603/s40.

[88] Gaspar-pintiliescu, A.; Stanciuc, A.; Craciunescu, O. Natural composite dressings based on collagen, gelatin and plant bioactive compounds for wound healing: A review. *Int. J. Biol. Macromol.* **2019**, 138, 854–865. doi: 10.1016/j.ijbiomac.2019.07.155.

[89] Hussain, Z.; Thu, H.E.; Shuid, A.N.; Katas, H.; Hussain, F. Recent Advances in Polymer-based Wound Dressings for the Treatment of Diabetic Foot Ulcer : An Overview of State-of-the-art. *Curr. Drug Targets* **2017**, 18, 527–550. doi: 10.2174/1389450118666170704132523.

[90] Kenawy, E.; Omer, A.M.; Tamer, T.M.; Elmeligy, M.A.; Eldin, M.S.M. Fabrication of biodegradable gelatin / chitosan / cinnamaldehyde crosslinked membranes for antibacterial wound dressing applications. *Int. J. Biol. Macromol.* **2019**, 139, 440–448.doi: 10.1016/j.ijbiomac.2019.07.191.

[91] Alven, S.; Nqoro, X.; Aderibigbe, B.A. Polymer-Based Materials Loaded with Curcumin for Wound Healing Application. *Polymers (Basel).* **2020**, 12, 2286. doi: 10.3390/polym12102286.

[92] Borda, L.J.; Macquhae, F.E.; Kirsner, R.S. Wound Dressings: A Comprehensive Review. *Curr. Dermatol. Rep.* **2016**, 5, 287–297. doi: 10.1007/s13671-016-0162-5.

[93] Alven, S.; Buyana, B.; Feketshane, Z.; Aderibige, B.A. Electrospun Nanofibers / Nanofibrous Scaffolds Loaded with Silver Nanoparticles as Effective Antibacterial Wound Dressing Materials. *Pharmaceutics* 2021, 13, 964. doi: 10.3390/pharmaceutics13070964.

[94] Alven, S.; Aderibigbe, B.A. Chitosan and Cellulose-Based Hydrogels for Wound Management. *Inter. J. Mol. Sci.* **2020**, 21, 9656. doi: 10.3390/ijms21249656.

[95] Gupta, B.; Agarwal, R.; Alam, M. Textile-based smart wound dressings. *Indian J. Fibre Text. Res.* 2010, 35, 174–184.

[96] Ndlovu, S.P.; Ngece, K.; Alven, S.; Aderibigbe, B.A. Gelatin-Based Hybrid Scaffolds : Promising Wound Dressings. *Polymers (Basel).* 2021, 13, 2959. doi: 10.3390/polym13172959.

[97] Benskin, L.L. Evidence for Polymeric Membrane Dressings as a Unique Dressing Subcategory, Using Pressure Ulcers as an Example. *Adv. Wound Care* **2018**, 7, 419–426. doi: 10.1089/wound.2018.0822.

[98] Ramos-e-silva, M.; Cristina, M.; Castro, R.D.E. New Dressings, Including Tissue-Engineered Living Skin. *Clin. Dermatol.* **2002**, 20, 715–723, 2002. doi: 10.1016/s0738-081x(02)00298-5.

[99] Everett, E.; Mathioudakis, N. Update on management of diabetic foot ulcers," *Ann. NEW YORK Acad. Sci.* **2018**, 1411, 153–165. doi: 10.1111/nyas.13569.

[100] BOATENG, J.S.; MATTHEWS, K.H.; STEVENS, H.N.E.; ECCLESTON, G.M. Wound Healing Dressings and Drug Delivery Systems: A Review. *J. Pharm. Sci.* **2008**, 97, 2892–2923. doi: 10.1002/jps.

[101] Pott, F.S.; Meier, M.J.; Stocco, J.G.D.; Crozeta, K.; Ribas, J.D. The effectiveness of hydrocolloid dressings versus other dressings in the healing of pressure ulcers in adults and older adults: a systematic review and meta-analysis. *Rev. Lat. Am. Enfermagem.* **2014**, 22, 511–520. doi: 10.1590/0104-1169.3480.2445.

[102] Lee, O.J.; Kim, J.H.; Moon, B.M.; Chao, J.; Yoon, J.; Ju, H.W.; Lee, J.M.; Park, H.J.; Kim, D.W.; Kim, S.J.; Park, H.S.; Park, C.H. Fabrication and characterization of hydrocolloid dressing with silk fibroin nanoparticles for wound healing. *Tissue Eng. Regen. Med.* **2016**, 13, 218–226. doi: 10.1007/s13770-016-9058-5.

[103] Boateng, J.S.; Matthews, K.H.; Stevens, H.N.; Eccleston, G.M.Wound Healing Dressings and Drug Delivery Systems: A Review. *Indian J Pharml Sci* 2008, 97, 2892–923. doi: 10.1002/jps.21210.

[104] Aderibigbe, B.A.; Buyana, B. Alginate in Wound Dressings. *Pharmaceutics* **2018**, 10,

42. doi: 10.3390/pharmaceutics10020042.

[105] Alven, S.; Aderibigbe, B.A. Hyaluronic Acid-Based Scaffolds as Potential Bioactive Wound Dressings. *Polymers (Basel)* 2021, 13, 2102. doi: 10.3390/polym13132102.

[106] Paul, W.; Sharma, C. Chitosan and AlginateWound Dressings: A Short Review. *Trends Biomater. Artif. Organs* **2004**, 18, 18–23.

[107] Talikowska, M.; Fu, X.; Lisak, G. Application of conducting polymers to wound care and skin tissue engineering: A review. *Biosens. Bioelectron.* **2019**, 135, 50–63. doi: 10.1016/j.bios.2019.04.001.

[108] Portela, R.; Leal, C.R.; Almeida, P.; Sobral, R.G. Bacterial cellulose: A versatile biopolymer for wound dressing applications. *Microb. Biotechnol.* **2019**, 12, 586–610. doi: 10.1111/1751-7915.13392.

[109] Negut, I.; Dorcioman, G.; Grumezescu, V. Scaffolds for Wound Healing Applications. *Polymers (Basel)* **2020**, 12, 2010. doi: 10.3390/polym12092010.

[110] Naseri-nosar, M.; Ziora, Z. Wound dressings from naturally-occurring polymers: a review on homopolysaccharide-based composites. *Carbohydr. Polym.* **2018**, 189, 379–398. doi: 10.1016/j.carbpol.2018.02.003.

[111] Lv, L.; Huang, Q.; Ding, W.; Xiao, X.-H.; Zhang, H.-Y.; Xiang, L.-X. Fish gelatin: The novel potential applications. *J. Funct. Food* **2019**, 63, 103581. doi: 10.1016/j.jff.2019.103581.

[112] Liu, D.; Nikoo, M.; Boran, G.; Zhou, P.; Regenstein, J.M. Collagen and gelatin. *Annu. Rev. Food Sci. Technol.* **2015**, 6, 527–557. doi: 10.1146/annurev-food-031414-111800.

[113] Pati, F.; Datta, P.; Adhikari, B.; Dhara, S.; Ghosh, K.; Mohapatra, P.K.D. Collagen scaffolds derived from fresh water fish origin and their biocompatibility. *J. Biomed. Mater. Res. Part A* **2012**, 100, 1068–1079. doi: 10.1002/jbm.a.33280.

[114] Hayashi, Y.; Yamada, S.; Guchi, K.Y.; Koyama, Z.; Ikeda, T. Chitosan and fish collagen as biomaterials for regenerative medicine. *Adv. Food Nutr. Res.* **2012**, 65, 107–120. doi: 10.1016/B978-0-12-416003-3.00006-8.

[115] Suarato, G.; Bertorelli, R.; Athanassiou, A. Borrowing From Nature : Biopolymers and Biocomposites as Smart Wound Care Materials. *Front. Bioeng. Biotechnol.* **2018**, 6,

1–11. doi: 10.3389/fbioe.2018.00137.

[116] Zheng, Y.; Liang, Y.; Zhang, D.; Sun, X.; Liang, L.; Li, J.; Liu, Y. Gelatin-Based Hydrogels Blended with Gellan as an Injectable Wound Dressing. *ACS Omega* **2018**, 3, 4766–4775. doi: 10.1021/acsomega.8b00308.

[117] Hussain, Z.; Thu, H.E.; Shuid, A.N.; Katas, H.; Hussain, F. Recent Advances in Polymer-based Wound Dressings for the Treatment of Diabetic Foot Ulcer: An Overview of State-of-the-art. *Curr. Drug Targets* 2017, 19, 527–550. doi: 10.2174/1389450118666170704132523

[118] Mano, J.F.; Silva, G.A.; Azevedo, H.S.; Malafaya, P.B.; Sousa, R.A.; Silva, S.S.; Boesel, L.F.; Oliveira, J.M.; Santos, T.C.; Marques, A.P.; Neves, N.M.; Reis, R.L. Natural origin biodegradable systems in tissue engineering and regenerative medicine: present status and some moving trends. *J R Soc Interface* **2007**, 4, 999–1030. doi: 10.1098/rsif.2007.0220.

[119] Sannino, A..; Demitri, C.; Madaghiele, M. Biodegradable cellulosebased hydrogels: design and applications. *Materials (Basel)* 2009, 2, 353–373. doi: 10.1016/j.cis.2021.102415.

[120] Serafica, G.; Mormino, R.; Oster, G.; Lentz, K.; Koehler, K. Microbial cellulose wound dressing for treating chronic wounds. **2010**, US7704523 B2,.

[121] Pettignano, A.; Charlot, A.; Fleury, E. Carboxyl-functionalized derivatives of carboxymethyl cellulose: towards advanced biomedical applications. *Polym. Rev.* **2019**, 59, 510–560. doi: 10.1080/15583724.2019.1579226

[122] Wong, T.; Ramli, N.A. Carboxymethylcellulose film for bacterial wound infection control and healing. *Carbohydr. Polym.* **2014**, 112, 367–375. doi: 10.1016/j.carbpol.2014.06.002.

[123] Kanikireddy, V.; Varaprasad, K.; Jayaramudu, T.; Karthikeyan, C.; Sadiku, R. Carboxymethyl cellulose-based materials for infection control and wound healing: A review. *Int. J. Biol. Macromol.* **2020**, 164, 963–975. doi: 10.1016/j.ijbiomac.2020.07.160.

[124] Bacakova, M.; Pajorova, J.; Sopuch, T.; Bacakova, L. Fibrin-modified cellulose as a promising dressing for accelerated wound healing. *Mater.* **2018**, 11, 2314. doi:

10.3390/ma11112314.

[125] Barnea, Y.; Weiss, J.; Gur, E. A review of the applications of the hydrofiber dressing with silver (Aquacel Ag®) in wound care. *Ther. Clin. Risk Manag.* **2010**, 6, 21–27; doi: 10.2147/tcrm.s3462.

[126] Mathew-Steiner, S.S.; Roy, S.; Sen, C.K. Collagen in wound healing. *Bioengineering* **2021**, 8, 63. doi: 10.3390/bioengineering8050063.

[127] Vasconcelos, A.; Gomes, A.C.; Cavaco-Paulo, A. Novel silk fibroin/elastin wound dressings. *Acta Biomater.* **2012**, 8, 3049–3060. doi: 10.1016/j.actbio.2012.04.035.

[128] Jayakumar, R.; Prabaharan, M.; Kumar, P.T.S.; Nair, S.V.; Tamura, H. Biomaterials based on chitin and chitosan in wound dressing applications. *Biotechnol. Adv.* **2011**, 29, 322–337. doi: 10.1016/j.biotechadv.2011.01.005.

[129] Varaprasad, K.; Jayaramudu, T.; Kanikireddy, V.; Toro, C.; Sadiku, E.R. Alginate-based composite materials for wound dressing application: A mini review. *Carbohydr. Polym.* **2020**, 236, 116025. doi: 10.1016/j.carbpol.2020.116025.

[130] Graça, M.F.P.; Miguel, S.P.; Cabral, C.S.D.; Correia, I.J. Hyaluronic acid — Based wound dressings: A review. *Carbohydr. Polym.* **2020**, 241, 116364. doi: 10.1016/j.carbpol.2020.116364.

[131] Wen, Q.; Mithieux, S.M..; Weiss, A.S. Elastin Biomaterials in Dermal Repair. *Trends Biotechnol.* **2020**, 38, 280–291. doi: 10.1016/j.tibtech.2019.08.005.

[132] Chen, S.-L.; Fu, R.-H.; Liao, S.-F.; Liu, S.-P.; Lin, S.-Z.; Wang, Y.-C. A PEG-Based Hydrogel for Effective Wound Care Management. *Cell Transplant.* **2018**, 27, 275–284. doi: 10.1177/0963689717749032.

[133] Kardan, T.; Mohammadi, R.; Taghavifar, S.; Cheraghi, M.; Yahoo, A.; Mohammadnejad, K. Polyethylene Glycol–Based Nanocerium Improves Healing Responses in Excisional and Incisional Wound Models in Rats. *Int. J. Low. Extrem. Wounds* **2021**, 20, 1–9. doi: 10.1177/1534734620912102.

[134] Yang, Y.; Xia, T.; Chen, F.; Liu, C.; He, S.; Li, X. Electrospun fibers with plasmid bFGF polyplex loadings promote skin wound healing in diabetic rats. *Mol. Pharm.* **2012**, 9, 48–58. doi: 10.1021/mp200246b.

[135] Percival, S.L.; Chen, R.; Mayer, D.; Salisbury, A.M. Mode of action of poloxamer-based surfactants in wound care and efficacy on biofilms. *Int. Wound J.* **2018**, 15, 749–755. doi: 10.1111/iwj.12922.

[136] McLain, V. Safety assessment of poloxamers 101, 105, 108, 122, 123, 124, 181, 182, 183, 184, 185, 188, 212, 215, 217, 231, 234, 235, 237, 238, 282, 284, 288, 331, 333, 334, 335, 338, 401, 402, 403, and 407, poloxamer 105 benzoate, and poloxamer 182 dibenzoate as use. *Int J Toxicol.* **2008**, 27, 93–128. doi: 10.1080/10915810802244595.

[137] Babickaite, L.; Grigonis, A.; Ramanauskiene, K.; Matusevicius, A.P.; Zamokas, G.; Daunoras, G.; Ivaskiene, M. Therapeutic activity of chlorhexidine-poloxamer antiseptic gel on wound healing in rats: A preclinical study. *Pol. J. Vet. Sci.* **2018**, 21, 175–183. doi: 10.24425/119036.

[138] Contardi, M.; Kossyvaki, D.; Picone, P.; Summa, M.; Guo, X.; Heredia-Guerrero, J.A.; Giacomazza, D.; Carzino, R.; Goldoni, L.; Scoponi, G.; Rancan, F. Electrospun polyvinylpyrrolidone (PVP) hydrogels containing hydroxycinnamic acid derivatives as potential wound dressings. *Chem. Eng. J.* **2021**, 409, 128144. doi: 10.1016/j.cej.2020.128144.

[139] Kamoun, E.A.; Kenawy, E.S.; Chen, X. A review on polymeric hydrogel membranes for wound dressing applications: PVA-based hydrogel dressings. *J. Adv. Res.* **2017**, 8, 217–233. doi: 10.1016/j.jare.2017.01.005.

[140] Kim, S.E.; Heo, D.N.; Lee, J.B.; Kim, J.R.; Park, S.H.; Jeon, S.H.; Kwon, I.K. Electrospun gelatin/polyurethane blended nanofibers for wound healing. *Biomed. Mater.* **2009**, 4, 044106. doi: 10.1088/1748-6041/4/4/044106.

[141] Ghaee, A.; Bagheri-khoulenjani, S.; Amir, H.; Bogheiri, H. Biomimetic nanocomposite scaffolds based on surface modified PCL-nanofibers containing curcumin embedded in chitosan / gelatin for skin regeneration. *Compos. Part B* **2019**, 177, 107339. doi: 10.1016/j.compositesb.2019.107339.

[142] Cui, S.; Sun, X.; Li, K.; Gou, D.; Zhou, Y.; Hu, J.; Liu, Y. Polylactide nano fi bers delivering doxycycline for chronic wound treatment. *Mater. Sci. Eng. C* **2019**, 104, 109745. doi: 10.1016/j.msec.2019.109745.

[143] Armentano, I.; Dottori, M.; Fortunati, E.; Mattioli, S.; Kenny, J. Biodegradable

polymer matrix nanocomposites for tissue engineering: a review. *Polym Degrad Stab*. **2010**, 95, 2126–46. doi: 10.1016/j.polymdegradstab.2010.06.007

[144] Liu, S.; Kau, Y.; Chou, C.; Chen, J.; Wu, R.; Yeh, W. Electrospun PLGA / collagen nanofibrous membrane as early-stage wound dressing. *J. Memb. Sci.* **2010**, 355, 53–59. doi: 10.1016/j.memsci.2010.03.012.

[145] Kim, Y.; Kim, J.E.; Jung, Y.; Sun, J. Non-swellable , cytocompatible pHEMA-alginate hydrogels with high stiffness and toughness. *Mater. Sci. Eng. C* **2019**, 95, 86–94. doi: 10.1016/j.msec.2018.10.045.

[146] Etebu, E.; Arikekpar, I. Antibiotics: Classification and mechanisms of action with emphasis on molecular perspectives. *Int. J. Appl. Microbiol. Biotechnol. Res.* **2016**, 4, 90–101. ISSN 2053-18188.

[147] Friedman, N.D.; Temkin, E.; Carmeli, Y. The negative impact of antibiotic resistance. *Clin. Microbiol. Infect.* **2016**, 22, 416–422, 2016. doi: 10.1016/j.cmi.2015.12.002.

[148] Ceruelos, H.A.; Romero-Quezada, L.C.; Ledezma, R.J.C. Contreras, L.L. Therapeutic uses of metronidazole and its side effects: An update. *Eur. Rev. Med. Pharmacol. Sci.* **2019**, 23, 397–401. doi: 10.26355/eurrev_201901_16788.

[149] Dingsdag, S.A. Hunter, N. Metronidazole: An update on metabolism, structure-cytotoxicity and resistance mechanisms. *J. Antimicrob. Chemother.*2018, 73, 265–279. doi: 10.1093/jac/dkx351.

[150] Kurian, M.; Ganapathy, D.; Jain, A.R. Recent advances of metronidazole - A review. *Drug Invent. Today* **2018**, 10, 3536–3541.

[151] Ousey, K. The role of topical metronidazole in management of infected wounds. *Wounds UK* **2018**, 14, 105–109.

[152] Castro, D.L.V.D.; Santos, V.L.C.D.G. Controlling wound odor with metronidazole: A systematic review. *J. Sch. Nurs.* **2015**, 49, 858–863. doi: 10.1590/S0080-623420150000500021.

[153] Abousamra, M.M. Nanoparticles as Safe and Effective Drug Delivery Systems for Wound Healing. *Austin J. Nanomedicine Nanotechnol.* **2019**, 7, 1056.

[154] de Souza, M.L.; dos Santos, W.M.; de Sousa, A.L.M.D.; de Albuquerque Wanderley

Sales, V.; Nóbrega, F.P.; de Oliveira, M.V.; Rolim-Neto, P.J. Lipid Nanoparticles as a Skin Wound Healing Drug Delivery System: Discoveries and Advances. *Curr. Pharm. Des.* **2020**, 26, 4536–4550. doi: 10.2174/1381612826666200417144530.

[155] Rajendran, N.K.; Kumar, S.S.D.; Houreld, N.N.; Abrahamse, H. A review on nanoparticle based treatment for wound healing. *J. Drug Deliv. Sci. Technol.* **2018**, 44, 421–430. doi: 10.1016/j.jddst.2018.01.009.

[156] Gupta, A.; Briffa, S.M.; Swingler, S.; Gibson, H.; Kannappan, V.; Adamus, G.; Kowalczuk, M.; Martin, C.; Radecka, I. Synthesis of Silver Nanoparticles Using Curcumin-Cyclodextrins Loaded into Bacterial Cellulose-Based Hydrogels for Wound Dressing Applications. *Biomacromolecules* **2020**, 21, 1802–1811. doi: 10.1021/acs.biomac.9b01724.

[157] Das, C.A.; Kumar, V.G.; Dhas, T.S.; Karthick, V.; Govindaraju, K.; Joselin, J.M.; Baalamurugan, J. Antibacterial activity of silver nanoparticles (biosynthesis): A short review on recent advances. *Biocatal. Agric. Biotechnol.* **2020**, 27, 101593. doi: 10.1016/j.bcab.2020.101593.

[158] Konop, M.; Damps, T.; Misicka, A.; Rudnicka, L. Certain Aspects of Silver and Silver Nanoparticles in Wound Care: A Minireview. *J. Nanomater.* 2016, 2016, 7614753. doi: 10.1155/2016/7614753.

[159] Silva, M.M.P.; Aguiar, M.I.F.D.; Rodrigues, A.B.; Miranda, M.D.C.; Araújo, M.Â.M.; Rolim, I.L.T.P. The use of nanoparticles in wound treatment: a systematic review," *J. Sch. Nurs.* **2017**, 51e03272, DOI: http://dx.doi.org/10.1590/S1980-220X201604350.

[160] Negut, I.; Grumezescu, V.; Grumezescu, A.M. Treatment Strategies for Infected Wounds. *Molecules* **2018**, 23, 2392. doi: 10.3390/molecules23092392.

[161] Kavoosi, G.; Dadfar, S.M.M.; Purfard, A.M.; Mehrabi, R. Antioxidant and Antibacterial Properties of Gelatin Films Incorporated with Carvacrol. *J. Food Saf.* **2013**, 33, 423–432. doi: 10.1111/jfs.12071

[162] Nogueira, M.N.M.; Aquino, S.; Rossa Junior, C.; Spolidorio, D.M.P. Terpinen-4-ol and alpha-terpineol (tea tree oil components) inhibit the production of IL-1b, IL-6 and IL-10 on human macrophages. *Inflamm. Res.* **2014**, 63, 769–778. doi: 10.1007/s00011-014-0749-x.

[163] Ge, Y.; Ge, M. Sustained Broad-spectrum Antimicrobial and Haemostatic Chitosan-based Film with Immerged Tea Tree Oil Droplets. *Fibers Polym.* **2015**, 16, 308–318. doi: 10.1007/s12221-015-0308-2.

[164] Mahmood, H.; Khan, I.U.; Asif, M.; Khan, R.U.; Asghar, S.; Khalid, I.; Khalid, S.H.; Irfan, M.; Rehman, F.; Shahzad, Y.; Yousaf, A.M. In vitro and in vivo evaluation of gellan gum hydrogel films: Assessing the co impact of therapeutic oils and ofloxacin on wound healing. *Int. J. Biol. Macromol.* 2021, 166, 483–495. doi: 10.1016/j.ijbiomac.2020.10.206.

[165] Najafi-taher, R.; Ghaemi, B. Kharazi, S. Rasoulikoohi, S.; Amani, A. Promising Antibacterial Effects of Silver Nanoparticle-Loaded Tea Tree Oil Nanoemulsion: a Synergistic Combination Against Resistance Threat. *AAPS PharmSciTech* **2018**, 19, 1133-1140. doi: 10.1208/s12249-017-0922-y.

[166] Lee, R.; Leung, P.; Wong, T. A randomized controlled trial of topical tea tree preparation for MRSA colonized wounds. *Int. J. Nurs. Sci.* **2014**, 1, 7–14. doi:10.1016/j.ijnss.2014.01.001

[167] Evandri, M.G.; Battinelli, L.; Daniele, C.; Mastrangelo, S.; Bolle, P.; Mazzanti, G. The antimutagenic activity of Lavandula angustifolia (lavender) essential oil in the bacterial reverse mutation assay. *Food Chem. Toxicol.* **2005**, 43, 1381–1387. doi: 10.1016/j.fct.2005.03.013.

[168] Cavanagh, H.M.A.; Wilkinson, J.M. Biological activities of lavender essentials oil," *Phytother. Res.* **2002**, 16, 301–308. doi: 10.1002/ptr.1103.

[169] Sofi, H.S.; Akram, T.; Tamboli, A.H.; Majeed, A.; Shabir, N.; Sheikh, F.A. Novel lavender oil and silver nanoparticles simultaneously loaded onto polyurethane nano fi bers for wound-healing applications. *Internatinal J. Pha* **2019**, 569, 118590. doi: 10.1016/j.ijpharm.2019.118590.

[170] EĞRİ, O. Production of lavender oil loaded antibacterial polymeric membranes. *Cumhur. Sci. J.* **2020**, 41, 160–168.. doi:10.17776/csj.624419

[171] Tajik, F.; Eslahi, N.; Rashidi, A.; Rad, M.M. Hybrid antibacterial hydrogels based on PVP and keratin incorporated with lavender extract. *J. Polym. Res.* **2021**, 28, 316. doi: 10.1007/s10965-021-02681-0.

[172] Yang, X.; Liu, W.; Xi, G.; Wang, M.; Liang, B.; Shi, Y.; Feng, Y.; Ren, X.; Shi, C. Fabricating antimicrobial peptideimmobilized starch sponges for hemorrhage control and antibacterial treatment. *Carbohydr. Polym.* 2019, 22, 115012. doi: 10.1016/j.carbpol.2019.115012.

[173] Feng, Y.; Li, X.; Zhang, Q.; Yan, S.; Guo, Y.; Li, M.; You, R. Mechanically robust and flexible silk protein/polysaccharide composite sponges for wound dressing. *Carbohydr. Polym.* **2019**, 216, 17-24. doi: 10.1016/j.carbpol.2019.04.008.

[174] Villamizar-Sarmiento, M.G.; Moreno-Villoslada, I.; Martínez, S.; Giacaman, A.; Miranda, V.; Vidal, A.; Orellana, S.L.;Concha, M.; Pavicic, F.; Lisoni, J.G.; Leyton, L. Ionic Nanocomplexes of Hyaluronic Acid and Polyarginine to Form Solid Materials: A Green Methodology to Obtain Sponges with Biomedical Potential. *Nanomaterials* 2019, 9, 944. doi: 10.3390/nano9070944

[175] Ma, R., Wang, Y., Qi, H., Shi, C., Wei, G., Xiao, L., Huang, Z., Liu, S., Yu, H., Teng, C. and Liu, H. Nanocomposite sponges of sodium alginate/ graphene oxide/ polyvinyl alcohol as potential wound dressing: In vitro and in vivo evaluation. *Compos. Part B*, **2019**, 167, 396–405. doi: 10.1016/j.compositesb.2019.03.006.

[176] Simões, D.; Miguel, S.P.; Ribeiro, M.P.; Coutinho, P.; Mendonça, A.G. Correia, I.J. Recent advances on antimicrobial wound dressing: A review. *Eur. J. Pharm. Biopharm.* **2018**, 127, 130–141. doi: 10.1016/j.ejpb.2018.02.022.

[177] Naghshineh, N.; Tahvildari, K.; Nozari, M. Preparation of Chitosan, Sodium Alginate, Gelatin and Collagen Biodegradable Sponge Composites and their Application in Wound Healing and Curcumin Delivery. *J. Polym. Environ.* **2019**, 27, 2819–2830. doi: 10.1007/s10924-019-01559-z.

[178] Wen, Y.; Yu, B.; Zhu, Z.; Ynang, Z.; Shao, W. Synthesis of Antibacterial Gelatin / Sodium Alginate Sponges and Their Antibacterial Activity. *Polymers (Basel)* **2020**, 12, 1926. doi: 10.3390/polym12091926.

[179] Tamahkar, E.; Özkahraman, B.; Özbaş, Z.; Izbudak, B.; Yarimcan, F.; Boran, F.; Öztürk, A.B. Aloe vera-based antibacterial porous sponges for wound dressing applications. *J. Porous Mater.* **2021**, 28, 741–750. doi: 10.1007/s10934-020-01029-1.

[180] Wang, X.; Guo, J.; Zhang, Q.; Zhu, S.; Liu, L.; Jiang, X.; Wei, D.H.; Liu, R.S.; Li, L.

Gelatin sponge functionalized with gold/ silver clusters for antibacterial application. *Nanotechnology* **2020**, 31, 134004. doi: 10.1088/1361-6528/ab59eb.

[181] Zou, Y.; Xie, R.; Hu, E.; Qian, P.; Lu, B.; Lan, G.; Lu, F. protein-reduced gold nanoparticles mixed with gentamicin sulfate and loaded into konjac/ gelatin sponge heal wounds and kill drug-resistant bacteria. *Int. J. Biol. Macromol.* **2020**, 148, 921–931.doi: 10.1016/j.ijbiomac.2020.01.190.

[182] Ye, S.; Jiang, L.; Su, C.; Zhu, Z.; Wen, Y.; Shao, W. Development of gelatin / bacterial cellulose composite sponges as potential natural wound dressings. *Int. J. Biol. Macromol.* **2019**, 133, 148–155. doi: 10.1016/j.ijbiomac.2019.04.095.

[183] Das, S.; Dey, T.K.; De, A.; Banerjee, A.; Chakraborty, S.; Das, B.; Mukhopadhyay, A.K.; Mukherjee, B.; Samanta, A. Antimicrobial loaded gum odina - gelatin-based biomimetic spongy scaffold for accelerated wound healing with complete cutaneous texture. *Int. J. Pharm.* **2021**, 606, 120892. doi: 10.1016/j.ijpharm.2021.120892.

[184] Sneha Letha, S.; Shukla, S.K.; Haridas, N.; Smitha, R.P.; Sidharth Mohan, M. In vitro and In vivo Biocompatibility Evaluation of Freeze-Dried Gelatin Haemostat. *Fibers Polym.* **2021**, 22, 621–628. doi: 10.1007/s12221-021-0268-7.

[185] Kaur, L.P.; Garg, R.; Gupta, G. Topical Gels: A Review. *Res. J. Pharm. Tech.* **2010**, 3, 17–24.

[186] Hagen, M.; Baker, M. Skin penetration and tissue permeation after topical administration of diclofenac. *Curr. Med. Res. Opin.* **2017**, 33, 1623–1634.

[187] Buyana, B.; Aderibigbe, B.A.; Ndinteh, D.T.; Fonkui, Y.T.; Kumar, P. Alginate-pluronic topical gels loaded with thymol, norfloxacin and ZnO nanoparticles as potential wound dressings. *J. Drug Deliv. Sci. Technol.* **2020**, 60, 101960. doi: 10.1016/j.jddst.2020.101960.

[188] Lipsky, B.A.; Hoey, C. Topical antimicrobial therapy for treating chronic wounds. *Clin. Infect. Dis.* **2009**, 49, 1541–1549. doi: 10.1086/644732.

[189] Patil, S.; George, T.; Mahadik, K. Green synthesized nanosilver loaded silk fibroin gel for enhanced wound healing. *J. Drug Deliv. Sci. Technol.* **2015**, 30, 30–36. doi: 10.1016/j.jddst.2015.09.001.

[190] Pérez-díaz, M.; Alvarado-gomez, E.; Magaña-aquino, M.; Sánchez-sánchez, R.;

Velasquillo, C.; Gonzalez, C.; Ganem-Rondero, A.; Martinez-Castanon, G.; Zavala-Alonso, N.; Martinez-Gutierrez, F. Anti-biofilm activity of chitosan gels formulated with silver nanoparticles and their cytotoxic effect on human fibroblasts. *Mater. Sci. Eng. C* **2016**, 60, 317–323. doi: 10.1016/j.msec.2015.11.036.

[191] Kaler, A.; Mittal, A.K.; Katariya, M.; Harde, H.; Agrawal, A.K.; Jain, S. Banerjee, U.C. An investigation of in vivo wound healing activity of biologically synthesized silver nanoparticles. *J. Nanoprt. Res*. **2014**, 16, 2605. doi: 10.1007/s11051-014-2605-x.

[192] Ontong, J.C.; Singh, S.; Nwabor, O.F.; Chusri, S.; Voravuthikunchai, S. P. Potential of antimicrobial topical gel with synthesized biogenic silver nanoparticle using Rhodomyrtus tomentosa leaf extract and silk sericin. *Biotechnol. Lett.* 2020, 42, 2653–2664. doi: 10.1007/s10529-020-02971-5.

[193] Sharma, D.; Sharma, N.; Roy, B.G.; Pathak, M.; Kumar, V.; Ojha, H. Healing efficacy and dermal toxicity of topical silver nanoparticles - loaded hydrogel in Sprague–Dawley rats. *Radiat. Prot. Environ.* **2021**, 44, 34–41. doi: 10.4103/rpe.

[194] Jain, J.; Arora, S.; Rajwade, J.; Omray, P.; Khandelwal, S.; Paknikar, K. Silver Nanoparticles in Therapeutics: Development of an Antimicrobial Gel Formulation for Topical Use. *Mol. Pharm.* **2009**, 6, 1388–1401. doi: 10.1021/mp900056g.

[195] Fatima, F.; Aldawsari, M.F.; Ahmed, M.M.; Anwer, M.K.; Naz, M.; Ansari, M.J.; Hamad, A.M.; Zafar, A.; Jafar, M. Green Synthesized Silver Nanoparticles Using Tridax Procumbens for Topical Application: Excision Wound Model and Histopathological Studies. *Pharmaceutics* **2021**, 13, 1745. 54. doi:10.3390/pharmaceutics13111754

[196] Reichling, J.; Landvatter, U.; Wagner, H.; Kostka, K.; Schaefer, F. In vitro studies on release and human skin permeation of Australian tea tree oil (TTO) from topical formulations. *Eur. J. Pharm. Biopharm.* **2006**, 64, 222–228. doi: 10.1016/j.ejpb.2006.05.006.

[197] Wroblewska, M.; Szymanska, E.; Winnincka, K. The Influence of Tea Tree Oil on Antifungal Activity and Pharmaceutical Characteristics of Pluronic ® F-127 Gel Formulations with Ketoconazole. *Int. J. Mol. Sci.* **2021**, 2021, 11326. doi: 10.3390/ijms222111326.

[198] Sharma, P.; Nautiyal, U. Formulation and evaluation of anti-microbial gel using lavender oil and rosemary oil. *Int. J. Heal. Clin. Res.* **2020**, 3, 1–6. e-ISSN: 2590-3241, p-ISSN: 2590-325X.

CHAPTER 3: METHODOLOGY

3. Experimental

3.1. Reagents

Distilled water was utilized for the formulation of the wound dressing scaffolds (sponges and topical gels). Gelatin was purchased from (Sigma Aldrich, South Africa), Polyethylene glycol (PEG) from (Merck Chemicals, South Africa), metronidazole, Silver Nitrate ($AgNO_3$), trisodium citrate, calcium chloride ($CaCl_2$), CMC, and poloxamer 407 were also purchased from (Merck Chemicals, South Africa), Essential Oils (Tea tree and Lavender) were purchased from Clicks Pharmacy, Fort Beaufort, South Africa. Propylene glycol and methylparaben were bought from Merck Chemicals, South Africa. The reagents were utilized without additional purification.

3.2. Methodology

3.2.1. Preparation of Silver Nanoparticles

The Ag nanoparticles were formulated by employing the Turkevich method [1]–[4]. Briefly, $AgNO_3$ solution (60 mL, 1 mM) was poured into a 100 mL beaker and covered with aluminium foil and heated with stirring until it reached its boiling. When boiling, 6 mL of 10 mM trisodium citrate was added dropwise with continuous stirring until a yellow-brown colour appeared, indicating the formation of Ag nanoparticles. The solution (Ag nanoparticles) was left to cool at room temperature (r.t.) and then kept in the refrigerator for further use without further purification process.

3.2.2. Preparation of Sponges

The sponges were prepared using a freeze-drying procedure [5]–[12]. Gelatin was dissolved in 20 ml of distilled water at r.t. PEG was dissolved separately in 20 ml of distilled water at r.t. also. These solutions were blended and stirred for 1 hour. After 1 hour, 80 mg of metronidazole was added, followed by the addition of 10 ml of Ag nanoparticle solution after an hour. The reaction was stirred for 1 hour at r.t followed by adding 2 or 5% $CaCl_2$ as a cross-linking agent and then stirred for 2 hours. After 2 hours, the solution was frozen at −20 °C overnight and freeze-dried in a freeze-dryer at −60 °C for 24 hours to afford sponges. The sponges were stored in the desiccator for further analysis. The compositions of the formulated sponges are presented in **Table 3.**

Table 3. Composition of sponges

Sample Name	Gelatin	PEG	Metronidazole	Ag Nanoparticles	Cross-linking agent
SA 1	200 mg	200 mg	80 mg	10 ml	5%
SA 2	200 mg	200 mg	80 mg	10 ml	2%
SA 3	300 mg	200 mg	80 mg	10 ml	5%
SA 4	300 mg	200 mg	80 mg	10 ml	2%
SA 5	400 mg	200 mg	80 mg	10 ml	5%
SA 6	400 mg	200 mg	80 mg	10 ml	2%
SA 6	500 mg	200 mg	80 mg	10 ml	5%
SA 8	500 mg	200 mg	80 mg	10 ml	2%
SA 9	600 mg	200 mg	80 mg	10 ml	5%
SA 10	600 mg	200 mg	80 mg	10 ml	2%
SA 11	700 mg	200 mg	80 mg	10 ml	5%
SA 12	700 mg	200 mg	80 mg	10 ml	2%
SAA2%	200 mg	200 mg		10 ml	2%
SAA5%	200 mg	200 mg		10 ml	5%
SAM2%	200 mg	200 mg	80 mg		2%
SAB2%	200 mg	200 mg			5%
SAB5%	200 mg	200 mg			5%

70
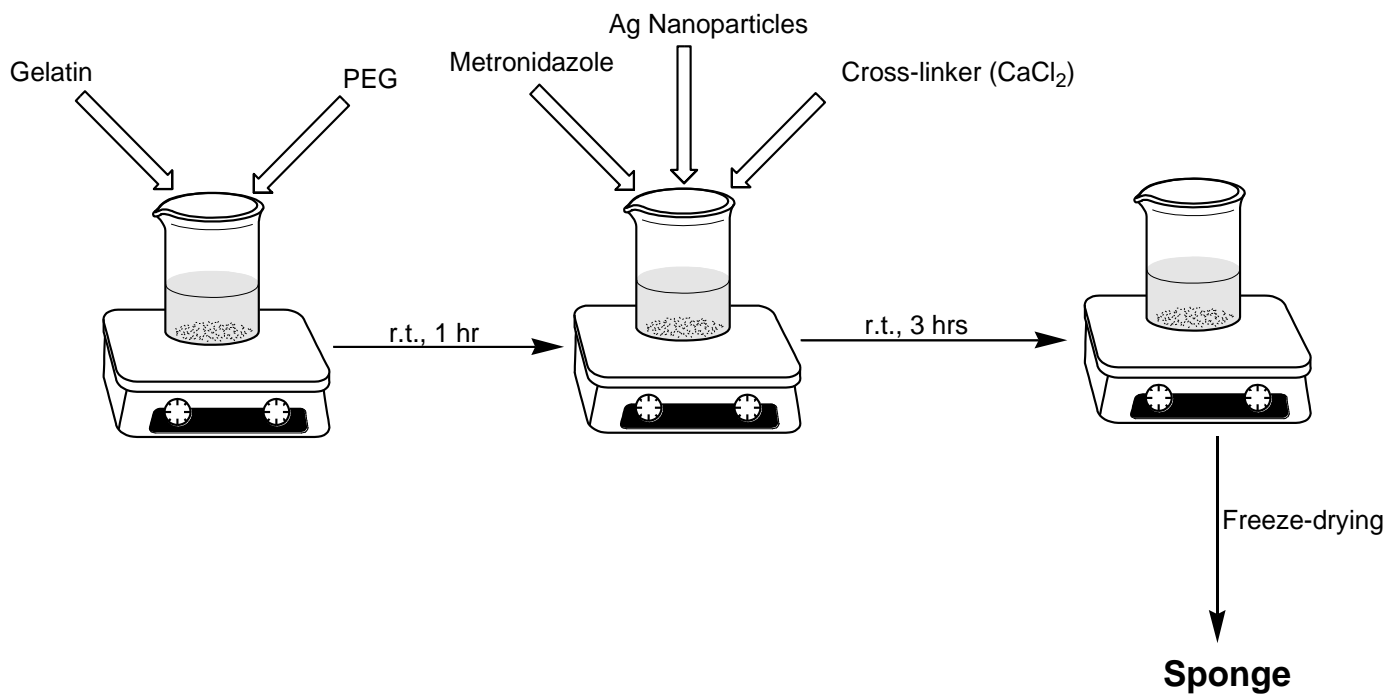
Scheme 1. Preparation of gelatin/PEG sponges loaded with metronidazole and Ag nanoparticles
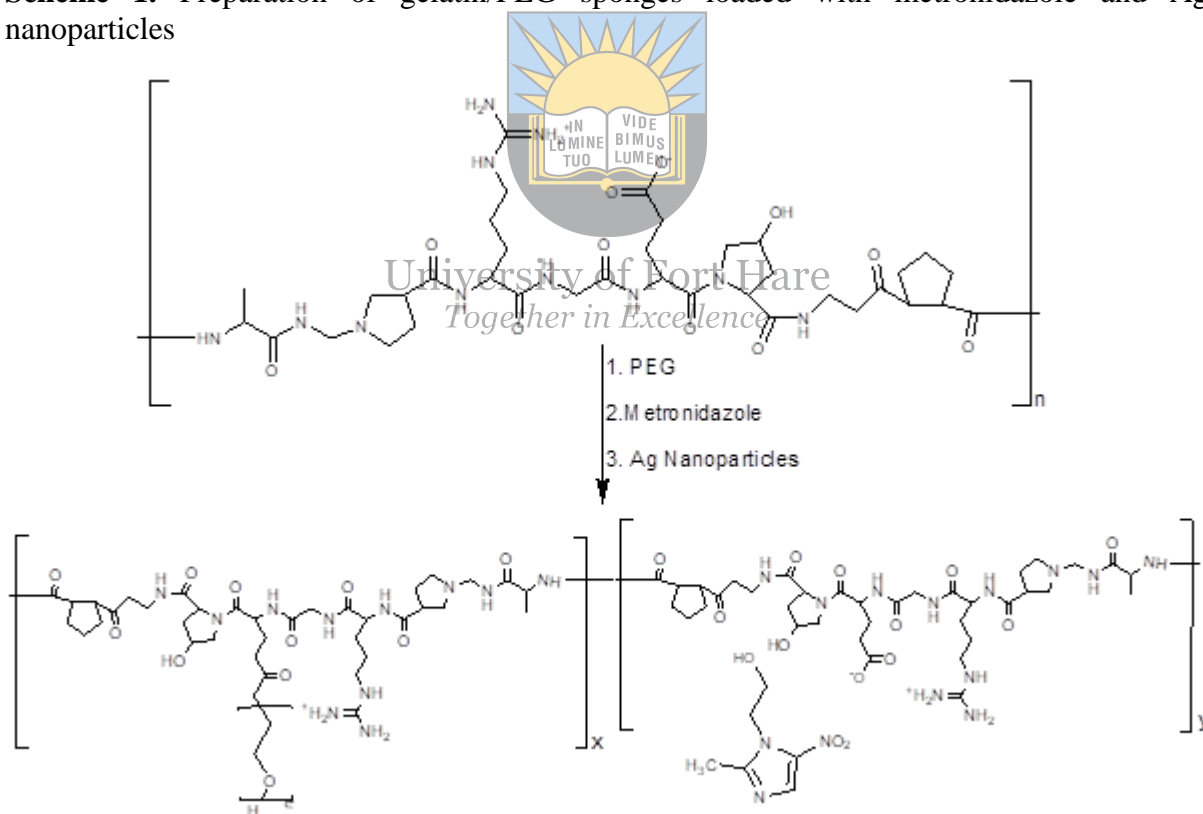
Scheme 2. Preparation of SA1 to SA12
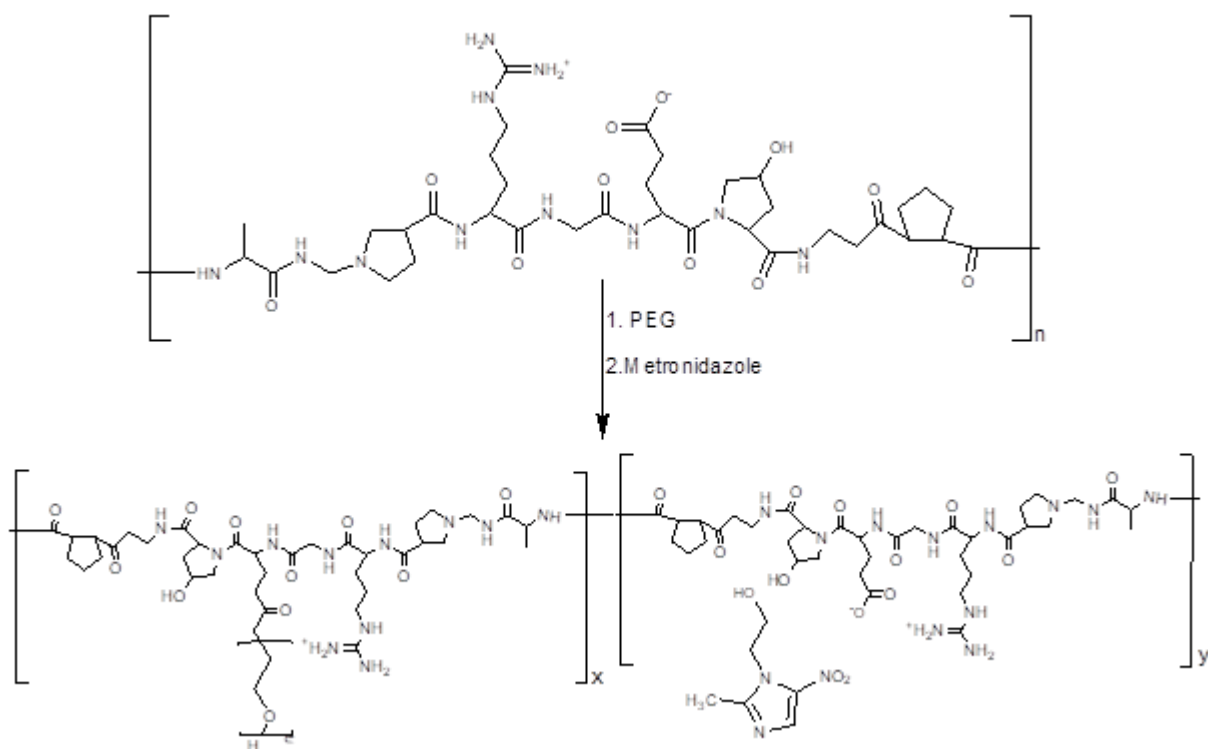
Scheme 3. Preparation of SAM2%
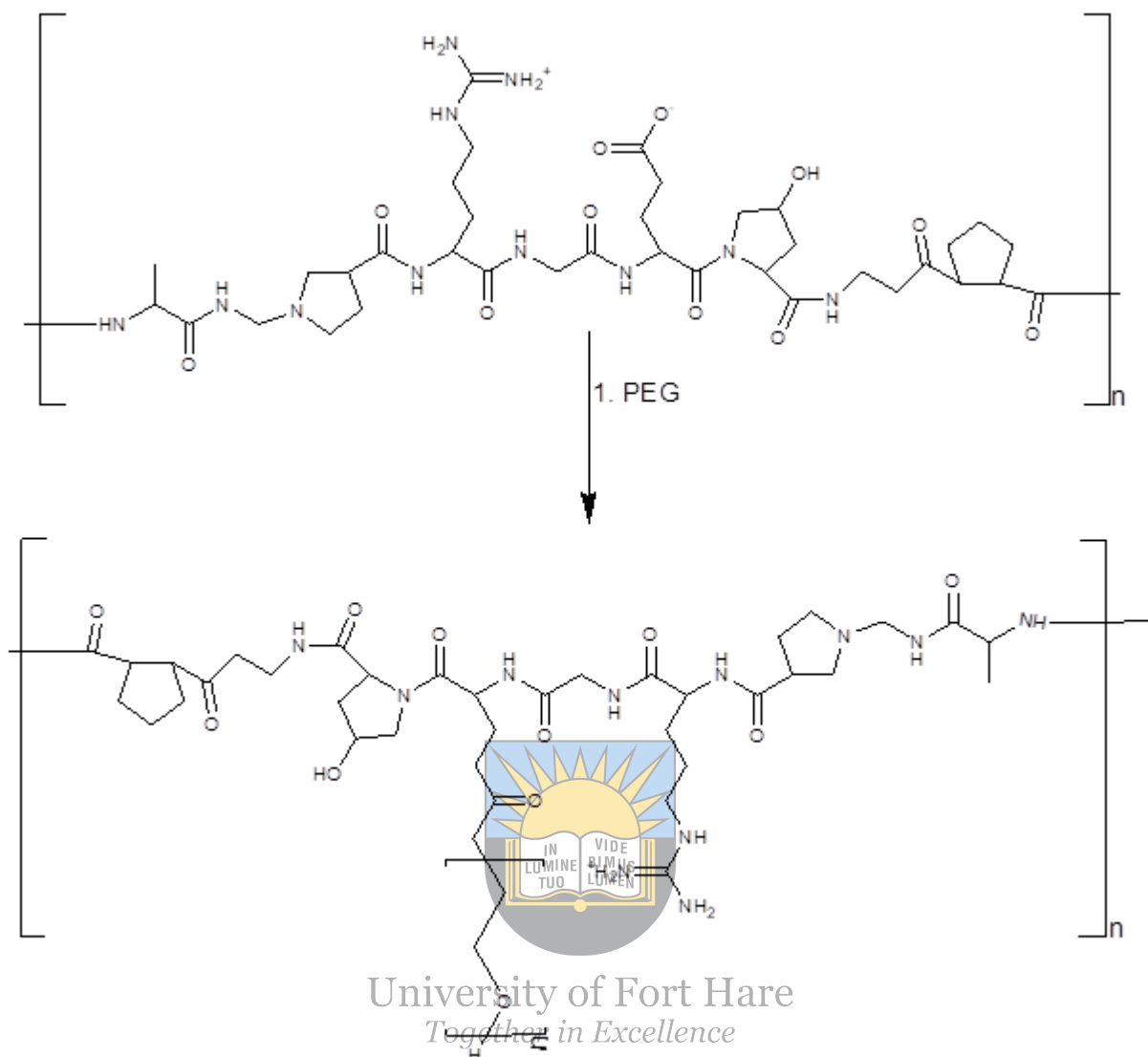
Scheme 4. Preparation of Blanks (SAB2% and SAB5%)

3.2.3. Preparation of Topical Gels

The topical gels were formulated according to a modified procedure from what was reported by Buyana *et al.* [13]. The list of gels is presented in **Table 4** below. Firstly, 20 mg of methylparaben was dissolved in distilled water (10 ml) at 90°C. After the solution was cooled, 100 mg of poloxamer was added and stirred at r.t. for 1 hour and then stored in the refrigerator overnight. While the frozen solution was melting at r.t., 100 mg of CMC was slowly added and stirred for 1 hour. After an hour, 2 ml of tea tree oil or lavender oil was added, followed by adding Ag nanoparticles after 1 hour. Propylene glycol (1 ml) was added, and the reaction was stirred for 1 hour. The formulated topical gels were stored in the refrigerator for further analysis.

Table 4. Composition of topical gels

Sample Name	CMC	Poloxamer	Tea tree Oil	Lavender Oil	Ag Nanoparticles	Propylene Glycol	Methyl Paraben
TG 1	100 mg	100 mg	2 ml		2 ml	1 ml	20 mg
TG 2	100 mg	100 mg	2 ml			1 ml	20 mg
TG 3	100 mg	100 mg			2 ml	1ml	20 mg
TG 4	100 mg	100 mg		2 ml		1 ml	20 mg
TG 5	100 mg	100 mg		2 ml	2 ml	1 ml	20 mg
TG 0	10 mg	100 mg				1 ml	20 mg
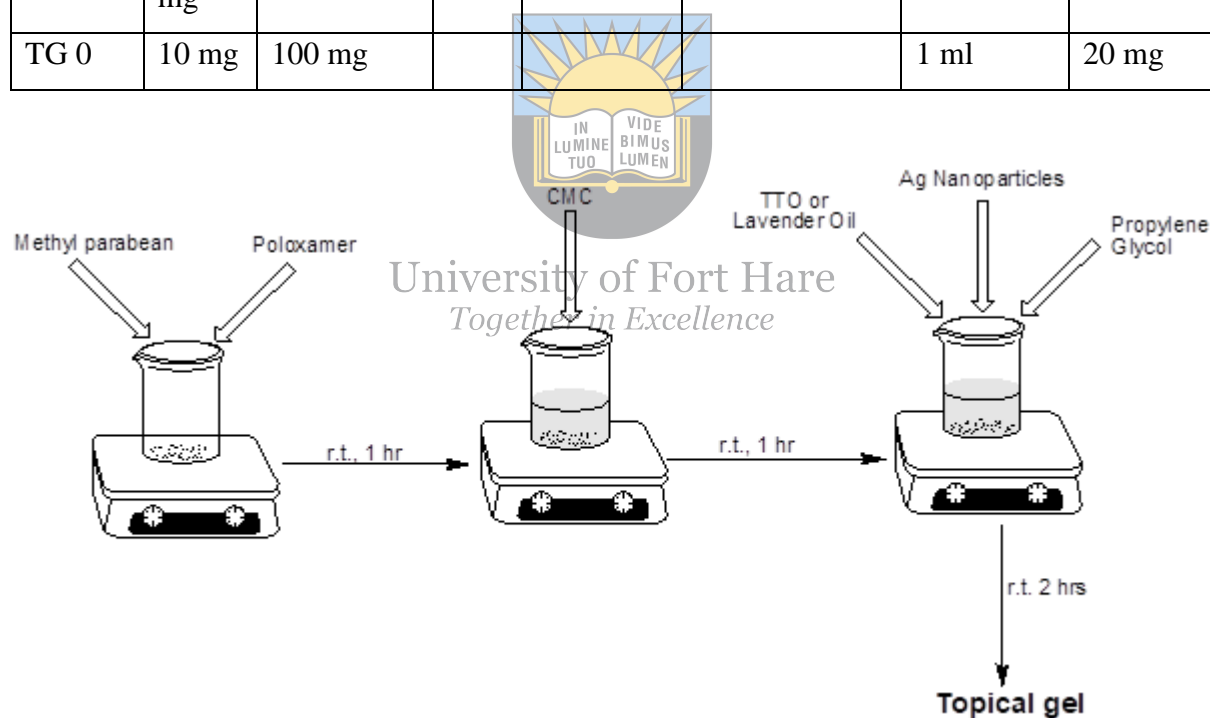
Equation 5. Preparation of Topical gels Loaded with Essential Oils and Ag nanoparticles

3.3. Instruments and Characterizations of Sponges and Gels

3.3.1. Freeze-drying

It was performed on the sponges to get rid of water employing VirTis benchtop K, Gardiner, New York.

3.3.2. UV-Vis Spectroscopy

UV-Vis analysis was performed to confirm the Ag nanoparticles formation by evaluating the absorption peak using Perkin Elmer Lambda 365, Korea.

3.3.3. Fourier Transform Infrared Spectroscopy (FTIR)

FTIR analysis was performed on the sponges and topical gels to determine the presence of functional groups in them. It was done using Perkin Elmer Spectrum 100 FTIR Spectrometer, USA. The spectra were conducted in the range of 4000–500 cm^{-1} utilizing OMNIC software.

3.3.4. Scanning Electron Microscopy (SEM)

The sponges were sputtered with gold particles before SEM analysis. SEM was employed to evaluate the morphology of the sponges. This analysis was conducted at an accelerating voltage of 15kV on JEOL JSM-6390LV Scanning Electron Microscope, Japan.

3.3.5. Thermogravimetric Analysis (TGA)

TGA was utilized to evaluate sponges' moisture content and thermal stability over a selected range of temperatures. TG-analyser (TGA-4000, Rheometric Scientific, South Africa) was used. Between 9-20 mg of the sponges was loaded on the TG-analyser. The weight loss profile was recorded from 20-700 ºC at a rate of 10 ºC per minute with a constant nitrogen flow of 50 mL/ min.
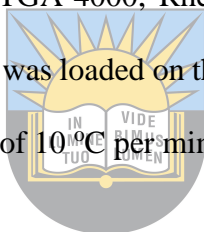
3.3.6. Porosity

The porosity studies were conducted to determine the degree of porosity of the sponges corresponding to the SEM micrographs. The porosity of the sponges was determined by the liquid displacement procedure using ethanol as the displacement liquid due to its ability to easily penetrate through the pores of the wound dressing scaffolds, which will not cause swelling or shrinking as a non-solvent of the polymers [14]–[19]. The freeze-dried sponges (10 mg) were absorbed in 2 ml of ethanol and weighed after an hour.

The sponge porosity was calculated using the following equation:

$$Porosity = \frac{W2 - W1}{p.V}$$

Where W_2 is the mass of sponges after immersion
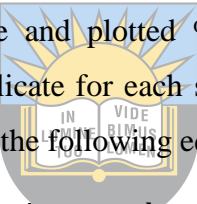
W_1 is the mass of sponges before immersion

V is the volume of the sponges

P is the density of ethanol

3.3.7. In vitro Drug Release Studies

The *in vitro* drug release experiments were conducted on sponges and topical gels following the method by Wen *et al*. [6] and Tawfeek *et al*. [20]. 20 mg of sponge or topical gel was dissolved in 3 mL of phosphate buffer saline (PBS) with a pH of 7.4. The solution was poured into the dialysis membrane and incubated in 40 mL of PBS (pH 7.4, 37ºC), simulating the physiological pH of the skin with slow shaking. 5 mL of PBS was taken at 1-hour intervals for 8 hrs, 24 hrs, and 48 hrs to check the concentration of drug released from the formulations using UV-vis analysis by completely emptying the release media and replacing it with fresh 40 mL buffer solution at every time interval. The UV-vis experiments of the released bioactive agents from the sponges and gels were performed at the wavelengths of 320 nm, 430 nm, 230 nm, and 260 nm for metronidazole, Ag nanoparticles, TTO, and lavender oil, respectively. The obtained data were expressed as % cumulative drug release. The concentration of metronidazole, Ag nanoparticles, TTO, and lavender oil released from the sponges or gels was investigated using a calibration curve and plotted % drug release against time. All the measurements were carried out in triplicate for each sponge or topical gels. The percentage drug release was calculated employing the following equation:

$$\% \text{ drug release} = \frac{\text{Amount drug released}}{\text{Amount drug} - \text{loaded}} \times 100\%$$

The selected drug release mathematical models that were used to determine the release mechanisms of loaded bioactive agents from the sponges and topical gels are Zero-order, Korsmeyer-Peppas, and Higuchi equations.

i.   Zero-order release equation

The equation of the Zero-order release model is:

Q = K.t + Qo

Where Q is the amount of the bioactive agent dissolved in time t, Qo is the initial amount of drug in the sponge or gel, and K is the Zero-order release constant expressed. This equation refers to a release profile where the release rate of the drug is independent of the pharmaceutical dosage concentration and time. This drug release model is more applicable to the slow drug release mechanism. The data from *in vitro* drug release experiments were plotted as % cumulative drug release versus time.

ii. Korsmeyer-Peppas release equation

The equation of the Korsmeyer-Peppas release model is:

$Q = M_t / M_\infty$

$M_t / M_\infty = K.t^n$

Where M_t/M_∞ is the amount of released bioactive agent at time t, while K and n are the release rate constant release exponent, respectively. The n value is utilized to describe different releases for the matrices. This release model illustrates drug release from a polymeric system equation. Only the first 60% of drug release data can be fitted in the Korsmeyer-Peppas model to determine the drug release mechanism. To evaluate the release kinetics, data from the *in vitro* drug release experiments were plotted as log cumulative percentage drug release versus log time.

Table 5. The diffusion coefficient (n) is used to calculate the mechanism of release

Coefficient of diffusion value	Mechanism of release
n<0.5	Quasi-Fickian diffusion
n=0.5	Fickian diffusion
0.5<n<1.0	Anomalous (non-Fickian)
n=1.0	Non-Fickian case II. It means a zero-order release profile.
n>1	Non-Fickian super case II.

iii. Higuchi release equations

The equation of the Higuchi release model is:

$Q = K\sqrt{t}$

Where K is the Higuchi dissolution constant and Q is the amount of drug released in time t. This equation refers to a system where the drug release of bioactive agents is by diffusion. This model is suitable for porous wound dressing scaffolds. The data were plotted as % cumulative drug release versus square root of time.

3.3.8. *In vitro* Biodegradation Studies

The biodegradation studies were done to examine the degradability of the sponges against time [21][22]. Briefly, 10 mg of SA3, SA4, SA11, SA12, SAB2%, and SAB5% sponges were immersed in 10 mL PBS solutions of pH 5.4 (simulating pH of chronic wounds) and 7.4 (physiological pH), over 1, 2, and 3 weeks in an incubator at 37ºC. Then, the sponges were freeze-dried and evaluated using FTIR and SEM to observe the degradability nature of the sponges. The biodegradation studies were performed to determine their potential capability to induce skin regeneration.

3.3.9. Viscosity

The viscosity of the topical gels was evaluated utilizing a Brookfield viscometer (DV-1). The topical gel was poured into a sample vial and rotated at a speed of 50 rpm and 100 rpm at r.t. of 25ºC, employing spindle 63 (LV3), and the viscosity was measured in cP. The viscosity of the topical gels was performed to evaluate their suitability for skin application and patient compliance. Topical gels for skin application exhibit viscoelastic flow properties and high viscosity is appropriate for the application manually to the skin.

3.3.10. Spreadability

The topical gels (0.1 g) were put between two glass slides and a second glass slide was placed followed by the addition of a known mass on top of the two glass slides for 5 minutes and the spreadability was measured in cm [13][23]–[26]. This technique was used to evaluate the capability of the gels to spread uniformly on the skin. Their spreadability influences their therapeutic efficacy.

3.3.11. pH

The pH was employed to evaluate the basicity or acidity of the topical gels. The pH of the gels was determined using MColorplastTM, pH indicator strips (non-bleeding) with a pH range of 0-14, a universal indicator. The pH of the gels was performed to determine their appropriateness for application on the skin. The pH suitable for the skin should be close to neutral to avoid irritation.

3.3.12. In vitro cytotoxicity evaluation

The *in vitro* cytotoxicity analysis of the wound dressings was performed to evaluate the biocompatibility of the developed transdermal patches employing the MTT assay. The sponges and topical gels were screened against HaCaT cells (immortalized human keratinocytes) which were cultured at a density of 5×10^4 cells/ml in 96-well plates at a volume of 90

µL/well. Twenty-four hours later, the cells were treated in triplicates with 10 µL of patch solution per sample, making final concentrations of 100, 50, 25, and 12.2 µg/mL. Cells treated with 1X PBS and 10% DMSO served as the negative and positive controls, respectively. The 96-well plates were incubated for 48 hrs after which MTT reagent was added, the plates were incubated for 4 hrs, solubilized overnight using the solubilization reagent, and the absorbance values were measured at 570 nm [42]. The experiments were run in triplicate. The cytotoxicity results of the wound dressings were analysed by calculating the percentage cell viability of each sponge and topical gel against untreated cells using the equation below:

$$\% \; cell \; viability = \frac{ODs - ODb}{ODu - ODb} x100\%$$

Where OD_S is the absorbance of the compound and OD_b is the absorbance of the blank. OD_u is the absorbance of the untreated compound.

3.3.13. *In vitro* Antibacterial Studies

The minimum inhibitory concentration (MIC) of the evaluated samples was carried out following Fonkui *et al*. (2018) [27]. Each compound was dissolved in d H_2O to a stock concentration of 1 mg/mL. These solutions were then serially diluted (6 times) in 100 uL of nutrient broth in 96 well plates to the anticipated concentrations (500, 250, 125, 62.5, 31.25 and 15.625 µg/mL). Then, 100 µL of each of these solutions was prepared in duplicate and incubated with 100 µL of an overnight bacterial culture brought to 0.5 Mc Farland in nutrient broth. Ampicillin, nalidixic acid, and streptomycin were utilized as positive control and negative control was formulated to contain 50% nutrient broth in DMSO.

3.3.14. *In vitro* scratch wound healing assay

It is an affordable study utilized to analyse fibroblast cell movement in two dimensions to induce wound healing. *In vitro* wound-healing assay was evaluated based on a procedure adapted from Felice *et al*., 2015, Suarez-Arnedo *et al*. 2020, Cheng *et al*. 2019 and Ranzato et al., 2008 [28]–[31]. Immortalized human keratinocyte (HaCaT) cells were cultured in a humidified incubator at 37°C and 5% CO_2 to 90% confluency in DMEM containing 10% (v/v) fetal bovine serum (FBS) and 1% (v/v) penicillin-streptomycin (Penstrep) antibiotics. The cells were then trypsinized, and viable cells were quantified employing the trypan blue dye

elimination method. The cell density was adjusted to 2.5 X 10^5 cells/ml, and the cells were incubated in 6-well plates until cell monolayers were formed (48 hours later). Single scratch wounds per well were generated utilizing a 200 µL micropipette tip. The cells were washed once per well with 2 ml of 1X phosphate-buffered saline (1X PBS) to remove dislodged cells. Serum-poor DMEM medium (containing 1% FBS) was added to the wells (1800 µl per well), and cells were treated with 200 µl of blank and patch 4 of various concentrations that showed the highest viability on the MTT assay screen.

Untreated cells seeded in Dulbecco's Modified Eagle's Medium (DMEM) containing 10% FBS were used as a positive control, while those cultured in 1% FBS in DMEM were employed as the negative control. The images were captured in duplicates at 0, 24, 48, 72, and 96 hours using the 4X objective and phase-contrast feature of an inverted light microscope (Olympus CKX53, Olympus, Tokyo, Japan). Cell migration was quantified using ImageJ image processing software.

University of Fort Hare
Together in Excellence

References

[1]   Arif, D.; Niazi, M.B.K.; Ul-haq, N.; Anwar, M.N.; Hashmi, E. Preparation of

Antibacterial Cotton Fabric Using Chitosan-silver Nanoparticles. *Fibers Polym.* **2015**, 16, 1519–1526. doi: 10.1007/s12221-015-5245-6.

[2] Nerkar, D.; Rajwade, M.; Jaware, S.; Jog, M. Synthesis and characterization of Polyvinyl Alcohol-Polypyrrole- Silver nanocomposite polymer films with core-shell structure. *Int. J. Nano Dimns.* **2020**, 11, 205–214.

[3] Jaiswal, A.; Sanpui, P.; Chattopadhyay, A.; Ghosh, S.S. Investigating Fluorescence Quenching of ZnS Quantum Dots by Silver Nanoparticles. *Plasmonics* **2011**, 6, 125–132. doi: 10.1007/s11468-010-9177-0.

[4] Gorup, L.F.; Longo, E.; Leite, E.R.; Camargo, E.R. Moderating effect of ammonia on particle growth and stability of quasi-monodisperse silver nanoparticles synthesized by the Turkevich method. *J. Colloid Interface Sci.* **2011**, 360, 355–358. doi: 10.1016/j.jcis.2011.04.099.

[5] Neto, A.D.N.P.; dos Santos Cruz, C.F.; Serafini, M.R.; dos Passos Menezes, P.; de Carvalho, Y.M.B.G.; Matos, C.R.S.; Nunes, P.S. Usnic acid-incorporated alginate and gelatin sponges prepared by freeze-drying for biomedical applications. *J. Therm. Anal Calorim.* **2017**, 127, 1707–1713. doi: 10.1007/s10973-016-5760-8.

[6] Wen, Y.; Yu, B.; Zhu, Z.; Ynang, Z.; Shao, W. Synthesis of Antibacterial Gelatin / Sodium Alginate Sponges and Their Antibacterial Activity. *Polymers (Basel)* **2020**, 12, 1926. doi:10.3390/polym12091926.

[7] Naghshineh, N.; Tahvildari, K.; Nozari, M. Preparation of Chitosan, Sodium Alginate, Gelatin and Collagen Biodegradable Sponge Composites and their Application in Wound Healing and Curcumin Delivery. *J. Polym. Environ.* **2019**, 27, 2819–2830. doi: 10.1007/s10924-019-01559-z.

[8] Sankar, P.C.K.; Rajmohan, G.; Rosemary, M.J. Physico-chemical characterisation and biological evaluation of freeze-dried chitosan sponge for wound care. *Mater. Lett.* **2017**, 208, 130–132. doi: 10.1016/j.matlet.2017.05.010.

[9] Ye, S.; Jiang, L.; Su, C.; Zhu, Z.; Wen, Y.; Shao, W. Development of gelatin / bacterial cellulose composite sponges as potential natural wound dressings. *Int. J. Biol. Macromol.* **2019**, 133, 148–155. doi: 10.1016/j.ijbiomac.2019.04.095.

[10] He, Y.; Zhao, W.; Dong, Z.; Ji, Y.; Li, M.; Hao, Y.; Zhang, D.; Yuan, C.; Deng,

J.;Zhao, P.; Zhou, Q. A biodegradable antibacterial alginate/carboxymethyl chitosan/Kangfuxin sponges for promoting blood coagulation and full-thickness wound healing. *Int. J. Biol. Macromol.* **2021**, 167, 182–192. doi: 10.1016/j.ijbiomac.2020.11.168.

[11] Hu, S.; Bi, S.; Yan, D.; Zhou, Z.; Sun, G.; Cheng, X.; Chen, X. Preparation of composite hydroxybutyl chitosan sponge and its role in promoting wound healing," *Carbohydr. Polym.* **2018**, 184, 154–163. doi: 10.1016/j.carbpol.2017.12.033.

[12] Ye, H.; Cheng, J.; Yu, K. In situ reduction of silver nanoparticles by gelatin to obtain porous silver nanoparticle/ chitosan composites with enhanced antimicrobial and wound-healing activity. *Int. J. Biol. Macromol.* **2019**, 121, 633–642. doi: 10.1016/j.ijbiomac.2018.10.056.

[13] Buyana, B.; Aderibigbe, B.A.; Ndinteh, D.T.; Fonkui, Y.T.; Kumar, P. Alginate-pluronic topical gels loaded with thymol, norfloxacin and ZnO nanoparticles as potential wound dressings. *J. Drug Deliv. Sci. Technol.* **2020**, 60, 101960. doi: 10.1016/j.jddst.2020.101960.

[14] Yang, G.; Xiao, Z.; Long, H.; Ma, K.; Zhang, J.; Ren, X.; Zhang, J. Assessment of the characteristics and biocompatibility of gelatin sponge scaffolds prepared by various crosslinking methods. *Sci. Rep.* **2018**, 8, 1616. doi: 10.1038/s41598-018-20006-y.

[15] Xie, Y.; Yi, Z.; Wang, J.; Hou, T.; Jiang, Q. Carboxymethyl konjac glucomannan - crosslinked chitosan sponges for wound dressing. *Int. J. Biol. Macromol.* **2018**, 112, 1225–1233. doi: 10.1016/j.ijbiomac.2018.02.075.

[16] Arif, M.M.A.; Fauzi, M.B.; Nordin, A.; Hiraoka, Y.; Tabata, Y.; Heikal, M.; Yunus, M.H.M. Fabrication of Bio-Based Gelatin Sponge for Potential Use as A Functional Acellular Skin Substitute. *Polymers (Basel).* **2020**, 12, 2678. doi:10.3390/polym12112678.

[17] Singaravelu, S.; Ramanathan, G.; Raja, M.D.; Nagiah, N.; Padmapriya, P.; Kaveri, K.; Sivagnanam, U.T. Biomimetic interconnected porous keratin-fibrin-gelatin 3D sponge for tissue engineering application. *Int. J. Biol. Macromol.* **2016**, 86, 810–819.doi: 10.1016/j.ijbiomac.2016.02.021.

[18] de Lacerda Bukzem, A.; dos Santos, D.M.; Leite, I.S.; Inada, N.M.; Campana-Filho,

S.P. Tuning the properties of carboxymethylchitosan-based porous membranes for potential application as wound dressing. *Int. J. Biol. Macromol.* **2021**, 166, 459–470. doi: 10.1016/j.ijbiomac.2020.10.204.

[19]   Salehi, M.; Niyakan, M.; Ehterami, A.; Haghi-Daredeh, S.; Nazarnezhad, S.; Abbaszdeh-Goudarzi, G.; Vaez, A.; Hashemi, S.; Rezaei, N.; Mousavi, S.R. Porous electrospun poly (ε -caprolactone)/ gelatin nanofibrous mat containing cinnamon for wound healing application: in vitro and in vivo study. *Biomed. Eng. Lett.* **2020**, 10, 149–161. doi: 10.1007/s13534-019-00138-4.

[20]   Tawfeek, H.M.; Abou-Taleb, D.A.E.; Badary, D.M.; Ibrahim, M.; Abdellatif, A.A.H. Pharmaceutical, clinical, and immunohistochemical studies of metformin hydrochloride topical hydrogel for wound healing application. *Arch. Dermatol. Res.* **2020**, 312, 113–121. doi: 10.1007/s00403-019-01982-1.

[21]   Tamahkar, E.; Özkahraman, B.; Özbaş, Z.; İzbudak, B.; Yarimcan, F.; Boran, F.; Ozturk, A.B. Aloe vera-based antibacterial porous sponges for wound dressing applications. *J. Porous Mater.* **2021**, 28, 741–750. doi: 10.1007/s10934-020-01029-1.

[22]   Buyana, B.; Aderibigbe, B.A.; Suprakash, S.; Ndinteh, D.; Fonkui, Y.T. Development, characterization, and in vitro evaluation of water soluble poloxamer/pluronic-mastic gum-gum acacia-based wound dressing. *J. Appl. Polym. Sci.* **2020**, 137, 48728.

[23]   Shukr, M.H.; Metwally, G.F. Evaluation of topical gel bases formulated with various essential oils for antibacterial activity against methicillin- resistant Staphylococcus aureus. *Trop. J. Pharm. Res.* 2013, 12, 877–884. ISSN: 1596-5996.

[24]   Choudhary, M.; Chhabra, P; Tyagi, A.; Singh, H. Scar free healing of full thickness diabetic wounds: A unique combination of silver nanoparticles as antimicrobial agent, calcium alginate nanoparticles as hemostatic agent, fresh blood as nutrient/growth factor supplier and chitosan as base matrix. *Int. J. Biol. Macromol.* **2021**, 178, 41–52. doi: 10.1016/j.ijbiomac.2021.02.133.

[25]   Khan, A.W.; Kotta, S.; Ansari, S.H.; Sharma, R.K.; Kumar, A.; Ali, J. Formulation development, optimization and evaluation of aloe vera gel for wound healing. *Pharmacogn. Mag.* **2013**, 9, S6–S10. doi: 10.4103/0973-1296.117849.

[26]   Siang, R.; Teo, S.Y.; Lee, S.Y.; Basavaraj, A.K.; Koh, R.Y.; Rathbone, M.J.

Formulation and evaluation of topical pentoxifylline-hydroxypropyl methylcellulose gels for wound healing application. *Int. J. Pharm. Pharm. Sci.* **2014**, 6, 535–539.

[27] Fonkui, T.Y.; Ikhile, M.I.; Muganza, F.M.; Fotsing, M.C.D.; Arderne, C.; Siwe-Noundou, X. Synthesis, Characterization and Biological Applications of Novel Schiff Bases of 2-(Trifluoromethoxy)aniline. *J. Chin. Pharm. Sci*. **2018**, 27, 307–323.

[28] Felice, F.; Zambito, Y.; Belardinelli, E.; Fabiano, A.; Santoni, T.; Di Stefano, R. International Journal of Biological Macromolecules Effect of different chitosan derivatives on in vitro scratch wound assay: A comparative study. *Int. J. Biol. Macromol.* **2015**, 76, 236–241.doi: 10.1016/j.ijbiomac.2015.02.041.

[29] Suarez-arnedo, A.; Figueroa, F.T.; Clavijo, C.; Arbela, P.; Cruz, J.C.; Munoz-Camargo, C. An image J plugin for the high throughput image analysis of in vitro scratch wound healing assays. *PLoS One* **2020**, 5, e0232565.doi: 10.1371/journal.pone.0232565.

[30] Cheng, Y.; Hu, Z.; Zhao, Y.; Zou, Z;. Lu, S.; Zhang, B.; Li, S. Sponges of Carboxymethyl Chitosan Grafted with Collagen Peptides for Wound Healing. *Int. J. Mol. Sci.* **2019**, 20, 3890. doi:10.3390/ijms20163890.

[31] Ranzato, E.; Patrone, M.; Mazzucco, L.; Burlando, B. Platelet lysate stimulates wound repair of HaCaT keratinocytes. *Br. J. Dermatol.* **2008**, 159, 537–545.

CHAPTER 4: RESULTS AND DISCUSSION FOR SPONGES

4.0. UV-Vis Analysis of Ag Nanoparticles

UV-vis spectroscopy was utilized to confirm the successful synthesis of Ag nanoparticles by analysing the absorbance data. The UV-vis spectrum of Ag nanoparticles exhibited a broad visible absorbance band at 426 nm (**Figure 6**), which corresponded with the theoretical UV-vis results of Ag nanoparticles. Alim-Al-Razy et al. synthesized Ag nanoparticles using the Turkevich procedure. The UV-Vis results of synthesized Ag nanoparticles displayed peaks between 417 and 444 nm, depending on the percentage of $AgNO_3$ used during their preparation [1]. The Ag nanoparticles formulated by Singh et al. employing green synthesis showed an absorbance band at 427 nm, corresponding to the results found in this research study [2]. Anandalakshmi prepared Ag nanoparticles with absorption at 430 nm [3]. The UV-vis results obtained from the various studies were aligned with the results found in this research study
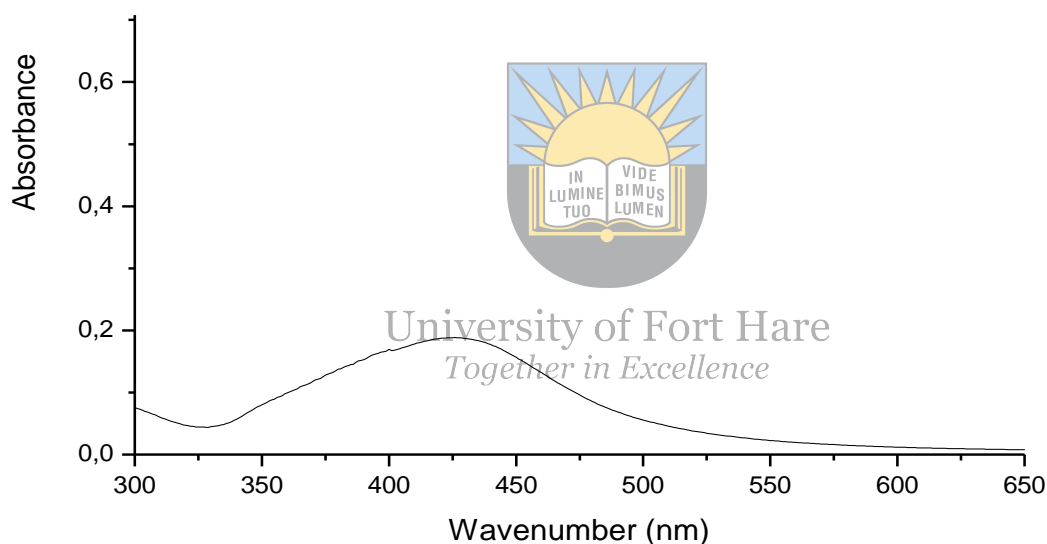
Figure 6: UV-Vis spectrum of Ag nanoparticles

4.1. FTIR

Functional groups present on the molecular structure of sponges give characteristic vibrational peaks (stretching, bending, etc.) on the FTIR spectra. The IR spectra for gelatin/PEG hybrid sponges loaded with metronidazole and Ag nanoparticles are shown in **Figures 7**-**15**, including the blank sponges. The FTIR spectra of hybrid sponges displayed similar characteristic absorption peaks due to their composition. The spectra of dual drug-loaded sponges are shown in **Figures 7**-**12**. The FTIR spectra of hybrid sponges loaded with one drug (Ag nanoparticles or metronidazole) are shown in **Figures 13** and **14,** while IR spectra in Figures **14** and **15** are for blank sponges cross-linked with 2% and 5% $CaCl_2$, respectively. All the spectra of sponges exhibited three characteristic peaks between 1637-1628 cm^{-1} (amide I), 1545 or 1536 cm^{-1}

(amide II), and 1261-1243 cm^{-1} (amide III), due to the C=O stretching vibrations of amides for gelatin. Furthermore, the C=O stretching vibrations of amide III of gelatin at 1261-1243 cm^{-1} overlapped with C-O stretching vibrations that confirm the presence of PEG in sponges. Several researchers reported similar FTIR results for gelatin-based scaffolds for wound dressing application [4]–[7].

The C=N stretching vibration at 1545 or 1536 cm^{-1} (overlapped with amide II of gelatin), N=O asymmetric stretching at 1472-1436 cm^{-1} (overlapped with amide III of gelatin), C-C stretching at 1426 or 1416 cm^{-1}, CH$_3$ bending vibration at 1371-1343 cm^{-1}, C-N stretching vibration at 1078-1059 cm^{-1}, and =C-H bending at 900-1000 cm^{-1} confirmed the functional groups of metronidazole revealing its successful loading in the sponges (SA1-SA12, and SAM2%). Furthermore, the peaks between 3351-3218 cm^{-1} denote the O-H stretching vibrations of metronidazole. These results are similar to the spectroscopic outcomes of metronidazole that were reported by Trivedi et al. [8]. The CH$_3$ bending at 1371-1344 cm^{-1} is ascribed to the metronidazole and gelatin methyl group. Furthermore, the FTIR spectra of sponges containing Ag nanoparticles (SA1 to SA12, SAA2%, and SAA5%) exhibited peaks between 3351-3218 cm^{-1} denoting O-H stretching vibrations (overlapping with the O-H stretching vibration of metronidazole), 1545 or 1536 cm^{-1} signifying N-H bending vibration of primary amines overlapped with C=N stretching, 1078-1059 cm^{-1} (stretching vibrations of all amines), and the peaks between 958 cm^{-1} and 821 cm^{-1} (C-H bending vibrations out of plane). Arif *et al*. reported similar results for FTIR analysis of Ag nanoparticles [9]. The peak at the wavenumber of 556 cm^{-1} represents the vibration frequency of Ag-O ionic bond groups [10]. Furthermore, the FTIR spectra of the drug-loaded sponges did not reveal any interaction of the therapeutic agents with the wound dressing polymer matrix, indicating that the loaded drug will not lose its biological activity. The functional groups of pure polymers (gelatin and PEG) and drugs (metronidazole) that are also displayed by IR spectra of respective sponges are shown in **Table 6**.
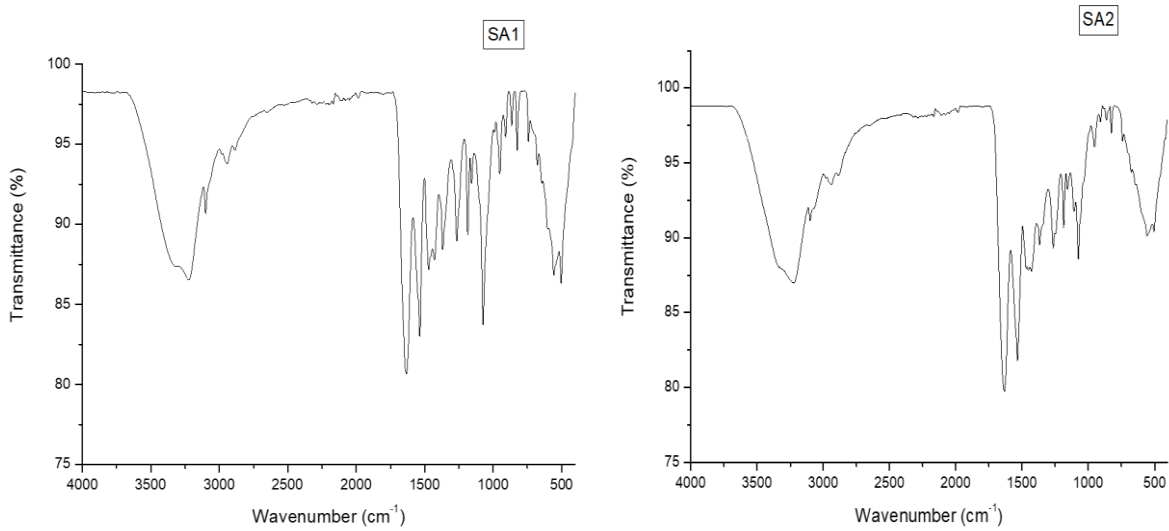
Figure 7: IR spectra of SA1 and SA2
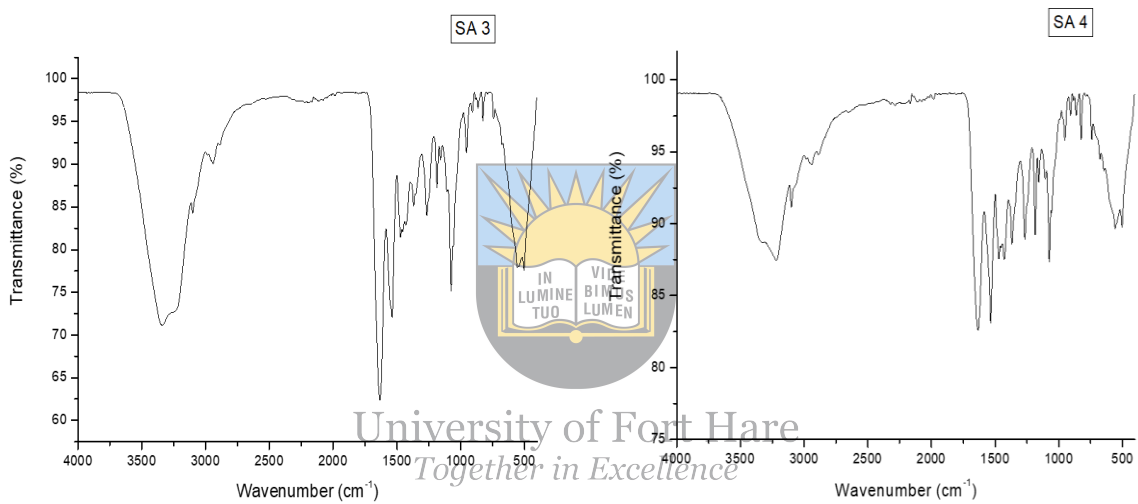
Figure 8: IR spectra of SA3 and SA4
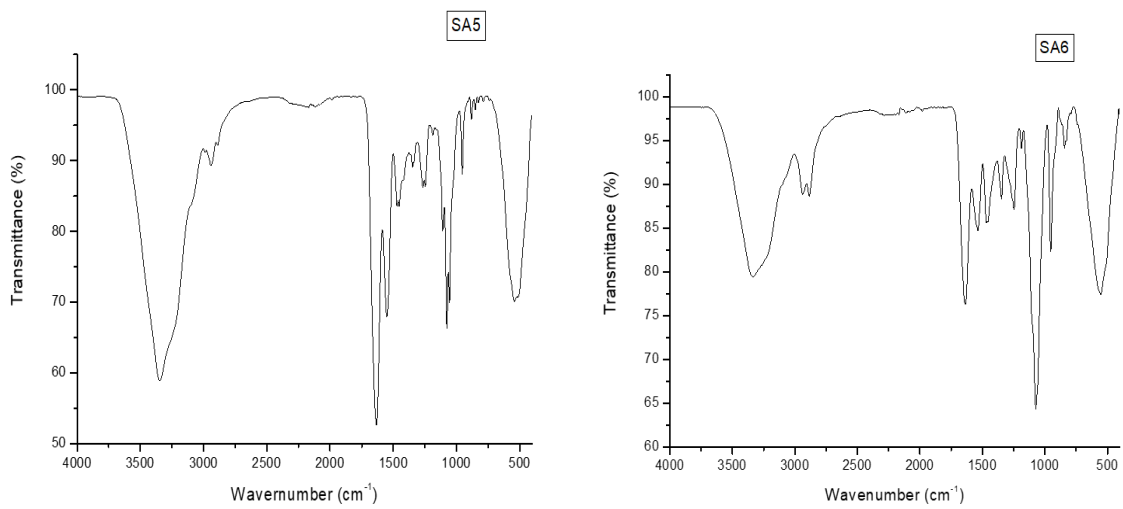
Figure 9: IR spectra of SA5 and SA6
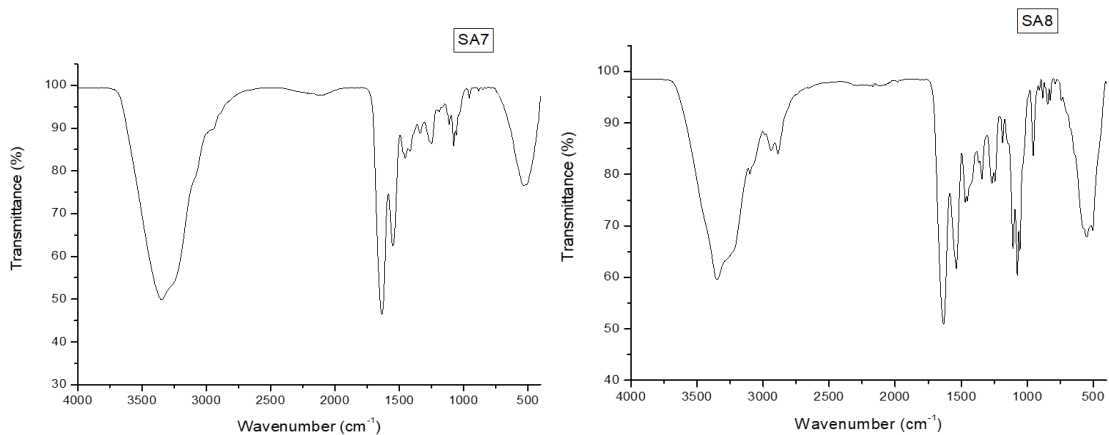
Figure 10: IR spectra of SA7 and SA8
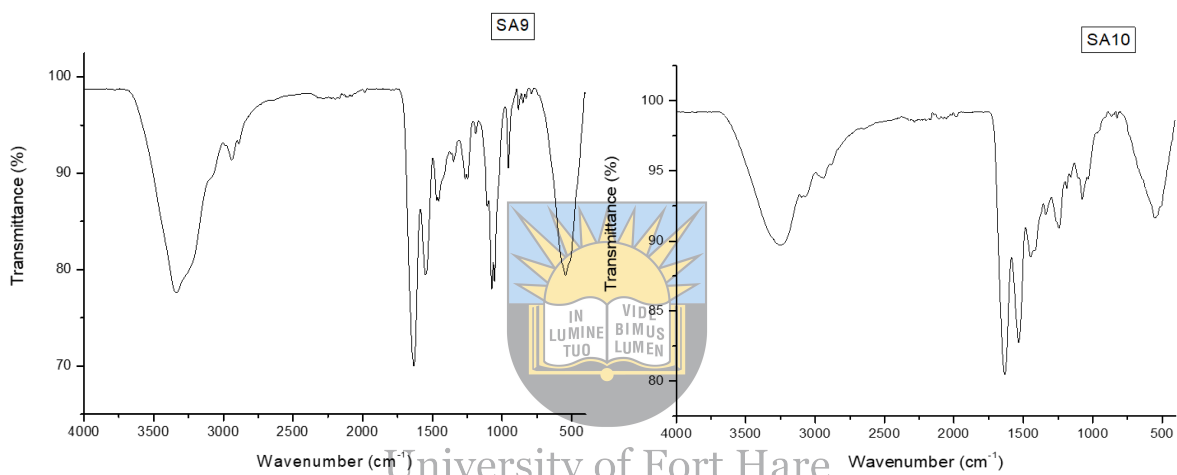
Figure 11: IR spectra of SA9 and SA10
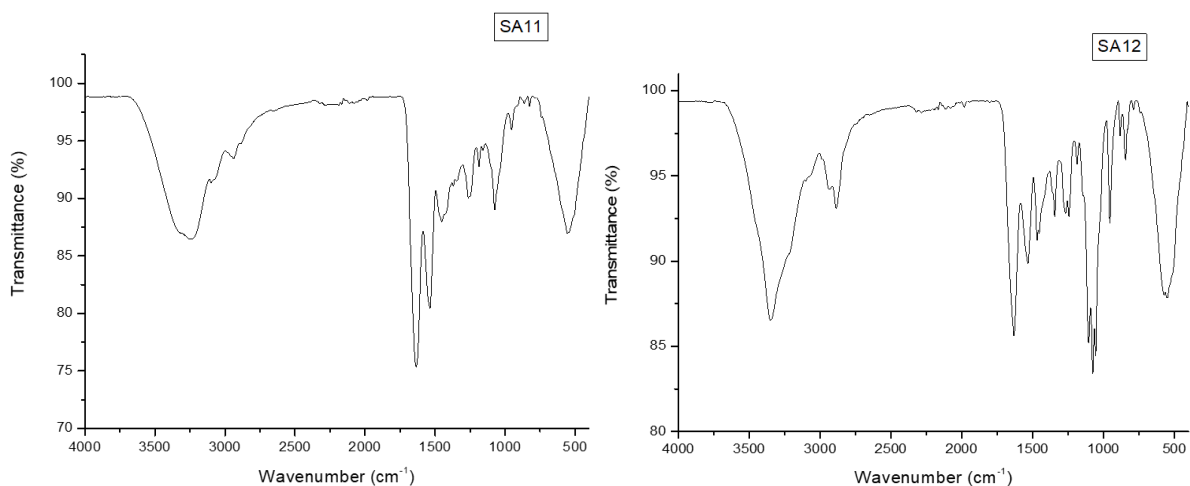
Figure 12: IR spectra of SA11 and SA12
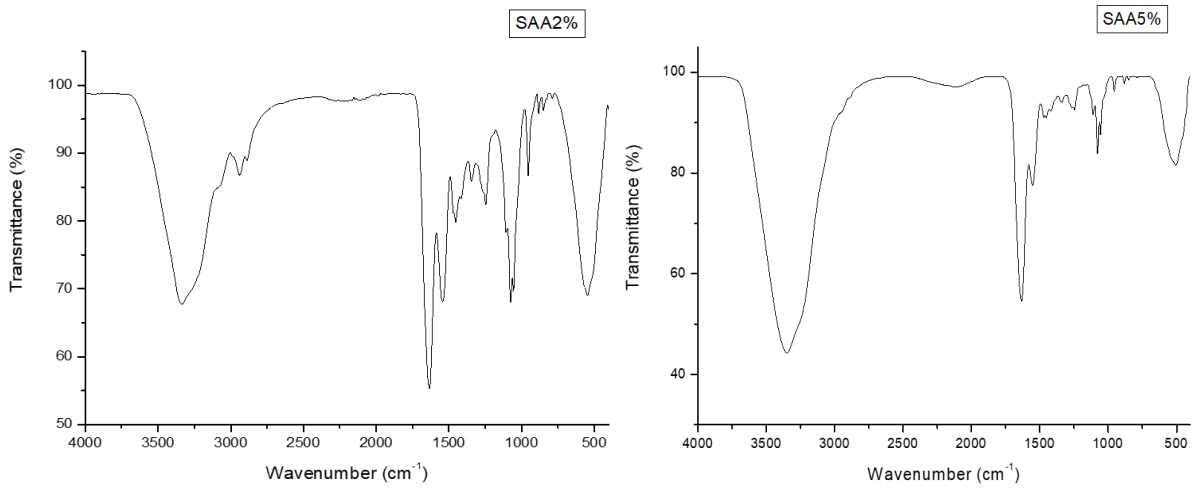
Figure 13: IR spectra of SAA2% and SAA5%
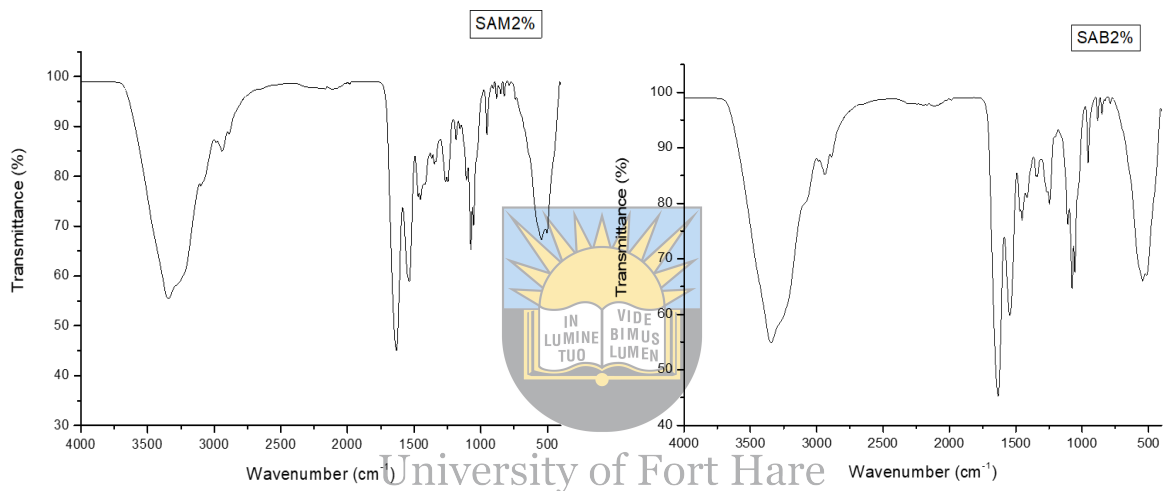
Figure 14: IR spectrum of SAM2% and SAB2%
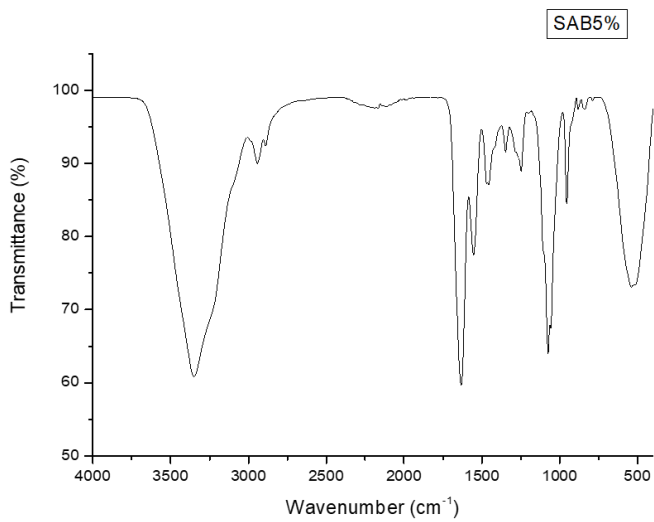
Figure 15: IR spectrum of SAB5%

Table 6. FTIR data of used polymers and antibiotics for preparation of sponges

Polymer or Drug Used	Functional Groups	Absorption peak (cm^{-1})
Gelatin	N-H	3288
	C=O (Amide I)	1631
	C=O (Amide II)	1525
	C=O (Amide III)	1240
PEG	C-O	1100
Metronidazole	C=N	1533
	N=O	1479
	C-C	1435
	C-N	1070
	=C-O	740

4.2. SEM/EDX

The SEM images of gelatin/PEG hybrid sponges are shown in **Figures 16**-**24**, displaying the surface morphology of the sponges. The SEM images of SA1, SA3, and SA5 exhibited a combination of plate-like morphology and a few spheres morphology. The surface morphology of SA2, SA6, SA12, SAA2%, and SAB2% also displayed plate-like morphology. The SEM images of SA4 and SA7 showed globular morphology with very few micropores. The surface morphology of SA10 exhibited swollen morphology. The surface morphology of SA8, SA9, SA11, and SAM2% displayed a highly porous network structure. The SEM images of SAA5% and SAB5% demonstrated a combination of globular and sphere-like morphology. Similar micrographs were reported by Wang et al. for ECM-loaded gelatin sponges for wound healing application. Their SEM images showed irregular porous morphology and highly porous network structures [11]. Several researchers have reported similar morphologies for gelatin-based sponges, especially porous morphology, due to the high amount of gelatin in the prepared sponges [12]–[16].

The CaCl$_2$ concentration did not lead to any significant effect on the morphology of the gelatin-based hybrid sponges. Ngece et al. reported SEM results of biopolymer-based sponges crosslinked with CaCl$_2$ in which the concentration of the crosslinker did not result in any significant effect on the SEM images of the sponges [17]. The porous structure of wound dressing is important for good gas permeation and suitable to induce high cell proliferation and attachment, and nutrient migration, and stimulating the acceleration of wound healing

mechanism. Furthermore, porous morphology can also influence the water adsorption capacity of the sponges [12].

The EDX analysis was used to determine the chemical composition of gelatin/PEG sponges co-loaded metronidazole and Ag nanoparticles (SA1-SA12), gelatin/PEG sponges loaded with only Ag nanoparticles (SAA2% and SAA5%), gelatin/PEG sponges loaded with only metronidazole (SAM2%), and blank sponges (SAB2% and SAB5%). The results are reported as mean ± SD (**Table 7**). Oxygen was visible in some sponges with a higher percentage of 13.95 and 49.20% compared to other elements (carbon, nitrogen, and silver). Nitrogen was visible in all sponges, with the composition percentage ranging from 0.66 to 21.39%. The mass percentage of carbon and Ag in the sponges was 14.71-40% and 0-0.92%, respectively. The EDX results of SAB2%, SAB5%, and SAM2% did not show the presence of Ag because they were not loaded with Ag nanoparticles. These EDX results revealed the successful fabrication of gelatin hybrid sponges encapsulated with metronidazole and Ag nanoparticles.
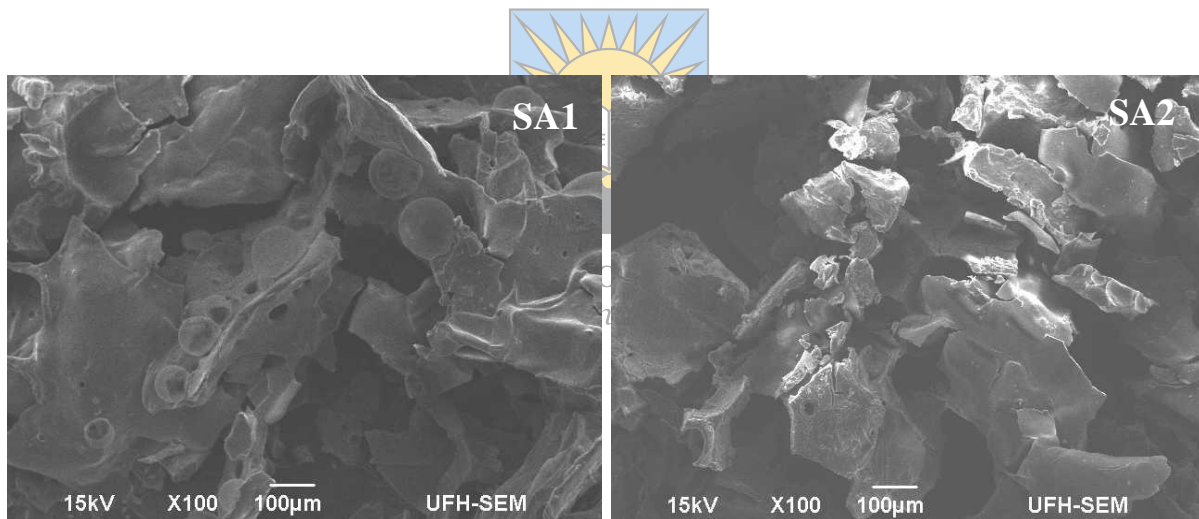
Figure 16: SEM images of SA1 and SA2
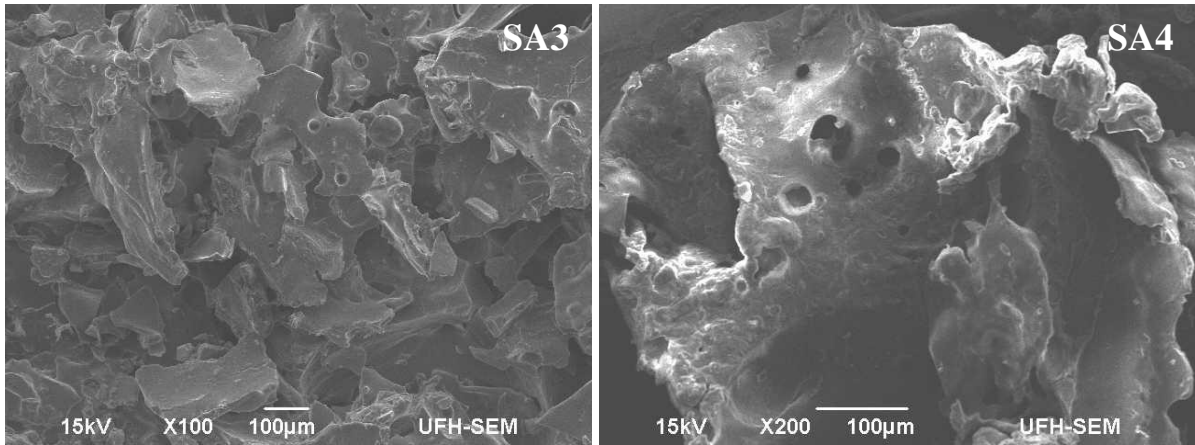
Figure 17: SEM images of SA3 and SA4
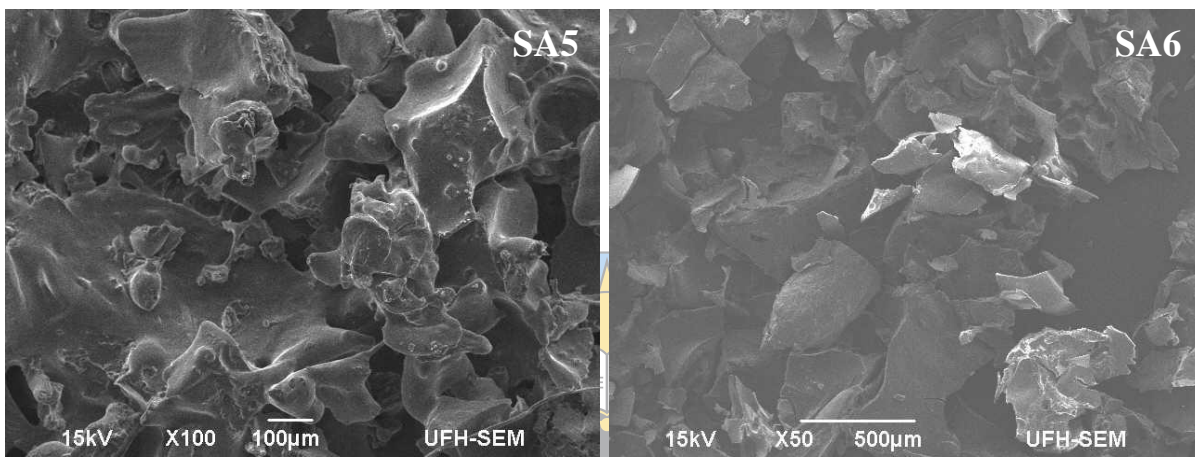
Figure 18*:* SEM images of SA5 and SA6
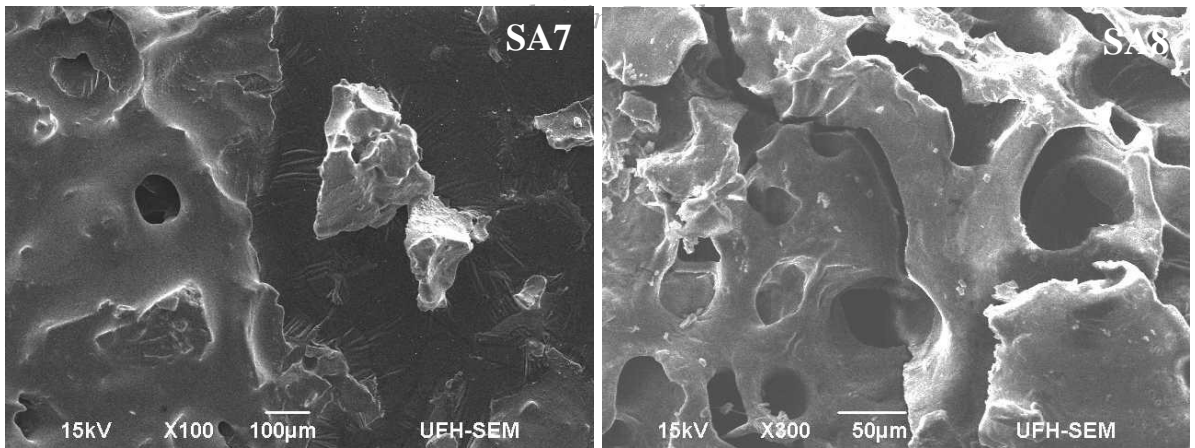
Figure 19: SEM images of SA7 and SA8
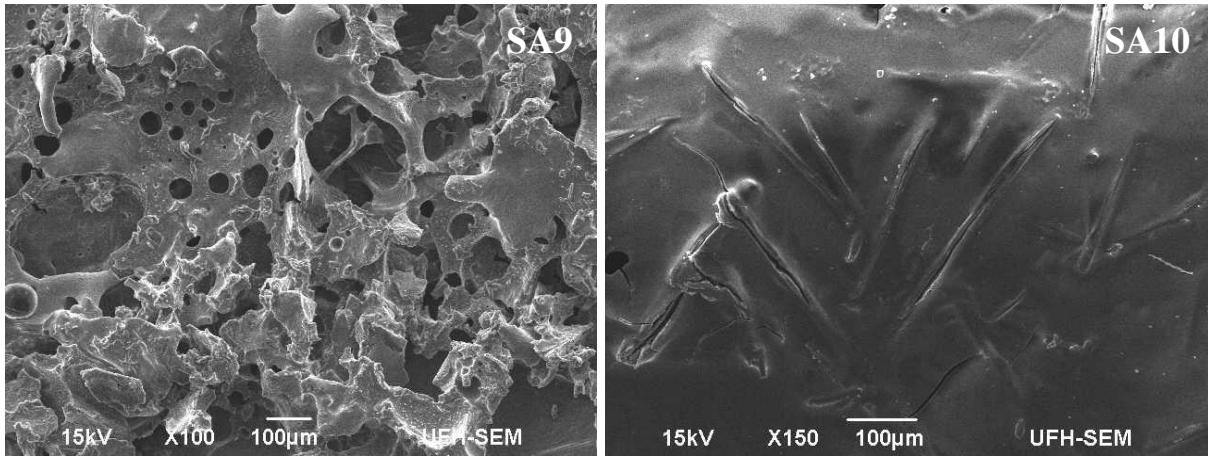
Figure 20: SEM images of SA9 and SA10
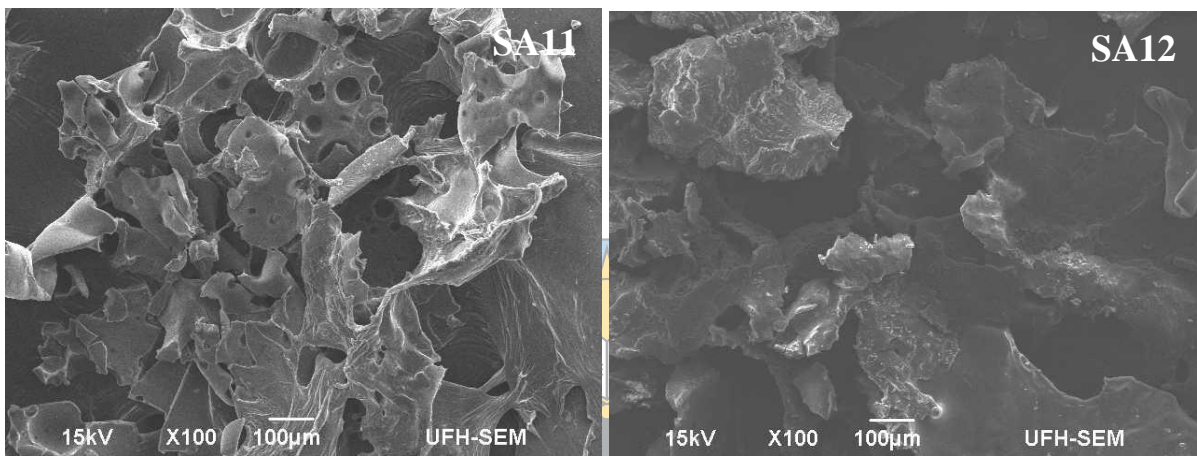
Figure 21: SEM images of SA11 and SA12
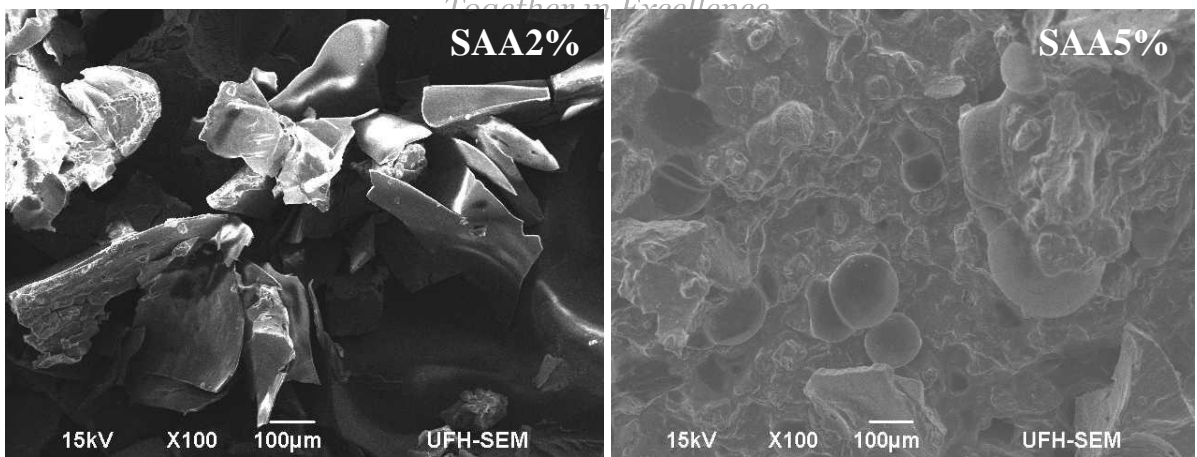
Figure 22: SEM images of SAA2% and SAA5%
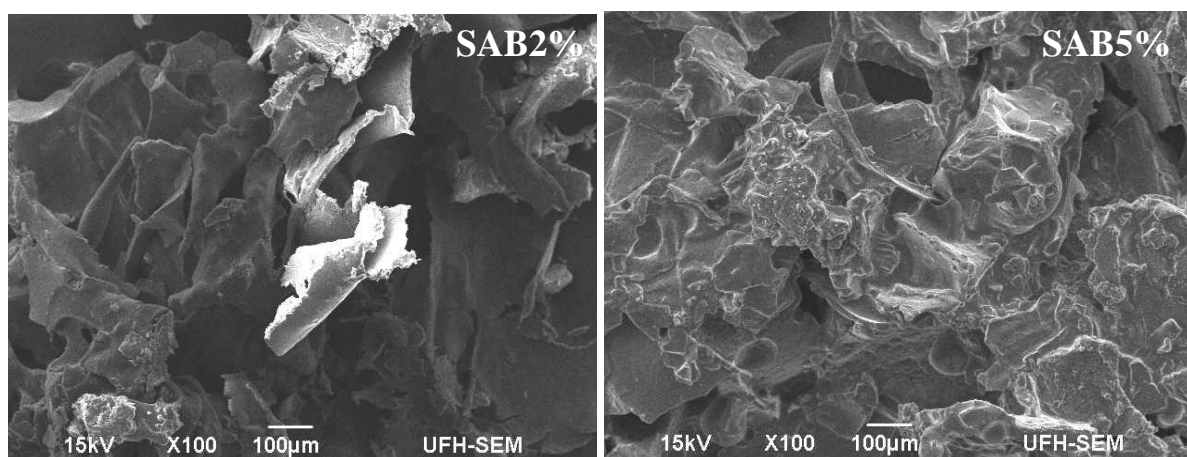
Figure 23: SEM images of SAB2% and SAB5%
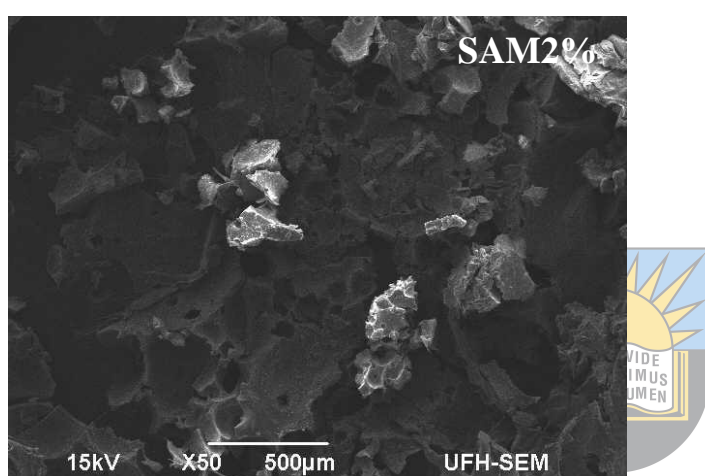
Figure 24: SEM images of SAM2%

Table 7. Elemental composition of the sponges

Sponges	Carbon (%)	Nitrogen (%)	Oxygen (%)	Silver (Ag) (%)
SA1	-	15.21	34.59	0.52
SA2	-	7.82	32.83	-
SA3	14.71	0.66	13.95	-
SA4	-	17.0	50.21	0.48
SA5	-	12.67	28.31	0.92
SA6	-	11.28	44.06	0.20
SA7	27.31	21.82	-	0.26
SA8	-	15.68	47.69	0.85
SA9	-	15.00	23.70	-
SA10	40.00	20.13	37.04	0.10
SA11	-	13.82	26.47	0.15
SA12	-	18.08	49.20	1.13
SAA2%	34.51	21.39	30.37	-
SAA5%	16.72	20.51	20.51	0.91
SAM2%	32.64	14.11	28.09	0.00
SAB2%	28.29	14.32	24.80	0.00
SAB5%	16.62	18.32	-	0.00

4.3. Thermogravimetric Analysis (TGA)

The Thermogravimetric analysis (TGA) was performed to evaluate the moisture content of the pristine and gelatin/PEG sponges loaded with metronidazole and Ag nanoparticles. Ideal moisture content is effective in providing an appropriate environment for the acceleration of the process of wound healing. The TGA graphs of the gelatin-based hybrid sponges showed a decrease in the weight of the gelatin/PEG sponges when they were heated at a temperature that ranges between 20 and 700 °C (**Figure 25-33**). These graphs exhibited a significant loss of weight in either three or four phases of temperature for the sponges. Sponge SA1 showed four phases of weight loss of 22.76% at 39-106ºC, 18% at 106-256ºC, 20.10% at 256-448 ºC, and 2.55% at 448-497ºC. SA2 also revealed four significant phases of weight loss of 14.78% at 39-125ºC, 11.80% at 125-258ºC, 31.26% at 258-355ºC, and 17.97% at 355-530 ºC. SA3 exhibited three distinct stages of weight loss at 28-152ºC (27.28%), 152-421ºC (30.50%), and 421-519ºC (11.36%). SA4 showed four phases of weight loss of 13.60% at 40-128ºC, 10.21% at 128-250ºC, 35.25% at 250-399ºC, and 18.95% at 250-549ºC. SA5 displayed three weight loss phases of 26.75% at 33-158ºC, 32.80% at 152-432ºC, and 12.74% at 432-543ºC. SA6 revealed four phases of weight loss of 13.65% at 37-122ºC, 10.44% at 122-243ºC, 37.68% at 243-420ºC, and 18.03% at 420-566ºC.
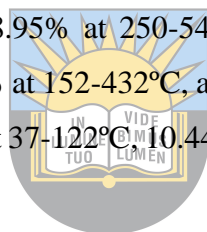
 Sponge SA7 showed three significant stages of weight loss of 28.81% at 30-224ºC, 28.38% at 224-421ºC, and 18.15% at 421-561ºC. SA8 revealed four significant phases of weight loss of 12.96% at 32-126ºC, 9.07% at 126-247ºC, 34.16% at 247-385ºC, and 26.70% at 385-585ºC. SA9 displayed three significant stages of weight loss of 18.89% at 35-155ºC, 35.06% at 155-404ºC, and 21.60% at 404-571 ºC. SA10 revealed three significant stages of weight loss at 32-126ºC (15.70%) 126-233ºC, 233-411ºC, and 411-591ºC. SA11 revealed three phases of weight loss of 14.70% at 37-153ºC, 35.39% at 153-400 ºC, and 22.48% at 400-552ºC. SA12 displayed three significant stages of weight loss of 19.21% at 30-133ºC, 44.19% at 133-399ºC, and 26.61% at 399-610ºC. SAA2% exhibited three important stages of weight loss at 35-142ºC, 142-377 ºC, and 377-560ºC of 23.71%, 38.46%, and 20.92%, respectively. SAA5% displayed three significant stages of weight loss of 40.65% at 28-156ºC, 27.52% at 156-423ºC, and 8.21% at 423-504ºC. SAB2% revealed three phases of weight loss of 19.51% at 37-144ºC, 38.74% at 144-400, and 16% at 400-568ºC. SAB5% exhibited three significant stages of weight loss of 48.75% at 35-138 ºC, 27.61% at 138-429 ºC, and 7.62% at 429-509 ºC. Lastly, SAM2%

exhibited three important stages of weight loss at 35-135ºC, 135-258ºC, 258-370, and 370-562ºC, of 25.55%, 13%, 33.07%, and 17.97%, respectively.

The first stage of weight loss for the gelatin/PEG sponges was due to the presence of moisture. Almost all the sponges exhibited ideal moisture content (10-30%) of wound dressing with excellent moisture content that ranged between 12.96 and 27.28% (**Table 8**), except SAA5% (40.65%) and SAB5% (48.75%), indicating their ability to offer a moist environment for the injury which is appropriate for the acceleration of wound healing process. The moisture content of the sponges was observed at a temperature between 28 and 224ºC. The final two or three phases of weight loss occur when the temperature increases from 106 to 585ºC; this effect is due to the degradation of the sponges. These TGA results were similar to those of gelatin-chitosan hybrid sponges incorporated with tannins and platelet-rich plasma fabricated by Lu et al. for application in wound healing. The TGA analysis of gelatin-based hybrid sponges exhibited three stages of weight; the first stage, at a temperature between 40 and 217ºC, displayed a weight loss of about 8.4%, which was attributed to the moisture content of sponges [18]. Wen et al. prepared gelatin/sodium alginate hybrid sponges encapsulated with tetracycline hydrochloride to treat bacteria-infected injuries. The TGA results showed that the first phase of weight took place below 120ºC owing to the evaporation of moisture (presenting moisture content of sponges). The weight loss that occurs at a temperature that ranged between 180 and 370ºC was due to the degradation of gelatin (similar to the case of gelatin/PEG sponges) [19]. Naghshineh et al. reported that the first stage of weight loss (10%) at the range of 170-300ºC from TGA studies of curcumin-loaded gelatin-based sponges could be attributed to the moisture content of sponges, while the second and third phases can happen because of the various factors, such as the release of volatile compounds, depolymerization of the polymer chain in sponges, etc. [20].

Table 8. The calculated moisture content of the sponges

Sponges	Moisture Content (%)
SA1	22.76
SA2	14.78
SA3	27.28
SA4	13.60
SA5	25.75
SA6	13.65

SA7	28.81
SA8	12.96
SA9	18.89
SA10	15.70
SA11	14.70
SA12	19.21
SAA2%	23.71
SAA5%	40.65
SAB2%	19.51
SAB5%	48.75
SAM2%	25.55
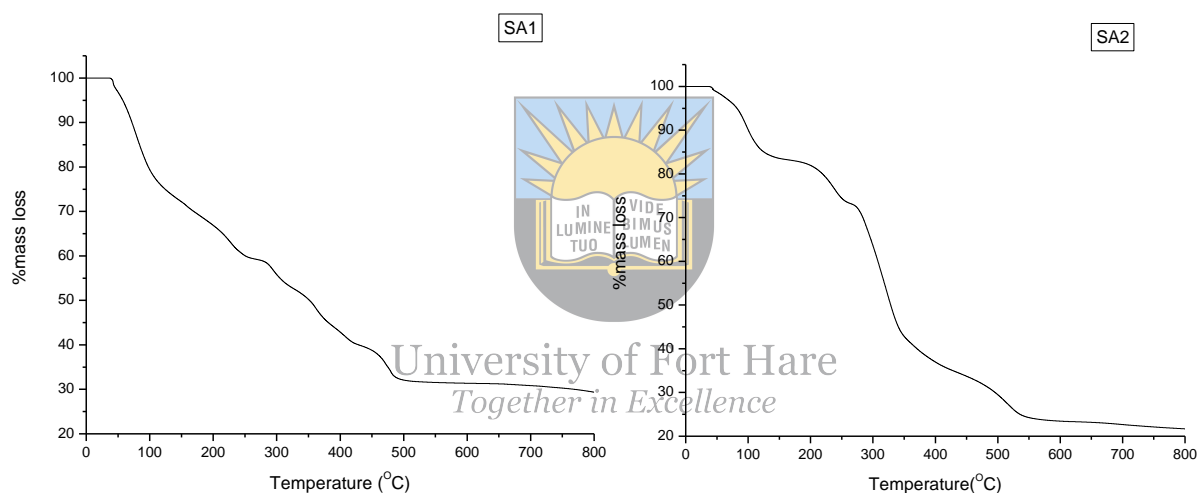
Figure 25: TGA spectra of SA1 and SA2
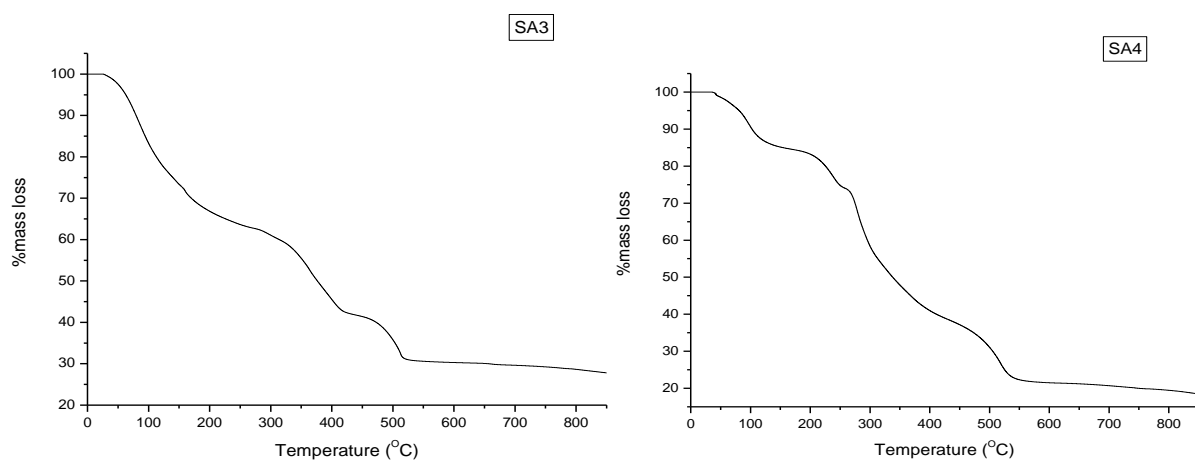
Figure 26:TGA spectra of SA3 and SA4
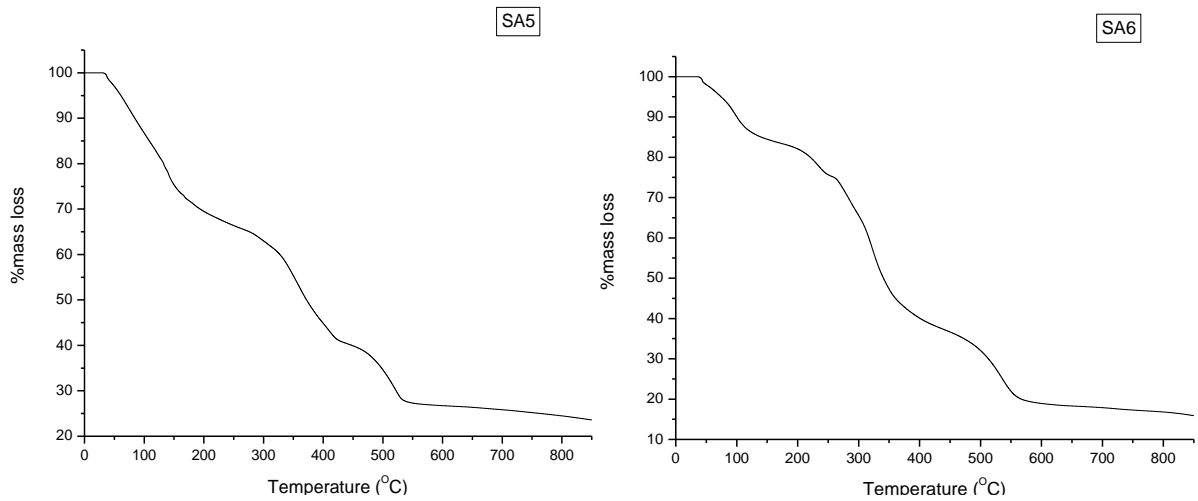
Figure 27: TGA spectra of SA5 and SA6
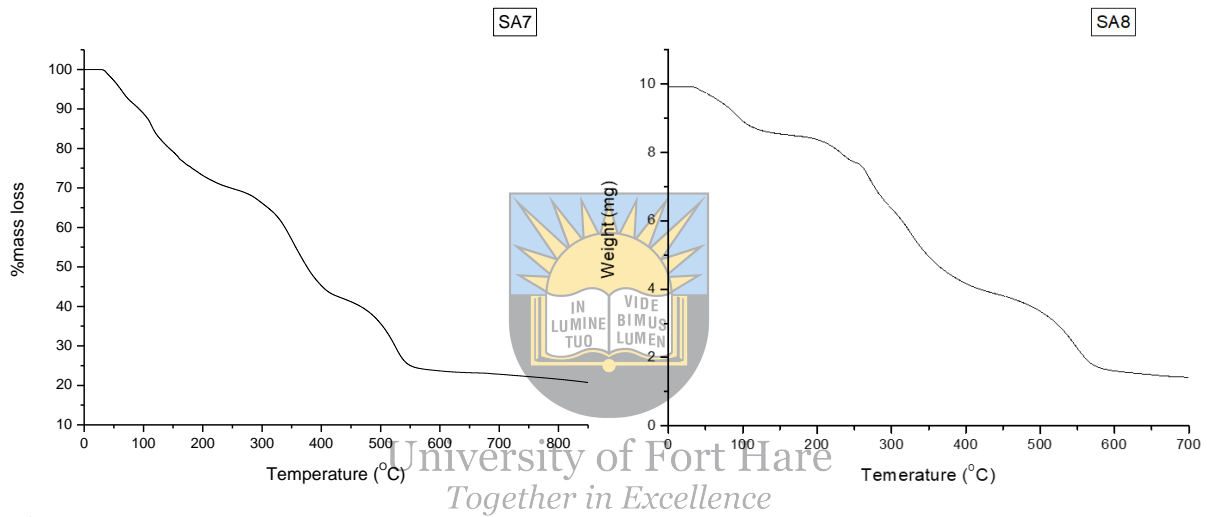
Figure 28: TGA spectra of SA7 and SA8
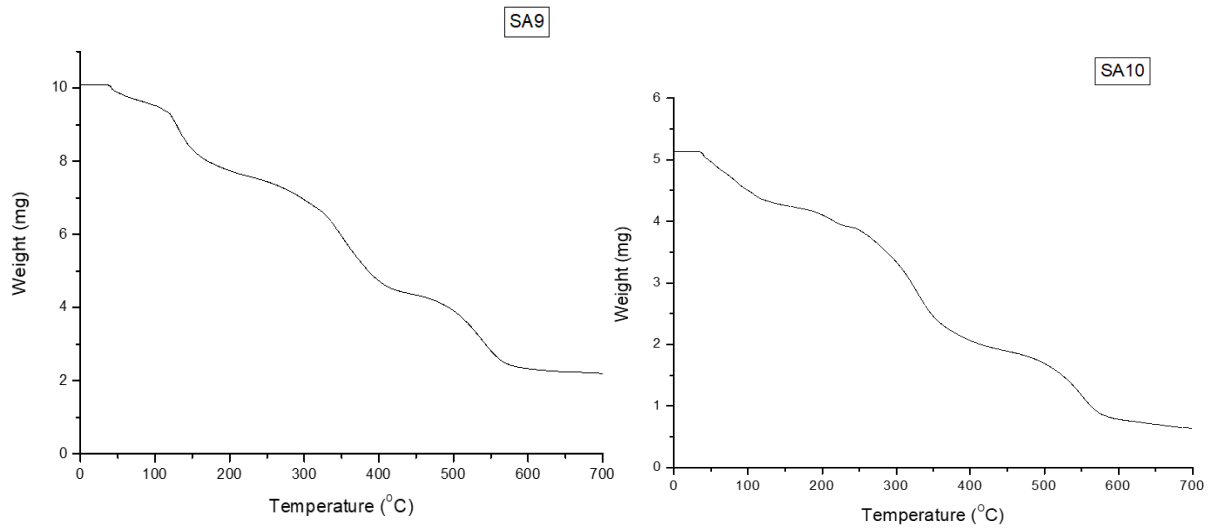
Figure 29: TGA spectra of SA9 and SA10
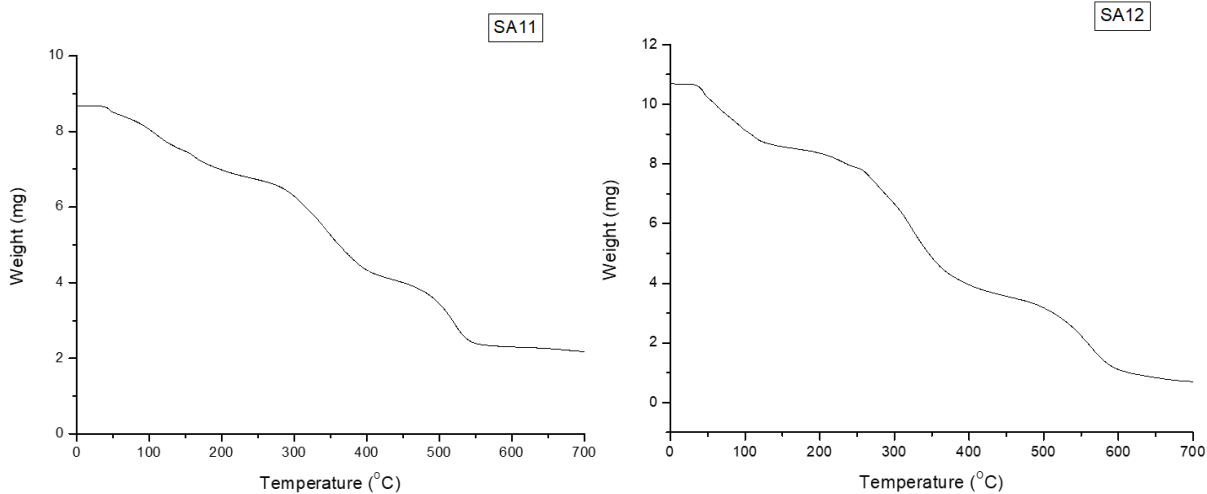
Figure 30: TGA spectra of SA11 and SA12
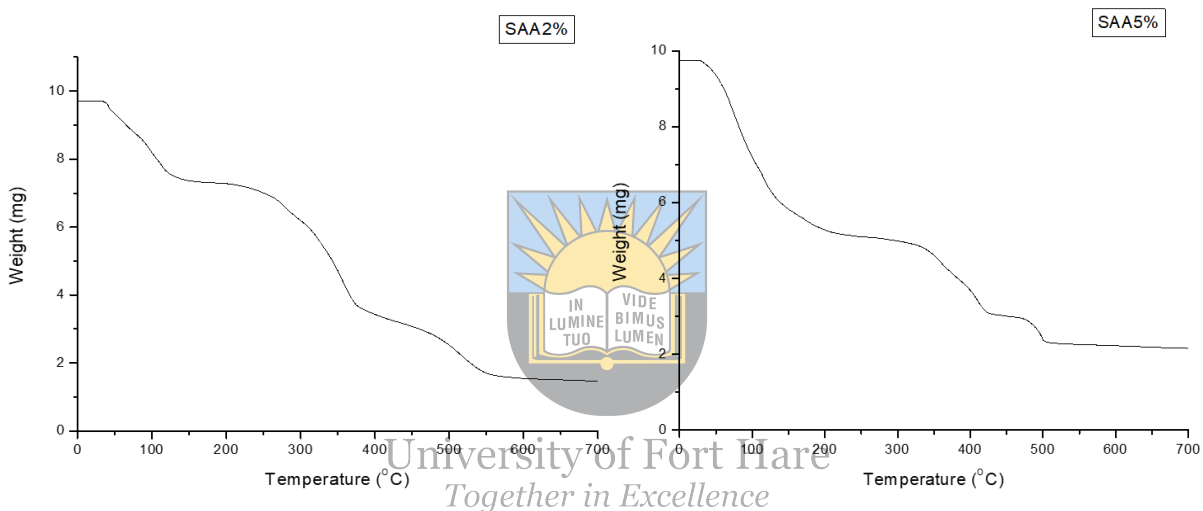
Figure 31: TGA spectra of SAA2% and SAA5%
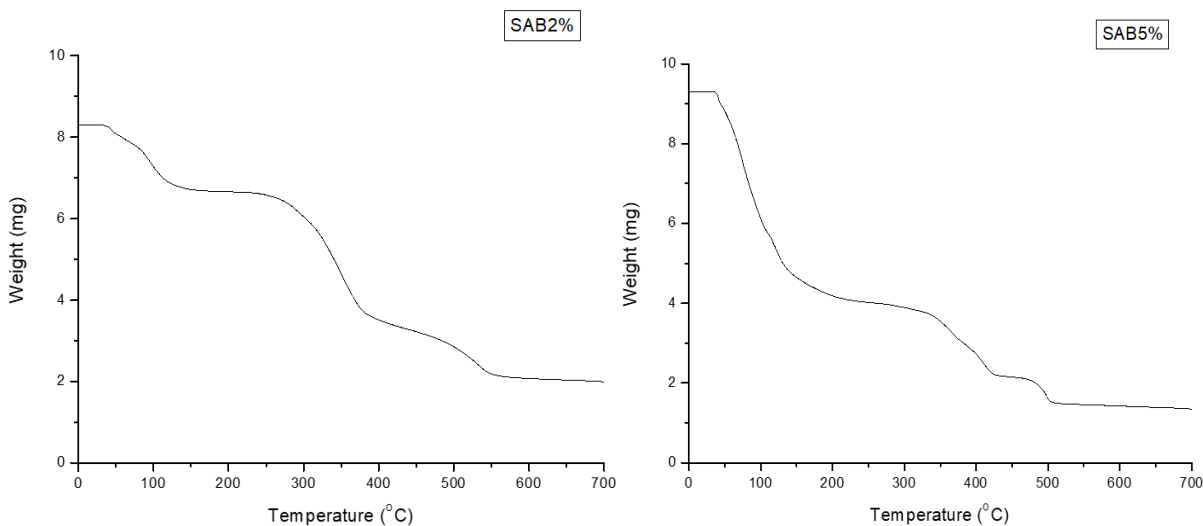
Figure 32: TGA spectra of SAB2% and SAB5%
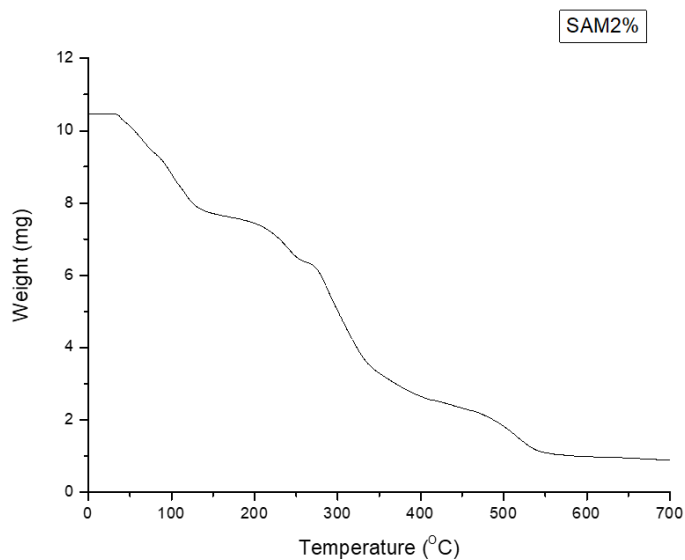
Figure 33: TGA spectrum of SAM2%

4.4. XRD

The XRD spectrum of metronidazole revealed significant crystalline characteristic peaks at 2Ө=12.50, 13.90,21.50, 24.90, 29.50, and 33.95 (**Figure 34**). The XRD spectra of gelatin/PEG sponges showed broad peaks demonstrating the amorphous nature of the sponge wound dressings (**Figures 34 to 39**)). The characteristic crystalline peaks of the metronidazole were not significant in the XRD spectrums of the sponges. Nevertheless, the distinctive peak of the antibiotics was visible in all the sponges at 2Ө=12.50, revealing the successful loading of the antibiotics in the sponge-based wound dressings. Several researchers that prepared drug-loaded gelatin-based hybrid scaffolds for wound treatment reported similar results [21][22].
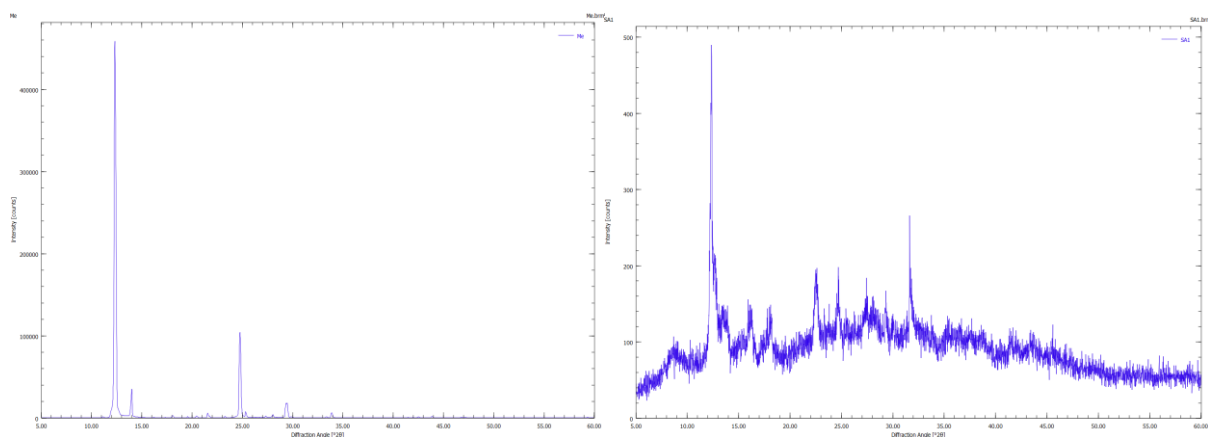
Figure 34: XRD spectrum of Metronidazole and SA1
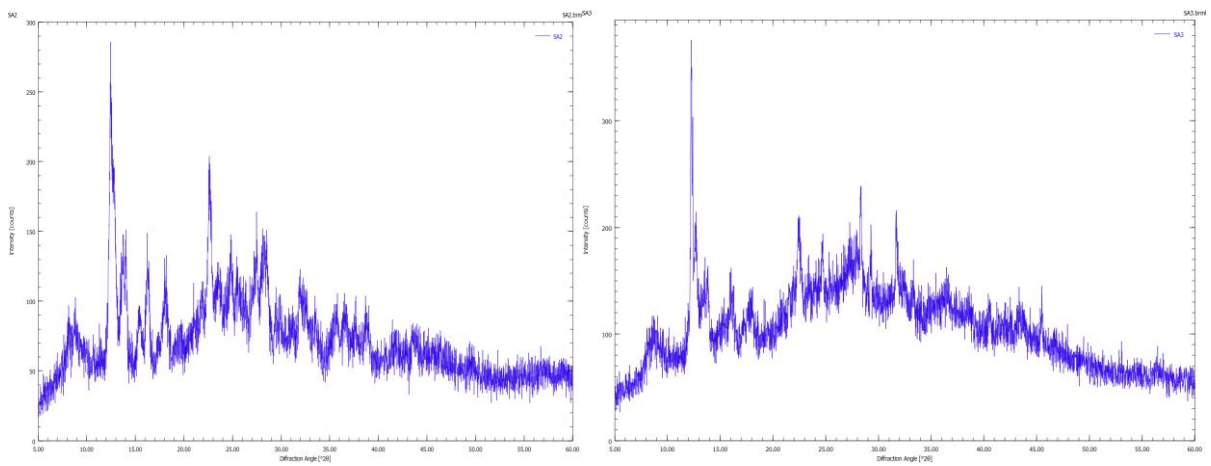
Figure 35: XRD spectrum of SA2 and SA3
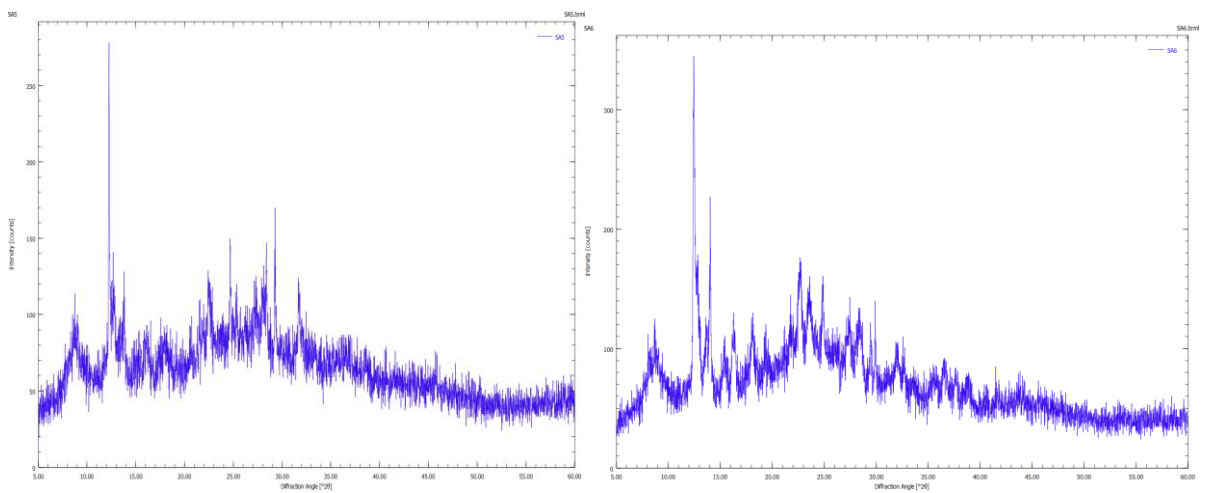
Figure 36: XRD spectrum of SA6 and SA6
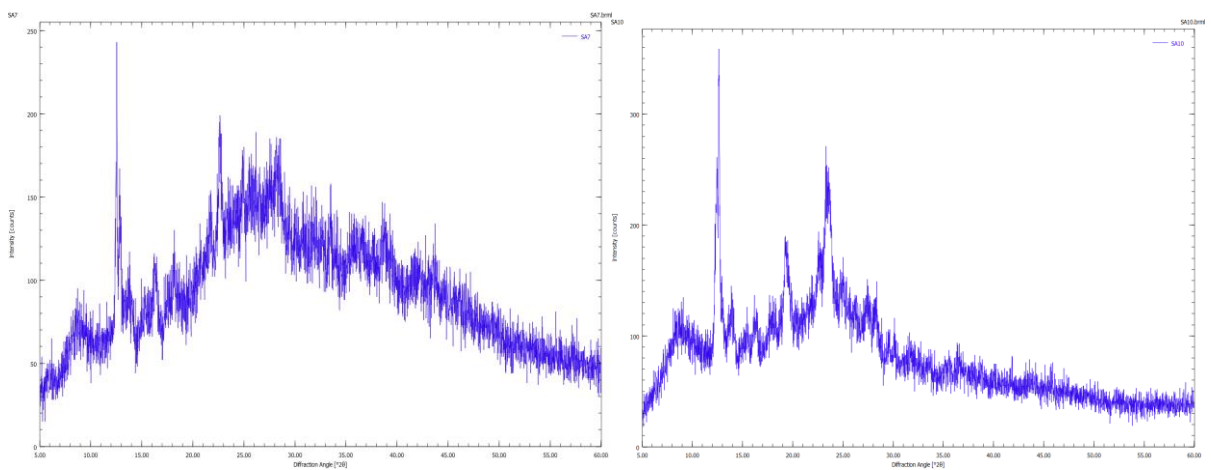
Figure 37: XRD spectrum of SA7 and SA10
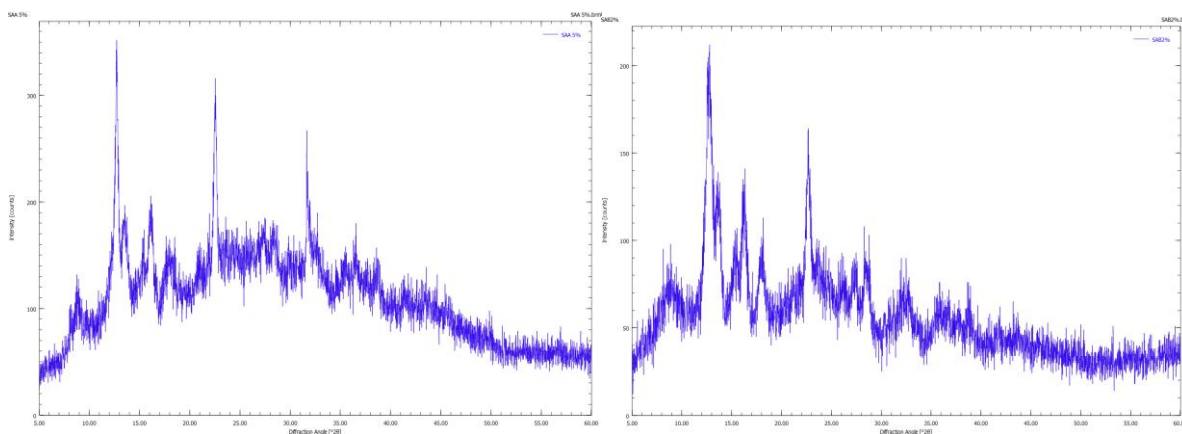
Figure 38: XRD spectrum of SAA5% and SAB2%
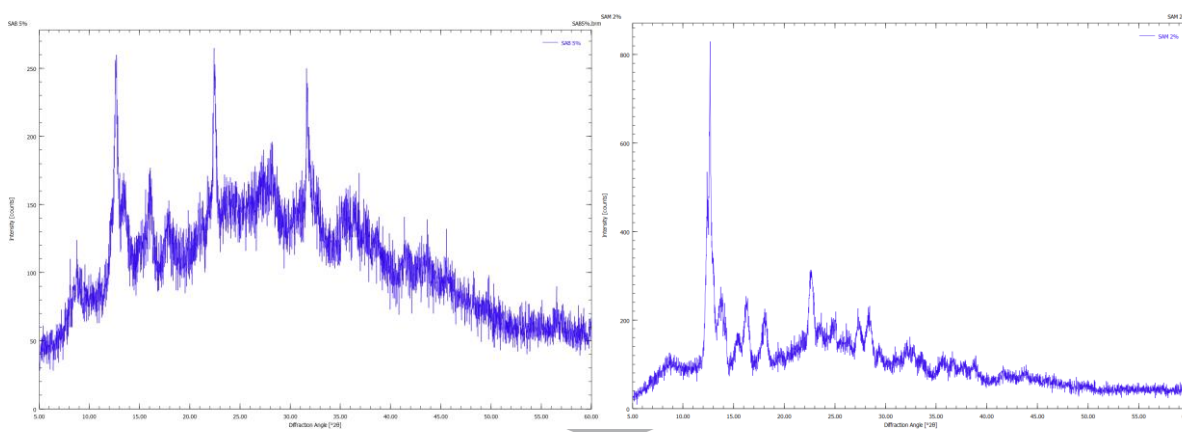
Figure 39: XRD spectra SAB5% and SAM2%

4.5. *In vitro* Biodegradability Studies

The *in vitro* biodegradability experiments were performed at pH 7.4 and pH 5.5, mimicking physiological pH and the pH of a chronic wound environment, respectively. The biodegradability of the sponges was analysed and confirmed by employing FTIR and SEM. The sponge samples that were selected for *in vitro* biodegradability are SA3, SA4, SA11, SA12, SAB2%, and SAB5%, due to their different polymer composition and percentage of cross-linking agents. The naming of the biodegraded sponge samples at pH 7.4 are as follows: the names of SA3 samples are A3W1 (freeze-dried sample after week 1), A3W2 (freeze-dried sample after week 2), and A3W3 (freeze-dried sample after week 3). The names of SA4 samples are A4W1 (freeze-dried sample after week 1), A4W2 (freeze-dried sample after week 2), and A4W3 (freeze-dried sample after week 3). The names of SA11 samples are A11W1 (freeze-dried sample after week 1), A11W2 (freeze-dried sample after week 2), and A11W3 (freeze-dried sample after week 3). The names of SA12 samples are A12W1 (freeze-dried

sample after week 1), A12W2 (freeze-dried sample after week 2), and A12W3 (freeze-dried sample after week 3). The names of SAB2% samples are B2W1 (freeze-dried sample after week 1), B2W2 (freeze-dried sample after week 2), and B2W3 (freeze-dried sample after week 3). The FTIR spectra of the samples after biodegradation experiments at pH 7.4 are shown in **Figures 40-48**.

The O-H stretching vibration at 3351-3218 cm^{-1} confirmed the alcohol group of metronidazole or Ag nanoparticles was replaced by some peaks in all sponges after biodegradation. New peaks that appeared for SA3 were around 3377, 3130, and 3689 cm^{-1} after one, two, and three weeks of the biodegradation experiment, respectively, indicating the degradable nature of the sponges. The O-H vibration peak on SA4 disappeared after one week, and two new peaks were formed at 3355 and 3376 cm^{-1} after two weeks of biodegradation studies. Also, the intensity of the O-H vibration peak of the SA4 sponge was reduced after three weeks of biodegradation studies. The O-H vibration peak of the SA11 sponge was broader after three weeks of the biodegradation experiment, and a new peak was visible at 2429 cm^{-1}. The O-H peak of SA12 was much broader during one and two weeks of biodegradation and a new vibration peak was formed at 2409 cm^{-1} after three weeks of biodegradation studies.

Also, the O-H peak of SAB2% was broader after 1-2 weeks of biodegradation experiments and a new peak was visible at 2434 cm^{-1} after three weeks of biodegradation. Furthermore, two new peaks were visible in the O-H range (3432 and 3376 cm^{-1}) during the third week of biodegradation studies. For SAB5%, the intensity of O-H vibration stretching was reduced during the first and second weeks of biodegradation, and two new peaks were visible at 3451 and 3377 cm^{-1}. A new broad peak was visible at 2397 cm^{-1} after 3 weeks of the biodegradation studies. The C=O vibration stretching assigned at 1637-1628 cm^{-1} for all the gelatin-hybrid sponges loaded with metronidazole was less intense after the biodegradation experiments. All the changes and formation of new peaks after the 3 weeks of biodegradation studies confirmed that the sponges are biodegradable under physiological conditions. The SEM micrographs of the sponges that are shown in **Figures 49-54** exhibited rough morphology for all the sponges after one, two, and three weeks of the biodegradation experiments. The change in the morphology of the sponges was significant after the biodegradation experiments. The FTIR spectra and SEM micrographs of the selected sponges demonstrated the potential capability of gelatin-based hybrid sponges to induce skin regeneration.
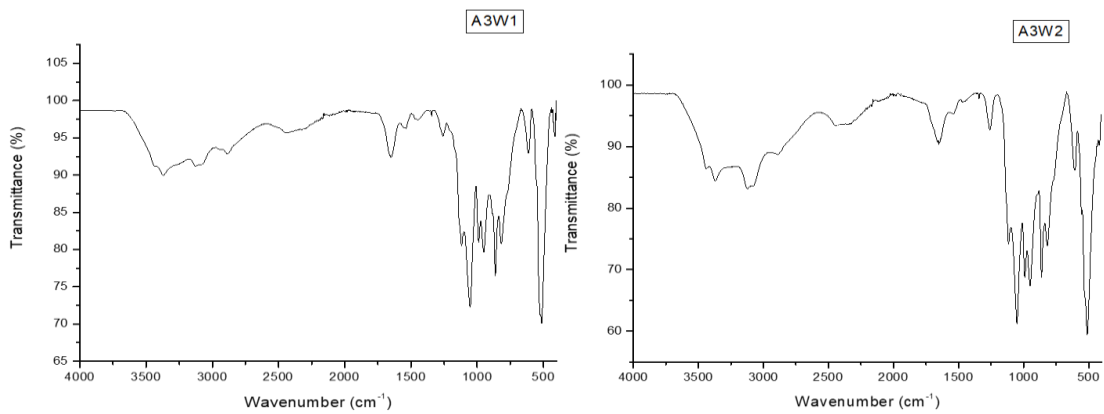
Figure 40: IR spectrum of A3W1 and A3W2
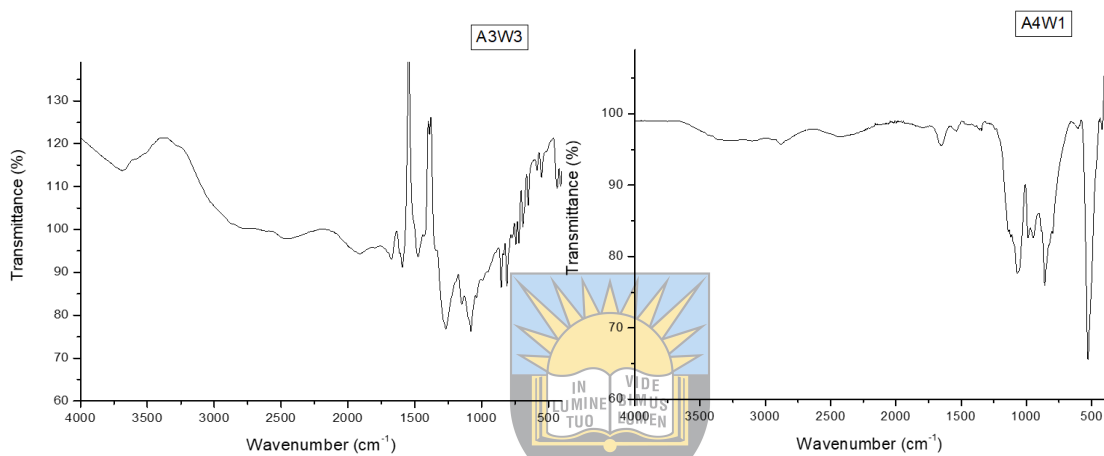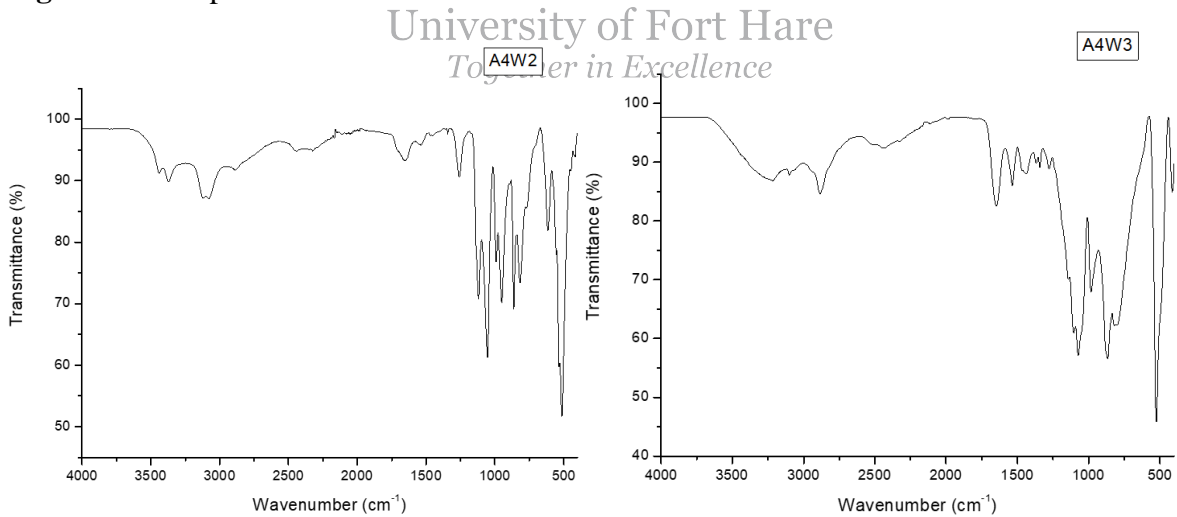

Figure 41: IR spectrum of A3W3 and A4W1

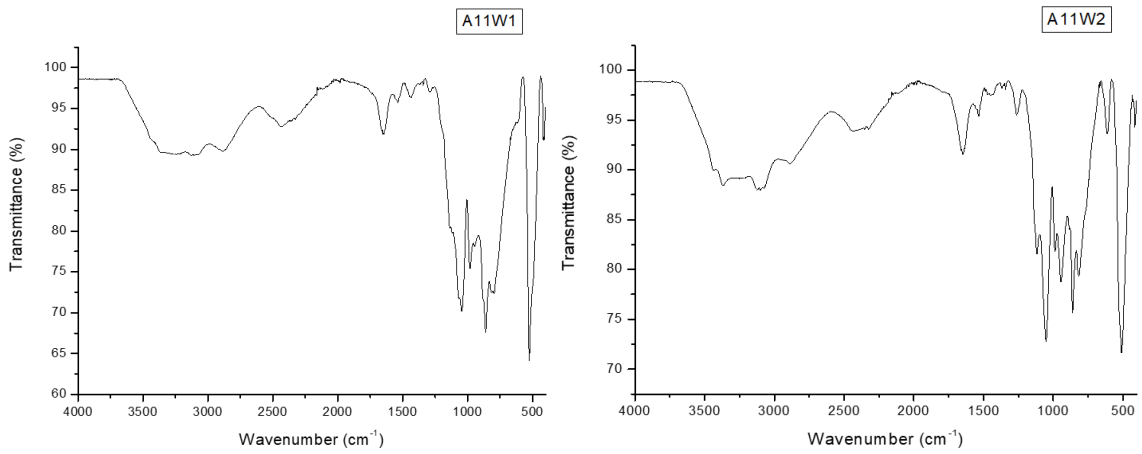**Figure 42:** IR spectrum of A4W2 and A4W3

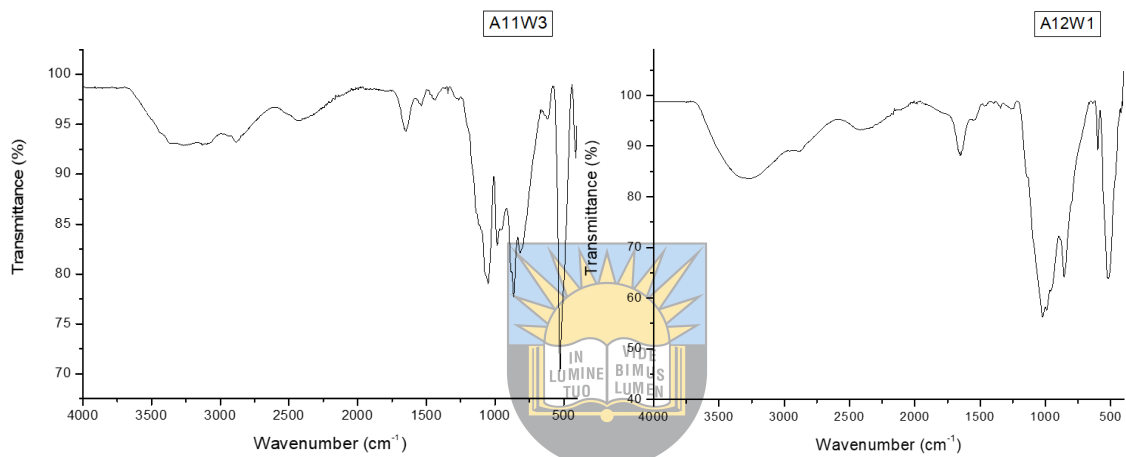**Figure 43:** IR spectrum of A11W1 and A11W2

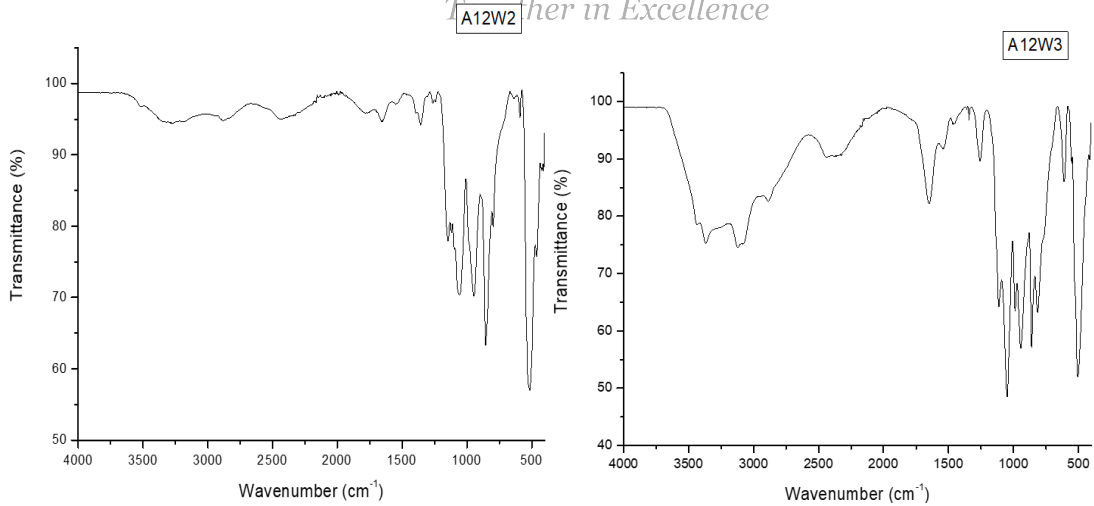**Figure 44:** IR spectrum of A11W3 and A12W1

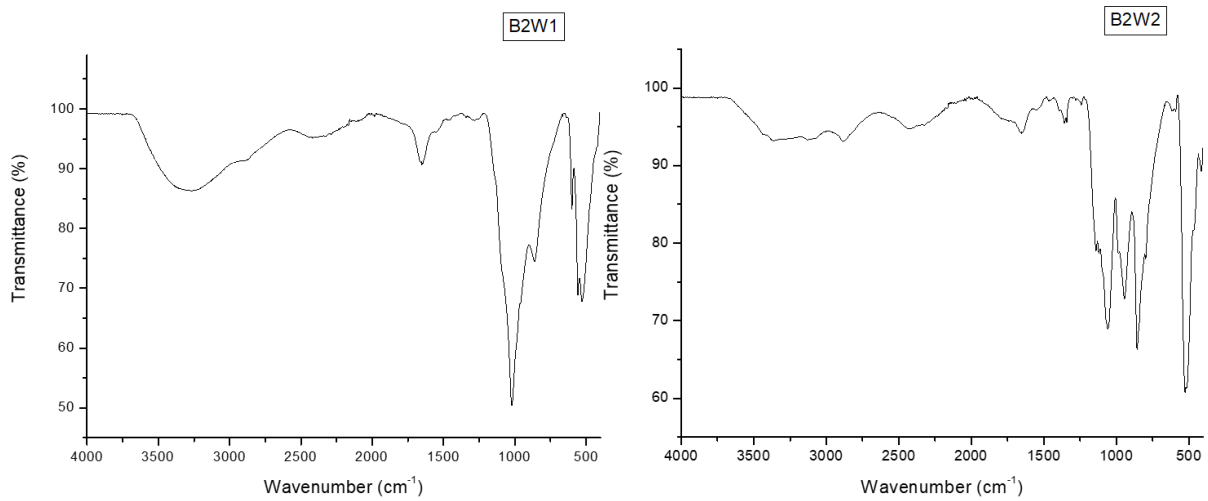**Figure 45:** IR spectrum of A12W2 and A12W3

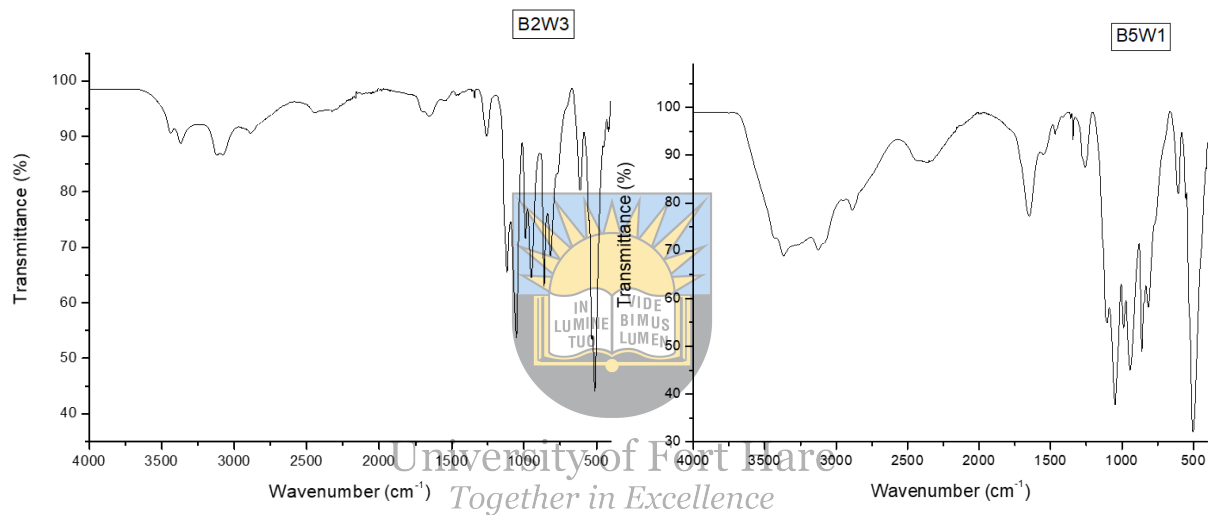**Figure 46:** IR spectrum of B2W1 and B2W2

Figure 47: IR spectrum of B2W3 and B5W1
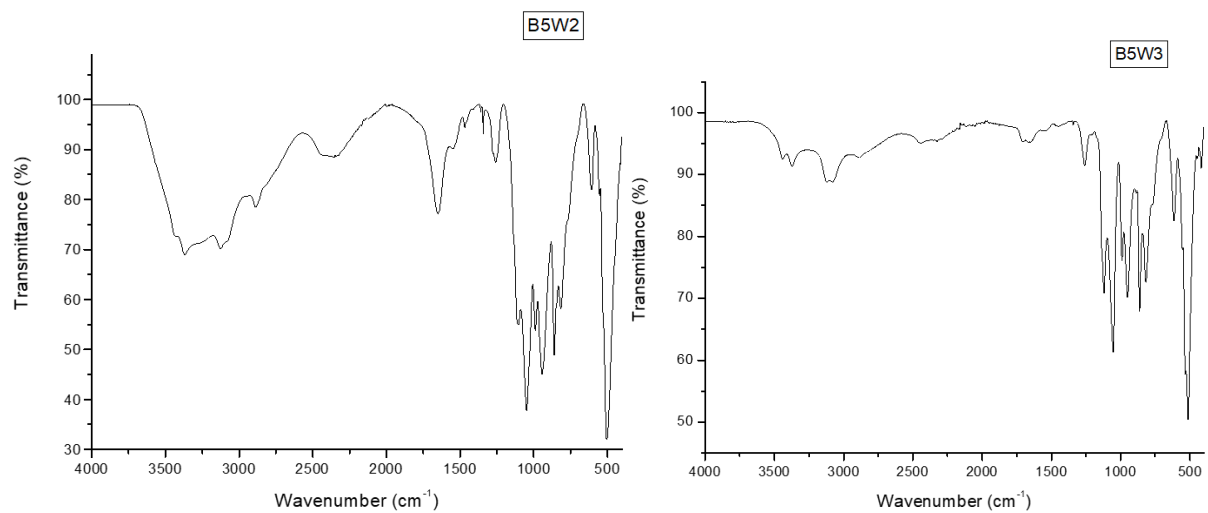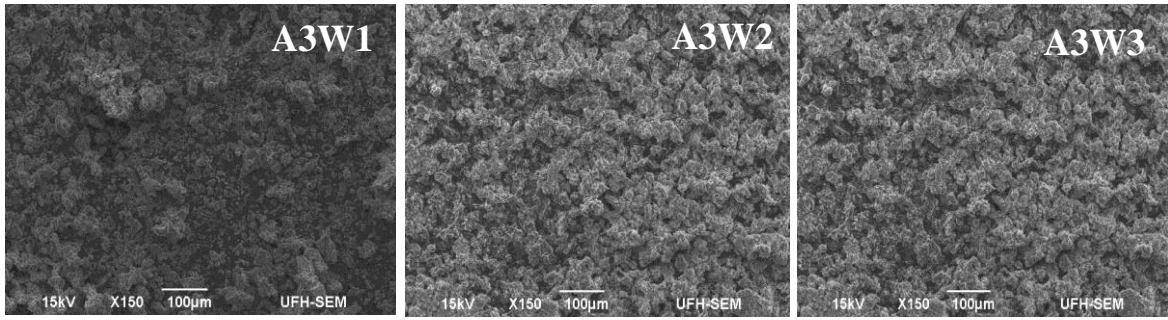

Figure 48: IR spectrum of B5W2 and B5W3
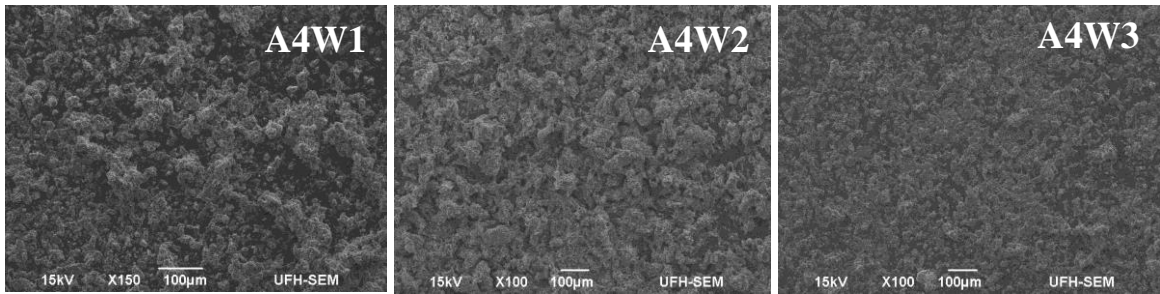
Figure 49: SEM images of A3W1, A3W2, and A3W3

Figure 50: SEM images of A4W1, A4W2, and A4W3
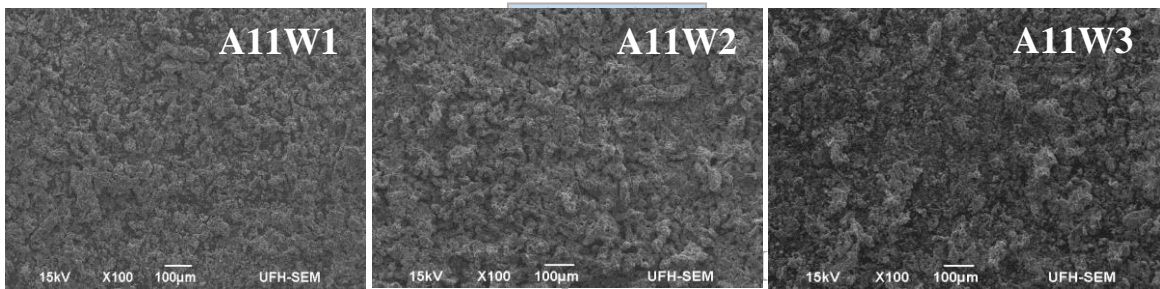
Figure 51: SEM images of A11W1, A11W2, and A11W3
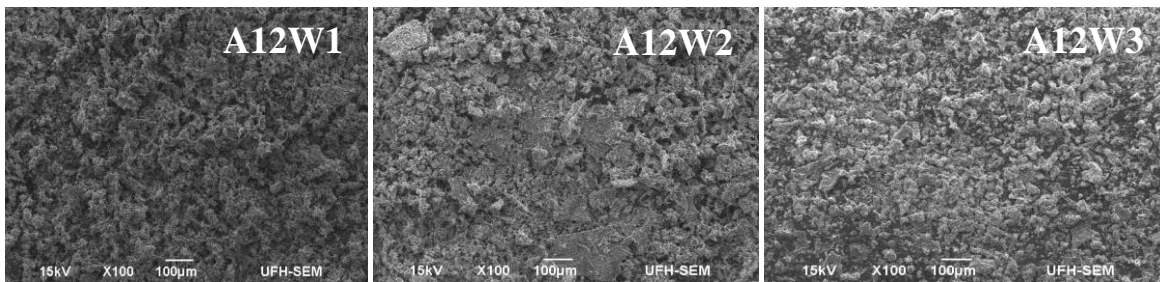
Figure 52: SEM images of A12W1, A12W2, and A12W3
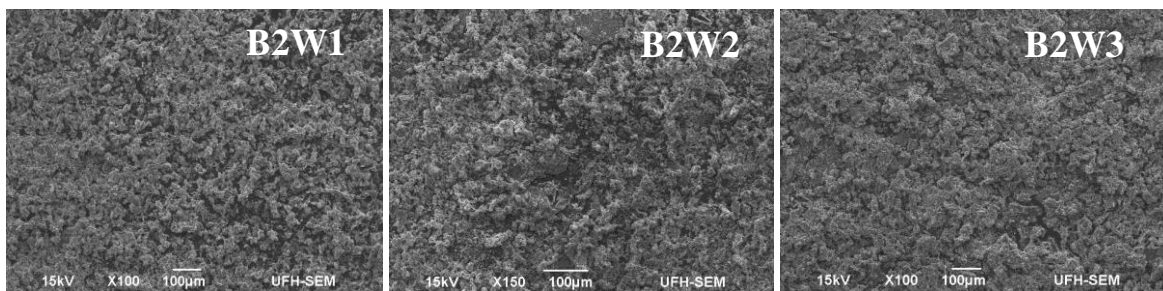
Figure 53: SEM images of B2W1, B2W2, and B2W3
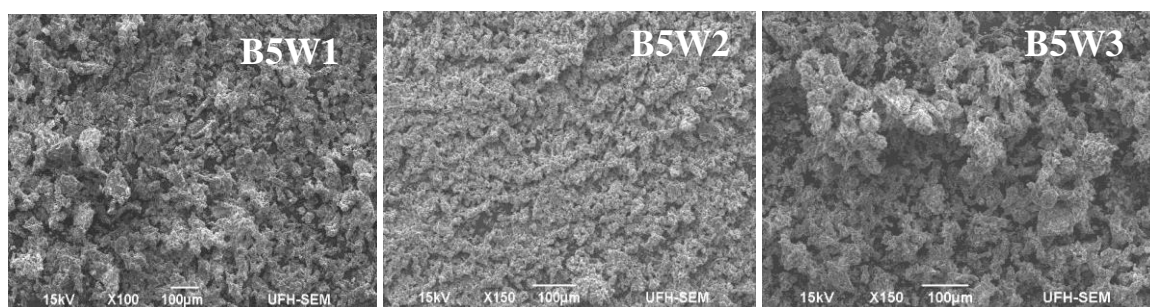
Figure 54: SEM images of B5W1, B5W2, and B5W3

The naming of the biodegradable sponge samples at pH 5.5 was as follows: the names for SA3 samples are A3X1 (freeze-dried sample after week 1), A3X2 (freeze-dried sample after week 2), and A3X3 (freeze-dried sample after week 3). The names for SA4 samples are A4X1 (freeze-dried sample after week 1), A4X2 (freeze-dried sample after week 2), and A4X3 (freeze-dried sample after week 3). The names for SA11 samples are A11X1 (freeze-dried sample after week 1), A11X2 (freeze-dried sample after week 2), and A11X3 (freeze-dried sample after week 3). The names for SA12 samples are A12X1 (freeze-dried sample after week 1), A12X2 (freeze-dried sample after week 2), and A12X3 (freeze-dried sample after week 3). The names for SAB2% samples are B2X1 (freeze-dried sample after week 1), B2X2 (freeze-dried sample after week 2), and B2X3 (freeze-dried sample after week 3). The FTIR spectra for the pH 7.4 sample are shown in **Figures 55-63**. The peaks between 3351-3218 cm^{-1} denote the O-H stretching vibrations of metronidazole and Ag nanoparticles were absent in all the sponges after three weeks. The following peaks were reduced after three weeks in most of the sponges: the C=N stretching at 1545 or 1536 cm^{-1} (overlapped with amide II of gelatin), N=O asymmetric stretching at 1472-1436 cm^{-1} (overlapped with amide III of gelatin), CH$_3$ bending at 1371-1344 cm^{-1}, C-C stretching at 1426 or 1416 cm^{-1}, CH$_3$ bending vibration at 1371-1343 cm^{-1}, C-N stretching at 1078-1059 cm^{-1}, and =C-H bending at 785-785 cm^{-1}.

These changes confirmed that the sponges are biodegradable. The SEM micrographs further confirmed the biodegradability of sponges (**Figures 64-69**). The morphology of sponge SA3 changes from plate-like surface to rough morphology at weeks 1 and 2, and a mixture of a sphere and rod-shaped morphology at week 3. Sponges SA4 altered from globular morphology with micropores to rough rod-like surface at week 1, globular morphology at week 2, and rough block-like surface. SA11 sponge changes from porous morphology to rough globular morphology in week 1, rod-like morphology in week 2, and rough morphology in week 3. The sponge SA12 that originally exhibited plate-like morphology changed to a rough block surface at weeks 1 and 2 of biodegradation studies and rough globular morphology at week 3. SAB2%

changed from a plate-like surface to rough globular morphology, while SAB5% changed from a globular surface with sphere-like morphology to rough morphology throughout the biodegradation studies.
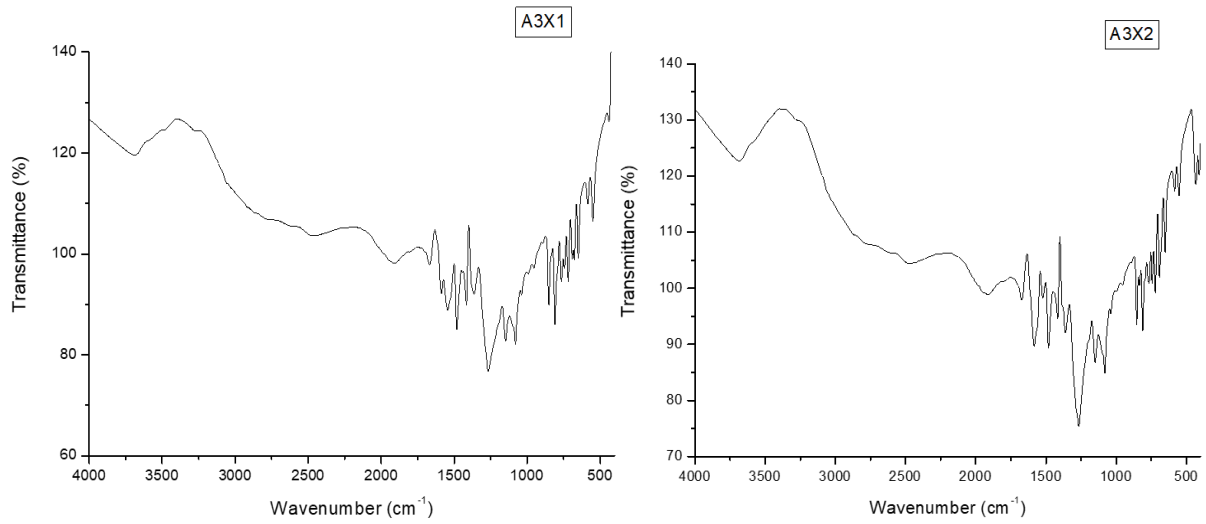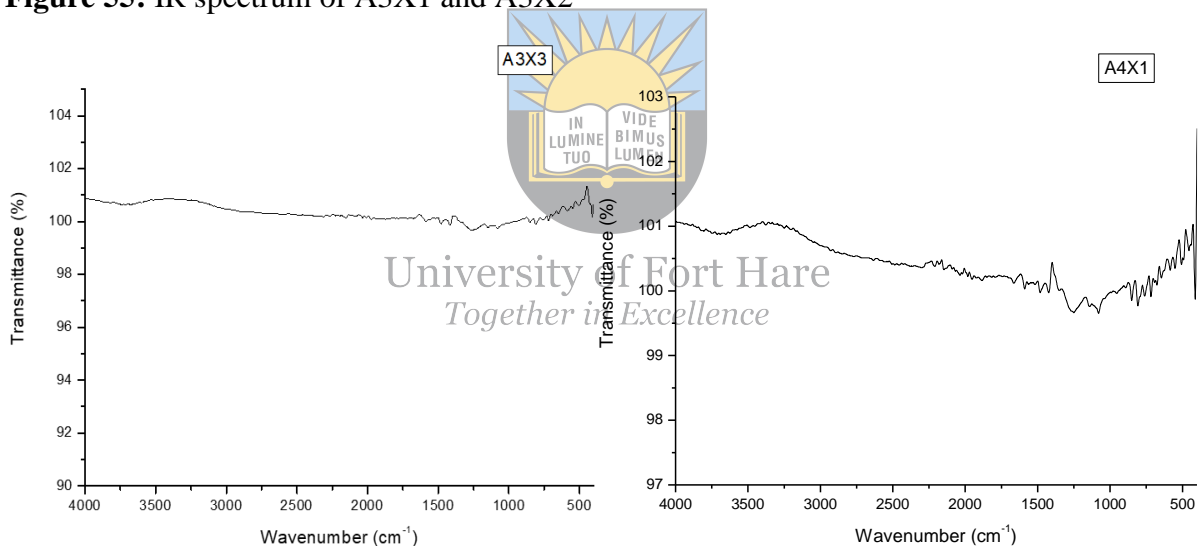

Figure 55: IR spectrum of A3X1 and A3X2

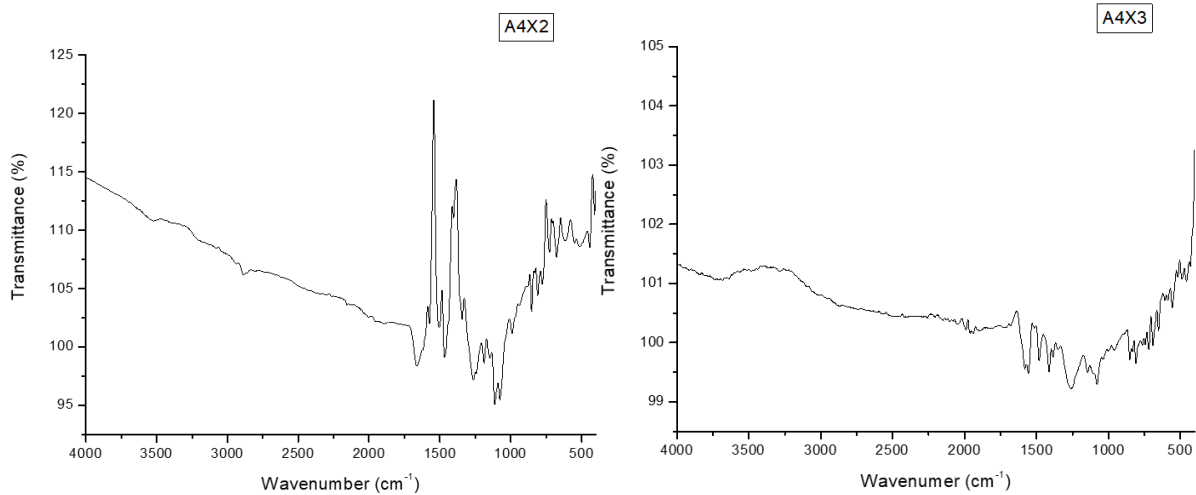**Figure 56:** IR spectrum of A3X3 and A4X1

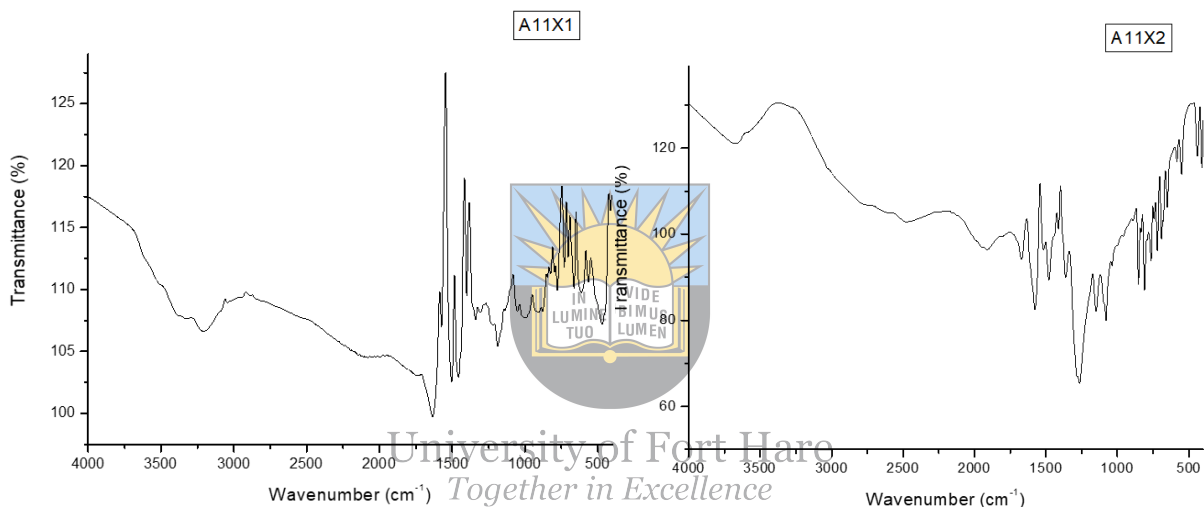**Figure 57:** IR spectrum of A4X2 and A4X3

Figure 58: IR spectrum of A11X1 and A11X2

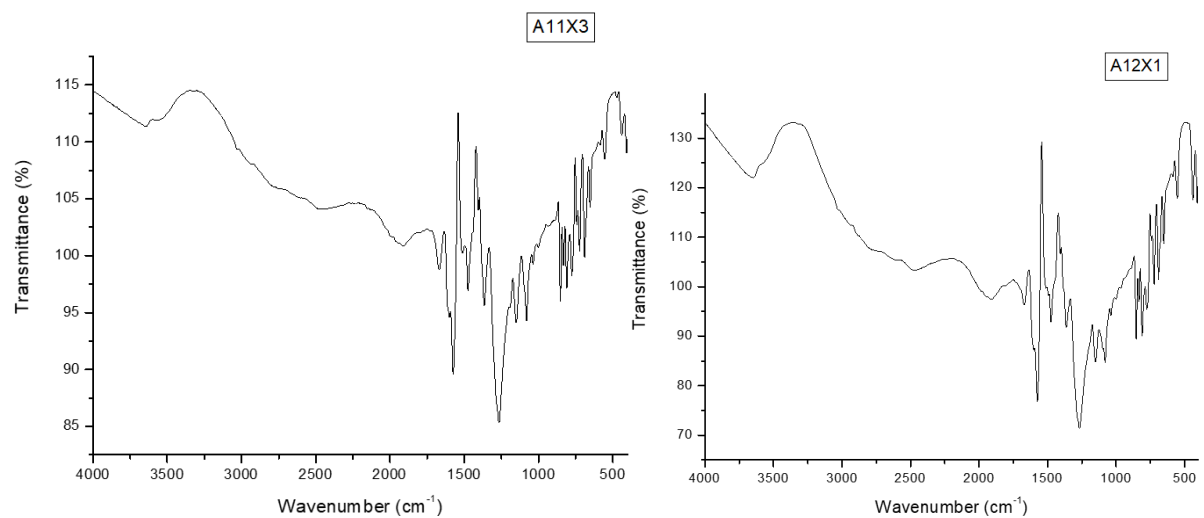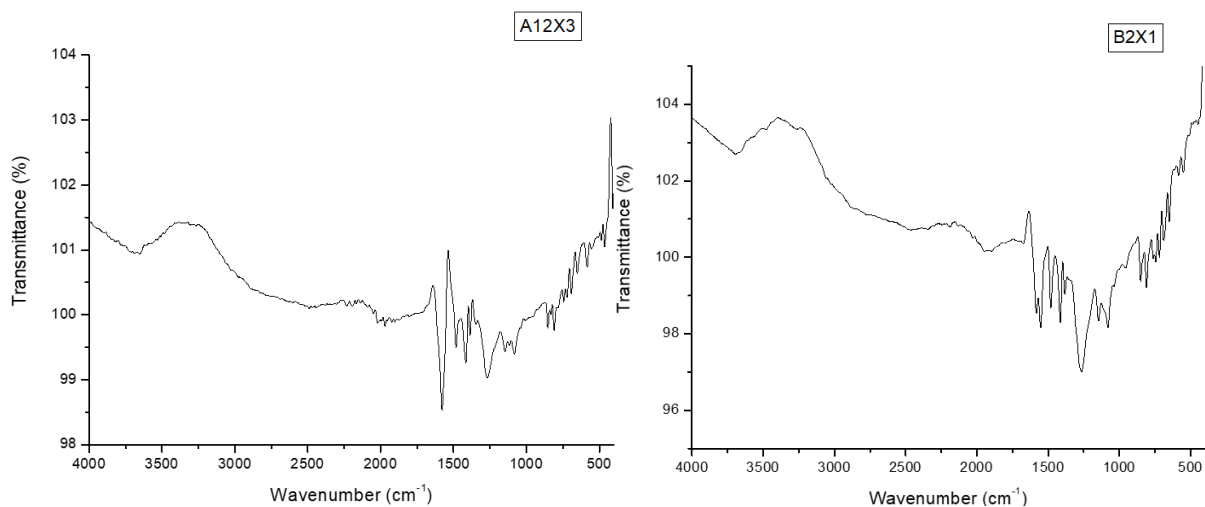**Figure 59:** IR spectrum of A11X3 and A12X1

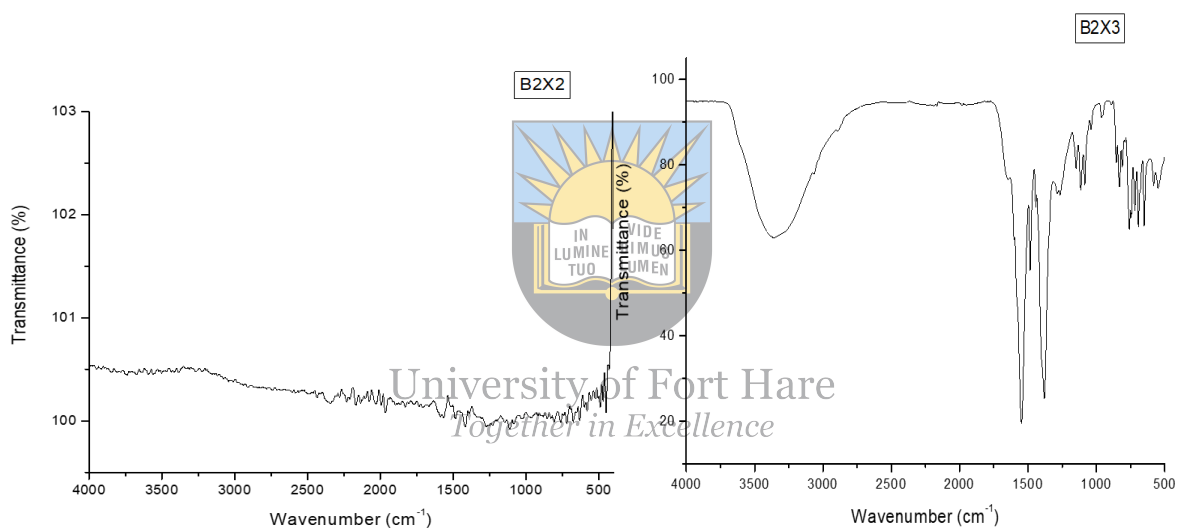**Figure 60:** IR spectrum of A12X3 and B2X1

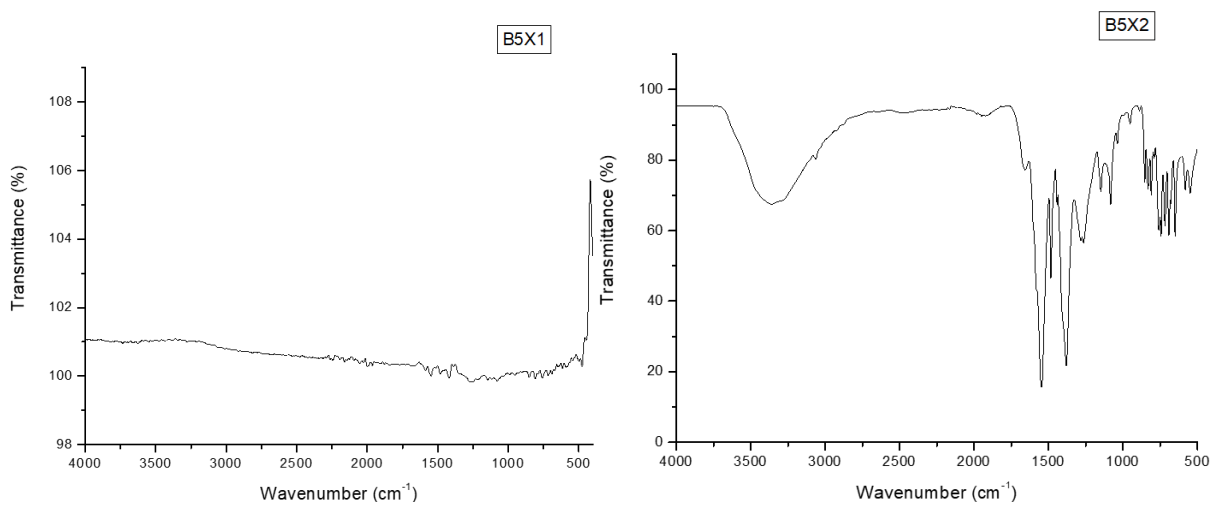**Figure 61:** IR spectrum of B2X2 and B2X3

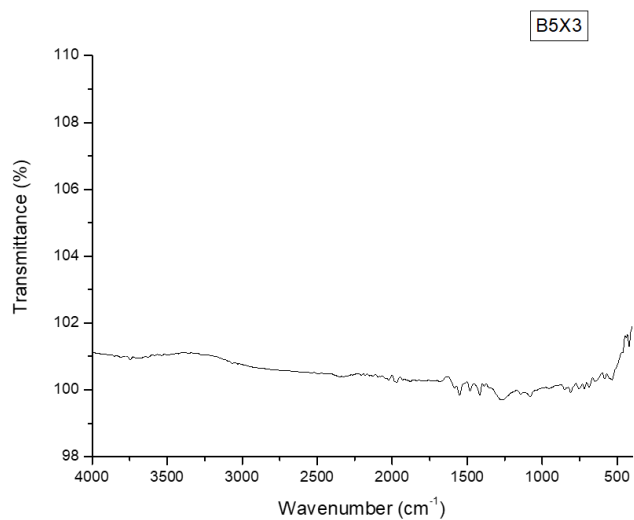**Figure 62:** IR spectrum of B5X1 and B5X2
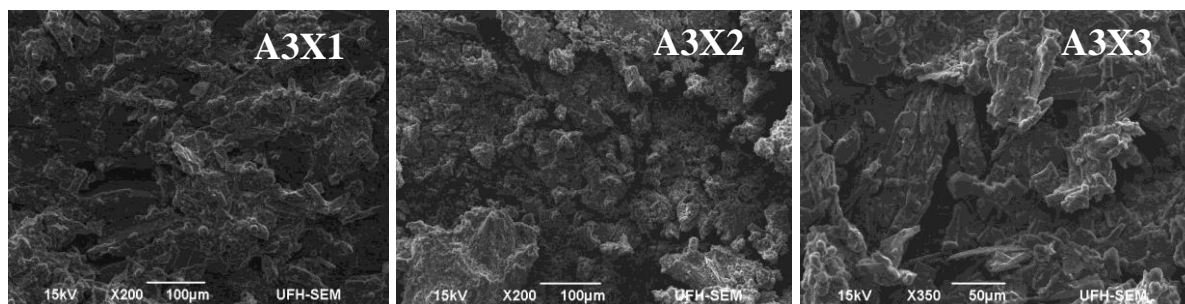
Figure 63: IR spectrum of B5X3

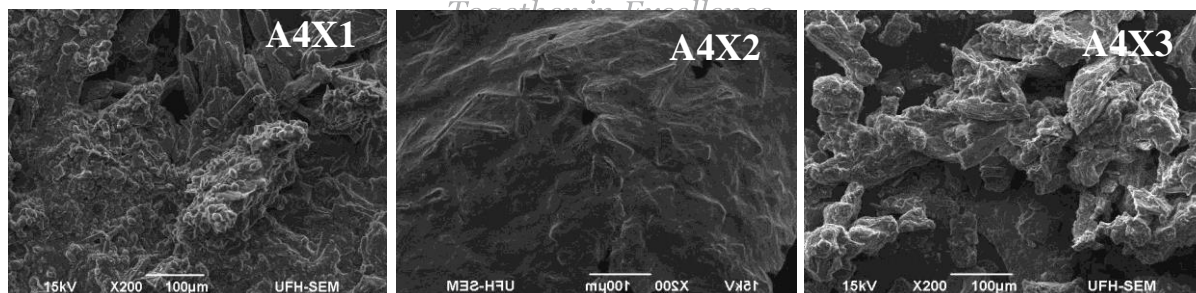**Figure 64:** SEM images of A3W1,A3W2, and A3W3

Figure 65: SEM images of A4W1, A4W2, and A4W3

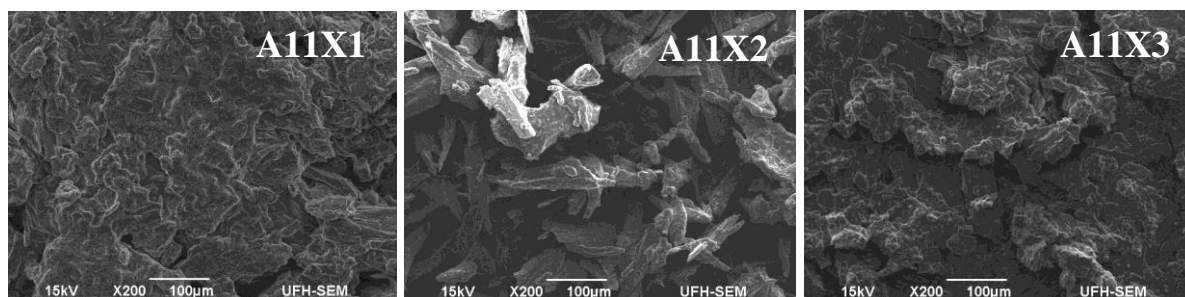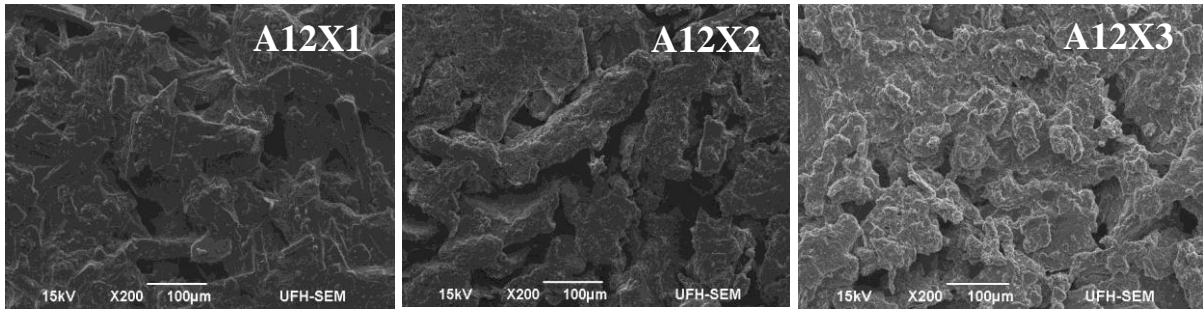**Figure 66:** SEM images of A11W1, A11W2, and A11W3

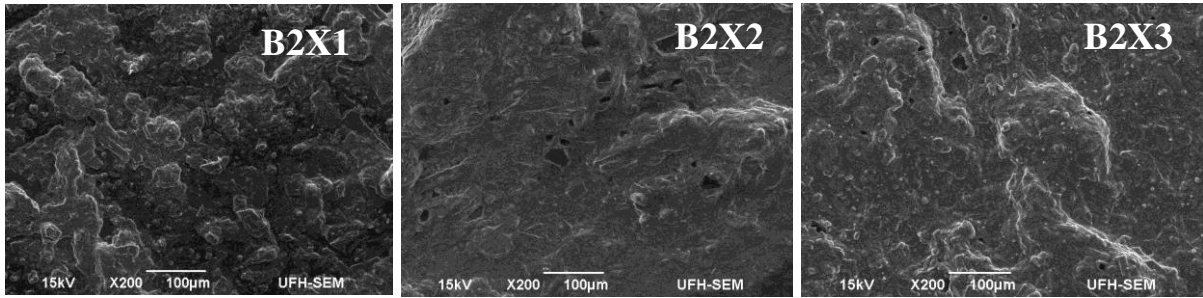**Figure 67:** SEM images of A12W1, A12W2, and A12W3

Figure 68: SEM images of B2X1, B2X2, and B2X3
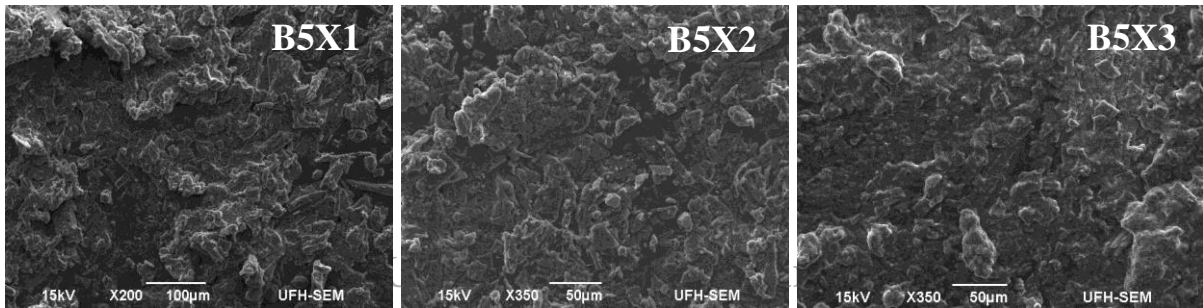

Figure 69: SEM images of B5X1, B5X2, and B5X3

4.6. Porosity

The % porosity of the gelatin-based hybrid sponges is shown in **Table 9**. The porosity of the hybrid sponges ranged between 15.64 and 91.10%. The increasing amount of gelatin utilized for the formulation of the hybrid sponges improved the % porosity of most of the hybrid sponges. In the case of sponges prepared using the same amount of gelatin, the sponges crosslinked with 2% $CaCl_2$ led to higher porosity than the sponges crosslinked with 5% $CaCl_2$, suggesting that the percentage of crosslinking agent affected the porosity of wound dressing. Sponge SAA2% displayed the highest porosity (91.10%) compared to all the sponges, and it contains Ag nanoparticles only and is crosslinked with 2% $CaCl_2$. The sponge (SAA5%) that displayed the lowest porosity (15.64%) was prepared with similar polymer composition as SAA2% but crosslinked with 5% $CaCl_2$. These results demonstrate that the percentage of the crosslinking agents influenced the porosity of the sponges. Furthermore, the high % porosity

113

of the sponges demonstrates that biopolymers (such as gelatin) can play an essential role in enhancing the porosity of the wound dressings.

Ngece et al. formulated sponges using biopolymers (sodium alginate and gum acacia) using $CaCl_2$ as a crosslinking agent for wound dressing applications. The porosity studies showed that the increase in the amount of biopolymers employed for the formulation of the hybrid sponges significantly improved the % porosity of the biopolymer-based sponges. Furthermore, utilizing 2% of $CaCl_2$ for crosslinking of the sponges leads to higher porosity for most of the formulated scaffolds than those fabricated with 1% $CaCl_2$ [17]. Most reported gelatin-based hybrid sponges exhibit good porosity, a feature useful in wound dressings for gaseous diffusion, migration of nutrients to the injury, permitting the exchange of substances between the cells of the skin, promoting the absorption of wound exudates, and stimulating high cell adhesion and proliferation useful for an acceleration of wound healing [23].

Table 9. Porosity (%) of gelatin-based sponges

Sponge	Porosity (%)
SA1	21.59
SA2	81.84
SA3	42.85
SA4	76.70
SA5	71.76
SA6	77.99
SA7	43.44
SA8	64.60
SA9	39.71
SA10	89.81
SA11	78.71
SA12	77.39
SAA2%	91.10
SAA5%	15.64
SAM2%	81.30
SAB2%	68.00
SAB5%	22.56

4.7. *In vitro* Drug Release Studies

The *in vitro* drug release experiments were conducted on the selected gelatin/PEG sponges (SA1, SA2, SA5, SA6, SA11, SA12, SAM2%, SAA2%, and SAA5%) loaded with bioactive agents (metronidazole and Ag nanoparticles). These studies were performed to evaluate the mode of drug release from the sponges at physiological conditions (pH 7.4, 37ºC). The graphs

that display the mechanism of release of metronidazole are shown in **Figures 70-76**. The % cumulative drug release of metronidazole from gelatin-based hybrid sponges was 78.95%, 89.88%, 85.88%, 91.76%, 80.45%, 88.61%, and 86.41 % for sponges SA1, SA2, SA5, SA6, SA11, SA12, and SAM2% over a period of 24 h, respectively. The % cumulative drug release of metronidazole from hybrid sponges were 88.35%, 95.02%, 97.22%, 97.16%, 94.64%, 98.00%, and 98.64% for sponges SA1, SA2, SA5, SA6, SA11, SA12, and SAM2% for 2 days (48 hrs), respectively, indicating that almost all the loaded metronidazole was released from the sponges after 48 hours.

All the hybrid sponges exhibited an initial drug release mechanism of 47.55%, 40.09%, 33.76%, 71.97%, 28.32%, 37.36%, and 51.41% of metronidazole after 1 h from SA1, SA2, SA5, SA6, SA11, SA12, and SAM2% respectively. The initial rapid drug release mechanism was because of the low molecular weight of the loaded drug and its high solubility in aqueous systems, making it easily released through the porous scaffolds, especially those with high porosity [24]. This mechanism was followed by a sustained release profile of metronidazole from the sponges for 48 hours. The initial rapid release can be advantageous in managing wounds by offering immediate relief followed by sustained release to stimulate continuing healing. The initial burst release followed by the sustained drug release can also significantly result in the fast killing of bacterial strains and the inhibition of persisting bacteria, as well as protecting the wound from further infections [25]. Ye and co-workers reported the drug release mechanism of ampicillin from gelatin/ bacterial cellulose hybrid sponges for antibacterial wound dressing application. They reported an initial burst release of ampicillin in the first hours that may be caused by the accumulation of this antibiotic on the surface of composite sponges, followed by a sustained release mechanism, and ultimately a full drug release for 48 hours [26].

Three mathematical models were utilized to evaluate the mechanisms of drug release from the sponges: Zero-order, Higuchi, and Korsmeyer Peppas model. The values of R^2, n and K of the drug release mechanism of each sponge are summarized as shown in **Table 10**. The determined correlation coefficient (R^2) is the standard to evaluate the most appropriate model to describe the mechanism of drug release. The drug release mechanisms of the sponges (SA1, SA2, SA5, SA6, SA11, SA12, and SAM2%) for metronidazole were best fitted into the Korsmeyer Peppas model when compared to Zero-order and Higuchi model with R^2 ranging between 0.9189 and 0.9964 while the n values were 0.9616, 0.8671, and 0.9118 for SA1, SA5, and SA12, respectively, representing a non-Fickian release mechanism (n values greater than 0.5). The n

values for SA1, SA6, SA11, and SAM2% were 1.2383, 1.3771, 1.108, and 1.296, representing non-Fickian super case II release mechanism (n values greater than 1).

Table 10. The drug release analysis constants of sponges for the Zero-order, Higuchi, and Korsmeyer-Peppas

Sponge	Loaded Drug	Zero-order model		Higuchi model		Korsmeyer model		Peppas
		K	r^2	K	r^2	K	n	r^2
SA1	Metronidazole	0.067	0.9012	0.719	0.7072	0.2475	1.2383	0.9766
	Ag nanoparticles	0.1277	0.9981	3.8366	0.9881	0.8767	0.5405	0.9992
SA2	Metronidazole	0.0953	0.8668	2.9981	0.9407	0.3763	0.9616	0.9543
	Ag nanoparticles	0.1264	0.9884	3.7521	0.9555	0.8535	0.5213	0.9861
SA5	Metronidazole	0.098	0.9704	2.9906	0.9909	0.3783	0.8671	0.9891
	Ag nanoparticles	0.1265	0.9986	3.7744	0.9745	0.9345	0.7383	0.9964
SA6	Metronidazole	0.059	0.7429	0.668	0.6668	0.2198	1.3771	0.9189
	Ag nanoparticles	0.1083	0.9168	3.29240	0.9894	0.8025	0.3526	0.9750
SA11	Metronidazole	0.0958	0.9741	2.9231	0.9944	0.2743	1.108	0.9622
	Ag nanoparticles	0.0906	0.9842	2.7186	0.9726	0.5638	0.1896	0.9760
SA12	Metronidazole	0.096	0.9044	1.086	0.7379	0.3832	0.9118	0.9733

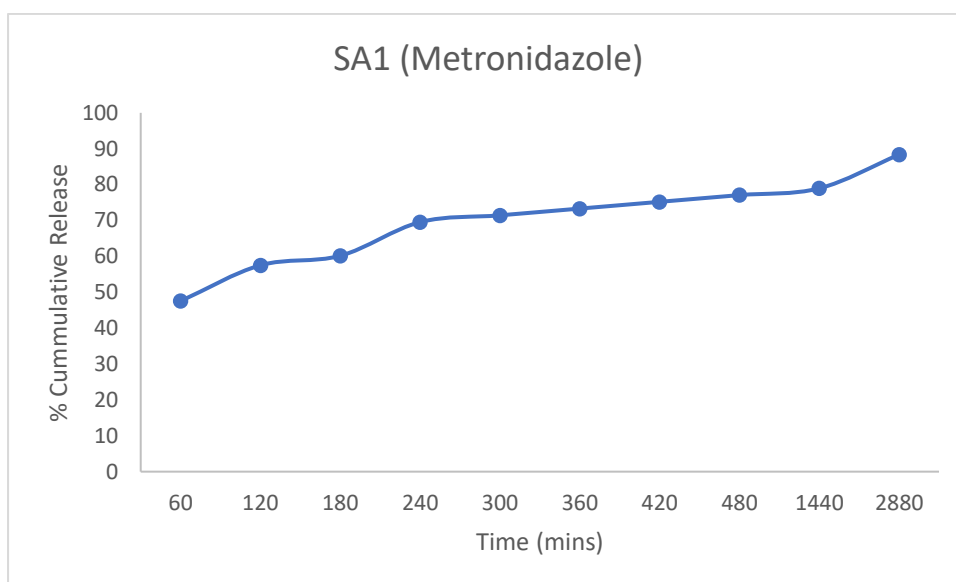|								
	Ag nanoparticles	0.0995	0.9886	3.0004	0.9870	0.7733	0.3443	0.9944
SAM2%	Metronidazole	0.068	0.9127	0.860	0.8082	0.2346	1.296	0.9964
SAA2%	Ag nanoparticles	0.1378	0.9948	4.1551	0.9924	0.7973	0.2716	0.9967
SAA5%	Ag nanoparticles	0.1004	0.9931	3.0239	0.9879	0.6023	0.1338	0.9913

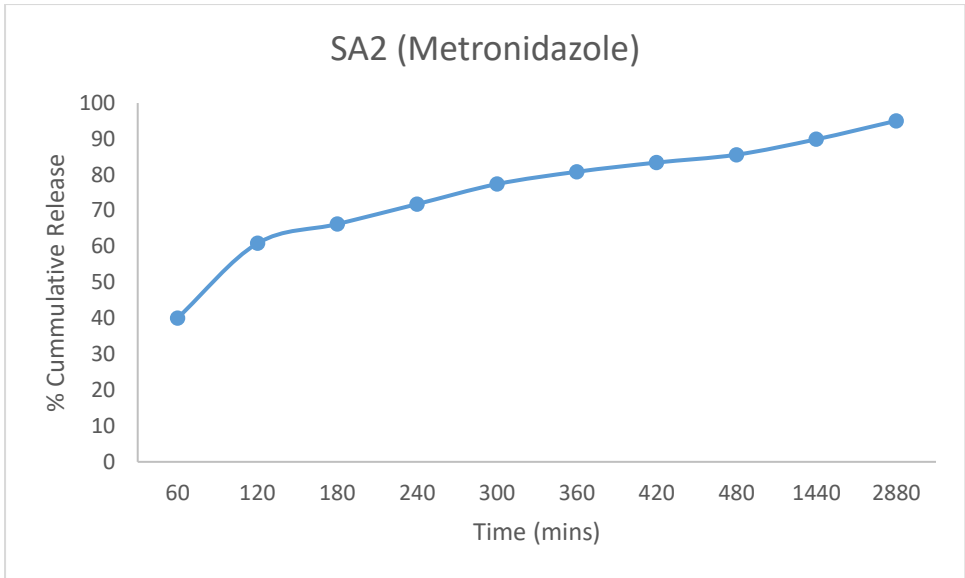**Figure 70:** Drug release of metronidazole from SA1

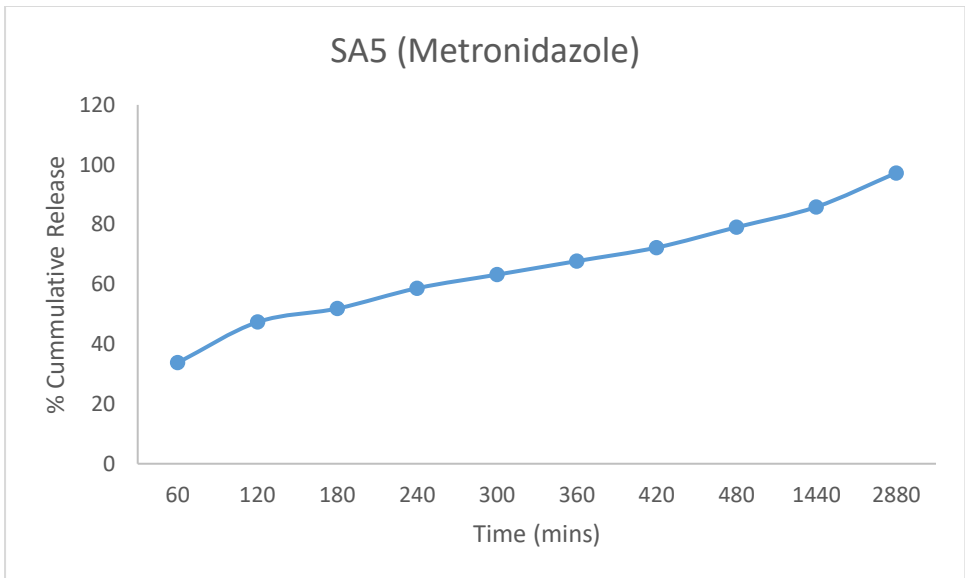**Figure 71:** Drug release of metronidazole from SA2

Figure 72: Drug release of metronidazole from SA5

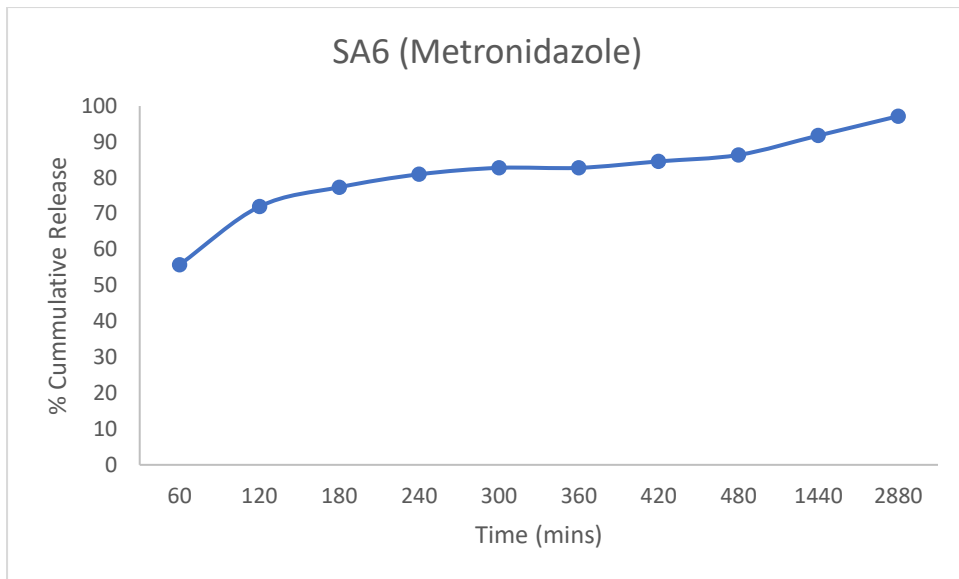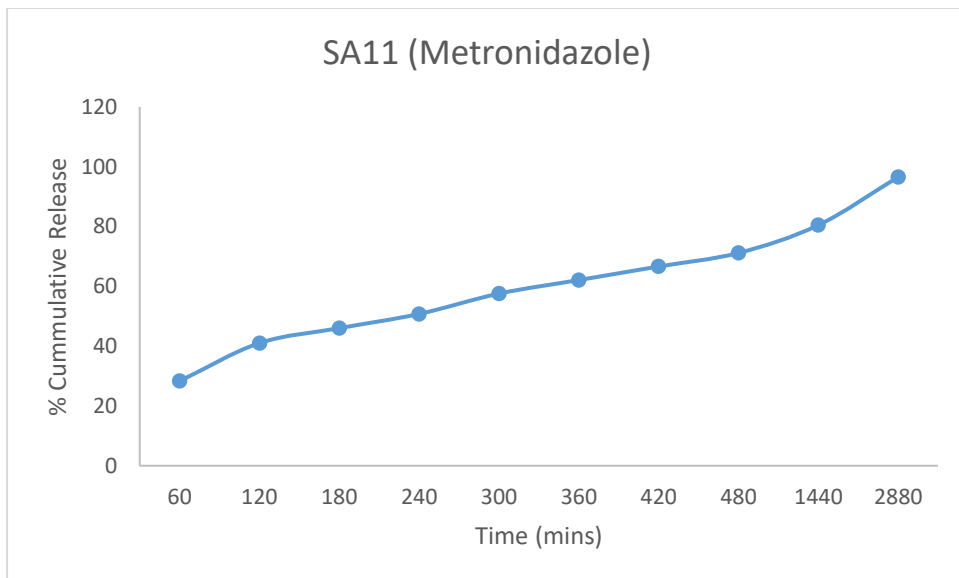**Figure 73:** Drug release of metronidazole from SA6

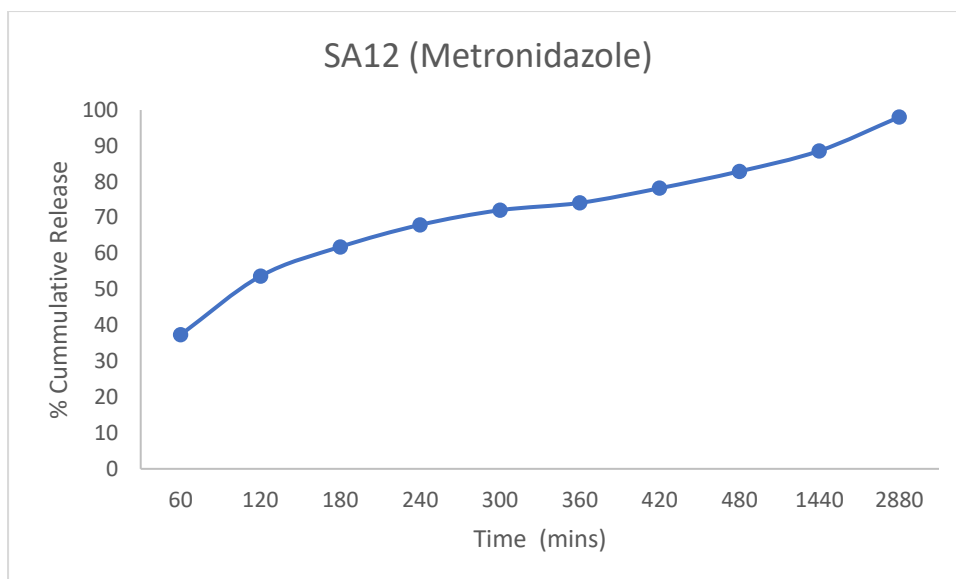**Figure 74:** Drug release of metronidazole from SA11

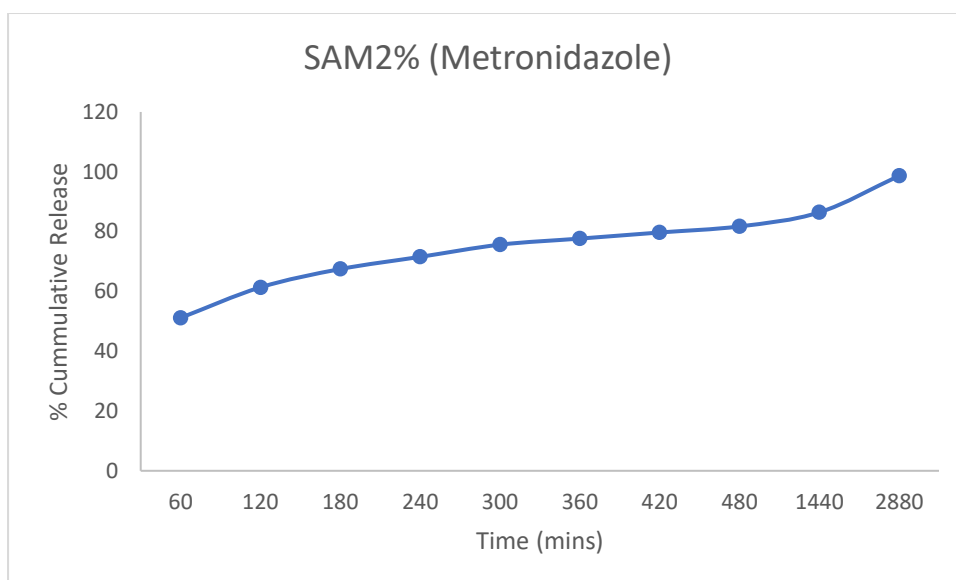**Figure 75:** Drug release of metronidazole from SA12

Figure 76: Drug release of metronidazole from SAM2%

The drug release studies were also conducted on the gelatin/PEG sponges (SA1, SA2, SA5, SA6, SA11, SA12, SAA2%, and SAA5%) to evaluate the release mechanism of Ag nanoparticles from the sponges under physiological conditions. The graphs that show the mechanism of drug release for Ag nanoparticles are displayed in **Figures 77-84**. The drug release results exhibited slow and sustained release of Ag nanoparticles from the gelatin-based hybrid sponges from the first hour by displaying % a cumulative release of 10.46% for SA1, 10.20% for SA2, 8.69% for SA5, 10.75% for SA6, 15.56% for SA11, 10.34% for SA12, 13.62% for SAA2%, and 15.77% for SAA5%. The sustained drug release profile protects the

wound from bacterial invasion and inhibits bacteria invasion during wound healing. The gelatin hybrid sponges exhibit slow and sustained drug release of Ag nanoparticles for 48 hours (The % cumulative drug release of Ag nanoparticles from sponges for 2 days were 94.09%, 95.13%, 93.85%, 96.69%, 95.10%, 96.46%, 97.01%, and 96.05% for sponges SA1, SA2, SA5, SA6, SA11, SA12, and SAA2%, SAA5%).

Three mathematical models were also used to evaluate the drug release mechanisms of Ag nanoparticles from the sponges: Zero-order, Higuchi, and Korsmeyer Peppas model. The values of R^2, n, and K of the drug release mechanism of each sponge are summarized as shown in **Table 9**. The drug release mechanisms of nanoparticles from the sponges (SA1, SA2, SA5, SA6, SA11, SA12, SA2%, and SAA5%) were best fitted into the Korsmeyer Peppas model in comparison to Zero-order and Higuchi model with R^2 ranging between 0.9750 and 0.9992. The n values were 0.5405, 0.5213, and 0.7383 for SA1, SA2, and SA5, respectively, representing a non-Fickian release mechanism (n values greater than 0.5). The n values for SA6, SA11, SA12, SAA2%, and SAA5% were 0.3526, 0.1896, 0.3443, 0.2716, and 0.1338, representing Quasi-Fickian diffusion release mechanism (n values less than 1).

Figure 77: Drug release of Ag nanoparticles from SA1

Figure 78: Drug release of Ag nanoparticles from SA2

Figure 79: Drug release of Ag nanoparticles from SA5

Figure 80: Drug release of Ag nanoparticles from SA6

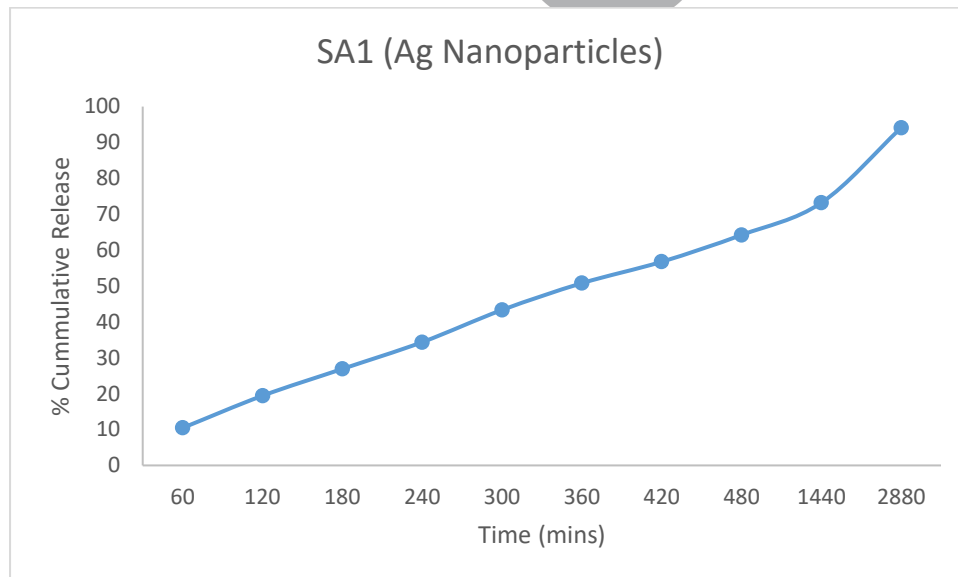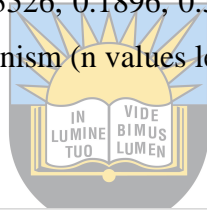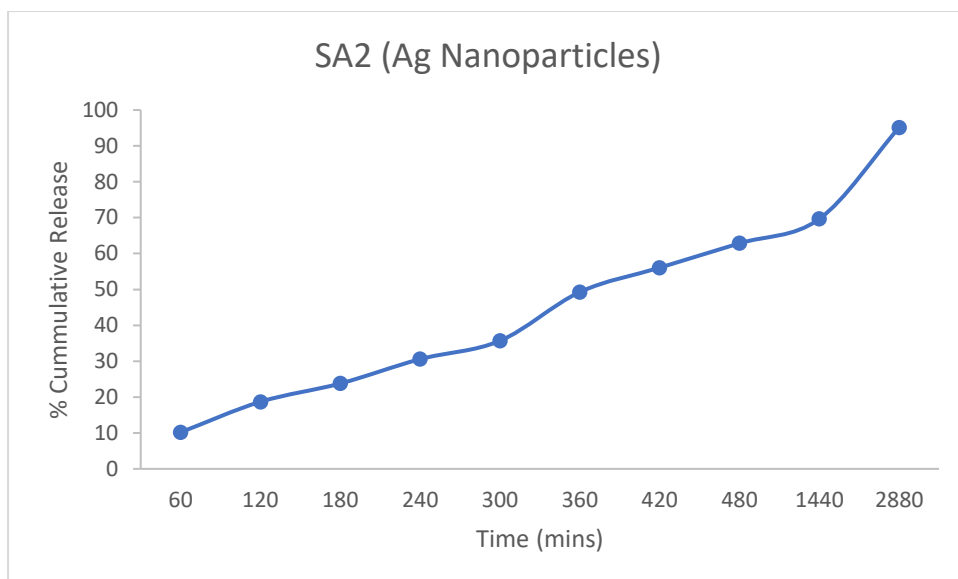**Figure 81:** Drug release of Ag nanoparticles from SA11
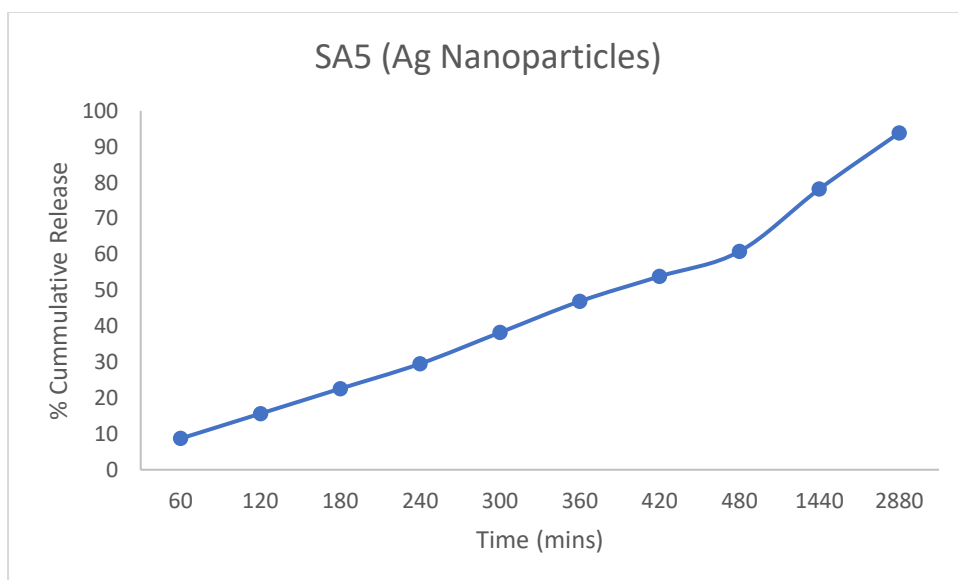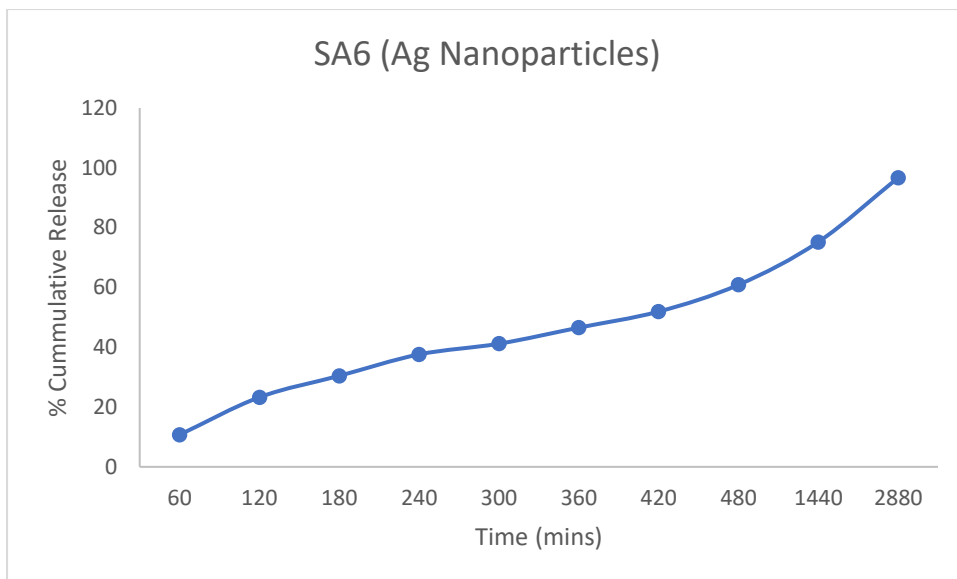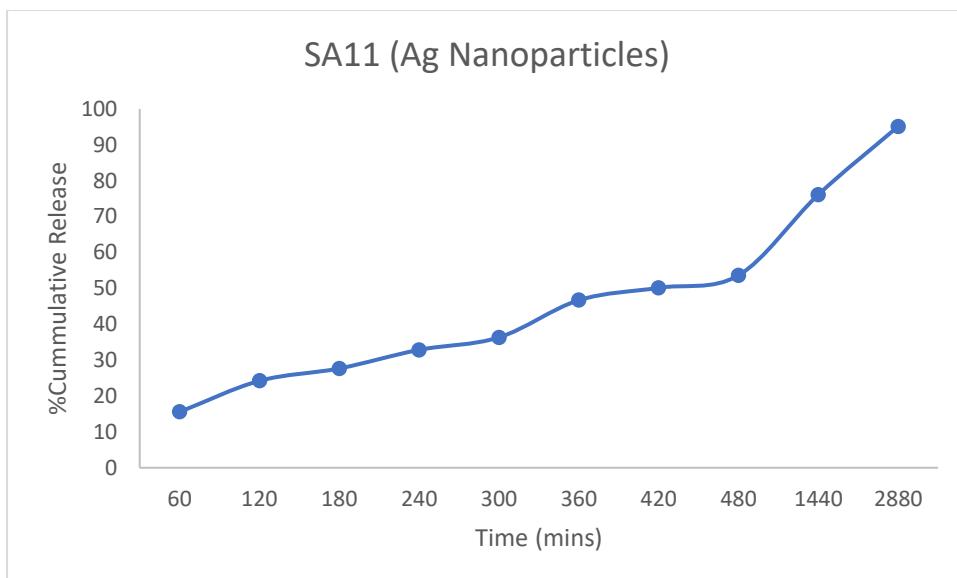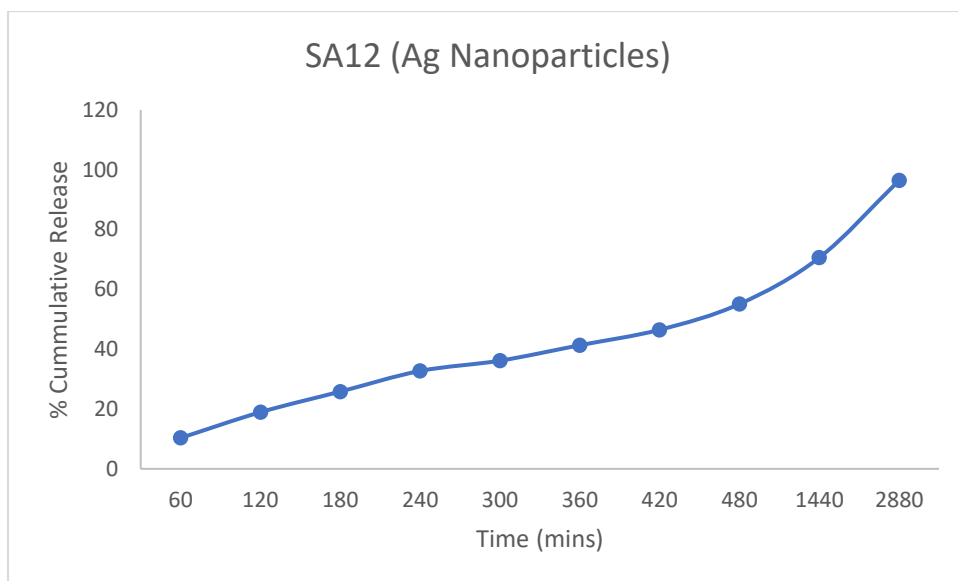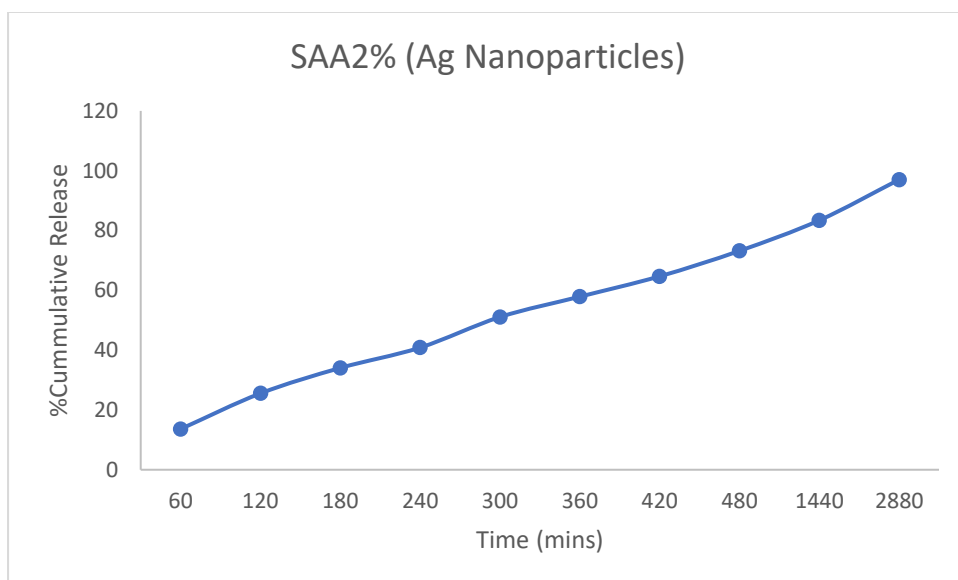
Figure 82: Drug release of Ag nanoparticles from SA12

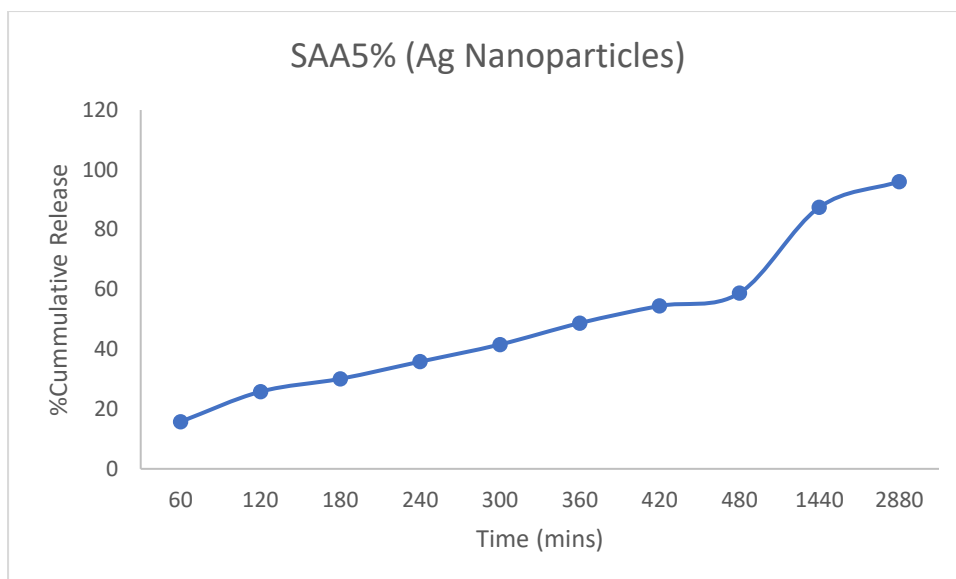**Figure 83:** Drug release of Ag nanoparticles from SAA2%

Figure 84: Drug release of Ag nanoparticles from SAA5%

4.8. *In Vitro* Cytotoxicity Studies

Three sponges (SA1, SAM2%, and SAB2%) were selected for *in vitro* cytotoxicity studies (**Table 11 and Figure 85**). The cytotoxicity of the sponge co-loaded with metronidazole and Ag nanoparticles (SA1), sponge loaded with only metronidazole (SAM2%), and plain sponge (SAB2%) was evaluated by screening these sponges at the concentration of 12.2, 25, 50, and 100 µM of sponges against immortalized human keratinocytes (HaCaT cells). The calculated % cell viability of each sponge against the untreated cells was used to analyse the cytotoxicity results of the sponges. The sponge that induced the highest cell viability at the highest concentration (100 µM) is SA1 with a % cell viability of 86.10%, followed by SAM2% with a % cell viability of 81.51% and SAB2% with a % cell viability of 71.71%. The loading of bioactive agents (metronidazole and Ag nanoparticles) into sponges revealed high % cell viability compared with a blank sponge, suggesting that loading drugs into the wound dressings did not induce any significant cytotoxic effect. All the sponges exhibited good cell viability, indicating non-toxicity and good biocompatibility (especially SA1), which are ideal features of an effective wound dressing.

Zou *et al*. fabricated gelatin/konjac sponges co-encapsulated with an antibiotic, gentamicin sulfate, and Au nanoparticles for wound healing applications. The *in vitro* cytotoxicity studies employing MTT assay exhibited that the cell viability of the murine fibroblast cell line (L929 cells) was more than 80% when incubated with dual drug-incorporated gelatin-based sponges, suggesting good biocompatibility and non-cytotoxicity [27]. These results are similar to the results reported in this study, revealing the non-toxic nature of the wound dressings.

Furthermore, Lan and co-workers demonstrated that gelatin/chitosan sponges induced the cell growth and adhesion of L929 cells, suggesting that these gelatin-based hybrid sponges are biocompatible and non-cytotoxic and therefore meet the requirements of an ideal wound dressing material [28].
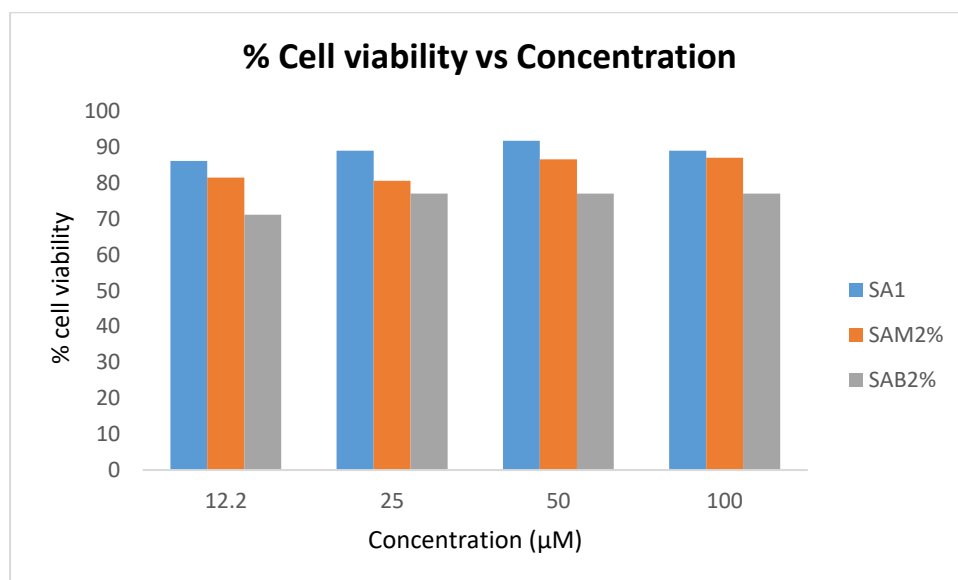
Figure 85: % Cell viability of sponges at different concentrations

Table 11. *In vitro* **cytotoxicity results of selected sponges at 100 µM**

Sponge	% Cell viability
SA1	86.10%
SAM2%	81.51%
SAB2%	71.17%

4.9. *In Vitro* Antibacterial Analysis

The antibacterial studies were performed to evaluate the antibacterial activity of gelatin/PEG sponges loaded with metronidazole and Ag nanoparticles. The antibacterial efficacy of the sponges against Gram-negative and Gram-positive bacteria strains was observed by comparing their minimum inhibition concentrations (MIC) values to those of the controls (**Table 12**). The lowest MIC values of the sponges, when compared to the control, were considered to be more effective. The outcomes exhibited that the antibacterial activity of the encapsulated antibiotics (metronidazole) in the sponge was retained. The co-loading of metronidazole and Ag nanoparticles into the sponges did not enhance the antibacterial efficacy. All the sponges

displayed superior antibacterial efficacy against *staphylococcus aureus* (SA) with a minimum inhibition concentration (MIC) value of 15.625 µg/ml except sponge SA12 (31.25 µg/ml) than the controls (Ampicillin (AMP) (26 µg/ml), streptomycin (STM) (256 µg/ml) and nalidixic acid (NLD) (64 µg/ml)). The antibacterial efficacy of all the sponges was excellent against *Bacillus subtilis* (BS) and *Enterococcus faecalis* (EF) with MIC values of 15.625 µg/ml each compared to the controls employed, AMP (26 µg/ml for both bacterial strains), STM (16 and 128 µg/ml, respectively), and NLD (16 and >512 µg/ml, respectively), excluding sponge SA6 that possessed MIC values of 500 µg/ml for both bacterial strains. Only SA7 and SA10 showed significant antibacterial efficacy against *Staphylococcus epidermidis* (SE) with MIC values of 15.625 µg/ml each in comparison with AMP and NLD with MIC values of 26 and 64 µg/ml, respectively.

The sponges exhibited good antibacterial efficacy against *Enterobacter cloacae* (ECL) with MIC value of 15.625 µg/ml except for SA10 (250 µg/ml), SA11 (500 µg/ml), and SA12 (250 µg/ml) in comparison with AMP, STM, NLD with MIC values of 26, 512, and 16 µg/ml, respectively. The antibacterial activity of sponges SA3, SA4, SAA5% SAM2%, and SAB5% against *Proteus vulgaris* (PV) was excellent with MIC values of 15.625 µg/mL each when compared to AMP, (416 µg/mL), STM (128 µg/mL) and NLD (128 µg/mL). All the gelatin hybrid sponges showed significant antibacterial activity against *Klebsiella oxytoca* (KO) and *Proteus mirabilis* (PM) with MIC values of 15.625 µg/mL each in comparison with AMP, STM, and NLD that possessed MIC values of 26 µg/mL for both bacterial strains, 16 and 28 µg/mL, and 8 (only this control that was superior when compared to sponges) and 32 µg/mL, respectively. The sponges SA1, SA5, and SA6 showed MIC values of 31.25 µg/mL against *Pseudomonas aeruginosa* (PA) while sponges SA2, SA3, SA4, SA10 and SA12 MIC value was 15.625 µg/mL, suggesting that they displayed superior antibacterial activity than controls AMP (64 µg/mL), STM (128 µg/mL), and NLD (128 µg/mL). The hybrid sponges SA1, SA2, SA3, SA4, SA8, SA9, SAA2%, SAA5%, and SAM2% displayed good antibacterial efficacy against *Escherichia coli* (EC) with MIC values of 15.625 µg/mL each than AMP (26 µg/mL), STM (64 µg/mL), and NLD (512 µg/mL). Sponge SAM2% demonstrated superior antibacterial efficacy against *Klebsiella pneumonia* (KP) with a MIC value of 15.625 µg/mL when compared to AMP, STM, and NLD, which displayed MIC values of 26, 512, and 256 µg/mL.

Almost all the sponges showed significant antibacterial efficacy against most gram-positive bacterial strains (BS, EF, SE, and SA) and gram-positive bacterial strains (ECL, KO, PM, PA, and EC) when compared to the controls used. Furthermore, these sponges showed selective

antibacterial activity. The gelatin/PEG sponges loaded with metronidazole and Ag nanoparticles demonstrated good antibacterial efficacy against the strains of bacteria (*Staphylococcus epidermidis, staphylococcus aureus*, *Escherichia coli,* and *Proteus vulgaris*) that commonly cause wound infections [29][30], demonstrating that these sponges are potential scaffolds that can be utilized for the management of infected chronic injuries. *Proteus vulgaris* and *Staphylococcus epidermidis* are responsible for antibiotic resistance genes, and they can cause biofilms that result in chronic wounds [31]. In addition, biofilms caused by *Pseudomonas aeruginosa* are normally related to difficult-to-heal chronic wounds [32]. Previous research has demonstrated that metronidazole is a potential antibiotic against resistant strains of *Pseudomonas aeruginosa* when utilized in combination therapies [33]. However, it suffers from drug resistance and known adverse effects.

Some research reports have demonstrated metronidazole-loaded wound dressing scaffolds as effective materials for the treatment of infected wounds. Brako *et al*. fabricated PVP/PCL nanofibers wound dressings loaded with metronidazole. The fibres were more effective against *Pseudomonas aeruginosa* cells than the control metronidazole creams [34], indicating that these fibres are potential materials that can be employed for the management of bacteria-infected wounds. The metronidazole-loaded gelatin/poly (3-hydroxy butyrate) nanofibrous scaffolds reported by El-Shanshory *et al*. exhibited the highest significant antibacterial activity by hindering the growth of *Escherichia aureus* by showing the diameter of inhibition zone of about 5.42 mm [35]. El-Newehy *et al*. prepared PVA/PEO nanofibers enriched with metronidazole and displayed a superior antimicrobial efficacy against *Pseudomonas aeruginosa*, *Escherichia coli*, *Penicillium notatum*, *Aspergillus niger*, and *Aspergillus flavus* [36]. The metronidazole-loaded gelatin/PEG-based composite hydrogels fabricated by Khade *et al*. showed potential antibacterial activity against *Escherichia coli* [37].

These preclinical research reports demonstrated that wound dressing scaffolds loaded with metronidazole are potential systems that can be employed in the treatment of infected chronic wounds. Furthermore, many studies have demonstrated Ag nanoparticles loaded materials as potential antibacterial wound dressing materials.

Ye et al. fabricated gelatin-gelatin sponges crosslinked with tannic acid and incorporated them with Ag nanoparticles for wound treatment. The antimicrobial experiments demonstrated that the addition of Ag nanoparticles improved the antibacterial effects of the sponges against *E. coli* and *S. aureus* [38]. The Ag nanoparticles-loaded gelatin-based sponges reported by Wu

and co-workers showed excellently and sustained antibacterial against *Streptococcus mutans* (gram-positive bacteria) with MIC values ranging between 0.5 and 2.1 mm [39]. Other antibacterial studies conducted by Rattanaruengsrikul et al. using colony count procedure demonstrated that gelatin wound dressings encapsulated with Ag nanoparticles possessed about 99.7% of bacterial growth inhibition against *P. aeruginosa*, *S. aureus*, and *E. coli*, demonstrating very good antibacterial activity against bacterial strains that commonly caused clinical wound infections [40]. Khanha et al. prepared gelatin-based composites co-encapsulated with Ag nanoparticles and curcumin for the management of bacteria-infected wounds. The antibacterial evaluation utilizing an agar diffusion method showed that the dual drug-loaded composites had excellent antibacterial efficacy against *S. aureus* and *P. aeruginosa* than the composites incorporated with only curcumin [41].

Aktürk et al. synthesized PVA nanofibrous mats incorporated with starch and coated with Ag nanoparticles. The *in vitro* antibacterial experiments exhibited potent growth-inhibitory and excellent antibacterial effects against *S. aureus* and *E. coli* when cultured with nanofibrous mats encapsulated with starch and coated with Ag nanoparticles [42]. Kohsari *et al*. prepared PEO-chitosan antibacterial nanofibrous mats loaded with Ag nanoparticles. The antibacterial studies of Ag nanoparticle-loaded nanofibrous mats displayed an antibacterial activity of more than 99% against *E. coli* and *S. aureus* [43]. Thomas et al. formulated PCL nanofibrous membranes incorporated with Ag nanoparticles for the management of bacteria-infected injuries. The antibacterial analysis showed that the prepared membranes incorporated with Ag nanoparticles had superior antimicrobial activity against *S. haemolyticus* and *S. epidermidis* in comparison to the pristine membranes (control) [44].

Table 12. Antibacterial results of sponges (MIC values were measured in µg/mL)

Tested Compounds	GRAM-POSITIVE					GRAM-NEGATIVE						
	BS	*EF*	*SE*	*SA*	*MS*	*ECL*	*PV*	*KO*	*PA*	*PM*	*EC*	KP
SA1	15.625	15.625	500	15.625	500	15.625	500	15.625	31.25	15.625	15.625	500
SA2	15.625	15.625	250	15.625	250	15.625	250	15.625	15.625	15.625	15.625	500
SA3	15.625	15.625	125	15.625	250	15.625	15.625	15.625	15.625	15.625	15.625	500
SA4	15.625	15.625	250	15.625	250	15.625	15.625	15.625	15.625	15.625	15.625	500
SA5	15.625	15.625	500	15.625	500	15.625	500	15.625	31.25	15.625	500	500

SA6	500	500	500	15.625	500	15.625	500	15.625	31.25	15.625	500	500
SA7	15.625	15.625	15.625	15.625	500	15.625	500	15.625	500	15.625	500	500
SA8	15.625	15.625	500	15.625	500	15.625	500	15.625	500	15.625	15.625	500
SA9	15.625	15.625	500	15.625	500	15.625	500	15.625	500	15.625	15.625	500
SA10	15.625	15.625	15.625	15.625	500	250	500	15.625	15.625	15.625	500	500
SA11	15.625	15.625	500	15.625	500	500	500	15.625	500	15.625	500	500
SA12	15.625	15.625	125	31.25	500	250	125	15.625	15.625	15.625	500	500
SAA2%	15.625	15.625	500	15.625	500	15.625	500	15.625	500	15.625	15.625	500
SAA5%	15.625	15.625	500	15.625	500	15.625	15.625	15.625	500	15.625	15.625	500
SAM2%	15.625	15.625	500	15.625	500	15.625	15.625	15.625	500	15.625	15.625	15.625
SAB2%	15.625	15.625	500	15.625	500	15.625	500	15.625	500	15.625	500	500
SAB5%	15.625	15.625	500	15.625	500	15.625	15.625	15.625	500	15.625	500	500
Metronidazole	15.625	15.625	125	15.625	500	125	500	15.625	500	15.625	500	500
Amp	26	26	26	26	26	26	416	26	64	26	26	26
STM	16	128	8	256	4	512	128	16	128	128	64	512
NLD	16	>512	64	64	512	16	128	8	128	32	512	256

4.10. *In Vitro* Scratch Wound Healing Assay

In vitro scratch wound-healing assay was conducted on sponges SA1 (sponge loaded with metronidazole and Ag nanoparticles) and SAM2% (sponge loaded with metronidazole only) that showed high % cell viability. Wound healing studies were performed at time points of 0, 24, 48, 72, and 96 hours to compare the rate of closure on treated and untreated cells. The wound healing results are shown in **Figures 86-88**. The cells treated with sponge SAM2% exhibited a higher rate of closure than the untreated cells and SA1 treated with HaCaT cells for 96 hours as shown in **Table 13**. SAM2% and SA1 treated with cells exhibited a reduction in the scratch area with a closure rate of 69.07% and 48.94, respectively, while the untreated cells displayed a rate of closure of 42.86% for 96 hours (4 days). These results demonstrated that the sponge containing metronidazole and Ag nanoparticles or loaded with metronidazole alone significantly accelerated the rate of closure when compared to the untreated scratched cells. Furthermore, SAM2% significantly showed the fastest reduction in the scratch area as compared to SA1, suggesting its effectiveness to accelerate the process of wound healing than SA1. Metronidazole loaded in sponges might have acted as a chemoattractant to improve cell migration of HaCaT cells, which is important for skin integrity.

The in vitro wound healing results of gelatin-based sponges were similar to those reported by Raja and Fathima incorporated cerium oxide nanoparticles in wound dressings. The *in vitro* scratch wound healing assay employing scratched NIH-3T3 fibroblast cells that were visualized using a light microscope showed the fastest % reduction in lesion area of 49.4 ± 0.2% for drug-loaded gelatin composite when compared to plain gelatin-based composite (47.3 ± 0.3%) and untreated stretched cells (44.8 ± 0.2%) throughout 10 h of the assay [45]. Furthermore, Zhang et al. fabricated gelatin sponges for the treatment of wounds. The *in vitro* scratch healing analysis displayed an accelerated rate of closure (about 78%) on day 2 of scratch human skin fibroblasts, demonstrating that a gelatin sponge might benefit wound healing [46]. The Growth factor-loaded gelatin methacryloyl/ poly(3-hydroxybutyrate-co-3-hydroxyvalerate) hybrid patches reported by Augustine *et al*. significantly promoted the acceleration of closure rate of stretched HaCat keratinocytes, 3T3 fibroblasts, and EA.hy926 endothelial cells [47].
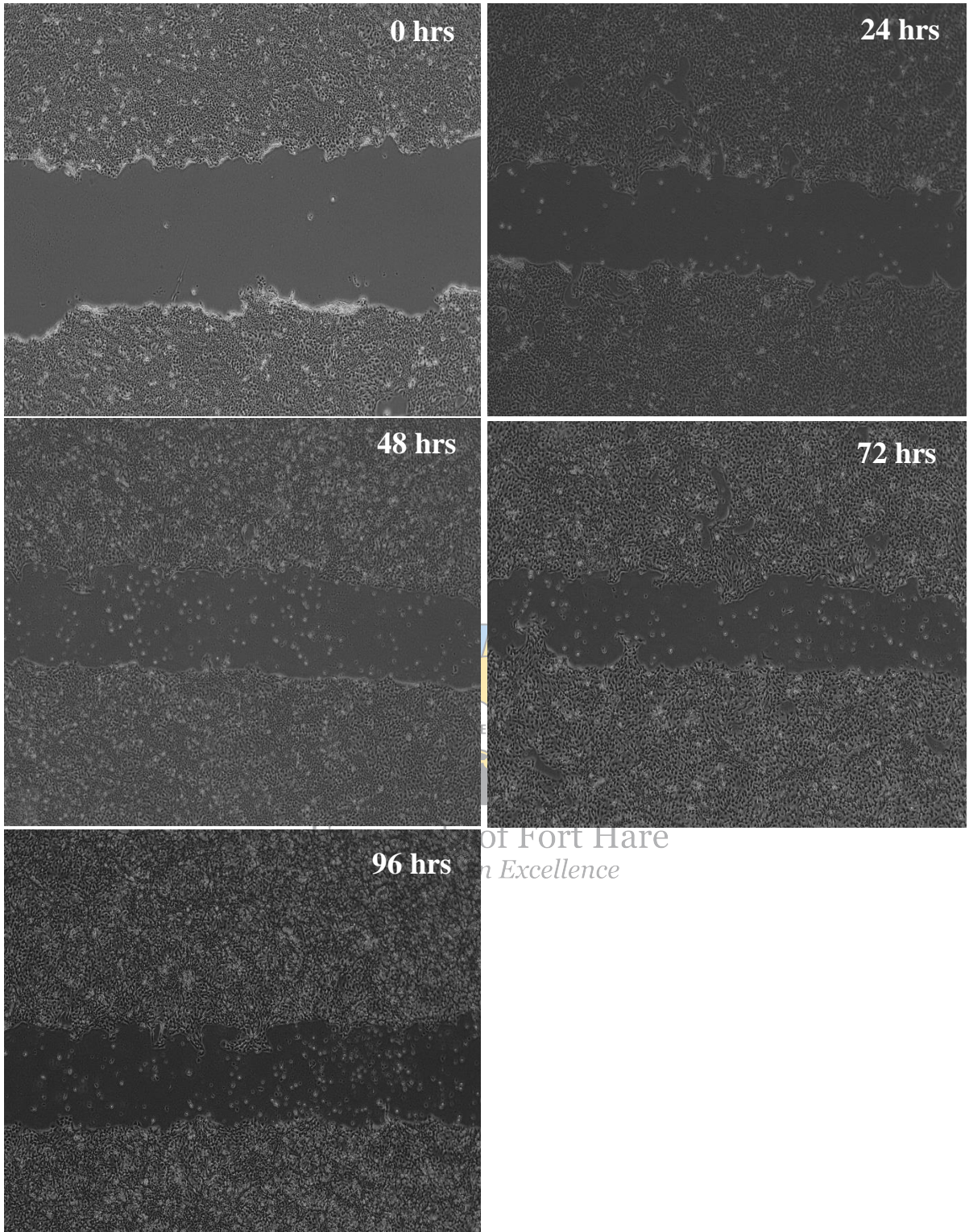
University of Fort Hare
Together in Excellence
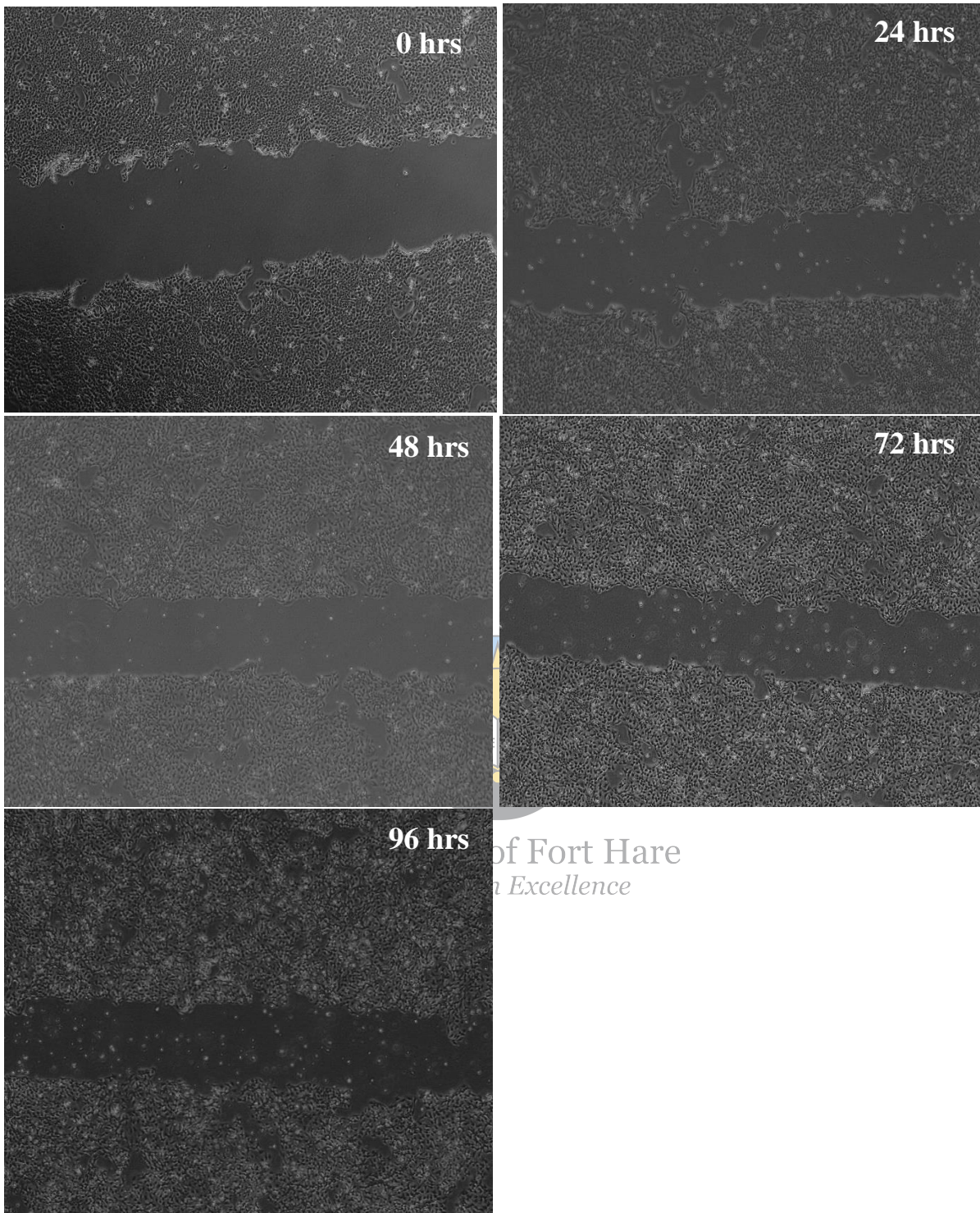
Figure 86: Wound scratch images of untreated cells

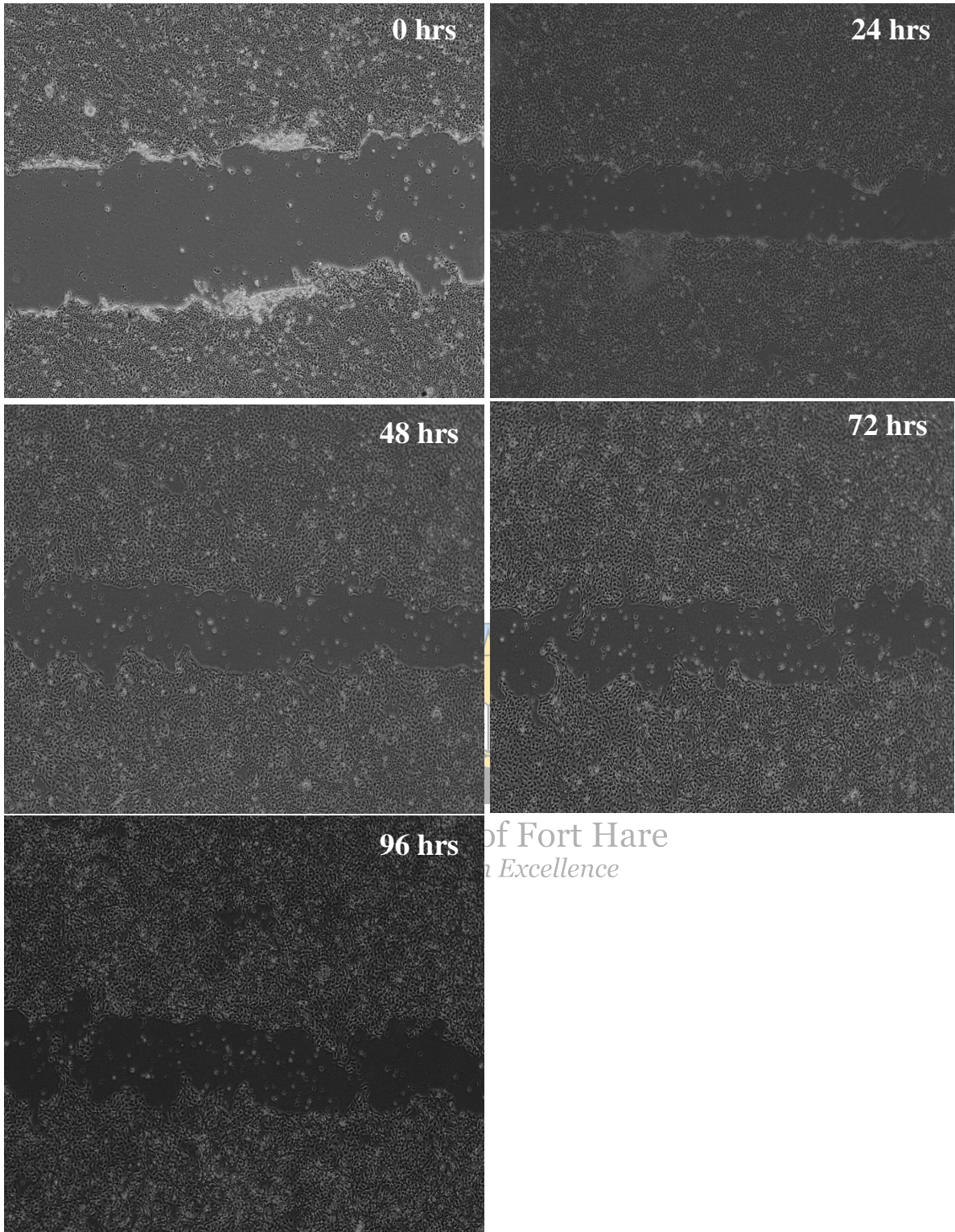**Figure 87:** Wound scratch images of treated cells with SA1

Figure 88: Wound Scratch images of treated cells with SAM2%

Table 13. Area of stretch over time for sponges

Time (h)	Area (mm)		
	Untreated cells	**SAM2%**	**SA1**
0	1058.630	944.031	823.383
24	650.330	300.004	604.810
48	605.236	238.915	541.960
72	511.619	194.102	427.446
96	604.881	292.061	420.371
Total reduction	453.749=42.86%	651.97=69.07%	403.021=48.94%

References

[1]   Alim-Al-Razy, M.; Bayazid, G.M.A.; Rahman, R.U.; Bosu, R.; Shamma, S.S. Silver nanoparticle synthesis, UV-Vis spectroscopy to find particle size and measure resistance of colloidal solution. *J. Phys. Conf. Ser.* **2020**, 1706, 012020. doi: 10.1088/1742-6596/1706/1/012020.

[2]   Singh, S.; Bharti, A.; Meena, V.K. Green synthesis of multi-shaped silver nanoparticles: optical, morphological and antibacterial properties. *J. Mater. Sci. Mater. Electron.* **2015**, 26, 3638–3648. doi: 10.1007/s10854-015-2881-y.

[3]   Anandalakshmi, K.; Venugobal, J.; Ramasamy, V. Characterization of silver nanoparticles by green synthesis method using Pedalium murex leaf extract and their antibacterial activity. *Appl. Nanosci.* **2016**, 6, 399–408. doi: 10.1007/s13204-015-0449-z.

[4]   Li, D.; Ye, Y.; Li, D.; Li, X.; Mu, C. Biological properties of dialdehyde carboxymethyl cellulose crosslinked gelatin-PEG composite hydrogel fibers for wound dressings. *Carbohydr. Polym.* **2016**, 137, 508–514.

[5]   Kim, S.E.; Heo, D.N.; Lee, J.B.; Kim, J.R.; Park, S.H.; Jeon, S.H.; Kwon, I.K. Electrospun gelatin/polyurethane blended nanofibers for wound healing. *Biomed. Mater.* **2009**, 4, 044106.doi: 10.1088/1748-6041/4/4/044106.

[6]   Chen, Y.; Lu, W.; Guo, Y.; Zhu, Y.; Song, Y. Electrospun Gelatin Fibers Surface Loaded ZnO Particles as a Potential Biodegradable Antibacterial Wound Dressing. *nanomaterials* **2019**, 9, 525. doi: 10.3390/nano9040525.

[7]   Fan, L.; Yang, H.; Yang, J.; Peng, M.; Hu, J. Preparation and characterization of chitosan/gelatin/PVA hydrogel for wound dressings. *Carbohydr. Polym. Polym.* **2016**, 146, 427–434.

[8]   Trivedi, M.K.; Patil, S.; Shettigar, H.; Bairwa, K.; Jana, S. Spectroscopic Characterization of Biofield Treated Metronidazole and Tinidazole. *Med. Chem. (Los. Angeles)* **2015**, 5, 7.doi: 10.4172/2161-0444.1000283.

[9]   Arif, D.; Niazi, M.B.K.; Ul-haq, N.; Anwar, M.N.; Hashmi, E. Preparation of Antibacterial Cotton Fabric Using Chitosan-silver Nanoparticles. *Fibers Polym.* **2015**, 16, 1519–1526. doi: 10.1007/s12221-015-5245-6.

[10] Gharibshahi, L.; Saion, E.; Gharibshahi, E.; Shaari, A.H.; Matori, K.A. Structural and Optical Properties of Ag Nanoparticles Synthesized by Thermal Treatment Method. *Materials (Basel)* **2017**, 10, 402. doi: 10.3390/ma10040402.

[11] Wang, B.; Johnson, A.; Li, W. Development of an extracellular matrix-enriched gelatin sponge for liver wound dressing. *J. Biomed. Mater. Res. - Part A* **2020**, 108, 2057–2068. doi: 10.1002/jbm.a.36965.

[12] Lu, B.; Wang, T.; Li, Z.; Dai, F.; Lv, L.; Tang, F.; Yu, K.; Liu, J.; Lan, G. Healing of skin wounds with a chitosan– gelatin sponge loaded with tannins and platelet-rich plasma. *Int. J. Biol. Macromol.* **2016**, 82, 884–891.doi: 10.1016/j.ijbiomac.2015.11.009.

[13] Ulubayram, K.; Cakar, A.N.; Korkusuz, P.; Ertan, C.; Hasirci, N. EGF containing gelatin-based wound dressings. *Biomaterials* **2001**, 22, 1345–1356.

[14] Hajosch, R.; Suckfuell, M.; Oesser, S.; Ahlers, M.; Flechsenhar, K.; Schlosshauer, B. A novel gelatin sponge for accelerated hemostasis. *J. Biomed. Mater. Res. B Appl. Biomater.* **2010**, 94B, 372–379. doi: 10.1002/jbm.b.31663.

[15] Imani, R.; Rafienia, M.; Emami, S.H. Synthesis and characterization of glutaraldehyde-based crosslinked gelatin as a local hemostat sponge in surgery: An in vitro study. *Biomed. Mater. Eng.* **2013**, 23, 211–224. doi: 10.3233/BME-130745.

[16] Choi, S.M.; Singh, D.; Kumar, A.; Oh, T.H.; Cho, Y.W.; Han, S.S. Porous Three-Dimensional PVA /Gelatin Sponge for Skin Tissue Engineering. *Int. J. Polym. Mater. Polym. Biomater.* **2013**, 62, 384–389. doi: 10.1080/00914037.2012.710862.

[17] Ngece, K.; Aderibigbe, B.A.; Ndinteh, D.T.; Fonkui, Y.T.; Kumar, P. Alginate-gum acacia based sponges as potential wound dressings for exuding and bleeding wounds. *Int. J. Biol. Macromol.* **2021**, 172, 350–359. doi: 10.1016/j.ijbiomac.2021.01.055.

[18] Lu, B.; Wang, T.; Li, Z.; Dai, F.; Lv, L.; Tang, F.; Yu, K. Liu, J.; Lan, G. Healing of skin wounds with a chitosan – gelatin sponge loaded with tannins and platelet-rich plasma. *Int. J. Biol. Macromol.* **2016**, 82, 884–891. doi: 10.1016/j.ijbiomac.2015.11.009.

[19] Wen, Y.; Yu, B.; Zhu, Z.; Ynang, Z.; Shao, W. Synthesis of Antibacterial Gelatin / Sodium Alginate Sponges and Their Antibacterial Activity. *Polymers (Basel)* **2020**, 12, 1926. doi:10.3390/polym12091926.

[20]   Naghshineh, N.; Tahvildari, K.; Nozari, M. Preparation of Chitosan, Sodium Alginate, Gelatin and Collagen Biodegradable Sponge Composites and their Application in Wound Healing and Curcumin Delivery. *J. Polym. Environ.* **2019**, 27, 2819-2830. doi: 10.1007/s10924-019-01559-z.

[21]   El Fawal, G.; Hong, H.; Mo, X.; Wang, H. Fabrication of scaffold based on gelatin and polycaprolactone (PCL) for wound dressing application. *J. Drug Deliv. Sci. Technol.* **2021**, 63, 102501, doi: 10.1016/j.jddst.2021.102501.

[22]   Sakthiguru, N.; Sithique, M.A. Fabrication of bioinspired chitosan/gelatin/allantoin biocomposite film for wound dressing application. *Int. J. Biol. Macromol.* **2020**, https://doi.org/10.1016/ j.ijbiomac.2020.02.289.

[23]   Mbese, Z.; Alven, S.; Aderibigbe, B.A. Collagen-Based Nanofibers for Skin Regeneration and Wound. *Polymers (Basel)* **2021***, 13, 4368. doi: 10.3390/polym13244368

[24]   Huang, X.; Brazel, C. S. On the importance and mechanisms of burst release in matrix-controlled drug delivery systems. *J. Control. Rel.* **2001**, 73, 121–136. doi: 10.1016/S0168-3659(01)00248-6.

[25]   Ndlovu, S.P.; Ngece, K.; Alven, S.; Aderibigbe, B.A. Gelatin-Based Hybrid Scaffolds: Promising Wound Dressings. *Polymers (Basel)* **2021**, 13, 2959. doi: 10.3390/polym13172959

[26]   Ye, S.; Jiang, L.; Su, C.; Zhu, Z.; Wen, Y.; Shao, W. Development of gelatin / bacterial cellulose composite sponges as potential natural wound dressings. *Int. J. Biol. Macromol.* **2019**, 133, 148–155. doi: 10.1016/j.ijbiomac.2019.04.095.

[27]   Zou, Y.; Xie, R.; Hu, E.; Qian, P.; Lu, B.; Lan, G.; Lu, F. Protein-reduced gold nanoparticles mixed with gentamicin sulfate and loaded into konjac/gelatin sponge heal wounds and kill drug-resistant bacteria. *Int. J. Biol. Macromol.* **2020**, 148, 921–931. doi: 10.1016/j.ijbiomac.2020.01.190.

[28]   Lan, G.; Lu, B.; Wang, T.; Wang, L.; Chen, J.; Yu, K.; Liu, J.; Dai, F.; Wu, D. Chitosan/gelatin composite sponge is an absorbable surgical hemostatic agent," *Coll. Surf. B Biointerf.* **2015**, 136, 1026–1034. doi: 10.1016/j.colsurfb.2015.10.039.

[29]   Alwan, M.J.; Lafta, I.J.; Hamzah, A.M. Bacterial isolation from burn wound infections

and studying their antimicrobial susceptibility. *Kufa J.Vet. Med. Sci.* **2011**, 2, 121–131.

[30] Almeida, G.C.; dos Santos, M.M.; Lima, N.G.; Cidral, T.A.; Melo, M.C.; Lima, K.C. Prevalence and factors associated with wound colonization by Staphylococcus spp. and Staphylococcus aureus in hospitalized patients in inland north eastern Brazil: a cross-sectional study. *BMC Infect. Dis.* **2014**, 14, 1–8.

[31] Kwiecinska-Pirog, J.; Skowron, K.; Bartczak, W.; Gospodarek-Komkowska, E. The ciprofloxacin impact on biofilm formation by Proteus mirabilis and P. vulgaris strains. *Jundishapur J. Microbiol.* **2016**, 9, e32656.

[32] Bjarnsholt, T.; Kirketerp-Møller, K.; Jensen, P.Ø.; Madsen, K.G.; Phipps, R.; Krogfelt, K.; Høiby, N.; Givskov, M.Why chronic wounds will not heal: A novel hypothesis," *Wound Repair Regen.* **2008**, 16, 2–10.

[33] Miller, B.; Popejoy, M.W.; Hershberger, E.; Steenbergen, J.N.; Alverdy, J. Characteristics and outcomes of complicated intra-abdominal infections involving Pseudomonas aeruginosa froma randomized, double-blind, phase 3 ceftolozane-tazobactam study. *Antimicrob. Agents Chemother.* 2016, 60, 4387–4390.

[34] Brako, F.; Luo, C.; Matharu, R.K.; Ciric, L.; Harker, A.; Edirisinghe, M.; Craig, D.Q.M. A Portable Device for the Generation of Drug-Loaded Three-Compartmental Fibers Containing Metronidazole and Iodine for Topical Application. *Pharmaceutics* **2020**, 12, 373. doi:10.3390/pharmaceutics12040373

[35] El-Shanshory, A.; Agwa, M.; Abd-Elhamid, A.; Soliman, H.; Mo, X.; Kenawy, E. Metronidazole Topically Immobilized Electrospun Nanofibrous Scaffold : Novel Secondary Intention Wound Healing Accelerator. *Polymers (Basel).* **2022**, 14, 4544. 4. doi: 10.3390/polym14030454

[36] El-Newehy, M.H.; Al-Deyab, S.S.; Kenawy, E.-R.; Abdel-Megeed, A. Fabrication of electrospun antimicrobial nanofibers containing metronidazole using nanospider technology. *Fibers Polym.* **2012**, 13, 709–717.

[37] Khade, S.M.; Behera, B.; Sagiri, S.S.; Singh, V.K.; Thirugnanam, A.; Pal, K.; Ray, S.S.; Pradhan, D.K.; Bhattacharya, M.K. Gelatin – PEG based metronidazole-loaded vaginal delivery systems: preparation, characterization and in vitro antimicrobial efficiency. *Iran Polym J.* **2014**, 23,171–184. doi: 10.1007/s13726-013-0213-8.

[38] Ye, H.; Cheng, J.; Yu, K. In situ reduction of silver nanoparticles by gelatin to obtain porous silver nanoparticle/chitosan com- posites with enhanced antimicrobial and wound-healing activity. *Int. J. Biol. Macromol.* **2019**, 121, 633–642.

[39] Wu, L.; Gareiss, S.K.; Morrow, B.R.; Babu, J.P.; Hottel, T.; Garcia, F.; Li, F.; Hong, L. Antibacterial Properties of silver-loaded gelatin sponges prepared with silver diamine floride. *Am. J. Dent.* 32, 276–280.

[40] Rattanaruengsrikul, V.; Pimpha, N.; Supaphol, P. In Vitro Efficacy and Toxicology Evaluation of Silver Nanoparticle-Loaded Gelatin Hydrogel Pads as Antibacterial Wound Dressings. *J. Appl. Polym. Sci.* 2011, 124, 1668–1682. doi: 10.1002/app.

[41] Khanha, L.L.; Truc, N.T.; Dat, N.T.; Nghi, N.T.P; Toi, V.V.; Hoai, N.T.T.; Quyen, T.N.; Loan, T.T.T.; Hiep, N.T. Gelatin-stabilized composites of silver nanoparticles and curcumin : characterization, antibacterial and antioxidant study. *Sci. Technol. Adv. Mater.* **2019**, 20, 276–290. doi: 10.1080/14686996.2019.1585131.

[42] Aktürk, A.; Taygun, M.E.; Guler, F.K.; Goller, G.; Kucukbayrak, S. Fabrication of antibacterial polyvinylalcohol nanocomposite mats with soluble starch coated silver nanoparticles. *Coll. Surf. A* **2019**, 562, 255–262. doi: 10.1016/j.colsurfa.2018.11.034.

[43] Kohsari, I.; Shariatinia, Z.; Pourmortazavi, S.M. Antibacterial electrospun chitosan – polyethylene oxide nanocomposite mats containing bioactive silver nanoparticles," *Carbohydr. Polym.* **2016**, 140, 287–298. doi: 10.1016/j.carbpol.2015.12.075.

[44] Thomas, R.; Soumya, K.R.; Mathew, J.; Radhakrishnan, E.K. Electrospun Polycaprolactone Membrane Incorporated with Biosynthesized Silver Nanoparticles as Effective Wound Dressing Material*Appied Biochem. Biotech.* **2015**, 176, 2213–2224. doi: 10.1007/s12010-015-1709-9.

[45] Raja, I.S.; Fathima, N.N. Gelatin-cerium oxide nanocomposite for enhanced excisional wound healing. *ACS Appl. Bio Mater.* 2018, 1, 487–495.doi: 10.1021/acsabm.8b00208.

[46] Zhang, H.; Liu, S.; Yang, X.; Chen, N.; Pang, F.; Chen, Z.; Wang, T.; Zhou, J.; Ren, F.; Xu, X.; Li, T. LED Phototherapy With Gelatin Sponge Promotes Wound Healing in Mice. *Photochem. Photobiol.* **2018**, 94, 4179–185.doi: 10.1111/ijlh.12426.

[47] Augustine, R.; Hasan, A.; Dalvi, Y.B.; Rehman, S.R.U.; Varghese, R.; Unni, R.N.; Yalcin, H.C.; Alfkey, R.; Thomas, S.; Al Moustafa, A.E. Growth factor loaded in situ

photocrosslinkable   poly(3-hydroxybutyrate-co-3-hydroxyvalerate)/gelatin
methacryloyl hybrid patch for diabetic wound healing. *Mater. Sci. Eng. C* **2021**, 118,
111519. doi: 10.1016/j.msec.2020.111519.

CHAPTER 5: RESULTS AND DISCUSSION FOR TOPICAL GELS

5.1. FTIR

FTIR spectroscopy was utilized to evaluate the functional groups available in the topical gels corresponding to the polymers (CMC and poloxamer) used for their formulation. FTIR spectra of all the gels (TG0 (blank gels) to TG5 are shown in **Figures 89-91**. It was CMC observed that the major vibrational bands associated with carboxylates (COO⁻) asymmetric stretch were visible at 1637 cm^{-1} and symmetric stretch at 1417 cm^{-1}. The C-O vibration from primary and secondary alcohols was visible at 1133 cm^{-1} (C2-OH), 1078 cm^{-1} (C3-OH), 1032 cm$^{-1,}$ and 986 cm^{-1} (C6-OH). β1-4 glycoside bonds between glucose units were detected at 913 cm^{-1}. Several researchers reported similar results for CMC-based wound dressings [1]–[3]. Furthermore, the FTIR spectra of gels exhibited an important peak at 1133 cm^{-1} that overlapped with the C-O stretching of CMC, which is related to the C-O vibration stretching of poloxamer [4]. In addition, C-O vibration stretch from alcohols (C2-OH) of CMC at 1133 cm^{-1} overlapped with C-O stretching vibrations that confirm the presence of poloxamer 407 in topical gels.

 The FTIR spectra of the gels loaded with TTO (TG1 and TG2) demonstrated a wide band at 3726–2892 cm^{-1} region due to the O–H stretching of terpinen-4-ol, the major constituent of TTO. The peak observed between 1462 and 1280 cm^{-1} illustrates overlap peaks of bending vibrations of CH$_3$ and CH$_2$ and aromatic carbon skeleton vibration. The peak at 1637 cm^{-1} (overlapped with carboxylate asymmetric stretch of CMC) is attributed to the stretching vibration absorption peak of the C=C bond. The peak at 1041 cm^{-1} is ascribed to the C–O bond in 1,8-cineole, which is the component of TTO. These results confirmed the successful loading of TTO into the gels. Similar results were reported by Jian and co-workers [5]. The FTIR spectra of the gels loaded with lavender oil (TG4 and TG5) exhibited C=O stretching vibration at 1637 cm^{-1} (overlapping with carboxylate asymmetric stretch of CMC), confirming the presence of two key components of lavender oil: linalyl acetate and linalool. Furthermore, the

spectra of lavender oil-loaded topical gels displayed a peak at 1462 cm^{-1} that represents an alkane group C-H bending vibration. Similar results of wound dressings loaded with lavender oil were reported by Jamróz and co-workers [6]. Significant chemical bonds in Ag nanoparticles loaded in topical gels (TG1, TG3, and TG5) are the broadband at 3726–2892 cm^{-1} region (C-H stretching vibrations of the amines), 1637 cm^{-1} (C=O stretching asymmetric in COO–), 1417 cm^{-1} (C=O stretching symmetric in COO–), and 583 cm^{-1} (Ag-O ionic bond groups) [7]. The functional groups of pure polymers (CMC and poloxamer) and essential oils (TTO and lavender oil) visible on FTIR spectra of corresponding topical gels are presented in **Table 14.**
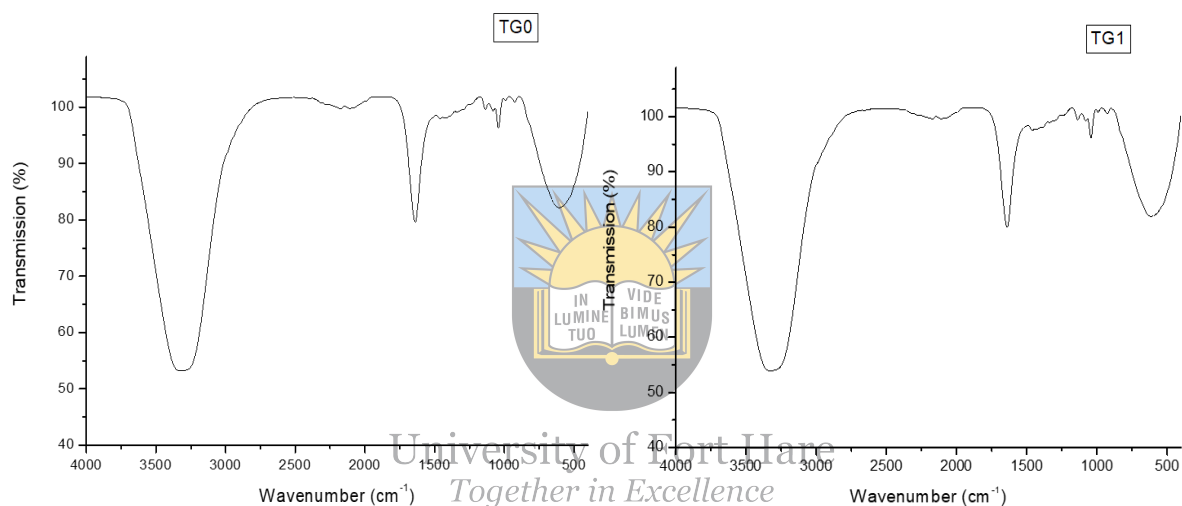
Figure 89: IR spectrum of TG0 and TG1
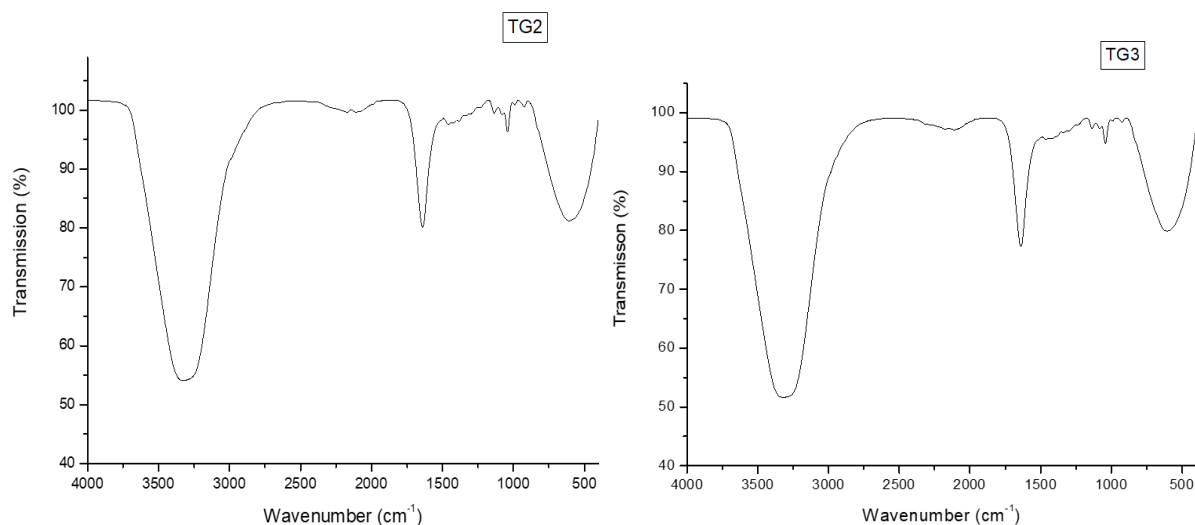
Figure 90: IR spectrum of TG2 and TG3
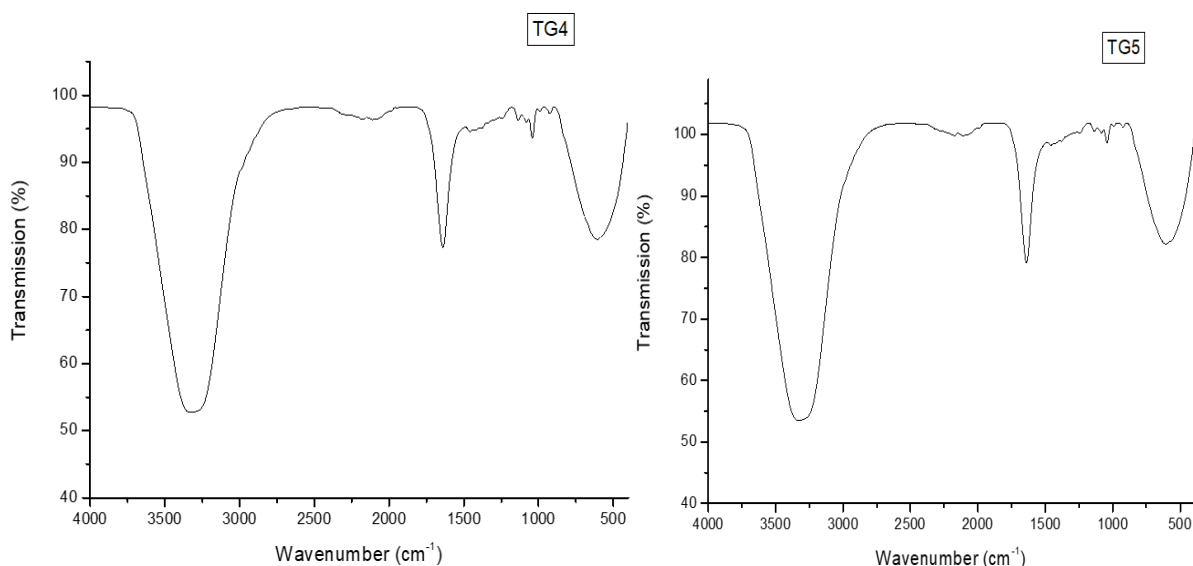
Figure 91: IR spectrum of TG4 and TG5

Table 14. FTIR data of used polymers and essential oils for preparation of topical gels

Polymer or Essential oil Used	Functional Groups	Absorption peak (cm^{-1})
CMC	C-O	1061
	Symmetric COO$^-$	1417
	Asymmetric COO$^-$	1604
	O-H	3314
Poloxamer	C-O	1112
TTO	O-H	3440
	C-O	1025
	C=C	1667
Lavender oil	C=O	1637
	Alkane C-H	1458

5.2. Viscosity

The viscosity of the CMC/poloxamer topical gels was studied employing the Brookfield viscometer and measured in cP at 50 and 100 revolutions per minute (rpm) at room temperature. The viscosity of the gels was performed at one-minute intervals for two minutes (**Table 15**). The viscosity results of the blank gel (TG0) were compared with the topical gels loaded with bioactive agents (TG1-TG5). The blank gel exhibited the highest viscosity, followed by TG4 (gel containing lavender oil only) when compared to the gels loaded with Ag nanoparticles and

143

TTO, both at 50 rpm and 100 rpm. The viscosity of the topical gels enriched with bioactive agents ranged between 216 and 732 cP at 50 rpm and 210–630 cP at 100 rpm, while the blank gel ranged from 810 to1200 cP. The order of viscosity for topical gels from the highest to the lowest was as follows: TG0>TG4>TG3>TG5>TG1>TG2. The gels containing TTO (TG1 and TG2) displayed very low viscosity indicating that TTO is less viscous when compared to lavender oil. The viscosity of all the topical gels decreased with the increase in rate and time. The viscosity range of the blank and topical gels loaded with lavender oil was higher when compared to those loaded with TTO, indicating that blank and lavender oil-loaded gels will not flow off from the skin during and after application, and further suggests their capacity to release the loaded bioactive agents in a sustained manner. The gels with higher viscosity will hinder a run-off of the gel from the site of application, thereby promoting slow drug release rates.

Table 15. The viscosity of topical gels

Gel	Time (min)	Viscosity (50 rpm)	Viscosity (100 rpm)
Blank (TG0)	1	**1200**	858
	2	**1104**	810
TG1	1	**516**	468
	2	**516**	462
TG2	1	**228**	210
	2	**216**	210
TG3	1	**732**	552
	2	**684**	534
TG4	1	**720**	636
	2	**708**	630
TG5	1	**636**	552
	2	**636**	546

5.3 pH and Spreadability of Topical Gels

The pH and spreadability results of topical gels are shown in **Table 16**. The pH of the topical gels determined their suitability for application in skin wound management. The topical gels displayed pH values in the range of 5.20-6.68, which are in the normal pH range of the skin. This is acceptable to avoid the risk of irritation upon application to the skin. The gels loaded with essential oils were in the range of 5.20-5.45 when compared to the pH of blank gel and gel loaded with

Ag nanoparticles that possessed pH of 6.43 and 6.68, respectively. These pH results showed that these topical gels are appropriate for topical application for the management of skin lesions because they were close to neutral to avoid skin irritation, especially blank (TG0) and Ag nanoparticle-loaded gel (TG3). Najafi-Taher *et al*. reported that pH values that are close to 7 are appropriate for dermal application [8]. The spreadability of topical gels (TG0-TG5) was determined after 3 mins. There was no significant difference in the spreadability of gels in the range of 5.4-5.9. TG0 (blank) displayed the highest spreadability. These results demonstrated that the loading of bioactive agents into the gels slightly reduced their spreadability. Their spreadability reveals that the topical gels can spread uniformly on the skin during wound dressing applications with improved therapeutic efficacy due to their high spreadability.

Table 16. pH and spreadability of topical gels

Gel	pH	Spreadability (cm)
TG0 (Blank)	6.43	5.9
TG1	5.37	5.5
TG2	5.21	5.5
TG3	6.68	5.5
TG4	5.45	5.4
TG5	5.20	5.8
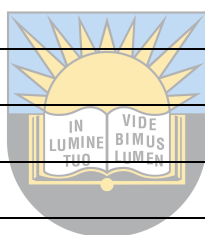
5.4. *In vitro* Drug Release Studies

The *in vitro* drug release experiments were conducted on three selected topical gels (TG1, TG3, and TG5) enriched with bioactive agents (TTO, lavender oil, and Ag nanoparticles). Gel TG1 is co-loaded with TTO and Ag nanoparticles, TG3 is only loaded with Ag nanoparticles, and TG5 is loaded with lavender oil and Ag nanoparticles. These experiments were performed to evaluate the mode of drug release from the topical at physiological conditions. The graphs that exhibit the mechanism of release of TTO and lavender oil are shown in **Figures 92-96**. The % cumulative drug release of TTO and Ag nanoparticles from gel TG1 was 82.27% and 79.12% over 24 hours, respectively, while it was 90.55% and 82.15% for lavender oil and Ag nanoparticles from TG5. The % cumulative drug release of Ag nanoparticles from gel TG3 was 77.08% over 24 hours. The % cumulative release of TTO and lavender oil from TG1 and TG5 were 91.55% and 96.06% over 2 days (48 h), respectively, while it was 99.40%, 98.37%, and 95.33% for Ag nanoparticles from TG1, TG3, and TG5, respectively, suggesting that almost

all the loaded essential oils and Ag nanoparticles were released from the topical gels after 48 hours. Interestingly, the mechanism of drug release of essential oils and Ag nanoparticles from gels was sustained from the first hour of the drug release studies with only 9.68% of TTO (and 9.12% Ag nanoparticles) and 8.20% of lavender oil (and 10.15% Ag nanoparticles) released from TG1 and TG5, respectively. It was also 10.15% of Ag nanoparticles released from TG3. This drug release mechanism can significantly result in consistent inhibition of persisting bacteria and protect the injury from further infections.

Three mathematical models were used to investigate the rate of drug release of bioactive agents from topical gels the Zero-order, Higuchi, and Korsmeyer Peppas models. The values of R^2, n, and K of the drug release mechanism of each topical gel are summarized as shown in **Table 17**. The drug release mechanism TTO from gel TG1 was best fitted into the Zero-order and Korsmeyer Peppas models with R^2 values of 0.9999 and 0.9998, respectively when compared to the Higuchi model. The n value was 0.7408 for TG1, representing a non-Fickian release mechanism. The drug release mechanism of gel TG5 for lavender oil was also well fitted into the Zero-order and Korsmeyer Peppas model compared to the Higuchi model with R^2 of 0.9885 and 0.9795, respectively. The n value was 0.9979 for TG5, also representing a non-Fickian release mechanism. The mechanism of drug release for TTO from gel TG1 was best fitted into the Zero-order and Korsmeyer Peppas models with R^2 values of 0.9999 and 0.9998, respectively. The drug release mechanism of Ag nanoparticles from gel TG1 was best fitted into the Zero-order models with R^2 values of 0.9986 than Higuchi and Korsmeyer Peppas model, while it was best fitted into the Korsmeyer Peppas model for TG3 and TG5 than Zero-order and Higuchi models with R^2 values of 0.9978 and 0.9992, respectively.
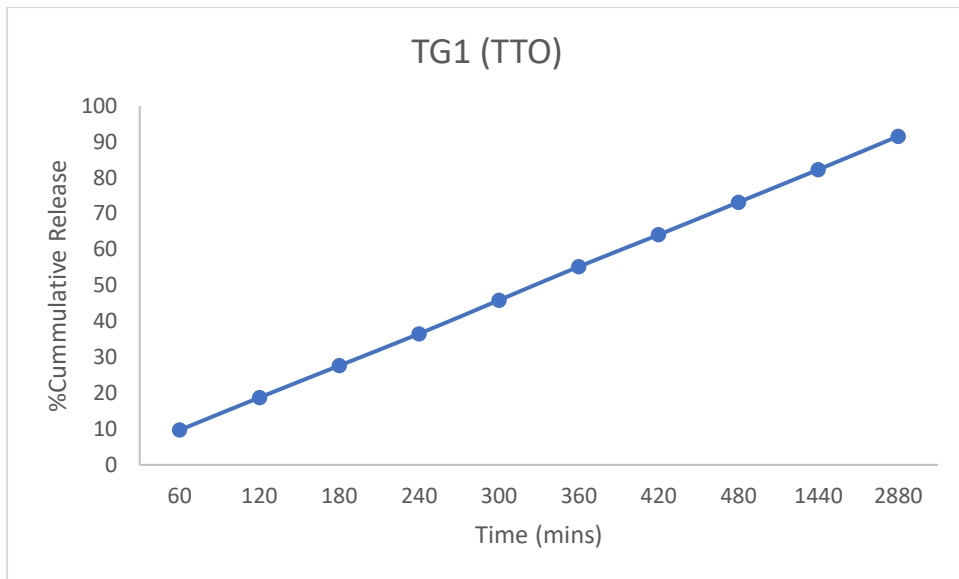
Figure 92: Drug release of TTO from TG1
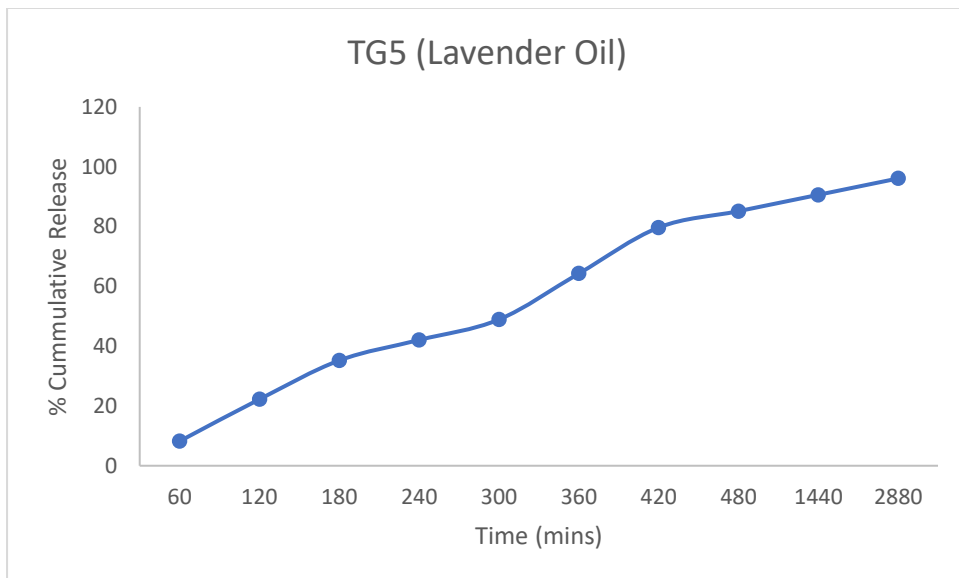
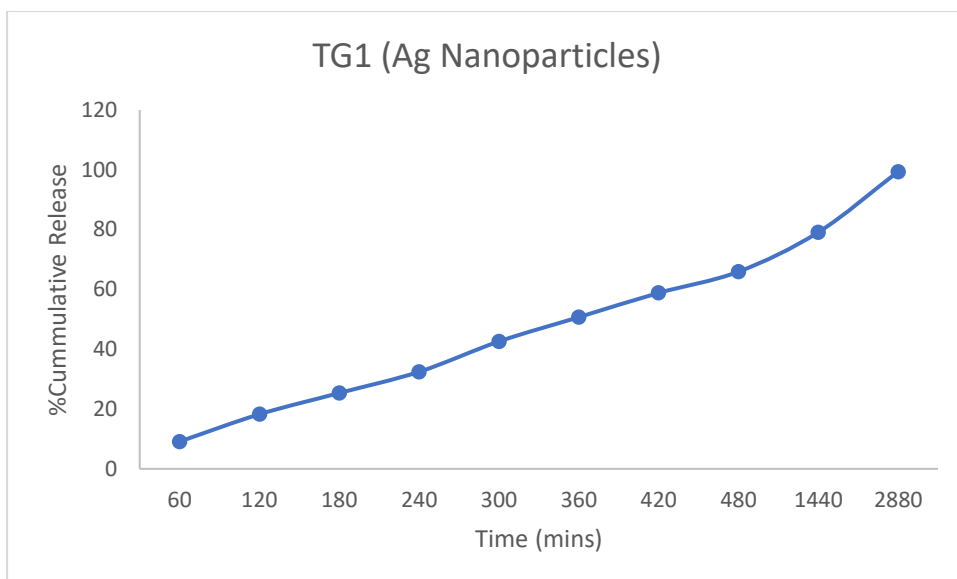**Figure 93:** Drug release of lavender oil from TG5

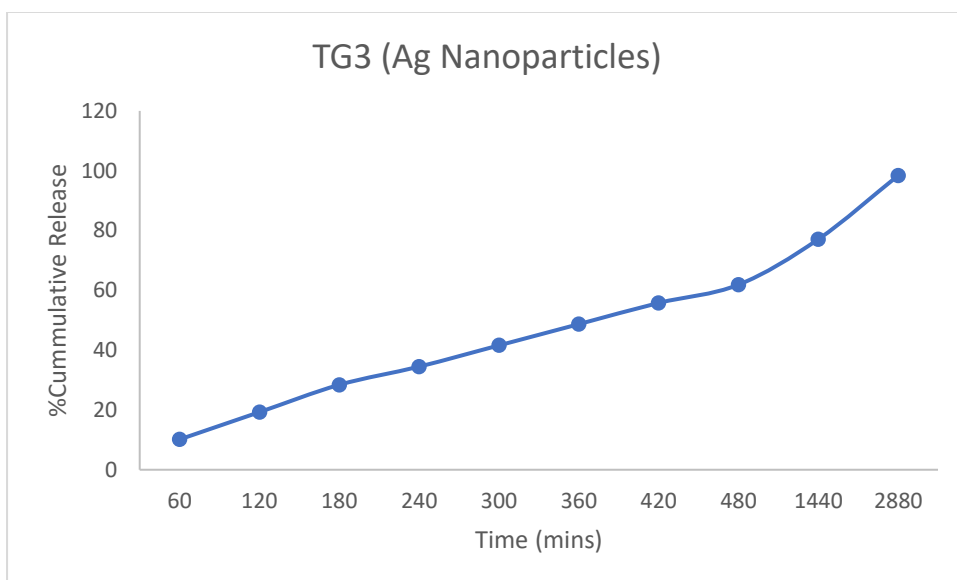**Figure 94:** Drug release of Ag nanoparticles from TG1

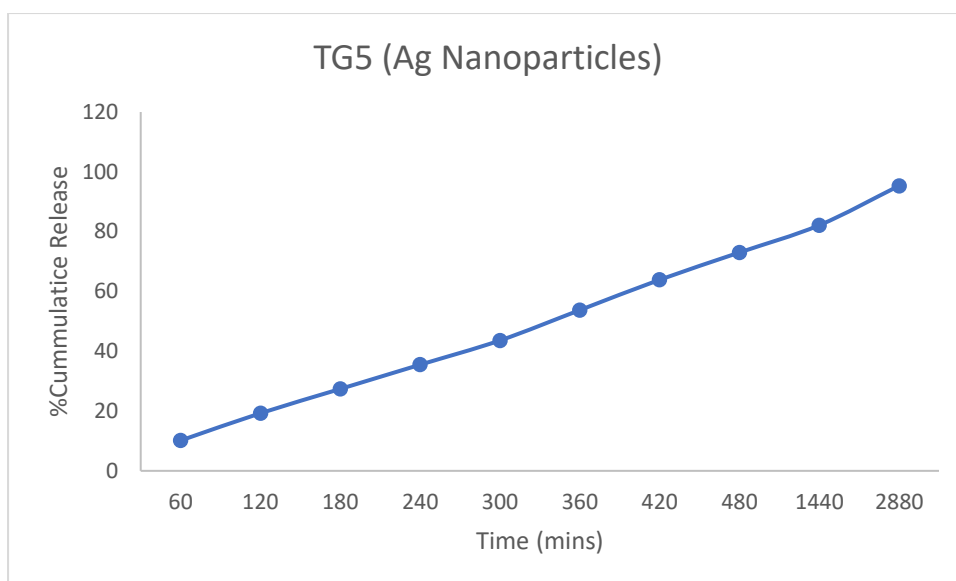**Figure 95:** Drug release of Ag nanoparticles from TG3

Figure 96: Drug release of Ag nanoparticles from TG5

Table 17. The drug release analysis constants of topical gels for the Zero-order, Higuchi, and Korsmeyer-Peppas.

Topical Gel	Loaded Drug	Zero-order model		Higuchi model		Korsmeyer Peppas model		
		K	r^2	K	r^2	K	n	r^2
TG1	TTO	0.1515	0.9999	4.5272	0.9801	0.9694	0.7408	0.9998
	Ag Nanoparticles	0.1363	0.9986	4.0742	0.9796	0.94390	0.7159	0.9978
TG3	Ag Nanoparticles	0.12151	0.9961	3.6636	0.9928	0.8709	0.5320	0.9978
TG5	Lavender Oil	0.1825	0.9885	5.4635	0.9721	1.1027	0.9979	0.9795
	Ag Nanoparticles	0.1489	0.9982	4.4342	0.9710	0.9172	0.6263	0.9992

5.5. *In Vitro* Cytotoxicity Studies

Four topical gels (TG0, TG1, TG3, and TG5) were selected for *in vitro* cytotoxicity studies, which were performed at 12.2, 25, 50, and 100 µM of gels. The selected topical gels are TG0

(blank gel), TG1 (gel co-loaded with TTO and Ag nanoparticles), TG3 (gel loaded with Ag nanoparticles only), and TG5 (gel co-loaded with lavender oil and Ag nanoparticle). All the topical gels exhibited high % cell viability of 90.83%, 91.62%, 89.18%, and 94.87% for TG0, TG1, TG3, and TG5 at the highest concentration (100 µM), respectively (**Table 18 and Figure 97**). Topical gels that were co-loaded with essential oils (TTO or lavender oil) and Ag nanoparticles showed excellent % cell viability showing that the topical gels demonstrated non-toxicity and excellent biocompatibility.
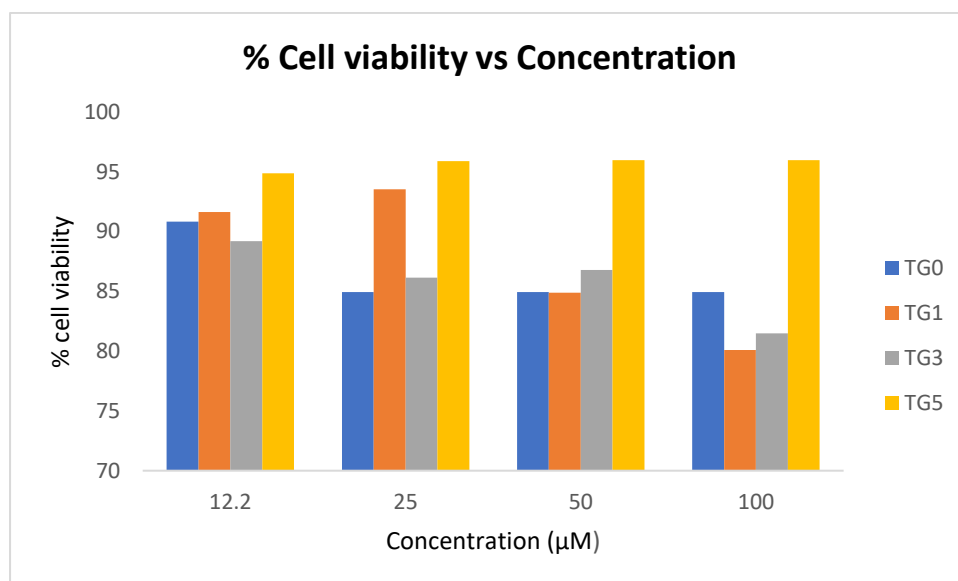
Figure 97: % Cell viability of topical gels at different concentrations

Table 18. *In vitro* cytotoxicity results of selected topical gels at 100 µM

Topical Gels	% Cell viability
TG0	90.83
TG1	91.62
TG3	89.18
TG5	94.87

5.6. *In vitro* Antibacterial Analysis

The antibacterial studies were performed to evaluate the antibacterial efficacy of CMC/poloxamer topical gels enriched with essential oils and Ag nanoparticles (**Table 19**). All the topical gels were evaluated: TG0 (blank gel), TG1 (topical gel co-loaded with TTO and Ag nanoparticles), TG2 (topical gel loaded with TTO only), TG3 (gel loaded with Ag nanoparticles only), TG4 (gel loaded with lavender oil only), and TG5 (gel co-enriched with lavender oil and Ag nanoparticles). The antimicrobial efficacy of the topical gels against Gram-positive and

Gram-negative bacteria strains was observed by comparing their MIC values to those of the controls used: AMP, STM, and NLD. All the topical gels exhibited excellent antibacterial efficacy against *Bacillus subtilis* (BS) and *Enterococcus faecalis* (EF) with a MIC value of 15.625 µg/ml each except blank gel (TG0) (100 µg/ml for both BS and EF) when compared to the controls, AMP (26 µg/ml against both bacteria strains), STM (16 µg/ml against BS and 128 µg/ml against EF), and NLD (16 µg/ml against BS and >512 µg/ml against EF). TG1 is the only topical gel that displayed superior antibacterial efficacy against *Staphylococcus epidermidis (SE) with a* MIC value of 15.625 µg/ml which could be because of the synergistic effect of TTO and Ag nanoparticles. Other gels (TG2, TG3, TG4, and TG5) showed a MIC value of 500 µg/ml while TG0, AMP, STM, and NLD exhibited MIC values of 200, 26, 8, and 64 µg/ml, respectively. TG2, TG3, and TG5 showed excellent antimicrobial efficacy against *Staphylococcus aureus* (SA) than controls with MIC value of 15.625 µg/ml each, while TG0, TG1, and TG4 exhibited MIC values of 200, 62.5, and 62.5 µg/ml, respectively. The MIC values of controls against SA were 26, 256, and 64 µg/ml for AMP, STM, and NLD, respectively. All the topical gels showed poor antibacterial activity against *Mycobaterium smegmatis* (*MS*) when compared to controls (AMP and STM) with MIC value of 200 µg/ml for blank gels and 500 µg/ml for all other gels (TG1, TG2, TG3, TG4, and TG5), MIC values of controls against *MS* were 26 µg/ml for AMP, 4 µg/ml for STM, and 512 µg/ml for NLD.

All the topical gels showed superior antibacterial efficacy against *Enterobacter cloacae* (ECL) with a MIC value of 15.625 µg/ml except TG0 (200 µg/ml) when compared to AMP, STM, NLD with MIC values of 26, 512, and 16 µg/ml, respectively. Surprisingly, blank gel (TG0) is the only gel that showed superior antibacterial efficacy against *Proteus vulgaris (PV)* with a MIC value of 12.5 µg/ml in comparison with all other gels (MIC value of 500 µg/ml each) and controls (MIC values of 416 for AMP and 128 µg/ml for both STM and NLD). All the topical gels exhibited excellent antibacterial activity against *Klebsiella oxytoca* (KO) and *Proteus mirabilis* (PM) with a MIC value of 15.625 µg/mL each except TG0 (200 µg/ml for each bacterial strain) in comparison with controls that displayed MIC values of 26 µg/mL (AMP) for both bacterial strains, 16 28 µg/mL against KO and 28 µg/mL against PM for STM, and 8 against KO (only this control that was superior when compared to topical gels) and 32 µg/mL against PM for NLD. The topical gel TG1, TG2, TG3, and TG5 showed good antibacterial efficacy against *Pseudomonas aeruginosa* (PA) with a MIC value of 15.625 µg/mL each than the controls AMP (64 µg/mL), STM (128 µg/mL), and NLD (128 µg/mL)., while TG0 and TG5 exhibited 200 and 250 µg/mL, respectively. Only gel TG5 displayed good antibacterial

efficacy against *Escherichia coli* (EC) with MIC values of 15.625 µg/mL when compared with AMP (26 µg/mL), STM (64 µg/mL), and NLD (512 µg/mL). There is not even one topical gel that showed antibacterial efficacy against *Klebsiella pneumonia* (KP).

The blank topical gel did not demonstrate any antibacterial effects against all bacterial strains except PV, which could be due to it not being loaded with bioactive agents (essential oils and Ag nanoparticles). Almost all the other topical gels revealed excellent antibacterial efficacy against most gram-positive bacterial strains (BS, EF, SE, and SA) and gram-positive bacterial strains (ECL, KO, PM, PA, and EC) when compared to the controls. TG1 and TG5 are the only topical gels that exhibited excellent antibacterial activity against *Staphylococcus epidermidis* (gram-negative bacteria) and *Escherichia coli* (gram-positive bacteria)*,* respectively; demonstrating that they are effective for the management of injuries that are infected by these clinical bacterial strains. Although research reports on topical gels enriched with TTO and lavender oil are very scarce, some reports demonstrated the antibacterial effects of wound dressing scaffolds loaded with these essential oils, even these oils co-loaded with Ag nanoparticles. Low *et al.* formulated chitosan hydrogels co-enriched with TTO and Ag^+ ions for wound dressing applications. The *in vitro* antimicrobial activity of dual drug-enriched hydrogels was excellent for *S. aureus*, *C. albicans*, and *P. aeruginosa* when incubated overnight with these infectious microorganisms [9].

The antibacterial analysis of TTO-enriched PVA/starch hydrogels conducted by Altaf and co-workers utilizing the disc diffusion procedure exhibited antibacterial efficacy against *E. coli* and MRSA, although it was not as good as the clove oil-loaded hydrogels which could be due to the major constituent of the TTO (terpinen-4-ol) that display the resistance against both *E. coli* and MRSA [10]. The topical gel TG1 (loaded with TTO only) did not display any antibacterial activity against *E. coli* and *S. aureus*, and TG2 (co-loaded with TTO and Ag nanoparticles) showed slight antibacterial activity against S. aureus with a MIC value of 16.2 µg/mL. Tajik et al. designed keratin/PVP hybrid hydrogels enriched with lavender oil extract for the management of bacteria-infected injuries. The antibacterial experiment of lavender oil extract-enriched hydrogels demonstrated good antibacterial activity against both *S. aureus* and *E. coli*, confirming their effectiveness as promising scaffolds for the treatment of bacteria-infected injuries [11]. Furthermore, The *in vitro* antibacterial experiments of gellan gum hydrogels co-enriched with lavender oil and ofloxacin performed by Mahmood and co-workers showed good antibacterial activity against *S. aureus* and *E. coli*, suggesting that these hydrogels

are also effective scaffolds that can be employed in the management of bacteria-infected injuries [12].

Table 19. Antibacterial results of topical gels (MIC values were measured in µg/mL)

Tested Compounds	GRAM-POSITIVE					GRAM-NEGATIVE						
	BS	*EF*	*SE*	*SA*	*MS*	*ECL*	*PV*	*KO*	*PA*	*PM*	*EC*	KP
TG0	100	100	200	200	200	200	12.5	200	200	200	200	200
TG1	15.625	15.625	15.625	62.5	500	15.625	500	15.625	15.625	15.625	500	500
TG2	15.625	15.625	500	15.625	500	15.625	500	15.625	15.625	15.625	500	500
TG3	15.625	15.625	500	15.625	500	15.625	500	15.625	15.625	15.625	500	500
TG4	15.625	15.625	500	62.5	500	15.625	500	15.625	15.625	15.625	500	500
TG5	15.625	15.625	500	15.625	500	15.625	500	15.625	250	15.625	15.625	500
AMP	26	26	26	26	26	26	416	26	64	26	26	26
STM	*16*	*128*	*8*	*256*	*4*	*512*	*128*	*16*	*128*	*128*	*64*	*512*
NLD	*16*	*>512*	*64*	*64*	*512*	*16*	*128*	*8*	*128*	*32*	*512*	*256*

5.7. In Vitro Scratch Wound Healing Assay

In vitro scratch wound healing assay was also performed on the selected topical gel co-loaded with lavender oil and Ag nanoparticles (TG5) (**Figure 98**), which showed high % cell viability *in vitro*. A wound healing study was conducted at time points of 0, 24, 48, 72, and 96 hours and compared to the rate of closure of the untreated cells. The cells treated with gel TG5 showed a 55.29% closure rate than the untreated cells (42.86%) for 96 hours against HACAT cells (**Table 20**). TG5 showed a significant rate of closure of cells as compared to untreated cells over 96 h, revealing the potential to induce wound healing. Research studies reporting the in vitro scratch wound healing of scaffolds enriched with lavender or tea tree oil are very scarce. However, some studies reported the in vitro wound healing of CMC-based systems.

Shin et al. fabricated CMC/PVA/PEG hydrogels to manage wounds. In vitro scratch wound healing assay employing L929 cells exhibited the fastest closure rate for the irradiated CMC/PVA/PEG hydrogels, indicating that the CMC-based hybrid hydrogels are wound healing scaffolds useful for skin regeneration [13]. Joorabloo et al. fabricated Heparinized CMC/PVA bionanocomposite hydrogels incorporated with ZnO nanoparticles for application in wound healing. The *in vitro* scratch wound healing assay employing L929 fibroblast cells

revealed the hydrogels' capability to heal the wounds properly after 24 h. It suggests they can promote wound cell migration [14]. The CMC-based hydrogel formulated by Zhang et al. showed proliferation-promoting activity with murine fibroblasts [15]. Bagheri *et al*. prepared CMC/chitosan–carboxymethyl cellulose nanogel co-enriched with *Nigella sativa* oil and atorvastatin for wound treatment. The *in vitro* wound healing studies showed that the migration of HDF cells enhanced after 24 and 48 h of the treatment with dual drug-enriched nanogels than the control [16]. The CMC-based hybrid scaffolds loaded with therapeutic agents or without bioactive agents are effective systems for treating wounds.
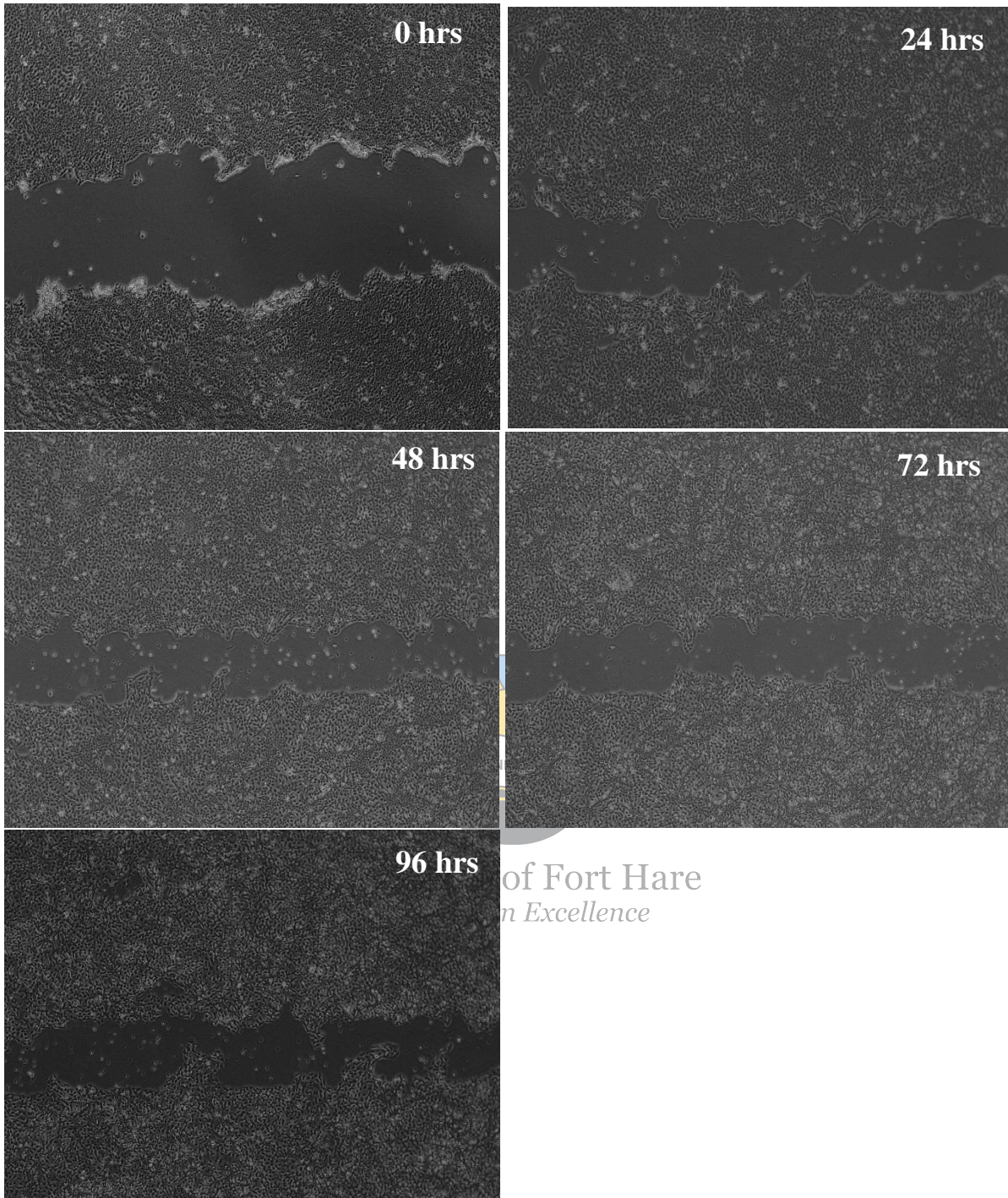
University of Fort Hare
Together in Excellence

Figure 98: Wound scratch images of treated cells with TG5

Table 20. Area of stretch over time for the selected topical gel

Time (h)	Area (mm)	
	Untreated cells	**TG5**
0	1058.630	830.269
24	650.330	425.653
48	605.236	422.134
72	511.619	392.669
96	604.881	371,177
Total reduction	453.749=42.86%	459.092=55.29%

31

References

[1]   Capanema, N.S.V.; Mansur, A.A.P.; De Jesus, A.C.; Carvalho, S.M.; De Oliveira, L.C.; Mansur, H.S. Superabsorbent crosslinked carboxymethyl cellulose-PEG hydrogels for potential wound dressing applications. *Int. J. Biol. Macromol.* 2018, 106, 1218–1234. doi: 10.1016/j.ijbiomac.2017.08.124.

[2]   Namazi, H.; Rakhshaei, R.; Hamishehkar, H.; Kafil, H.S. Antibiotic loaded carboxymethylcellulose / MCM-41 nanocomposite hydrogel films as potential wound dressing. *Int. J. Biol. Macromol.* 2016, 85, 327–334. doi: 10.1016/j.ijbiomac.2015.12.076.

[3]   Palem, R.R.; Rao, K.M.; Shimoga, G.; Saratale, R.G.; Shinde, S.K.; Ghodake, G.S.; Lee, S. Physicochemical characterization, drug release, and biocompatibility evaluation of carboxymethyl cellulose-based hydrogels reinforced with sepiolite nanoclay. *Int. J. Biol. Macromol.* **2021**, 178, 464–476. doi: 10.1016/j.ijbiomac.2021.02.195.

[4]   Khajeh, H.G.; Sabzi, M.; Ramezani, S.; Jalili, A.A.; Ghorbani, M. Fabrication of a wound dressing mat based on Polyurethane / Polyacrylic acid containing Poloxamer for skin tissue engineering. *Coll. Surf. A Physicochem. Eng. Asp.* **2022**, 633, 12789. doi: 10.1016/j.colsurfa.2021.127891.

[5]   Jiang, S.; Zhao, T.; Wei, Y.; Cao, Z.; Xu, Y.; Wei, J.; Xu, F.; Wang, H.; Shao, X. Preparation and characterization of tea tree oil /hydroxypropyl- β -cyclodextrin inclusion complex and its application to control brown rot in peach fruit. *Food Hydrocoll.* **2021**, 121, 107037 doi: 10.1016/j.foodhyd.2021.107037.

[6]   Jamróz, E.; Juszczak, L.; Kucharek, M. Investigation of the physical properties, antioxidant and antimicrobial activity of ternary potato starch-furcellaran-gelatin films incorporated with lavender essential oil. *Int. J. Biol. Macromol.* **2018**, 114, 1094–1101. doi: 10.1016/j.ijbiomac.2018.04.014.

[7]   Nerkar, D.; Rajwade, M.; Jaware, S.; Jog, M. Synthesis and characterization of Polyvinyl Alcohol-Polypyrrole- Silver nanocomposite polymer films with core-shell structure. *Int. J. Nano Dimns.* **2020**, 11205–214.

[8]   Najafi-Taher, R.; Ghaemi, B.; Amani, A. Delivery of adapalene using a novel topical

gel-based on tea tree oil nano-emulsion: Permeation, antibacterial and safety assessments. *Eur. J. Pharm. Sci.* **2018**, 120, 142–151. doi: 10.1016/j.ejps.2018.04.029.

[9]   Low, W.L.; Kenward, M.A.; Amin, M.C.Q.; Martin, C. Ionically Crosslinked Chitosan Hydrogels for the Controlled Release of Antimicrobial Essential Oils and Metal Ions for Wound Management Applications. *medicines* **2016**, 3, 8.doi: 10.3390/medicines3010008.

[10]   Altaf, F.; Niazi, M.B.K.; Jahan, Z.; Ahmad, T.; Akram, M.A.; Safdar, A.; Butt, M.S.; Noor, T.; Sher, F. Synthesis and Characterization of PVA / Starch Hydrogel Membranes Incorporating Essential Oils Aimed to be Used in Wound Dressing Applications. *J. Polym. Environ.* **2021**, 29, 156–174. doi: 10.1007/s10924-020-01866-w.

[11]   Tajik, F.; Eslahi, N.; Rashidi, A.; Rad, M.M. Hybrid antibacterial hydrogels based on PVP and keratin incorporated with lavender extract. *J. Polym. Res.* **2021**, 28, 316. doi: 10.1007/s10965-021-02681-0.

[12]   Mahmood, H.; Khan, I.U.; Asif, M.; Khan, R.U.; Asghar, S.; Khalid, I.; Khalid, S.H.; Irfan, M.; Rehman, F.; Shahzad, Y.; Yousaf, A.M.; Younus, A.; Niazi, Z.R.; Asim, M. In vitro and in vivo evaluation of gellan gum hydrogel fi lms : Assessing the co impact of therapeutic oils and ofloxacin on wound healing. *Int. J. Biol. Macromol.* **2021**, 166, 483–495. doi: 10.1016/j.ijbiomac.2020.10.206.

[13]   Shin, J.-Y.; Lee, D.Y.; Kim, B.-Y.; Yoon, J. I. Effect of polyethylene glycol molecular weight on cell growth behavior of polyvinyl alcohol/carboxymethyl cellulose/polyethylene glycol hydrogel. *J. Appl. Polym. Sci.* **2020**, 137, e49568, 2020, doi: 10.1002/app.49568.

[14]   Joorabloo, A.; Khorasani, M.T.; Adeli, H.; Mansoori-Moghadam, Z.; Moghaddam, A. Fabrication of heparinized nano ZnO/poly(vinylalcohol)/carboxymethyl cellulose bionanocomposite hydrogels using artificial neural network for wound dressing application.; *J. Ind. Eng. Chem.* 2019, 70, 253–263. doi: 10.1016/j.jiec.2018.10.022.

[15]   Zhang, W.; Wang, X.; Ma, J.; Yang, R.; Hu, Y.; Tan, X.; Chi, B. Adaptive injectable carboxymethyl cellulose/poly (γ-glutamic acid) hydrogels promote wound healing. *Biomater. Adv.* **2022**, 136, 212753.

[16]   Bagheri, F.; Darakhshan, S.; Mazloomi, S.; Varnamkhasti, B.S.; Tahvilian, R. Dual
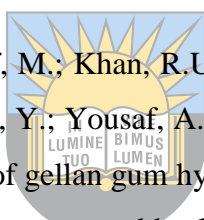
loading of Nigella sativa oil-atorvastatin in chitosan–carboxymethyl cellulose nanogel as a transdermal delivery system. *Drug Dev. Ind. Pharm.* **2021**, 47, 569–578. doi: 10.1080/03639045.2021.1892742.

CHAPTER 6: CONCLUSION

6.1 Conclusion

The FTIR and SEM/EDX results confirmed the successful formulation of the plain gelatin/PEG sponges and gelatin/PEG sponges loaded with metronidazole and Ag nanoparticles. The FTIR spectra of the gelatin-based sponges exhibited characteristic peaks that confirmed the successful crosslinking of the polymers (gelatin and PEG). FTIR spectra also revealed the absence of an interaction between the loaded bioactive agents (metronidazole and Ag nanoparticles) and the polymer network. The SEM images displayed the morphologies of the gelatin-based hybrid sponges, such as globular, plate-like, and spherical morphology. Most importantly some exhibited porous morphology, revealing their capability to support skin regeneration. The EDX results showed elemental analysis in which oxygen was in the range of 13.95-49.20%, carbon (14.71-40%), when compared to nitrogen (0.66 to 21.39%) and Ag (0 and 0.92%), further confirming the successful fabrication of gelatin hybrid sponges. The *in vitro* biodegradation studies revealed that all the sponges were biodegradable, an important feature in wound dressings to promote skin regeneration. Also, the SEM images of sponges exhibited rough morphology for all sponges after one, two, and three weeks of biodegradation studies further confirming the degradability of gelatin-based sponges. These biodegradation studies reveal that these gelatin-based sponges possess the potential ability to induce skin regeneration. The TGA results exhibited the ideal moisture content in the range of 12.96-27.28%, except for SAB5% (48.75%) and SAA5% (40.65%), indicating their capability to offer a suitable moist environment for the wound bed for the acceleration of wound healing process.

The porosity of the gelatin-based hybrid sponges was in the range of 15.64-91.10%, and it increased with an increase in the gelatin amount, indicating that these sponges can improve cell proliferation and movement and gaseous exchange during wound dressing applications. The *in vitro* drug release kinetics exhibited an initial burst drug release mechanism of metronidazole from gelatin-based hybrid sponges followed by sustained drug release, indicating that these sponges can quickly kill bacteria and inhibit persisting bacteria infections as well as protect the

injury from further infections. The drug release results of Ag nanoparticles exhibited slow, sustained release from the gelatin-based hybrid sponges. The *in vitro* cytotoxicity studies utilizing HaCaT cells showed that all the selected sponges possess good cell viability between 71.71% and 86.10%, suggesting non-toxicity and good cytocompatibility of the blank gelatin-based sponges and sponges loaded with metronidazole and Ag nanoparticles. The gelatin-based hybrid sponges loaded with metronidazole and Ag nanoparticles showed excellent antibacterial efficacy against the strains of bacteria (*Staphylococcus epidermidis, Escherichia coli, staphylococcus aureus*, and *Proteus vulgaris*) that are commonly found in wound infections with MIC value of 15.625 µg/mL each. The sponges revealed an important reduction in the scratch area of over 48.94% and 69.07% for the dual drug-loaded sponge and the metronidazole-loaded sponge, respectively, for 96 hours when compared to the untreated cells (42.86%), suggesting that the sponges have the potential to accelerate the process of wound healing.

The FTIR analysis of topical gels loaded with essential oils and Ag nanoparticles confirmed the successful preparation of the gels by exhibiting important peaks for major constituents of essential oils (TTO and lavender oil), and Ag nanoparticles. The viscosity of the blank and topical gels loaded with lavender oil was higher when compared to those loaded with TTO, suggesting that these gels with high viscosity will not flow off the skin during wound dressing application. The topical gels displayed pH values in the range of 5.20 and 6.68, which are close to neutral, especially blank and Ag nanoparticle-loaded gels, demonstrating that these gels do not have the potential to cause skin irritation. Furthermore, there was no significant difference in the spreadability of topical gels. They were all in the range of 5.4-5.9, indicating that the gels can spread uniformly on the skin with improved therapeutic activity due to their high spreadability. The *in vitro* drug release experiments of topical gels showed that the release of essential oils and Ag nanoparticles from gels was sustained. The *in vitro* cytotoxicity analysis of selected gels showed very high % cell viability ranging between 89.18% and 94.87%, suggesting excellent cytocompatibility of topical gels, a unique property of an ideal wound dressing material. The antibacterial analysis showed that dual drug loaded-topical gels (TG1 and TG2) are the only gels that possessed superior antibacterial efficacy against *S. epidermidis* (gram-positive bacteria) and *E. coli* (gram-negative bacteria)*,* respectively, suggesting that they are potential candidates that can be employed for the management of injuries infected by these clinical bacterial strains. *In vitro* scratch wound healing studies showed that the cells treated with gel co-enriched with lavender oil and Ag nanoparticles possessed a higher rate of closure

of 55.93% than the untreated cells (42.86%) for 96 hours against HACAT cells, suggesting the potential to induce accelerated wound healing process.

6.2. Contribution of new knowledge to the scientific community In this study

New knowledge was generated on the preparation of wound dressings based on biopolymers with the potential to accelerate wound healing, inhibit microbial invasion, and treat infected wounds. This is the first report to the best of my knowledge that reports gelatin-PEG-based sponges with high porosity and good moisture content loaded with the combination of metronidazole and AgNPs as potential scaffolds for the treatment of wounds. Chronic wounds resulting from microbial infections are challenging to treat. Therefore, this study contributes to the development of innovative antimicrobial wound dressings for managing chronic wounds.

6.3. Future Work

The results obtained from this research study are auspicious for the field of wound dressing. However, further characterizations (e.g., BET, TEM, particle size analysis) and *in vivo* wound healing studies, histological evaluation, and hemostasis analysis are required to fully understand the potential of gelatin/PEG sponges loaded with metronidazole and Ag nanoparticles, and topical gels enriched with essential oils and Ag nanoparticles as effective wound dressings.
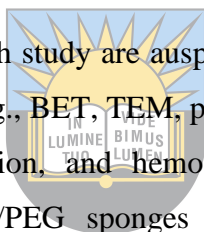
6.4. Appendix

5.3.1. FTIR Spectrums of Drugs and Polymers
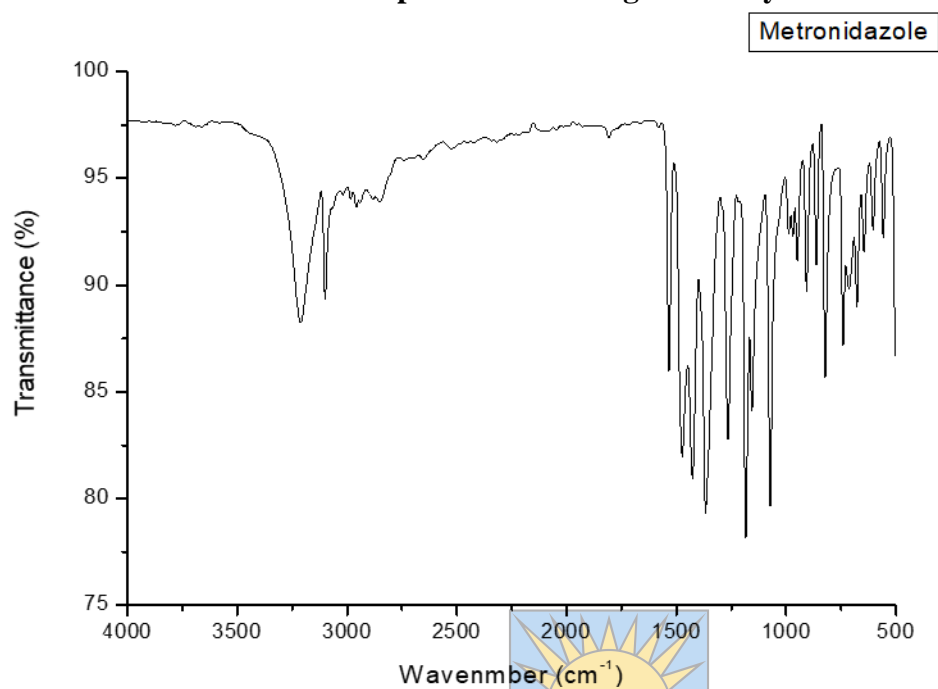
Figure 99: IR spectrum of metronidazole
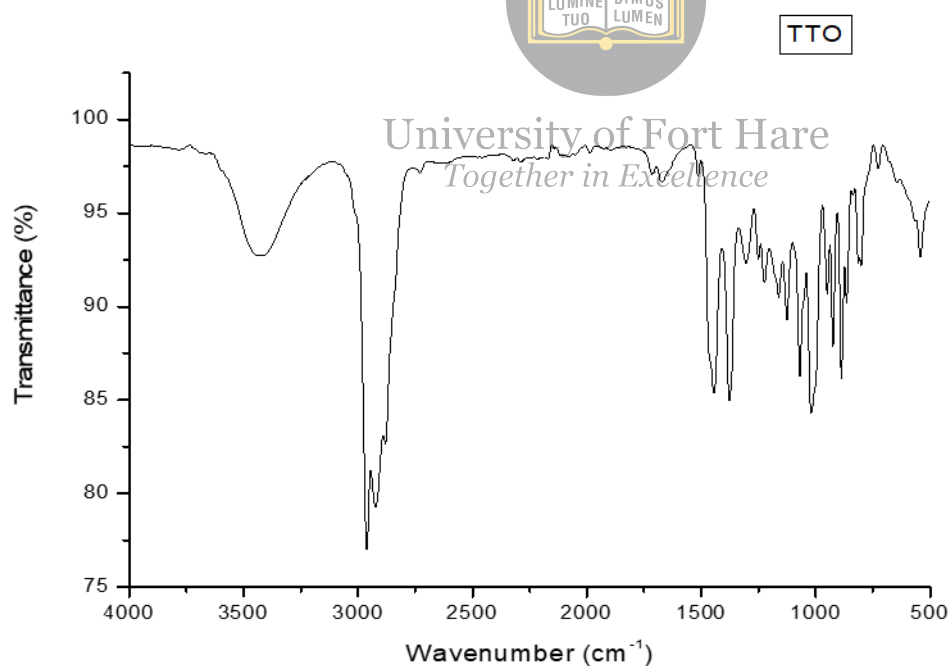
Figure 100: IR spectrum of TTO
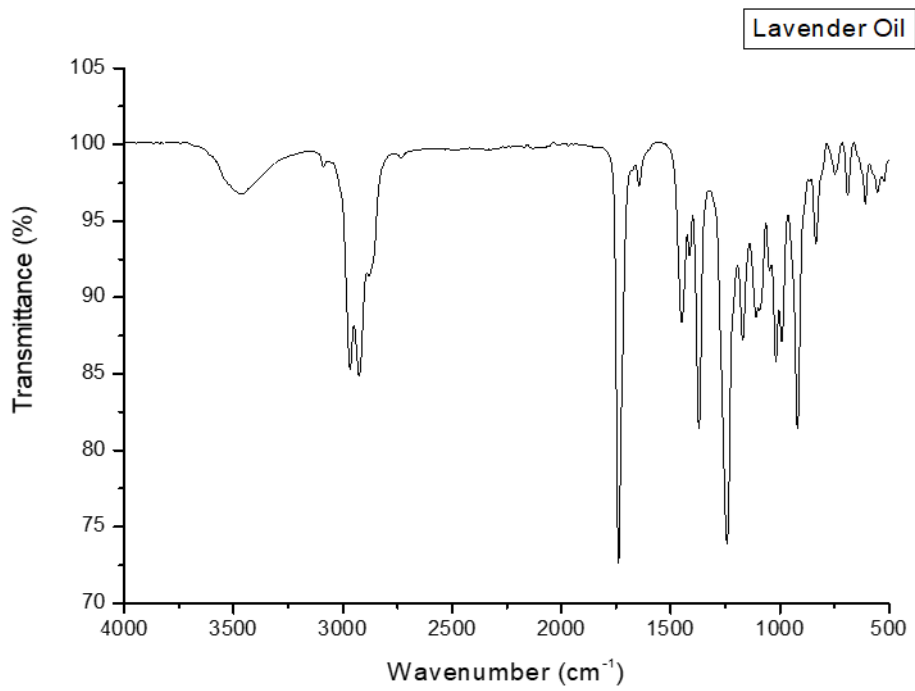
Figure 101: IR spectrum of lavender oil
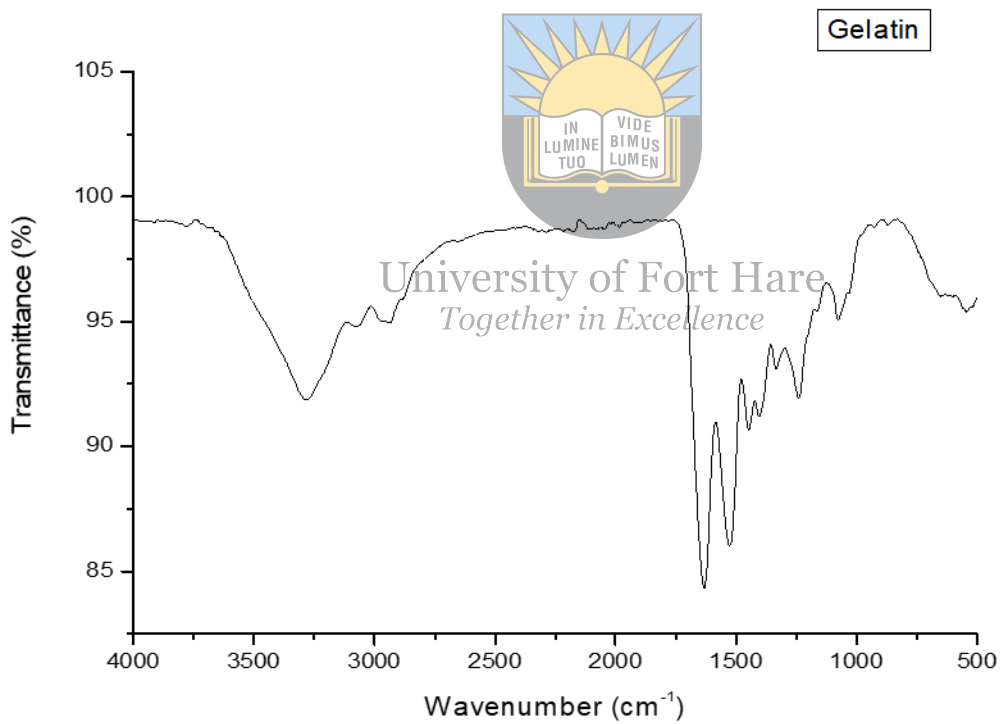
Figure 102: IR spectrum of gelatin

163
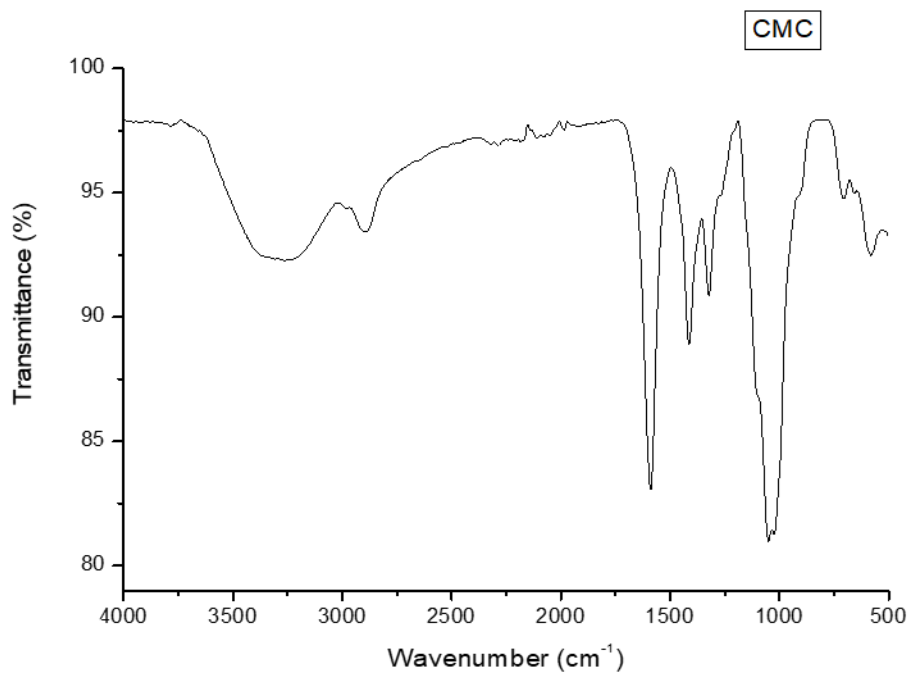
Figure 103: IR spectrum of CMC
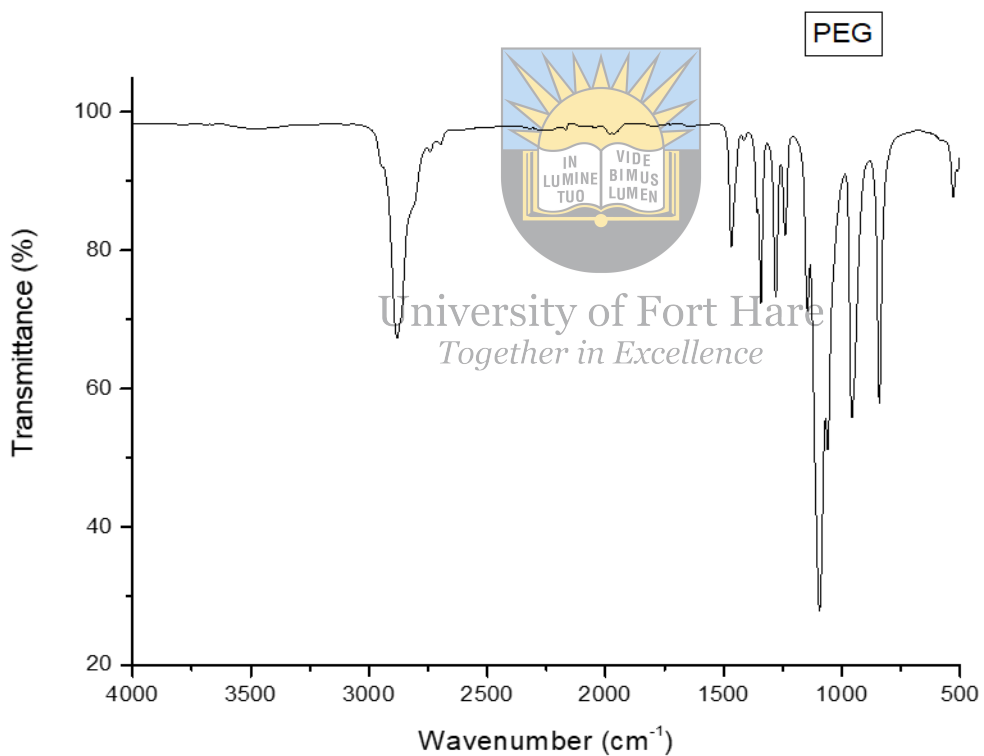
Figure 104: IR spectrum of PEG
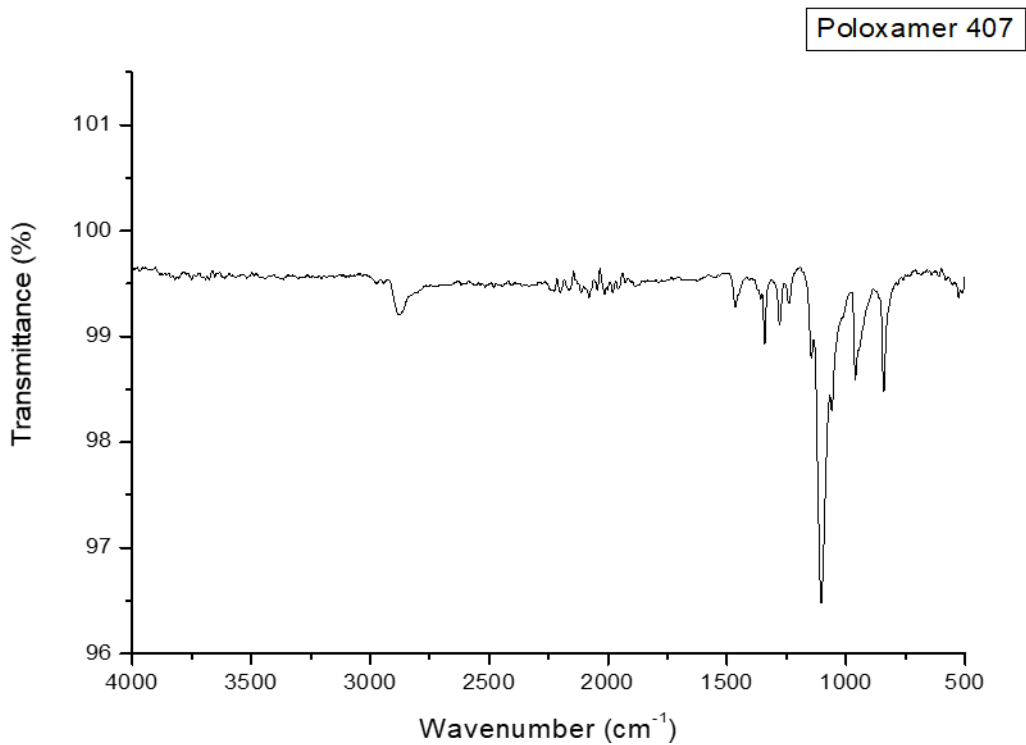
Figure 105: IR spectrum of Poloxamer 407

5.3.2. EDX Spectra of Sponges
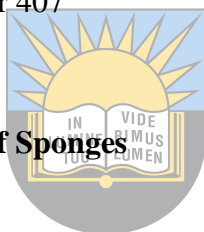
Figure 106: EDX of SA1
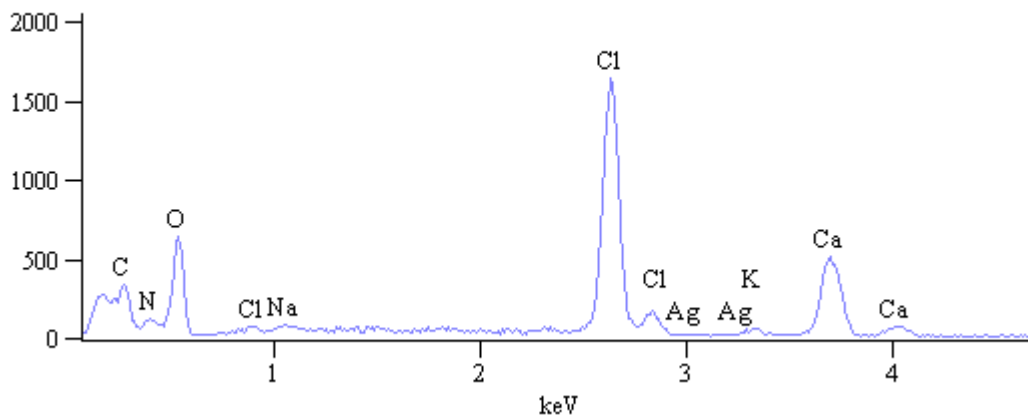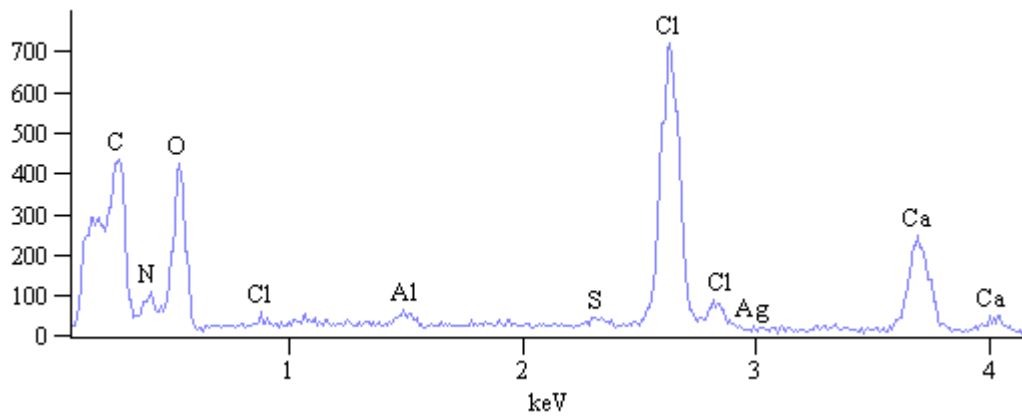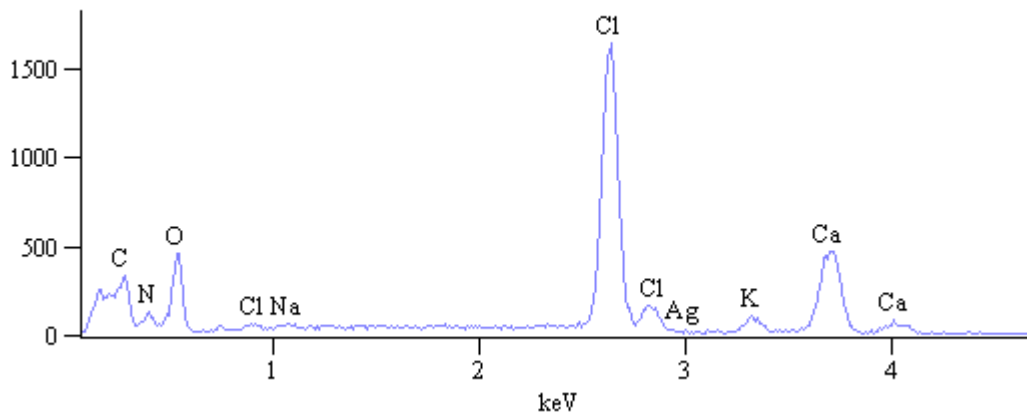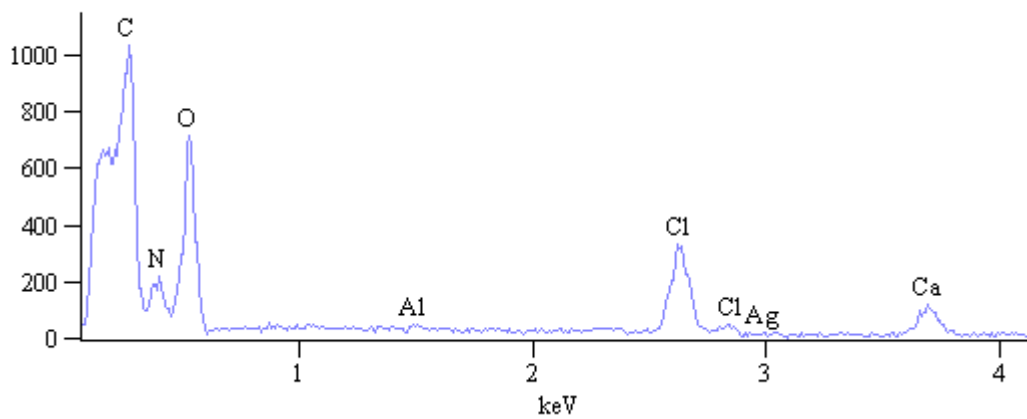
Figure 107: EDX of SA2

Figure 108: EDX of SA3

Figure 109: EDX of SA4
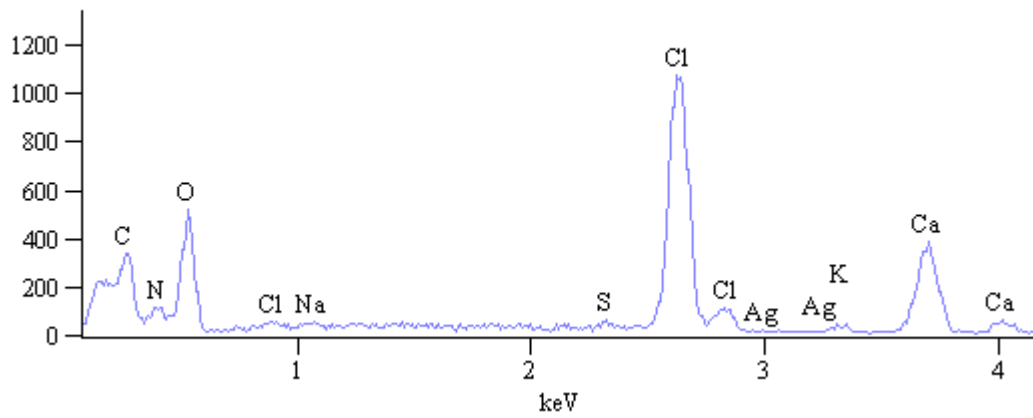
Figure 110: EDX of SA5
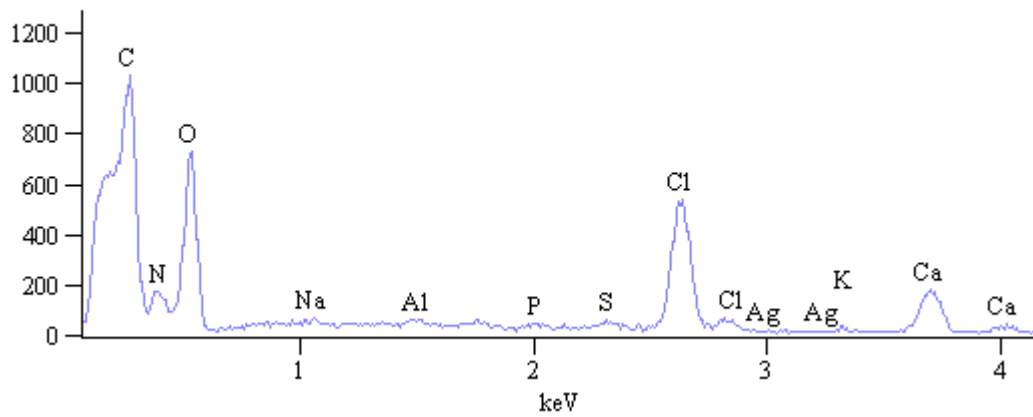
Figure 111: EDX for SA6

Together in Excellence
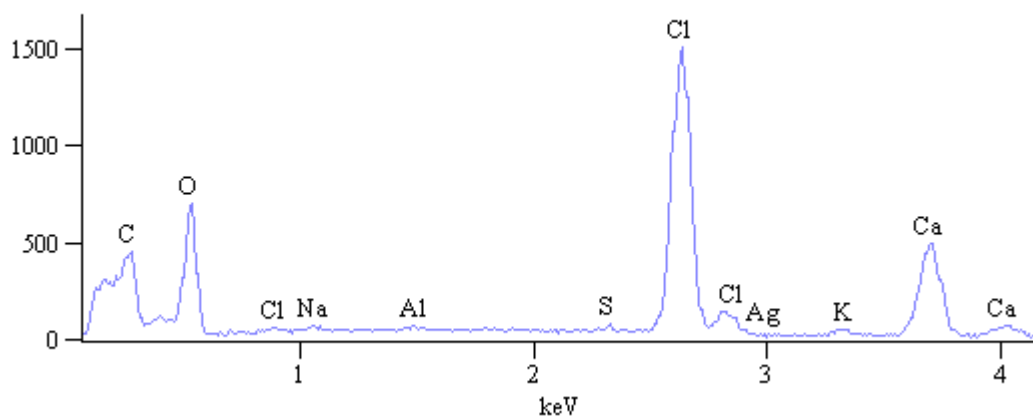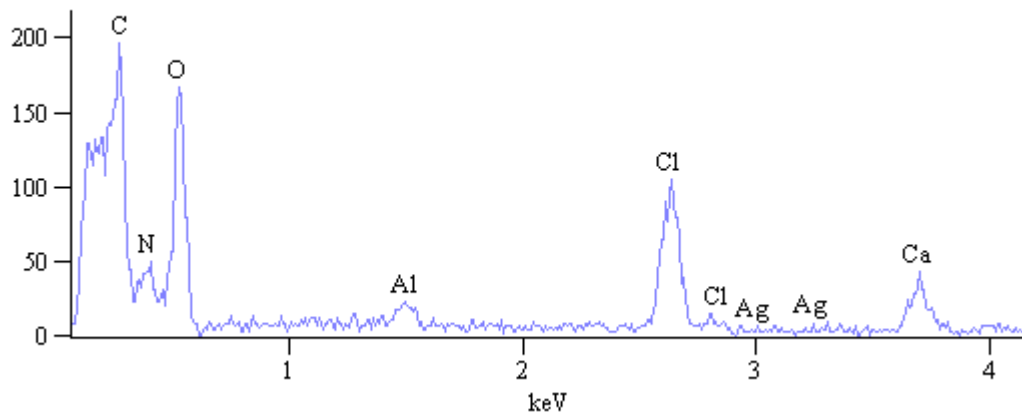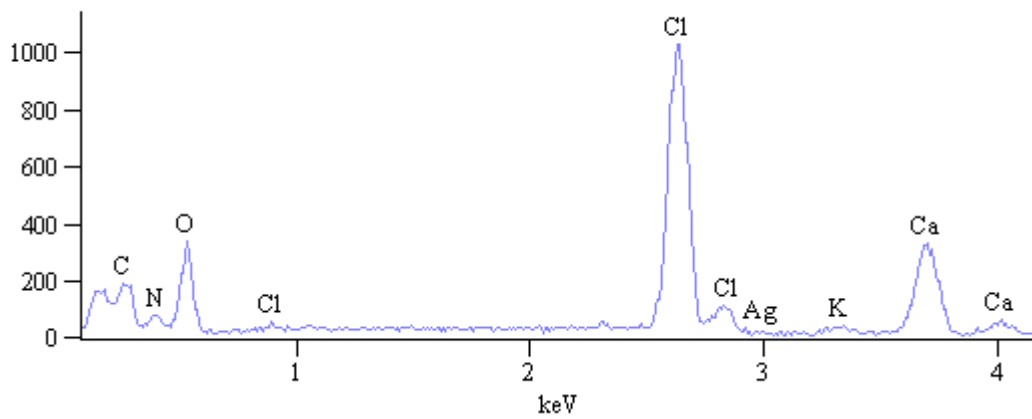
Figure 112: EDX for SA7

Figure 113: EDX for SA8

Figure 114: EDX for SA9
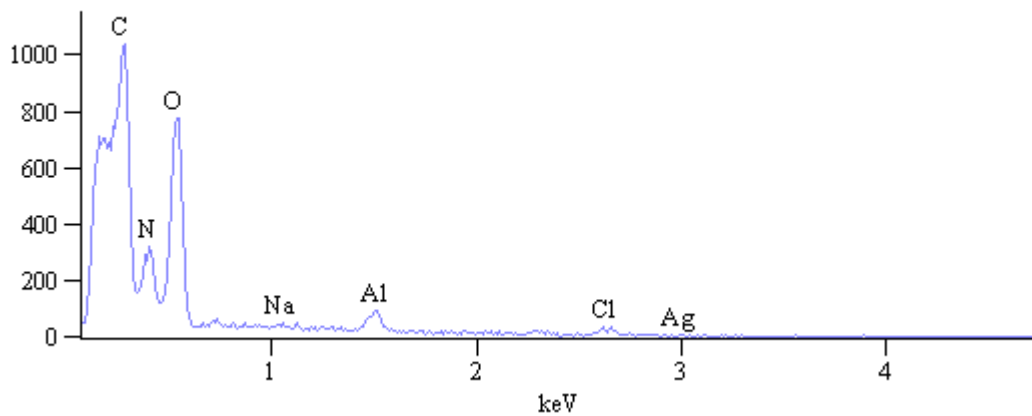
Figure 115: EDX for SA10

SA11(1)_pt1
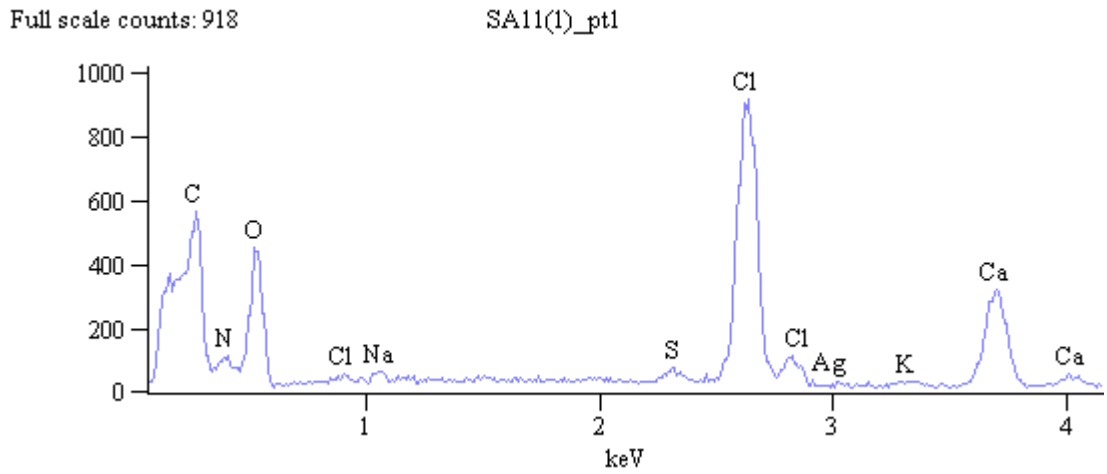
Figure 116: EDX for SA11
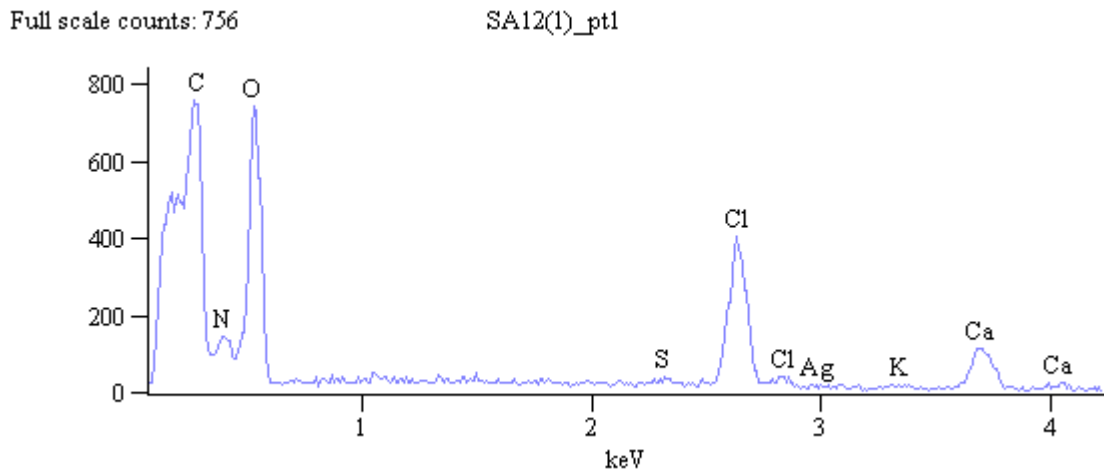
SA12(1)_pt1

Figure 117: EDX for SA12
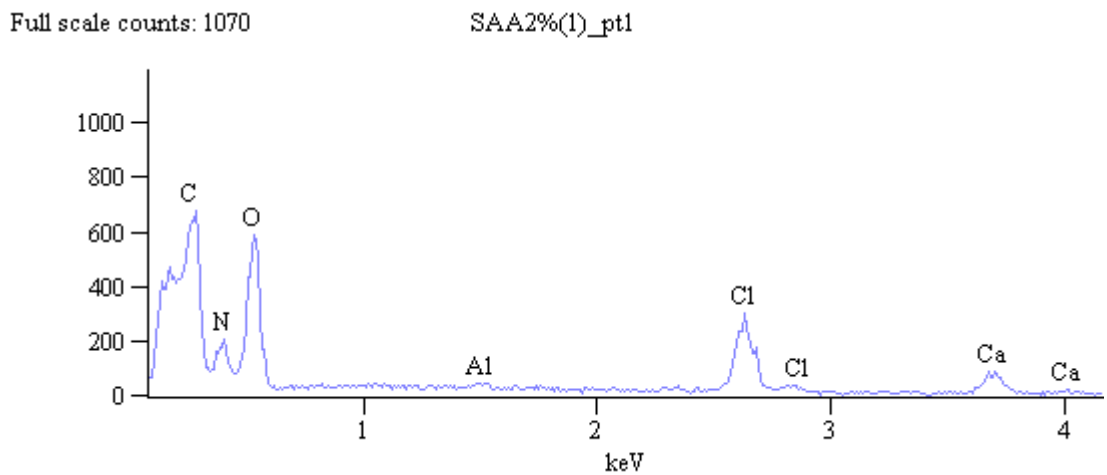
SAA2%(1)_pt1

Figure 118: EDX for SAA2%

Figure 119: EDX for SAA5%
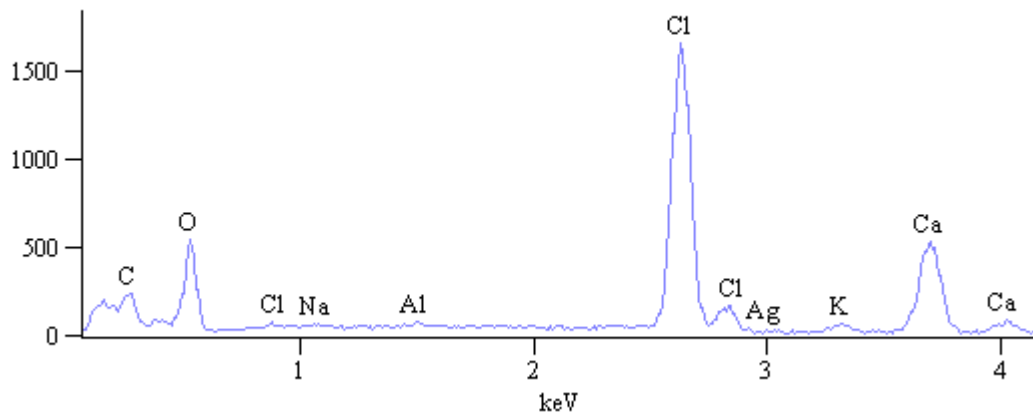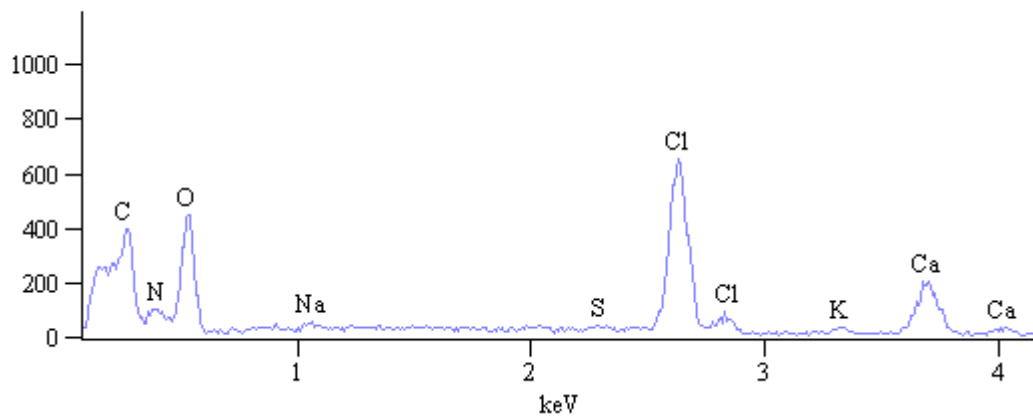
Figure 120: EDX for SAB2%   *Together in Excellence*

Figure 121: EDX for SAB5%

Figure 122: EDX for SAB5%